New developments in calcium phosphate bone cements: approaching spinal applications

Maria Daniela Vlad

PhD Thesis

Universitat Politècnica de Catalunya

New developments in calcium phosphate bone cements: approaching spinal applications

Maria Daniela Vlad

Supervisor : Prof. Dr. Enrique Fernández Aguado

Department of Materials Science and Metallurgical Engineering

Universitat Politècnica de Catalunya

December 2008

Părinților mei Ileana şi Ioan,

cărora niciodată nu le v-oi putea mulțumii îndeajuns.

Acknowledgements

Finally, this will be my PhD thesis. It has been a long way plenty of gratitude to many people: relatives, professors, colleagues and friends. I should thank the *Universitat Politècnica de Catalunya* (UPC) and the *Departament de Ciència dels Materials i Enginyeria Metal.lúrgica* (CMEM) for accepting me as a PhD student.

My sincere gratitude to Mr. Prof. Enrique Fernández Aguado, my PhD supervisor, for giving me the opportunity to commence and develop my research activity in the exciting field of calcium phosphate bone cements, for all your ideas, advices and explanations, for always sharing with me the further researches, for your great enthusiasm and patience, for your humanity, professionalism and scientific rigor. There are so many things I would like to say, so many feelings I would like to express, that it is difficult to find the words to express what I really want to leave on this page. In fact, it will prove an impossible task, and, this is why I decided to express myself, as always, to my way: *Thank you, Sir. Prof. Fernández, for giving me the opportunity to be Juan Salvador Gaviota, for giving me wings, thank you for having trusted and allowed me to fly in my own way, thank you for having always supported and defended my flight, thank you ... thank you so much for flying with me!* Deep gratitude also to Ms. Fernández and family for the attention, affection, friendship and concern towards me and my parents. ¡*Muchas gracias por todo!*

Thanks to my research group GRICCA *(Grupo Interdepartamental para la Colaboración Científica Aplicada)* whose support has been crucial in achieving this goal. In this regard, I am also grateful to Prof. José López López, Prof. Ricardo Torres Cámara and Prof. Jorge Alcalá Cabrelles for having offered me a suitable environment for work, for your collaboration, availability and concern, for your valuable and honest advices, for having

"contaminated" me with your enthusiasm and joviality. ¡*Todo lo que de más diga de Uds. sería poco!*

Special thanks to the *Escola Universitària d'Enginyeria Tècnica Industrial de Barcelona* (EUETIB – UPC) for the inconditional support given to GRICCA. Without this support this PhD thesis would not exist. Thanks for the research spaces allowed to GRICCA for the development of his research and educational activities and thanks for giving me access to all its facilities. Thanks for being my home during these years.

Thanks to Dr. Francesc Sepulcre and Dr. Luis J. del Valle *(Departamento de Ingeniería Agroalimentaria y Biotecnología, UPC)* for the experimental support and fruitful discussions, as well as for technical assistance in the cell cultures. ¡*Muchas gracias Sr. Lucho,* for sharing your knowledge in the cell culture field with me!

I am grateful to Dr. Mª Lluisa Mariñoso *(Servicio de Patologia, Hospital de Mar)* for giving me access to her laboratory and for the opportunity of enriching my knowledge with fruitful histology discussions; also, to Mª Andrea García and Rosa Mª Martínez for teaching and help me with the histology technique.

I thank Montserrat Marsal and Josep Palou *(Servicio de Microscopía Electrónica, CMEM, UPC)* for the many hours of dedication to my samples and excellent technical assistance, for your greatly patience and for the lovely pictures. ¡*Muchas gracias Josep por tu comprensión y disponibilidad hacia mi trabajo y por haberme coloreado la foto que ocupa la portada de mi tesis!*

Thanks to Xavier Alcobé *(Servicios Científico-técnicos, Universidad de Barcelona)* and Susana Valls *(Departamento de Ingeniería de Construcción, Sección Materiales, UPC)* for the X-ray diffraction analysis and helpful discussions.

Thanks to Ricard Álvarez and Jaume Comas *(Unidad de Granulometría y Citometría, Servicios Científico-técnicos, Universidad de Barcelona - UB)* for particle size analysis and useful comments.

Thanks to Maria Calvo, Anna Lladó and Anna Bosch for technical assistance in the cell's immunofluorescence staining and in the confocal imaging *(Unidad de Microscopía Confocal, Servicios Científico-técnicos, UB)*, and to Manel Bosch and Nieves Hernández for their useful advices.

Thanks to Eulalia Rius *(Departamento de Biología Celular, Facultad de Medicina, UB)* for the kindness shown at any time and for her technical advises concerning the microplate reader measurements.

Special thanks to Prof. Dr. Mercedes Durfort i Coll *(Faculdad de Biologia, UB)* and Prof. Dr. Cristina Manzanares *(Faculdad de Odontologia, UB)* for the great honour/opportunity of having meet her, for your kindness and availability in help me with my research and for your valuable discussions.

Thanks to Dr. Johan Carlson (Luleå University of Technology) for your experimental support with the ultrasound study and for fruitful discussions.

The list of colleagues, both in the biomaterials group of CMEM and EUETIB, I would like to mention is much too long, so I would like to say to all of them that I am thankful for having meet them and having have around. To mention just a few, thank to Dani, Lucía, Ana, Alex, Jorge, Montse, Camino, Naile, Crístian, Jordi, Albert and Eduardo for good advices, help and interesting or funny discussions.

I would like to thank all the teachers, PhD students and administrative staff of the UPC, EUETIB and UB with whom I interacted in one way or another; everyone contributed to enrich my doctoral stay in Barcelona.

I should also thank the *Faculty of Medical Bioengineering, University of Medicine and Pharmacy "Gr. T. Popa"* of Iasi (Romania) for the permission granted for coming to UPC to do this PhD thesis. In this regard, I would like to express my sincere gratitude to Mr. Prof. Ion Poeată, my PhD supervisor in the neurosurgery field, for your valuable advices and for always encourage me and support my scientific/research and professional activities, and this doctoral stage too.

The *Faculty of Veterinary Medicine* (Iasi, Romania) is acknowledged for permission granted for the animal experiments. I thank Prof. Dr. Corneliu Cotea and Dr. Eusebiu Sindilar and his team, for excellent collaboration concerning the animal experimental study.

Obviously, this PhD thesis would not be possible without funding. In this regard, I should thank funding allowed through projects HPMT-CT-2000-00003 (*European Commission*), SGR200500732 (*Generalitat de Catalunya*) and MAT200502778 (*Ministerio de Educacíon y Ciencia* of Spain). I am grateful again to the *Generalitat de Catalunya* for granting me a predoctoral fellowship within the program FIE2006 to do training activities at PROTECMO (*Procesos Técnicos del Molde S.A.*), an active company with research activities in the Biomedical Sector and the micromanufacturing field. Thanks to Mr. Ferran Picas, Mr. Ramón Porta and Mr. Enric Porta for giving me the opportunity to share ideas between the University and the Productive Sector around the same table. Thanks for good brainstormings and good luck for the future!

Last, but definitively not least, I would like to thank my mother and my father, for their love, for always being there for me and for always supporting me. *Fără dragostea voastră şi sprijinul vostru constant această teză, ca de altfel tot ceea ce am realizat până acum, nu ar fi fost posibilă. Niciodată nu am să vă pot mulțumii îndeajuns!*

"-Se ha roto la Hermandad- entonaron juntas las gaviotas, y todas de acuerdo cerraron solemnemente sus oídos y le dieron la espalda."

"Hay quien obedece sus propias reglas porque se sabe en lo cierto; quien cosecha un especial placer en hacer algo bien; quien adivina algo más que lo que sus ojos ven; quien prefiere volar a dormir y comer."

Richard Bach, Juan Salvador Gaviota

Abstract

The present PhD thesis (i.e., "New developments in calcium phosphate bone cements: approaching spinal applications") is aimed at contributing to close the gap between the research conducted on the field of calcium phosphate bone cements (CPBCs) and their specific spinal clinical use. The main working hypothesis was formulated as follows (see: *Motivation: objectives*):

> *"Apatitic cements could be (after further optimization) an alternative or better option (due to its natural setting, hardening and bioactive properties) to the present use of polymeric cements in vertebroplasty and kyphoplasty".*

In this regard, this thesis has approached new solutions to obtain apatitic bone cements with: (a) improved mechanical properties *(Chapter 2)*; (b) the ability to develop open-interconnected macroporosity included into a matrix of entangled micro-calcium-deficient apatite crystals *(Chapter 3)*; (c) improved chemical reactivity and stability *(Chapter 4 & 5)*; (d) suitable biocompatible and osteogenic properties *(Chapter 6, 7 & 8)*; and (e) improved injectability properties *(Chapter 7)*. Moreover, this thesis has also approached ultrasound, a non destructive testing technique, in order to monitor the early setting stages of ceramic based bone cements to link the evolution of acoustic and material properties with some intrinsic cement-injectability features *(Chapter 9 & 10)*.

Chapter 2 showed that workability, flowing and mechanical properties of apatitic bone cements can be improved by adding superplasticizers to the liquid cement phase. The results indicated that superplasticizers (if biocompatible) can be used to improve the injectability and the strength of apatitic bone cements.

Chapter 3 showed that calcium sulfate dihydrate (CSD) crystals can be added into the cement powder phase to modulate the macroporosity of the cement during its setting. This was proved with an alpha-tricalcium phosphate (α-TCP) bone cement. The setting properties of the new biphasic cements resulted from the progressive dissolution-precipitation of α-TCP into calcium-deficient hydroxyapatite (CDHA) crystals and the passive dissolution of the CSD phase, which render porosity homogeneously distributed into an entangled matrix of CDHA crystals. The biphasic cements showed suitable strength for trabecular bone applications.

Chapter 4 focused the manufacturing process of α-TCP (α-$Ca_3(PO_4)_2$), the main cement reactant of most commercial apatitic-based CPBCs. It has been shown that if calcium-to-phosphorous (Ca/P) ratio deviated from Ca/P=1.50, the resulting cements had worse setting and hardening properties. These deviations can result from sintering if reactives are not pure from batch to batch; in this case the α-TCP shows no-cement reactivity at all.

Chapter 5 approached new solutions to control and improve the chemical reactivity of the α-TCP phase. In this sense, new solid solutions like $(3.CaO\text{-}1.P_2O_5)_{1-x}(FeO)_x$ were investigated to replace the α-TCP of the present CPBCs. The results showed that iron modification of α-TCP recovered the chemical reactivity of unreactive α-TCP cements with even better setting and rheological end-cement properties.

Chapter 6 focused the attention into the cytocompatibility of the new cement formulations (investigated previously; chapters 3-5). It is showed that the new iron-modified calcium phosphate cements (IM-CPCs) have cytocompatible features (i.e. cells' adhesion and viability were not affected with culturing time by the iron concentration dose).

Chapter 7 concerned a new approach to improve the injectability of α-TCP based bone cements. It has been shown that the addition of iron oxide nanoparticles into the powder phase of α-TCP based cement improved both, the initial injectability and maximum

compressive strength of the cement without affecting their physico-chemical setting reactions and their cytocompatibility.

Chapter 8 pointed to the cytocompatibility, the biocompatibility and the osteogenic character of new biphasic porous/iron-modified cements (investigated previously; chapters 3-7). The results showed that biphasic cements made of CSD and iron-modified α-TCP had the ability to support cellular colonization *in vitro* and lead firm bone binding *in vivo*. It is concluded that these new formulations has cyto- and biocompatible features of interest as further cancellous bone replacement biomaterial for spinal surgery applications such as vertebroplasty or kyphoplasty.

Finally, *Chapter 9 & Chapter 10* approached ultrasound as more reliable characterisation technique of the early setting properties of bone cement-like materials than the *Gillmore* needles standard. This non-destructive technique allowed monitoring the whole setting period of experimental calcium sulphate and calcium phosphate bone cements. The results linked acoustic and material properties with the experimental factors studied and with cement flowing features. It is expected that, after further optimization, ultrasound monitoring should help, in combination with recent approaches that measure certain injectability characteristic for calcium-based bone cements (CBC's), to set up good practice protocols for CBC's injection during minimally invasive surgery.

Contents

List of Figures

LIST OF FIGURES

LIST OF FIGURES

LIST OF FIGURES

List of Tables

Preface

The present Thesis has been organized in eleven chapters. Chapter 1 contains the state of the art and Chapter 11 is a summary of the main findings. Chapters 2 to 10 form the nucleous of this Thesis. These chapters have been organized as individual units and are presented as closed studies. The information is presented in the classical form, i.e. “Introduction” (containing the relevant literature search, the key problem and the objectives of the study), “Materials and methods” (detailing the experimental materials, equipments and protocols), “Results” (presenting the main results of the study), “Discussion” (discussing the results obtained and comparing them to the relevant literature), and “References” (listing the main references supporting the findings of the study). In some chapters, the sections “Results” and “Discussion” have been joined together for convenience in only one section, i.e. “Results and discussion”.

Moreover, in order to facilitate a quick reading and remembering of contents of chapters 2 to 10, each is initiated with an “Structured abstract" (following the international peer-reviewed journal *Spine*) containing the short summarized subsections: “Mini abstract” (comprehend summary of the entire study), “Study Design” (research plan followed to limit the study), “Objectives” (clear definition of the objectives of the study), “Summary of Background Data” (research performed versus the relevant state of the art), “Methods” (main experimental methods used in the study), “Results” (presentation of the main results), “Conclusion” (main conclusion of the study), and “Key points” (listing the main key points of the study).

Finally, I would like to say that the present Thesis should be understood as forming part of a well stablished research line initiated at the Department of Materials Science and Metallurgy of the Technical University of Catalonia in 1990 by Prof. Dr. Ferdinand C.M.

Drieesens (who past away recently) and continue later on by his PhD students, now Dr. Maria Pau Ginebra Molins and Dr. Enrique Fernández Aguado (my supervisor). Be this Thesis a sensed offer also to the memory of Prof. Drieesens and a small contribution to the branched and continuous extending research of this very exciting field.

María Daniela Vlad

Barcelona, September 2008

Motivation: objectives

One of the main reported consequences of osteoporosis is Vertebral Compression Fractures (VCF). This is a worldwide problem that affects many people. The main effects are pain, loss of quality of life and dependence. VCF affects mainly old women and men (osteoporosis). However, nowadays, incidence has also increased in young people (high risk activities). The clinical cost is enormous.

Vertebroplasty (VP) and kyphoplasty (KP) are modern minimally invasive surgery techniques consisting in the injection of polymeric cement into the damaged vertebra. Moreover, KP tries to recover before injection the spine vertebral deformity caused by compression damage (kyphosis).

The present thesis was motivated by the clinical outcomes reported in the literature since 1985, when polymeric-VP started. Several recent studies and reviews (see Chapter 1) have indicated that polymeric-VP, despite its advantages (inmediate removal of pain, quality of life recovery, independency), has several inconveniences such as high polimerization exothermy (local necrosis), monomer residues (local and systemic toxicity), high stiffness after polimerization (adjacent vertebral fractures), extravasation of cement into the medular canal (spinal cord compression) or the blood system (pulmonary embolism). Moreover, the lack of bioactivity and bone-tissue regeneration capacity of polymeric cements make them even a worse option for the treatment of burst fractures in young people.

On the other hand, apatitic calcium phosphate cements are a sort of biomaterials that are bioactive (osteoclast and osteoblast activity), can be formulated to increase osteointegration and bone-tissue regeneration (porosity and bone-morphogenetic-protein, BMP), and are not exothermic (no local necrosis), do not contain toxic residues

(non toxic) and are less stiff than polymeric cements (expected low incidence of adjacent vertebral fractures).

Having in mind the above general picture, i.e. pros and contras reported for polymeric-VP and the possible benefits of calcium phosphate cements (CPCs) for the same clinical applications, the main hypothesis of the present thesis was formulated as follows:

> *"Apatitic cements could be (after further optimization) an alternative or better option (due to its natural setting, hardening and bioactive properties) to the present use of polymeric cements in vertebroplasty and kyphoplasty".*

It is worthmentioning that the above hypothesis was strongly supported by the carefull analysis performed during the study of the State of the Art (SoA) of this research field (see Chapter 1). Literature was abundant, with hundreds of references supporting the needs for future development of suitable injectable biomaterials for VP and KP. However, it was also clear from the SoA that optimum clinical performance of cement like materials will not be obtained at least new cements fit into the definition of an "ideal injectable biomaterial with optimum desirable properties for VP and KP", as stated in Table 1.1 (see Chapter 1). Although, the "desirable properties" were generally formulated, it was on the basis of the SoA of CPCs that it was made clear that these biomaterials can really close the gap between CPCs research and their specific clinical use in VP and KP spinal applications. In this sense, a small survey of important references used to close the circle around the main motivated hypothesis of the present Thesis were, concerning the: a) non cytotoxicity of CPCs (see: *Ooms E et al. Histological evaluation of the bone response to calcium phosphate cement implanted in cortical bone. Biomaterials. 2003;24(6):989-1000)*; b) osteoclast and osteoblast activity of CPCs (see: *Smartt JM et al. Repair of the immature and mature craniofacial skeleton with a carbonated calcium phosphate*

cement: Assessment of biocompatibility, osteoconductivity, and remodeling Capacity. Plastic & Reconstructive Surgery. 2005;115(6):1642-1650); c) osteointegration of CPCs (see: *Real RP et al. In vivo bone response to porous calcium phosphate cement. Journal of Biomedical Materials Research Part A. 2003;65A(1):30-36)*; d) bone-tissue regeneration of CPCs (see: *Seeherman HJ et al. rhBMP-2 delivered in a calcium phosphate cement accelerates bridging of critical-sized defects in rabbit radii. The Journal of Bone and Joint Surgery (American). 2006;88:1553-1565)*; e) non exothermy of CPCs as compared to acrylic cements (see: *Belkoff SM et al. Temperature measurement during polymerization of polymethylmethacrylate cement used for vertebroplasty. Spine. 2003;28(14):1555-1559)*; f) injectability improvements of CPCs (see: *Jansen J et al. Injectable calcium phosphate cement for bone repair and implant fixation. Orthopedic Clinics of North America. 2005;36(1):89-95*; or see: *Wang X et al. Effects of additives on the rheological properties and injectability of a calcium phosphate bone substitute material. Journal of Biomedical Materials Research (Applied Biomaterials). 2005;78B(2):259-264).*

Thus, the specific objectives of the present Thesis were formulated to solve some of the main problems that still need to be approach in order to obtain both confident new bioactive cement materials and characterisation procedures for the needed properties of the new ideal injectable bioactive spinal cements. In consequence, the specific objectives planned for this Thesis were delineated as follows:

a) Study of novel high-strength apatitic cements (see Chapter 2).
b) Study of novel high-porosity apatitic cements (see Chapter 3).
c) Study of the stability setting properties of alpha-tricalcium phosphate as the main reactant of apatitic bone cements (see Chapter 4)
d) Study of novel stable-setting iron-modified apatitic cements (see Chapter 5).
e) Study of the cytocompatibility properties of novel iron-modified apatitic bone cements (see Chapter 6).

f) Comprehensive study of the setting and hardening properties of novel iron-modified apatitic bone cements (see Chapter 7).

g) Preliminary *in vitro* and *in vivo* study of novel iron-modified apatitic bone cements (see Chapter 8).

h) Preliminary study of ultrasounds to characterise setting properties of calcium based bone cements (see Chapter 9).

i) Application of ultrasounds to further characterise material properties of calcium based bone cements (see Chapter 10).

In this sense, Chapters 2-8 were planned to increase step by step the new know-how necessary to address with confidence in the future the development of novel injectable bioactive cements with tissue regeneration efficiency and optimal rheological properties for VP and KP spinal applications. On the other hand, Chapters 9-10 were planned in order to apply ultrasound based data acquisition models to obtain suitable information on the initial physical and chemical cement's setting reactions. In VP and KP, cements should be injected far before of what is called the initial setting time *I* of the cement (see Chapter 1). However, nothing is practically known for times lower than *I*. Moreover, cement properties such as *swelling time*, *viscosity* or *injectability* change with time and these changes need to be monitor from the start of the powder and the liquid cement phases mixing.

Summarising, the present Thesis (i.e., "New developments in calcium phosphate bone cements: approaching spinal applications") is aimed at contributing to close the gap between CPCs' research and their specific clinical use in VP and KP, by studying and defining the actual needs of these special injectable bone cement biomaterials in terms of cement properties and by finding adequate clinical solutions. It is expected that recent and future developments will enable the commercialisation of better and more

differentiated products that should improve the clinical outcome of VP and KP and hence the patient life quality.

Finally, it is worthmentioning that this research field is becaming very active. At present, there are several international groups focussing on minimally invasive bone therapies using Injectable Bone Biomaterials. This year, they meet together at the 18th Interdisciplinary Research Conference on Biomaterials (Groupe de Recherche Interdisciplinaire sur les Biomateriaux Osteoarticulaires Injectables, GRIBOI; May 5-6, Montreal, Canada, 2008; http://www.griboi.org). This multidisciplinary conference showed that research on this field is growing exponentially due to the relevance, cost and social impact that osteoporosis induced fractures has in modern society.

Chapter 1

Calcium phosphate bone cements: state of the art

1.1. Background

It is well known that osteoporosis is responsible for weakening of the structural strength of bone to the extent that normal daily activities can create stresses that exceed the vertebra's strength, resulting in so-called osteoporosis-induced vertebral compression fractures (OIVCF) [1]. The incidence and associated socioeconomic costs of these fractures are very high and their health impact is far reaching: about 440000 and 700000 new cases per year in the European Union (EU) countries and in the United States, respectively [2,3]; direct annual costs estimated to be about US$440 million and US$750 million in the EU countries and in the United States, respectively [4,5]; a high degree of morbidity; a decrease in both the general and the health-related quality of life indexes [6]; an increase in various psychological disorders [7]; and an increase in mortality rate [8,9].

Vertebroplasty (VP) and Kyphoplasty (KP) are minimally invasive surgical procedures that have recently been introduced for the medical management of OIVCF [10-16]. Specifically, they aim to augment the weakened vertebral body, stabilize it, and/or restore it to as much of its normal height and functional state as possible. A dough of an Injectable Bone Cement (IBC) is carefully injected either directly into the fractured vertebral body (VP) or into a cavity created in the fractured vertebral body by the inflation of an inflatable balloon tamp (KP).

The central role that the IBC plays in the clinical outcome of VP and KP cannot be overemphasized. Nowadays, IBC's concept stands for a suitable injectable material with suitable properties for a specific clinical application. Historically, injectable acrylic cements and no other cemented materials were first used in VP [17] because their use in cemented arthroplasty was known since 1960 [18]. For this reason, there is a vast literature on the properties and clinical use of acrylic cements [19]. In particular, in VP and KP, the use of these materials have reported advantages (inmediate removal of pain,

quality of life recovery, independency) but several recent studies have indicated that polymeric-VP has several inconveniences such as high polimerization exothermy (local necrosis), monomer residues (local and systemic toxicity), high stiffness after polimerization (adjacent vertebral fractures), extravasation of cement into the medular canal (spinal cord compression) or the blood system (pulmonary embolism) [19,20]. Moreover, the lack of bioactivity and bone-tissue regeneration capacity of polymeric cements make them even a worse option for the treatment of burst fractures in young people [20].

The experience gained from polymeric-VP has led different researchers to identify a long list of desirable properties (see Table 1.1) that an optimum IBC for use in VP and KP should comply with [10,21]. Meanwhile, as some of those properties are difficult to obtain at the same time, a consensus appears to be that the most important of these properties are easy injectability, high radiopacity, a setting dough viscosity that does not change much between mixing and delivery into the vertebral body, a resorption rate that is neither too fast nor too slow, and mechanical properties that are comparable to those of a healthy intact vertebral body [21].

It is obvious from Table 1.1 that polymeric cements do not fulfil most of these desirable properties. For this reason other known cemented materials (calcium phosphates, calcium sulfates and composites) have came into the arena of VP and KP [22]. This explains the extensive research and development efforts that have been and continue to be expended on IBCs, spawning, in the process, an exponential growth of the specific literature [23]. In particular, researchers in the field of calcium phosphate cements (CPCs) have recently focussed their efforts in the development of new injectable CPCs because these materials (if injectable) can fulfil most of the desirable properties in Table 1.1. However, research in this topic has practically started and there are several

drawbacks that need to be solved before an optimum injectable apatitic cement is developed for VP and KP [24].

Table 1.1. Desirable properties of an Injectable Bone Cement for use in VP and/or KP.

• Easy preparation/handling	• Working time ≈6–10 min	• Setting time ≈15 min
• Very easy vertebral injectability (i.e. low cement viscosity)		• Low cost
• Very high radiopacity	• Low curing temperature	• No toxicity
• Optimum cohesion (i.e. no disintegration during setting; needed high viscosity for the dough)		
• Initial viscosity practically invariant with setting time and not low enough to have the potential for extravasation		• Excellent biocompatibility
• Comparable mechanical properties to healthy vertebral body for immediate reinforcement to ensure early ambulation of the patient		
• Excellent bioactivity	• Excellent osteoinductivity	• Excellent osteoconduction
• Microporosity (pores <10 μm), to allow circulation of body fluid		
• Macroporosity (pores >100 μm), to provide a scaffold for blood–cell colonization		• Resorption rate neither too high nor too low

For all these reasons, the present Thesis was motivated. As has been commented in previous section (see: "Motivation: objectives") CPCs are bioactive (osteoclast and osteoblast activity), can be formulated to increase osteointegration and bone-tissue regeneration (porosity and bone-morphogenetic-protein), are not exothermic (no local necrosis), do not contain toxic residues (non toxic) and are less stiff than acrylic cements (expected low incidence of adjacent vertebral fractures). However, despite all these advantages, new research is needed to approach CPCs to VP or KP, where optimum rheological properties are needed. Specifically, new studies on basic properties of CPCs (cohesion, injectability, setting time) and on surgeons' needs (clinical requirements) require more research and should be urgently addressed. To understand the importance of all these issues and the need for further improvements [25], it now follows an overview of the main scientific literature of the bioactive bone cements' field.

1.2. Introduction

Bioactive bone cements is just a topic of the fascinating field of *Biomaterials*. Before commenting on the concept of "bioactive cements", it could be interesting to start with some words of Professor Larry L. Hench who in 1998 wrote: *"It is time to accept that the revolution of the last 30 years, the revolution of replacement of tissues by transplants and implants has run its course. It has led to a remarkable increase in the quality of life for millions of patients... However, continuing the same approach of the last 30 years is not likely to reach a goal of 20-30 years implants survivability, a requirement of our ageing population. We need a change in emphasis in biomaterials research; in fact, we need a new revolution"* [26]. The words of Professor Jonathan Black can also help to understand where exactly this research field is now and what kind of new approaches are being looked for; in 1999 he wrote: *"Since my retirement... this... marks the end of a 30-year career as student, researcher and teacher in this field. It has been an interesting time, with gains and losses, both personally and for society. As I move on to other pursuits, I wish the very best to those who continue. May your efforts and insights continue to produce improvements in the human condition"* [27].

In order to improve our understanding of nowadays Biomaterials field, it is interesting to note that Prof. Hench [21] defined biomaterials as *"man-made materials to interface with living, host tissues"* while Prof. Black [27] expanded this definition to include *"materials of natural or man-made origin used to direct, supplement, or replace the functions of living tissue"*. A consensus definition is that of Prof. David F. Williams in 1987 [28], i.e. *"a material intended to interface with biological systems to evaluate, treat, augment, or replace any tissue, organ, or function of the body"*.

The above definitions lead us to the concept of biocompatibility that Prof. Black solves in the following manner [27]: *"The real issue of biocompatibility is not whether there are adverse biological reactions to a material, but whether that material performs satisfactorily (that is,*

in the intended fashion) in the application under consideration, and can be considered a successful biomaterial". According to this concept, biomaterials are nowadays classified as: a) *inert*, i.e. implantable materials that elicit little or no host response (local and systemic response, other than the intended therapeutic response, of living systems to the material); b) *interactive*, i.e. implantable materials designed to elicit specific, beneficial responses, such as ingrowth, adhesion, etc.; c) *viable*, i.e. implantable materials, incorporating or attracting living cells at the implantation site, that are treated by the host as normal tissue matrices and are actively resorbed or remodelled; and d) *replant*, i.e. implantable materials consisting of native tissue, cultured *in vitro* from cells obtained previously from the specific implant patient.

According to Prof. Black [27], a replant material (implantable, live tissue with identical genetic code and immunological determinants of the recipient patient) *"represents the fulfilment of the original search for biocompatibility: implantable materials demonstrating harmonious interaction"*. This is exactly the same idea reported by Prof. Hench [26]: *"The message for the next millennium... We need to shift the emphasis of biomaterials research towards assisting or enhancing the body's own reparative capacity... The proposal is that we seek biomaterials that behave in a manner equivalent to an autograft, i.e. a regenerative allograft"*.

The above conclusion helps to clarify the history of biomaterials where in the past the key question was the removal of tissue, in the present was/is the replacement of tissues and in the future is/will be the regeneration of tissues. If we consider the present, i.e. the replacement of tissues by implants *(man-made materials to interface with living, host tissues)*, such biomaterials have the advantages of availability, reproducibility and reliability (GMPs, standards, and regulations). On the other hand, the main reported disadvantage relates to the interfacial stability with host tissue, i.e. fixation of the implant [26]. Some partial solutions have promoted morphological fixation (press-fitting), cement fixation, biological fixation (porous ingrowth) and/or the trendy approach of Prof. Hench [26], the

bioactive fixation, i.e. interfacial bonding of an implant to tissue through a biologically active *hydroxyapatite* layer onto the implant surface. In this sense, materials showing bioactive fixation are called *bioactive implants*. A more general definition is that a bioactive material is a biomaterial that is designed to elicit or modulate biological activity [27].

However, the term bioactive is often related to the presence of the bone-like mineral phase hydroxyapatite. For this reason, Prof. Oonishi [29] has suggested that there are three types of bioactive bone cements: a) *bioactive bone cements* where the whole material is bioactive, i.e. calcium phosphate cements (the focus of the present chapter/Thesis); b) *surface-bioactive bone cements*, where, for example, a bioactive filler particle is added to a non-bioactive matrix, i.e. hydroxyapatite added to polymeric cements such as poly-methyl-methacrylate [30]; and c) *interface-bioactive bone cements* where a bioactive material is placed between the bone and the non-bioactive cement, i.e. layers of hydroxyapatite granules between bone cement.

In this Thesis, the term *bioactive bone cements* makes reference to those cementitious materials made exclusively by bioactive materials, i.e. calcium phosphate cements, that through setting reactions form a scaffold of interconnecting crystals of bone apatite-like mineral phase. The analysis of the SoA around this specific topic will bring forward some insights on the evolution of *bioactive bone cements* since their discovery in 1985 by Brown and Chow [31] until the present time, where *minimally invasive surgery* [32,33] and *tissue engineering* [34] are the key issues controlling further developments.

1.3. Calcium phosphate cements: state of the art

1.3.1. The concept of cement material

Cements are made up of a powder and a liquid phase that, on mixing, form slurry-like materials that set with time to a solid body. CPCs are made up of a mixture of calcium

phosphates [35] and an aqueous solution (see Fig. 1.1). The physical, the chemical or the mechanical properties $P(x_i,t)$ that characterize the setting of these materials can be approximated by mathematical functions $f(x_i,t)$ depending on the experimental factors x_i and the time t, i.e. $P(x_i,t) \equiv f(x_i,t)$, which can be analysed by design of experiments [36].

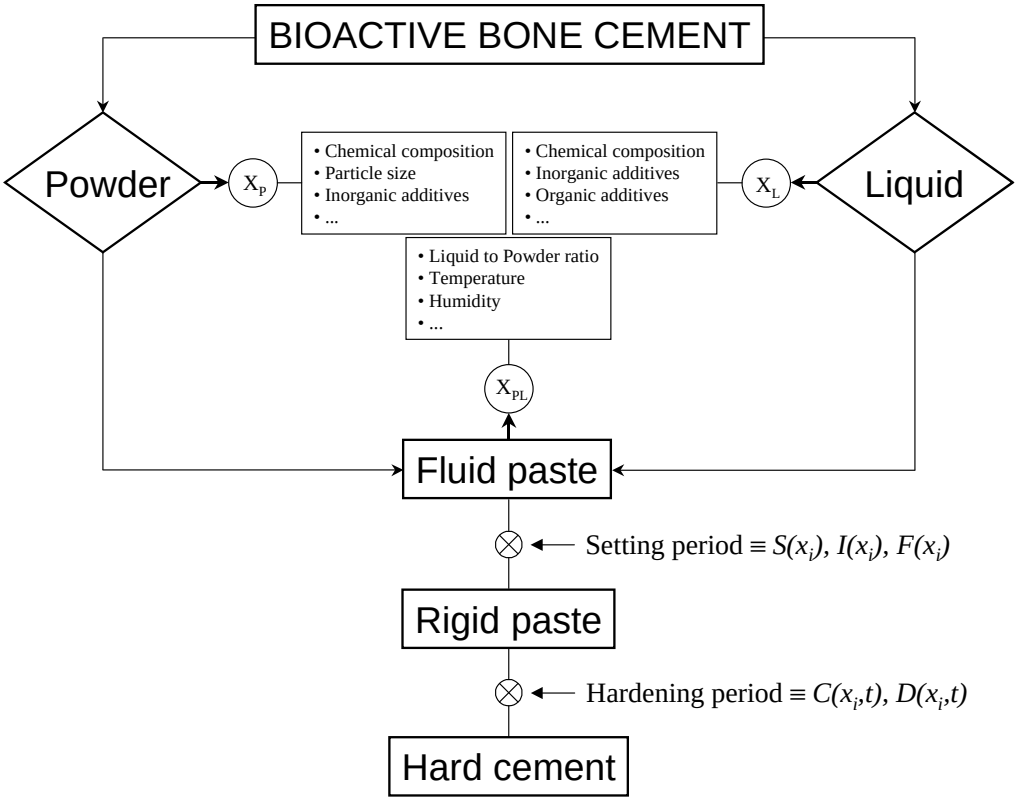

Figure 1.1. Block diagram of bone cement's technology. Some factors affecting the powder (X_P), the liquid (X_L) and the mixing (X_{PL}) are listed. Distinction between the setting and the hardening periods are clearly stated. (Note: S, I and F are the swelling, the initial and the final setting times, respectively; these characteristic times can be affected by X_P, X_L, and/or X_{PL} factors. C and D are the compressive and the diametral-tensile strength, respectively; these properties are also affected by the above factors but also change with time t (see the text for further details).

1.3.2. The concept of setting

The setting of bioactive bone cements is a continuous process that involves dissolution and precipitation chemical reactions [37]. During these processes, new crystals are formed; with time, the crystals grow and entangle, so the cement loses its viscofluid properties into a solid body [38]. The entire process is called setting. However, in CPCs, it is often distinguished between the setting and the hardening of the cement. The setting is identified to the period of time from the initial powder and liquid mixture until the cement starts to lose the viscofluid properties. On the other hand, the hardening makes reference to the period between the setting (as defined before) and the full transformation of the cement into a solid body, when no further chemical reactions are observed.

1.3.3. Characterization of the setting period

Some physical properties that are often measured to characterize the setting period are the swelling time $S(x_i)$, the initial setting time $I(x_i)$, and the final setting time $F(x_i)$ (see Fig. 1.1). $S(x_i)$, also called the cohesion time [39], is defined as the time needed, after mixing the cement's powder and liquid phase into a homogeneous paste, not to observe any cement disintegration upon early contact with liquid phases (water, Ringer's solution, simulated body fluid or blood) [40-42] (see Fig. 1.2). $I(x_i)$, which marks the start of the setting period, has been identified to the maximum time the surgeon has to implant the homogeneous cement paste into the body without affecting the microstructure of the cement and, as a result, its final properties after hardening [43,44]. Similarly, $F(x_i)$, which marks the end of the setting and the start of the hardening period, has been defined as the maximum time the surgeon must wait before closing and stressing the wound without affecting the mechanical stability and the end properties of the cement implant [43,44]. The above definitions are used in experimental design to optimize both research

and properties of commercial bioactive bone cements. In this sense, researchers are looking for CPCs with $S(x_i) \rightarrow 0$ [41,42] or at least with $S(x_i) << I(x_i)$ [45,46]; otherwise cement disintegrates upon contact with body fluids. Optimum values for $I(x_i)$ and $F(x_i)$ in clinical procedures have been reported to be $4<I(min)<8$ and $10<F(min)<15$ [44,47]. The setting times are measured using the standards *ASTM C191-92* (Vicat needles) [48] or *ASTM C266-89* (Gillmore needles) [49] (see Fig. 1.3).

Basically, both standards measure a static pressure. The procedure is as follows: (a) a needle of certain diameter and weight is rested, at control times, onto a flat surface of certain volume of cement; (b) when no visual mark is let down onto the surface by the resting needle, the cement is considered to be set. Whereas the Vicat method only uses a needle to determine $F(x_i)$, the Gillmore method uses two different needles: one for $I(x_i)$ and the other for $F(x_i)$. Most researchers prefer the Gillmore method because it also gives a measure for $I(x_i)$. The equivalent static pressures applied by the Gillmore needles are 0.3MPa for $I(x_i)$ and 5MPa for $F(x_i)$ [49]. It is found experimentally that $F(x_i) \approx 2I(x_i)$ [45].

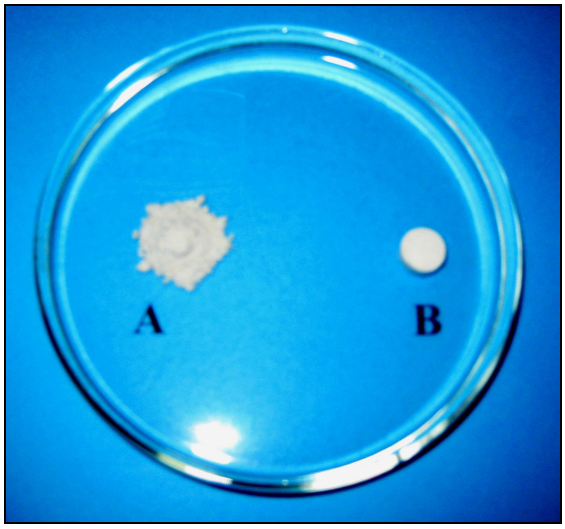

Figure 1.2. Cement disintegrates upon early contact with the liquid phase (left); after the swelling time the cement shows no disintegration (right).

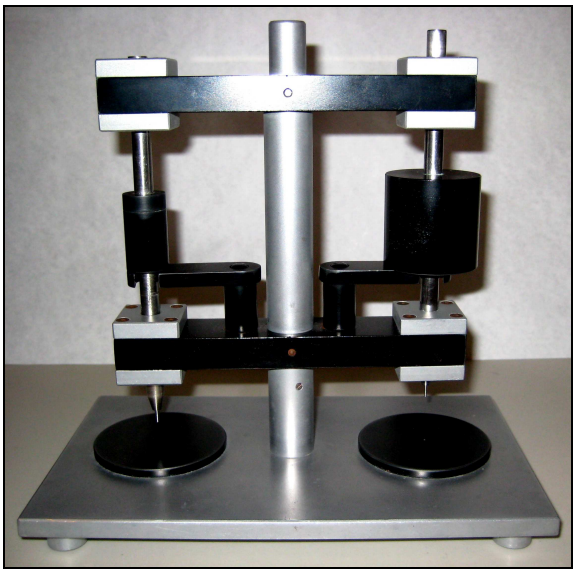

Figure 1.3. Gillmore needles (standard ASTM C266-89). Light (left) and heavy (right) needle measure the initial and final setting time, respectively.

The Vicat and Gillmore methods have been used since the discovery of CPCs [37,50]. However, these methods have not avoided criticism due to their subjectivity (visual inspection) and the relative value that setting times have in minimally invasive spinal surgery (VP and KP), where the cement should be injected far before the completion of the $I(x_i)$; otherwise, it is impossible to inject the cement into the implant site. For this reason, some authors have started to record the setting period continuosly by ultrasounds [51,52] (see also Chapters 9 and 10), as well as to point out that the lack of injectability of the present bioactive bone cements is the key issue to be solved in today's minimally invasive surgery [24,53].

1.3.4. Characterization of the hardening period

1.3.4.1. Mechanical point of view

The hardening period (transition from viscous to solid state; see Fig. 1.1.) is characterized by measuring the evolution of some mechanical property. For convenience, the compressive strength $C(x_i,t)$ or the diametral tensile strength $D(x_i,t)$ are often used [54]. Most authors use the compressive strength and follow the standard *ISO 9917-1* [55] for dental cements. Basically, compressive strength samples of 6mm of diameter and 12mm of height are made using Teflon or stainless-steel molds. Then, samples are allowed to set for different fixed times at near *in vivo* conditions (i.e., 37°C and 100% humidity, by immersion in a liquid solution (water, Ringer's solution, or simulated body fluid). Then, the cement samples are immediately tested under compression in an electromechanical testing machine at a normal cross-head speed of 1 mm/min, and the maximum compressive strength before fracture is recorded [56] (see Fig. 1.4).

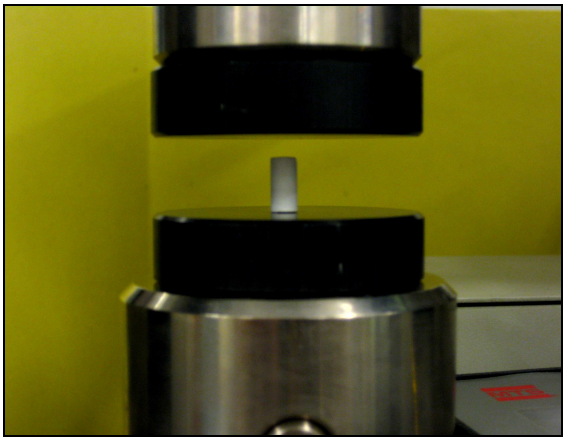

Figure 1.4. Cements are tested under compression in an electromechanical testing machine. The maximum compressive strength at failure is recorded against the reaction time to obtain the hardening curve, i.e. $C(x_i,t)$.

The optimum procedure to characterize the hardening of CPCs is by recording the whole hardening curve (i.e., the compressive strength $C(x_i,t)$ for a fixed and controllable number of experimental factors x_i as a function of time t), from after the $F(x_i)$ (if possible) until saturation with time (i.e., no further evolution of the compressive strength) [56-61]. This method allows obtaining relevant information on the chemical and physical mechanisms involved during the hardening period. Moreover, these mechanisms can be confirmed by other characterization techniques (Scanning Electron Microscopy, SEM; or X-ray Diffraction, XRD) [57-61], as is commented later on. On the other hand, this is the appropriate way by which two different cements (i.e., cements made with different experimental factors x_i) can be objectively compared in order to study the influence of several experimental factors x_i on the mechanical properties. Following this procedure, some authors have recorded the hardening curve and modeled the hardening process of bioactive bone cements following equation $C(x_i,t)=C_0(x_i)*[1-exp(-t/\tau_c(x_i)]$ [57-61]. For all these reasons, this is the method followed in this Thesis (see for example Chapter 3).

The information obtained through the mechanical characteristic time constant $\tau_c(x_i)$, which is a function of the experimental factors x_i, has linked the microstructural development of the crystal scaffold network, responsible for the mechanical strength, to the chemical reactivity of the powder cement's phases [57-61]. Moreover, this approximation has put forward the relevance of kinetic *versus* thermodynamic studies. Unfortunately, since the discovery of CPCs [31,37] most authors have reported the compressive strength after 24 h of setting [54,62], in accordance to the standard of dental cements [55], which has been the consequence of traditionally looking for CPCs passing certain ''required'' threshold to be considered for further optimization. In this sense, it is not rare to find in the past literature certain discrepancies among authors claiming for high, i.e., 90MPa , 55MPa, 40MPa [31,38,54,62-65], or low, i.e., 5–10MPa [56] compressive strength values, all suitable values for the claimed bone applications. Whatever the

strength threshold, experience has shown that CPCs (i.e., a ceramic material) should be intended for nonload bone bearing applications [33]. For this reason, strength values around the compressive strength of cancellous bone (i.e., 10–30MPa) are considered enough for these materials, and research has been focused on more relevant problems such as their injectability [24,32,33,57-70] or their stability and transformation into bone tissue *in vivo* [71,72].

1.3.4.2. Microstructural point of view

CPCs are intended for bone filling applications. It is important to remember that the trendy approach of biomaterials for this century is the replant type materials or tissue engineering (see, *1.2. Introduction*). In this sense, a key issue in bioactive cements' research has been how to improve the osteointegration and further transformation of the cement implant into real bone tissue. Some authors have used the concept of osteotransductive bone cements to explain that the microstructure of these materials (network of chemically entangled apatite-like crystals) are slowly resorbed and replaced by new bone tissue without loss of mechanical stability during transformation [73]. Since the discovery of CPCs [31,37], researchers have followed by SEM the evolution of the crystal-network structure developed during the cement's hardening, something like a function $\Omega(x_i,t)$, which obviously has not been measured but has been visually observed and reported. The information gained on the hardening behavior of CPCs has been tremendous. It has been possible to observe how the microstructure changed completely by only adding, for example, minor additions of citric acid [58] or polymeric additives [74] or how the porosity developed within the cement [60,74,75]. Most important, these observations have helped to explain the short-range and long-range mechanical stability of these materials during setting. The processes of dissolution, nucleation, precipitation, growth, and entanglement of apatite-like crystals (see Fig. 1.5) have been perfectly reported

[58,59,74,76]. This information has also served to point out the relevance of kinetic *versus* thermodynamic studies in CPCs. The present Thesis has also taken advantage of this knowledge.

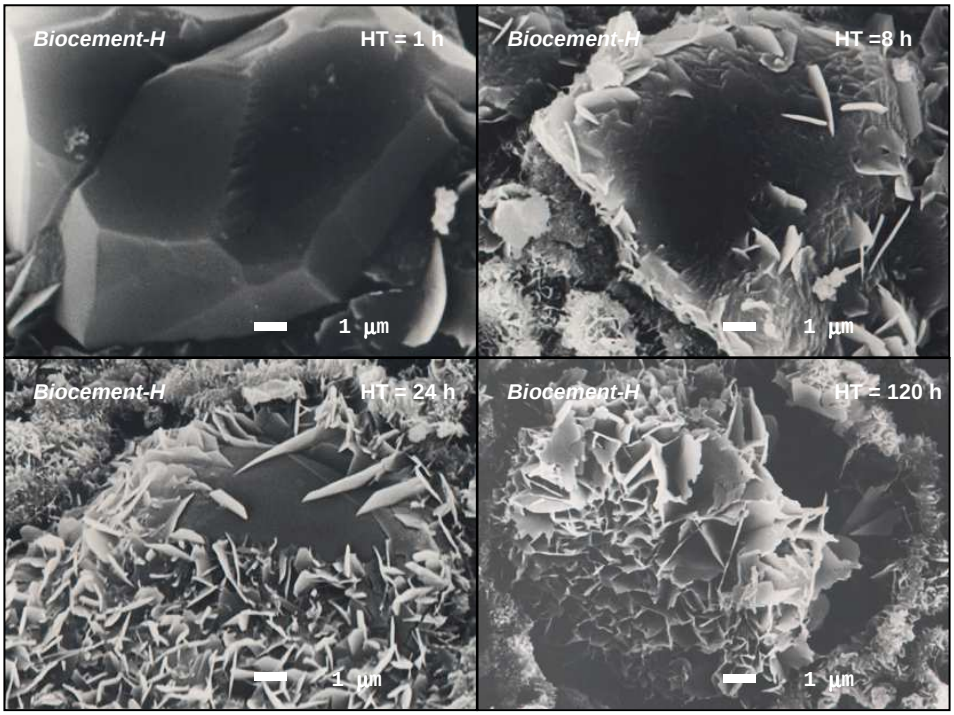

Figure 1.5. SEM microstructures showing different stages of Biocement-H®'s setting (left-top: dissolution of α-TCP particles after 1h of setting; right-top: nucleation and growth of apatite crystals after 8h; left-bottom: further surface-control growth after 24 h; right-bottom: further diffusion-control growth after 120 h) [from Ref. 74].

1.3.4.3. Chemical point of view

The chemistry (thermodynamics) of CPCs is well known and for a long time has been the basis for further material's development. In the literature, many good reviews exist that

explain the main facts of chemical cement's technology [31,33,35,37,77,78]. In particular, concepts such as solubility isotherms, singular points, supersaturated solution, dissolution, and precipitation should be well understood. Although this knowledge has served to identify those thermodynamically optimum calcium phosphate powder mixtures [33,77,78], as well as the expected crystallization steps, in practice, the actual evolution of the cement's chemistry has been followed by XRD [38,57-60,76,79], also in the present Thesis. Some authors have followed at the same time the evolution of the compressive strength (as reported before) and the evolution of the chemical phases disappearing (dissolution of cement's powder phases) or appearing (precipitation of new crystal phases) during the setting/hardening process. Similarly, the extent of chemical reaction [i.e., $R(x_i,t)$] has been calculated for both the dissolved or the new precipitated phases according to equation $R(x_i,t)=R_0(x_i)*[1-exp(-t/\tau_r(x_i)]$, and comparison with equation $C(x_i,t)=C_0(x_i)*[1-exp(-t/\tau_c(x_i)]$ has led to very interesting results and conclusions [57,58,60].

For example, it has been made clear throughout the values of $\tau_c(x_i)$ and $\tau_r(x_i)$ that the cement's strengthening and the extent of chemical reaction (chemical reactivity) are directly related, i.e., both are different measures (observations) of the same interrelated processes (dissolution, nucleation, precipitation, growth, and entanglement of apatite-like crystals) [57,58,60]. It has also been observed that the dissolution of the main cement's powder reactant, accounted by XRD through the time constant $\tau_r^d(x_i)$, is directly followed by the precipitation of the apatite phase [i.e., $\tau_r^p(x_i) \geq \tau_r^d(x_i)$], which means that some grade of dissolution is needed before precipitation can occur, which also agrees with the fact that some precipitation is also needed before some mechanical strength can be measured, i.e., $\tau_c(x_i) \geq \tau_r^p(x_i)$ [57,58,60]. Most complex analyses have also clarified, with the supporting help of SEM microstructure observations, when the chemical reactions were being controlled by the available surface area for dissolution of the main cement

powder reactant or by diffusion through a shell of precipitated apatite crystals surrounding the main reactant particles [58,59,76] (see Fig. 1.6).

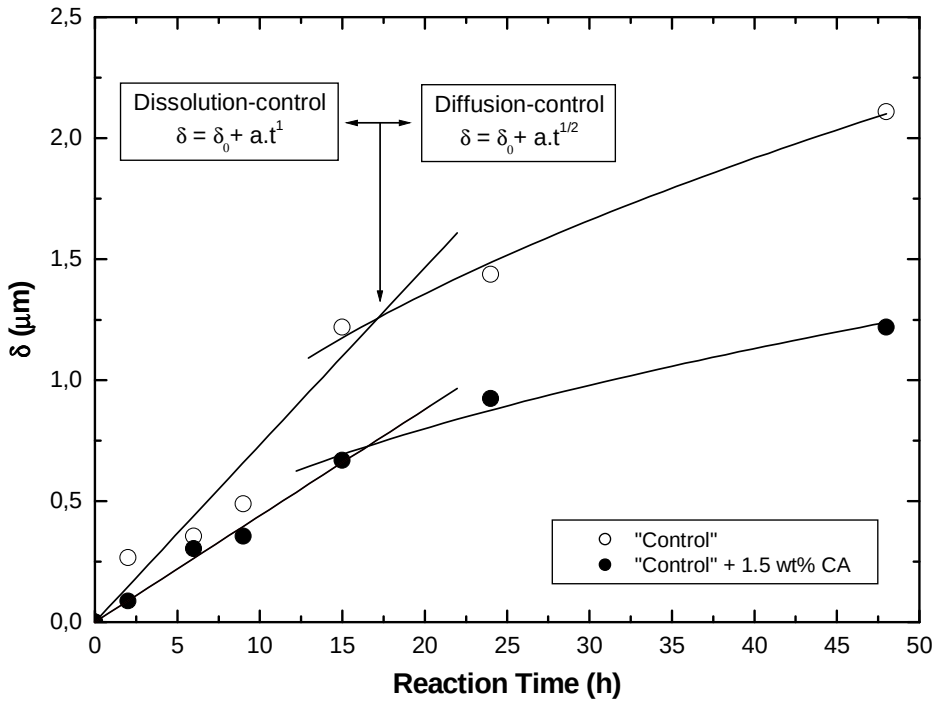

Figure 1.6. Bioactive bone cement modified with citric acid. Certain models determine when the setting reaction was controlled by dissolution and/or by diffusion [adapted from Ref. 37].

In general, these studies have put forward the relevance of the kinetic *versus* the thermodynamic approximation to the study of the setting of bioactive CPCs. Moreover, the understanding that cement's properties can be modulated, according to $P(x_i,t) \equiv f(x_i,t)$, by selecting a proper set of experimental factors x_i has been the start of a new revolution in the experimental design of CPCs [36]. In the next section, the attention is put on these experimental factors.

1.3.5. Factors affecting cement's properties

Equation $P(x_i,t) \equiv f(x_i,t)$ makes clear that any measurable cement property (at some time t) is a complicated function depending on several experimental factors x_i (controlled or not). Some of the main factors x_i affecting the powder phase (and so the end-setting properties of the cement) are: (a) the chemical nature of the reactants [33,78], (b) the number and the relative weight proportion of the reactants [45,56,78]; (c) the particle size of the reactants [59,70]; and (d) the presence of some minor additives (accelerators or retarders) [70,80]. Similarly, the main factor affecting the aqueous liquid phase is its chemical purity because of the presence of some additives (accelerators, retarders, fluidifiers, etc.) [46,70,74]. The main factor affecting the mixing is the liquid-to-powder (L/P) ratio, acting on both the setting times and the cement's rheology [70,81]; other factors are the temperature (i.e., at higher temperatures cements set faster) and the humidity [69,82,83] (see also Fig. 1.1). It is evident from the above description that cement optimization is an iterative and complicate process [25]. For example, optimum bioactive bone cement could be defined as that cement that shows no swelling, short setting times, maximum strength, good injectability, or the ability to develop porosity (see also Table 1.1). However, experience shows (as an example) that in order to shorten setting times and increase the ultimate strength, it is good to have reactants with small particle size [59], which is understandable because from thermodynamics small particle size (high surface area) shows high chemical reactivity (faster dissolution, supersaturation is attained earlier and, as a result, precipitation). However, if the L/P ratio is maintained constant the swelling often increases [45], which is also understandable because if surface area is increased, more liquid is adsorbed onto the particles and so the cement paste is dryer [45], which makes the cement impossible to inject despite the fact that it could show higher strength at saturation [45,59]. This example is clear on how factors x_i, interact between them in an

experimental design to favor certain properties (setting times or strength) in front of others (injectability or porosity). For this reason, CPCs should be optimized having in mind its final clinical application, which is why the opinion of the final user (i.e., the surgeon (clinical procedure)) is so important and should be considered from the start of any cement product development.

1.3.6. New research on fundamental properties

At present, there are not fundamental studies devoted to CPC's swelling time (i.e. $S(x_i)$). Some authors talk about "non-decay", whereas other authors used the term "cohesion" and "stability". As mentioned before, an ideal CPC should comply at least with $S(x_i)<<I(x_i)$ [23]. However, this condition is not enough for an injectable-CPC in VP or KP because CPC should be injected far before the completion of the $I(x_i)$, otherwise the cement is not injectable. For this reason, fundamental studies are needed to understand the equilibrium of forces between cement particles and fluid in order to develop injectable cements with $S(x_i)=0$ at any injection time. Basically, it appears that instead of $S(x_i)$ there is probably an unknown swelling property $S(x_i,t)$ to be determined. Some authors have reported that an increase of the cement viscosity, i.e. with the addition of a gel-forming polymer into the mixing solution, increases the cement cohesion [84-86]. However, recent studies contradict this finding. Moreover, the type of solution used to test the cohesion, strongly affects the results. So it is clear that there is presently a great need for more understanding concerning cohesion. The extreme importance of this topic is also ilustrated by recent findings that CPCs used for VP have been associated with an increased risk of blood clotting [87,88]. Considering the facts that (i) CPCs would be very appropriate for VP, (ii) vertebral bodies are intensively irrigated by blood, and (iii) the distance from the spine to the lungs and heart is short, it is of high importance to understand the reason why blood clotting occurs. A most likely explanation is that

clotting is provoked by interfacial reactions between solid particles and blood. So, the release of calcium phosphate particles from the cement into the blood stream should be prevented (perfect cohesion) and/or controlled. Therefore, cement cohesion and blood-calcium phosphate interactions should be also better understood [25].

Other fundamental property that should be reviewed is setting. Traditional methods to characterise the initial setting of cement use a mechanical approach: the cement is considered to be set when it can resist a given mechanical load applied onto its surface (Vicat and Gillmore needles methods) [48,49]. It is obvious that the information obtained is scarce and totally inadequate to understand the evolution of the time-dependent intrinsec cement's properties. Therefore, there is a need for more chemistry-based (thermal analysis) and physic-based (ultrasounds) [51,52] approaches to enable a better understanding of the kinetics of the setting reactions as a whole and not of single points in time (see also Chapters 9 and 10). Unfortunately, there is still too little known about initial setting kinetics in order to design a "perfect" CPC paste that would have a constant viscosity for a given time and then hardens very rapidly. To reach this goal, setting kinetics (and viscosity changes) have to be determined and well understood, for example by combining the very precise information retrieved from calorimetric studies [89,90] or ultrasonic studies [51,52] with the less precise information retrieved from mechanical evaluations [91].

1.3.7. New research based on surgeons' requirements

There is a large difference between the interests of CPC researchers and the needs of clinicians. Whereas the former group is interested in improving performance via an understanding of the chemistry and physics of CPC, the second is interested in a CPC that "works", regardless of the composition. A "working" cement must have several features (see Table 1.1.), such as low price, easy and reliable mixing and delivery, good

visualisation during injection (i.e. for VP) and good clinical outcome, particular fast replacement with bone or rapid bone apposition. Despite the improvements made in those directions other problems still remain. For example, the rheological behaviour of CPC is largely unknown. One important drawback of CPC compared to acrylic cements has been their poor injectability. Liquid-solid phase separation (so-called filter-pressing) has often been observed in commercial formulations. Recent efforts in the field of cement injectability have enabled a better understanding of CPC injectability and also provided innovative solutions [53,66,67,92-94]. Moreover, the large effect of temperature on the setting (and probably swelling) properties of CPC, particularly apatite CPC is a huge challenge for cement producers: the setting time of apatite is typically reduced three- to fourfold when temperature increases from 20 to 37°C [69]. This implies that composition and/or mixing systems should be optimised. Addition of radio-opacifiers into CPC might provide a better visualisation during injection, particularly for VP. However, solutions are not trivial. There is not information about the effect of these new additives on the rheological, setting and hardening properties of CPCs. Moreover, there is a concern to implant billions of non-resorbable particles in a matrix that is likely to be resorbed over time.

1.3.8. Conclusion

It is concluded from this critical analysis of the State of the Art that a real need for more innovative research exists to close the gap between CPC research and their specific clinical use in VP and KP. In this sense, engineers should approach this new research having in mind the specific clinical requirements that an ideal CPC should have for VP and KP. In this sense, the rheological behaviour of these materials should be understood. In particular CPC researchers should design programs to know the real functionality of viscosity, i.e. $\eta(x_i,t)$. Moreover, basic properties such as cohesion or swelling (i.e. $S(x_i,t)$)

should also carefully analysed. For all these reasons, the present Thesis (i.e., "New developments in calcium phosphate bone cements: approaching spinal applications") finds complete justification. It is expected to contribute with new ideas and improvements in order to approach better materials and solutions for spinal applications.

References

1. Ferguson SJ, Steffen T. Biomechanics of the aging spine. Eur Spine J 2003;12(2):S97–S103.

2. European Prospective Osteoporosis Study Working Group. Incidence of vertebral fracture in Europe: Results from the European Prospective Osteoporosis Study (EPOS). J Bone Miner Res 2002;17:716-24.

3. Akesson K, Adami S, Woolf AD, editors. The year in osteoporosis 2004. Boca Raton, FL; CRC Press; 2004.

4. Johnell O. Economic implication of osteoporotic spine disease: Cost to society. Eur Spine J 2003;12(2):S168 –S169.

5. Melton III LJ. Epidemiology of spinal osteoporosis. Spine 1997;22:2S–11S.

6. Adachi J, Loannidis G, Olszynski W, et al. The impact of incident vertebral and non-vertebral fractures of health related quality of life in postmenopausal women. BMC Musculoskelet Disord 2002;3:11.

7. Silverman SL. The clinical consequences of vertebral compression fracture. Bone 1992;13(2):S27–S31.

8. Kado DM, Browner W, Palermo L, et al. Vertebral body fractures and mortality in older women: A prospective study of the osteoporotic fracture research group. Arch Intern Med 1999;159:1215-20.

9. Grigoryan M, Guermazi A, Roemer FW, et al. Recognizing and reporting osteoporotic vertebral fractures. Eur Spine J 2003;2:S104–S112.

10. Phillips FM. Minimally invasive treatments of osteoporotic vertebral compression fractures. Spine 2003;28:S45–S53.

11. Bono C, Garfin S. Kyphoplasty and vertebroplasty for the treatment of painful osteoporotic vertebral compression fractures. In: Lewandrowski KU, Wise DL, Trantolo DJ, Yaszemski MJ, White III AA, editors. Advances in spinal fusion; Molecular science, biomechanics, and clinical management. New York: Marcel Dekker, Inc.; 2004. p 33–49.

12. Alvarez L, Pérez-Higueras A, Granizo JJ, de Miguel I, Quiñones D, Rossi RE. Predictors of outcomes of percutaneous vertebroplasty for osteoporotic vertebral fractures. Spine 2005;30:87-92.

13. Alvarez L, Alcaraz M, Pérez-Higueras A, Granizo JJ, de Miguel I, Ross RE, Quiñones D. Percutaneous vertebroplasty functional improvement in patients with osteoporotic compression fractures. Spine 2006;31:1113-18.

14. Alvarez L, Perez-Higueras A, Quinones D,Calvo E, Rossi RE. Vertebroplasty in the treatment of vertebral tumors: postprocedural outcome and quality of life. Eur Spine J 2003;12:356-60.

15. Martinez-Quiñones JV, Hernández-Sánchez G. Percutaneous vertebroplasty: tecnique and early results in 25 procedures. Neurocirugía 2003;14:323-32.

16. Martinez-Quiñones JV, Aso-Escari J, Arregui-Calvo R. Refuerzo vertebral percutáneo: vertebroplastia y cifoplastia. Procedimiento técnico. Neurocirugía 2005;16:427-40.

17. Galibert P, Deramond H, Rosat P, et al: Preliminary note on the treatment of vertebral angioma by percutaneous acrylic vertebroplasty. Neurochirurgie 33:166-168, 1987.

18. Charnley, J. Anchorage of the femoral head prosthesis to the shaft of the femur. J Bone Joint Surg 1960;43B:28–30.

19. Lewis G. Properties of acrylic bone cement: state of the art review. J Biomed Mater Res (Appl Biomater) 1997;38:155-82.

20. Burton AW, Rhines LD, Mendel E. Vertebroplasty and kyphoplasty: a comprehensive review. Neurosurg Focus 2005;18(3):E1,1-9.

21. Heini PF, Berlemann U. Bone substitutes in vertebroplasty. Eur Spine J 2001;10:S205–S213.

22. Lewis G. Injectable bone cements for use in vertebroplasty and kyphoplasty: state of the art review. J Biomed Mater Res Part B: Appl Biomater 2006;76B:456-68.

23. Fernández E. Bioactive bone cements. In: Wiley Encyclopedia of Biomedical Engineering, 6-Volume Set, ISBN: 0-471-24967-X, John Wiley & Sons, Inc. (USA), Metin Akay (Ed.), June 2006, pp. 1-9.

24. Bohner M, Baroud G. Injectability of calcium phosphate pastes. Biomaterials 2005;26:1553-1563.

25. Bohner M, Gbureck U, Barralet JE. Technological issues for the development of more efficient calcium phosphate bone cements: a critical assessment. Biomaterials 2005;26:6423-29.

26. Hench LL. Biomaterials: a forecast for the future. Biomaterials 1998;19:1419-1423.

27. Black J. In: Biological Performance of Materials: Fundamentals of Biocompatibility, Third Edition, Marcel Dekker, NY, 1999.

28. Williams DF (Ed.). In: Definitions in biomaterials (Proceedings of a Consensus Conference of the European Society for Biomaterials, Chester, UK, 3-5 March, 1986), Elsevier Science Publishers B.V., Amsterdam, 1987.

29. Oonishi H. Bioactive bone cements. In: The Bone-Biomaterial Interface (Ed. J.E. Davies), 1991, pp. 321-333 (University of Toronto Press, Toronto, Canada).

30. Harper EJ. Bioactive bone cements. Proc Instn Mech Engrs 1998; 212(H): 113-120.

31. Brown WE, Chow LC. Dental Restorative Cement Pastes, Patent No. US4518430. May 21 (1985).

32. Mushipe M. Injectable micro-particles and pastes for minimally invasive orthopaedic surgery. MD Technology Watch Series, Article 2, August 2003.

33. Bohner M. Physical and chemical aspects of calcium phosphates used in spinal surgery. Eur Spine J 2001;10:S114-S121.

34. Barralet JE, Grover L, Gaunt T, Wright AJ, Gibson LR. Preparation of macroporous calcium phosphate cement tissue engineering scaffold. Biomaterials 2002;23:3063-3072.

35. De Groot K(Ed.). In: Bioceramics of calcium phosphates, CRC Press Inc., Boca Raton, FL, 1983.

36. Box GEP, Hunter WG, Hunter JS. In: Statistics for experimenters: An introduction to design, data analysis, and model building. John Wiley & Sons, NY, 1978.

37. Brown WE, Chow LC. A new calcium phosphate water-setting cement. In: Cements Research Progress. Ed. by P.W. Brown. (American Ceramic Society, Westerville, Ohio, 1986) p. 351-379.

38. Ginebra MP, Fernández E, De Maeyer EAP, Verbeeck RMH, Boltong MG, Ginebra J, Driessens FCM, Planell JA. Setting reaction and hardening of an apatitic calcium phosphate cement. J Dent Res 1997;76(4):905-912.

39. Khairoun I, Boltong MG, Driessens FCM, Planell JA. Effect of calcium carbonate on the compliance of an apatitic calcium phosphate bone cement. Biomaterials 1997;18:1535-1539.

40. Fernández E, Boltong MG, Ginebra MP, Driessens FCM, Bermúdez O, Planell JA. Development of a method to measure the period of swelling of calcium phosphate cements. J Mater Sci Letters 1996;15:1004-1005.

41. Ishikawa K, Miyamoto Y, Kon M, Nagayama M, Asaoka K. Non-decay type fast-setting calcium phosphate cement: composite with sodium alginate. Biomaterials 1995;16:527-532.

42. Takechi M, Miyamoto Y, Ishikawa K, Yuasa M, Nagayama M, Kon M, Asaoka K. Non-decay type fast-setting calcium phosphate cement using chitosan. J Mater Sci Mater Med 1996;7:317-322.

43. Driessens FCM, Boltong MG, Bermúdez O, Planell JA. Formulation and setting times of some calcium orthophosphate cements: a pilot study. J Mater Sci Mater Med 1993;4:503-508.

44. Ginebra MP, Fernández E, Boltong MG, Bermúdez O, Planell JA, Driessens FCM. Compliance of an apatitic calcium phosphate cement with the short-term clinical requirements in bone surgery, orthopaedics and dentistry. Clinical Materials 1994;17:99-104.

45. Fernández E, Gil FJ, Ginebra MP, Driessens FCM, Planell JA, Best SM. Production and characterization of new calcium phosphate bone cements in the $CaHPO_4$-α-$Ca_3(PO_4)_2$ system: pH, workability and setting times. J Mater Sci Mater Med 1999;10:223-230.

46. Khairoun I, Driessens FCM, Boltong MG, Planell JA, Wenz R. Addition of cohesion promotors to calcium phosphate cements. Biomaterials 1999;20:393-398.

47. Khairoun I, Boltong MG, Driessens FCM, Planell JA. Limited compliance of some apatitic calcium phosphate bone cements with clinical requirements. J Mater Sci Mater Med 1998;9:667-671.

48. Standard Test Method for Time of Setting of Hydraulic Cement Paste by Vicat Needle, ASTM C191-92, Annual Book of ASTM Standards, vol. 04.01: Cement, Lime, Gypsum. Philadelphia: ASTM;1993:158-160.

49. Standard Test Method for Time of Setting of Hydraulic Cement Paste by the Gillmore Needles, ASTM C266-89, Annual Book of ASTM Standards, vol. 04.01: Cement, Lime, Gypsum. Philadelphia: ASTM;1993:189-191.

50. Takezawa Y, Doi Y, Shibata S, Wakamatsu N, Kamemizu H, Goto T, Iijima M, Moriwaki Y, Uno K,Kubo F, Haeuchi Y. Self-setting apatite cement. II. Hydroxyapatite as setting accelerator. J Japan Soc Dent Mater Devices 1987;6(4):426-431.

51. Nilsson M, Carlson J, Fernández E, Planell JA. Monitoring the setting of calcium-based bone cements using pulse-echo ultrasound. J Mater Sci Mater Med 2002;13:1135-41.

52. Carlson J, Nilsson M, Fernández E, Planell JA. An ultrasonic pulse-echo technique for monitoring the setting of $CaSO_4$-based bone cement. Biomaterials 2003;24:71-77.

53. Baroud G, Bohner M, Heini P, Steffen T. Injection biomechanics of bone cements used in vertebroplasty. Bio-medical Materials and Engineering 2004;14(4):487-504.

54. Bermúdez O, Boltong MG, Driessens FCM, Planell JA. Compressive strength and diametral tensile strength of some calcium-orthophosphate cements: a pilot study. J Mater Sci Mater Med 1993;4:389-393.

55. ISO 9917-1. "Dentistry. Water-based cements. P.1: Powder/liquid acid-base cements". By International Organization for Standardization (ISO). Geneva: ISO, 2003.

56. Fernández E, Gil FJ, Best SM, Ginebra MP, Driessens FCM, Planell JA. Improvement of the mechanical properties of new calcium phosphate bone cements in the $CaHPO_4$-α-$Ca_3(PO_4)_2$ system: compressive strength and microstructural development. J Biomed Mater Res 1998;41:560-567.

57. Fernández E, Ginebra MP, Boltong MG, Driessens FCM, Ginebra J, De Maeyer EAP, Verbeeck RMH, Planell JA. Kinetic study of the setting reaction of calcium phosphate bone cement. J Biomed Mater Res 1996;32:367-374.

58. Sarda S, Fernández E, Nilsson M, Balcells M, Planell JA. Kinetic study of citric acid influence on calcium phosphate bone cements as water-reducing agent. J Biomed Mater Res 2002;61:653-659.

59. Ginebra MP, Driessens FCM, Planell JA. Effect of the particle size on the micro and nanostructural features of a calcium phosphate cement: a kinetic analysis. Biomaterials 2004;25:3453-3462.

60. Fernández E, Vlad MD, Gel MM, López J, Torres R, Cauich JV, Bohner M. Modulation of porosity in apatitic cements by the use of α-tricalcium phosphate-calcium sulphate dihydrate mixtures. Biomaterials 2005;26:3395-3404.

61. Fernández E, Vlad MD, Hamcerencu M, Darie A, Torres R, López J. Effect of iron on the setting properties of α-TCP bone cements. J Mater Sci 2005;40:3677-3682.

62. Driessens FCM, Boltong MG, Bermúdez O, Planell JA, Ginebra MP, Fernández E. Effective formulations for the preparation of calcium phosphate bone cements. J Mater Sci Mater Med 1994;5:164-170.

63. Constantz BR. Formulation for in situ prepared calcium phosphate minerals. Patent No. EP0416761, March 13 (1993).

64. Constantz BR, Ison LC, Fulmer MT, Poser RD, Smith ST, VanWagoner M, Ross J, Goldstein SA, Jupiter JB, Rosenthal DI. Skeletal repair by in situ formation of the mineral phase of bone. Science 1995;267:1796-1799.

65. Fernández E, Planell JA, Best SM, Bonfield W. Synthesis of dahllite through a cement setting reaction. J Mater Sci Mater Med 1998;9:789-792.

66. Yin Y, Ye F, Cai S, Yao K, Cui J, Song X. Gelatin manipulation of latent macropores formation in brushite cement. J Mater Sci Mater Med 2003;14:255-261.

67. Khairoun I, Boltong MG, Driessens FCM, Planell JA. Some factors controlling the injectability of calcium phosphate bone cements. J Mater Sci Mater Med 1998;9:425-428.

68. Ginebra MP, Rilliard A, Fernández E, Elvira C, San Roman J, Planell JA. Mechanical and rheological improvement of a calcium phosphate cement by the addition of a polymeric drug. J Biomed Mater Res 2001;57:113-118.

69. Sarda S, Fernández E, Llorens J, Martínez S, Nilsson M, Planell JA. Rheological properties of an apatitic bone cement during initial setting. J Mater Sci Mater Med 2001;12:905-909.

70. Baroud G, Cayer E, Bohner M. Rheological characterization of concentrated aqueous β-tricalcium phosphate suspensions: The effect of liquid-to-powder ratio, milling time, and additives. Acta Biomaterialia 2005;1(3):357-363.

71. Saito T, Kin Y, Koshino. Osteogenic response of hydroxyapatite cement implanted into the femur of rats with experimentally induced osteoporosis. Biomaterials 2002;23:2711-2716.

72. Bohner M, Theiss T, Apelt D, Hirsiger W, Houriet R, Rizzoli G, Gnos E, Frei C, Auer JA, von Rechenberg B. Compositional changes of a dicalcium phosphate dihydrate cement after implantation in sheep. Biomaterials 2003;24:3463-3474.

73. Driessens FCM, Planell JA, Boltong MG, Khairoun I, Ginebra MP. Osteotransductive bone cements. Proc Inst Mech Eng 1998;212(H6):427-435.

74. Fernández E, Sarda S, Hamcerencu M, Vlad MD, Gel M, Valls S, Torres R, Lopez J. High-strength apatitic cement by modification with superplasticizers. Biomaterials 2005;26:2289-2296.

75. Sarda S, Nilsson M, Balcells M, Fernández E. Influence of surfactant molecules as air-entraining agent for bone cement macroporosity. J Biomed Mater Res 2003;65A:215-221.

76. Ginebra MP, Fernández E, Driessens FCM, Planell JA. Modelling of the hydrolysis of α-tricalcium phosphate. J Am Ceram Soc 1999;82(10):2808-2812.

77. Fernández E, Gil FJ, Ginebra MP, Driessens FCM, Planell JA, Best SM. Calcium phosphate bone cements for clinical applications. I: Solution chemistry. J Mater Sci Mater Med 1999;10:169-176.

78. Fernández E, Gil FJ, Ginebra MP, Driessens FCM, Planell JA, Best SM. Calcium phosphate bone cements for clinical applications. II: Precipitate formation during setting reactions. J Mater Sci Mater Med 1999;10:177-183.

79. Fernández E, Gil FJ, Best S, Ginebra MP, Driessens FCM, Planell JA. The cement setting reaction in the $CaHPO_4$-α-$Ca_3(PO_4)_2$ system: an x-ray diffraction study. J Biomed Mater Res 1998;42:403-406.

80. Yang Q, Troczynski T, Liu D. Influence of apatite seeds on the synthesis of calcium phosphate cement. Biomaterials 2002;23:2751-2760.

81. Friberg J, Fernández E, Sarda S, Nilsson M, Ginebra MP, Martínez S, Planell JA. An experimental approach to the study of the rheology behaviour of synthetic bone calcium phosphate cements. Key Engineering Materials 2001;192-195:777-780.

82. Ginebra MP, Boltong MG, Fernández E, Planell JA, Driessens FCM. Effect of various additives and temperature on some properties of an apatitic calcium phosphate cement. J Mater Sci Mater Med 1995;6:612-616.

83. Ginebra MP, Fernández E, Driessens FCM, Boltong MG, Muntasell J, Font J, Planell JA. The effects of temperature on the behaviour of an apatitic calcium phosphate cement. J Mater Sci Mater Med 1995;6:857-860.

84. Ishikawa K, Miyamoto Y, Kon M, Nagayama M, Asaoka K. Non-decay type fast-setting calcium phosphate cement: composite with sodium alginate. Biomaterials 1995;16:527–32.

85. Khairoun I, Boltong MG, Driessens FC, Planell JA. Effect of calcium carbonate on clinical compliance of apatitic calcium phosphate bone cement. J Biomed Mater Res 1997;38(4):356-60.

86. Andrianjatovo H, Lemaître J. Effects of polysaccharides on the cement properties in the monocalcium phosphate monohydrate/b-tricalcium phosphate system. Innovation Tech Biol Med 1995;16S1:140–7.

87. Bernards CM, Chapman JR, Mirza SK. Lethality of embolized norian bone cement varies with the time between mixing and embolization. Proceedings of the 50th Annual Meeting of the Orthopaedic Research Society (ORS), San Fransisco, p. 254.

88. Axen N, Ahnfelt N-O, Persson T, Hermansson L, Sanchez J, Larsson R. Clotting behavior of orthopaedic cements in human blood. Proceedings of the Nineth annual meeting "Ceramics, cells and tissues", Faenza, September 28–October 1, 2004.

89. Brown PW, Fulmer M. Kinetics of hydroxyapatite formation at low temperature. J Am Ceram Soc 1991;75(5):934-40.

90. Liu CS, Gai W, Pan SH, Li ZS. The exothermal behavior in the hydration process of calcium phosphate cement. Biomaterials 2003;24(18):2995-03.

91. Fernández E, Ginebra MP, Boltong MG, Driessens FC, Ginebra J, De Maeyer EA, Verbeeck RM, Planell JA. Kinetic study of the setting reaction of a calcium phosphate bone cement. J Biomed Mater Res 1996;32(3):367-74.

92. Vlad MD, Del Valle LJ, Barracó M, Torres R, López J, Fernández E. Iron oxide nanoparticles significantly enhances the injectability of apatitic bone cement for vertebroplasty. Spine 2008;33(21): 2290-2298.

93. Bohner M, Gasser B, Baroud G, Heini P. Theoretical and experimental model to describe the injection of a polymethylmethacrylate cement into a porous structure. Biomaterials 2003;24:2721-30.

94. Baroud G, Steffen T. A new cannula to ease cement injection during vertebroplasty. Eur Spine J 2005;14:474-79.

Chapter 2

Effect of superplasticizers on the setting properties of apatitic bone cement

2.0. Structured abstract

Mini Abstract. This study reports on novel method to improve the strength of apatitic bone cements by modifying the liquid cement phase with the addition of superplasticizers (SPs). It is showed that these additives can be used to improve the initial cement injectability and/or the maximum mechanical strength after setting.

Study Design. Experimental study to characterise the setting and hardening properties of superplasticizers-modified apatitic bone cements.

Objective. To investigate the effect of superplasticizers on the setting and hardening properties of apatitic bone cements.

Summary of Background Data. It is generally accepted that calcium phosphate bone cements (CPBCs) need further improvements to broad their potential clinical applications. Nowadays, further improvements should be obtained at the compromise between what is considered, for a certain clinical application, the optimum cement injectability, the fast-setting behaviour, the macroporosity and the mechanical strength. In particular, to extend the use of CPBCs to minimally invasive spinal applications such as *vertebroplasty* and *kyphoplasty* it is needed that present cements be injectable. For this reason, the objective of the present research was to study the effect of superplasticizer additives on the setting and hardening properties of an apatitic control cement.

Methods. *Biocement-H*©, an α-TCP based cement, was used as control. Its liquid phase was modified with several civil engineering commercial superplasticizers. The evolution of the compressive strength accounted for the cement hardening process. Scanning electron microscopy followed the evolution of the cement microstructure during hardening. X-ray diffraction analysis confirmed the evolution of the crystalline phases controlling the setting and the hardening processes.

Results. The results showed that the addition of small amounts (0.5 *vol.%*) of S500-HE (vinilic modified copolymer-SP) into the aqueous liquid phase improved the maximum compressive strength of *Biocement-H©* (35 MPa) by 71%, i.e. 60 MPa. On the other hand, high amounts of this additive (i.e. 50 *vol.%*), significantly reduced the liquid to powder L/P ratio needed (20% water reduction) to made the cement (from 0.32 to 0.256 mL/g) without affecting its maximum strength and/or its workability. In general, the results were SP-type dependent.

Conclusions. It is concluded that SPs: a) improved cement particles both dispersion and hydration during setting; b) did not affect the nature of the crystalline phases responsible for the setting and hardening; c) can be used to improve the final cement mechanical properties after hardening; and d) can be used to improve the initial injectability and workability of the cement.

Key Points.

- Superplasticizers affected the properties of apatitic calcium phosphate bone cements in a similar way as in civil engineering cements.
- Biocompatible superplasticizers will improve the development of better injectable and resistant CPBCs for *vertebroplasty* and *kyphophasty* minimally invasive spinal surgery applications.

2.1. Introduction

It is generally accepted that calcium phosphate bone cements need further improvements to broad their potential clinical applications [1]. However, further improvements on material properties should keep in mind the way surgeons apply bone cements through *Minimally Invasive Surgery Techniques* (MIST) [2]. For this reason, certain novel approaches reported to increase the strength of bone cements [1], by improving the particle packing of the powder reactants in the cement paste with a pressurising technique [3], do not apply to MIST applications such as *vertebro-* and/or *kypho-plasties* [4]. In this sense, further material improvements should be obtained at the compromise between what is considered, for a certain clinical application, the optimum cement injectability, fast-setting behaviour, macroporosity and mechanical strength (see Chapter 1).

Following the above approach, the first condition that bone cements should fulfil in spinal surgery applications is injectability. Although, compressive strength values of 180 MPa have been obtained by a compaction pressure technique [3], this method does not assure at the same time injectable and high-strength bone cements. The rheological behaviour of the cement pastes is the key point. In this sense, some studies have been focussed on how to improve the injectability of apatitic bone cements by the addition of citric acid and how these modifications affect the whole cement's setting and hardening processes [6-8]. This is, in fact, an important aspect because cement's property modification is a multifactorial problem where different manufacturing factors affect properties in different and controversial ways (see Chapter 1).

Concerning the fast setting behaviour, it should be noted that cement should set fast after implantation but not before. This has let to consider that temperature could be used as a setting control factor. In this sense, cement processing and handling should be performed, in a proper mixing device, at low temperatures (5-10°C) to delay the setting

reactions, while after implantation these will proceed faster at 37°C [7]. In fact, this approach has let to reconsider, for MIST applications, the clinical utility of the initial (IST) and the final (FST) setting times reported by the cement's manufacturer. For this reason, recent studies [9,10] have been trying to monitor *in situ*, from the beginning of the powder and the liquid mixing, the setting of cement-like materials and do not rely, for MIST applications, in the setting times measured by the *Gillmore* needles standard [11] (see also Chapters 9 and 10).

On the other hand, macroporosity is the property on which the most active research has been performed [12-17] (see also Chapter 3). This is because most commercial cements are apatitic, i.e. the end setting product is hydroxyapatite (HA; $Ca_{10}(PO_4)_6(OH)_2$) and/or calcium deficient hydroxyapatite (CDHA; $Ca_9HPO_4(PO_4)_5OH$), which indeed has very low resorbability *in vivo* [18,19]. For this reason, a recent study was focussed on the effect of surfactants on cement's macroporosity [13]. This approach showed advantages, from the rheological point of view, over other studies using oxygen peroxide [12], ice [15], sugar [16] and/or mannitol [17] crystals as porogenic agents inside the powder phase of the cement.

However, as the strength decreases exponentially with the porosity a compromise is needed between these two properties, otherwise the clinical applications are limited. For this reason, some authors have tried to improve the strength by reinforcing the porous apatitic matrix with aramide fibres [20]. Others have applied pressure to a mixture of cement powder and ice crystals, added to induce porosity, up to form solid compacts with setting property [15]. In fact, these authors formed porous compacts with denser cement matrix (higher strength) as compared to that of slurry systems. Unfortunately, this procedure, which results in gain strength of the cement, can not be applied for MIST applications where the main problem is still to assure cement's injectability. However, the

idea of having a more dense cement matrix is valid and should be used to find new approaches to improve the strength of the cement; this is the subject of this chapter.

In this study, it is reported on novel method (in this research field) to improve rheological or mechanical properties of calcium phosphate bone cements. The method, which is not unknown in Civil Engeneering, consists in the modification of the liquid cement phase with the addition of superplasticizer (SP). The advantage of the method relay on the fact that if cement liquid-to-powder (L/P) ratio is maintained constant then the fluidity of the cement is improved. Consequently, low L/P ratios can be used for the same workability property and as porosity decreases the strength of the cement increases, accordingly. This study addressed all these issues.

2.2. Materials and methods

2.2.1. Cement preparation

Biocement-H© was used as control [21]. It is a trademark bone cement (by *Merck GmbH*) made of 98 *wt%* alpha-tricalcium phosphate (α-TCP) and 2 *wt%* precipitated hydroxyapatite (PHA; *Merck-2143*) seeds setting accelerator. The liquid phase was an aqueous solution of 2.5 *wt%* disodium hydrogen phosphate (Na_2HPO_4; DHP; *Merck-6586*). The starting L/P ratio was 0.32 mL/g that assured suitable workability and cohesive property [21]. The control behaved as expected according to the setting and hardening data in the literature [22]. It was selected because it is ≈100 *wt%* α-TCP and so, the results of the present study should be also of interest to other α-TCP based bone cements [2].

The liquid phase of the control was modified (0.5, 5 and/or 50 *vol%*) with four commercial civil engineered SPs (by *Sika, Spain*): *Sikament-300®* (*S300*; synthetic modified melamine), *Sikament-500®* (*S500*; vinilic modified copolymer), *Sikament-500-HE®* (*S500-HE*; vinilic modified copolymer with organic-mineral agents) and *Sika-ViscoCrete-5-700®*

(*V5-700*; modified polycarboxilate); they were used as received (technical specifications can be found elsewhere [23]).

2.2.2. Cement hardening

Cement cylinders with aspect ratio of 2:1 (6 mm diameter x 12 mm length) were fabricated with L/P ratios from 0.256 to 0.320 mL/g. The specimens were removed from the moulds after 15 min and stored in Ringer's solution at 37°C for 5 days prior to testing. Compressive strength (CS; $n \geq 8$) was measured at a crosshead speed of 1 mm/min using universal testing machine Bionix-858 (*MTS, Eden Prairie, MN, USA)* with 100 kN load cell.

2.2.3. Chemical characterisation

After CS-testing, the broken samples were quenched immediately in acetone, to stop further setting, dried and powdered for X-Ray Diffraction (XRD; *Siemens-D500, Germany*). XRD data were collected from 2θ=4-70° with step size of 0.05° and count time of 3 s/step. The phase composition was checked by means of JCPDS (Joint Committee on Powder Diffraction Standards) reference patterns (9-348 for α-TCP, 9-169 for β-TCP and 9-432 for CDHA). The extent of conversion R(%) of α-TCP into CDHA (degree of reaction *vs.* hardening time), after 5 days of setting, was calculated as described in previous paper [25] (see also Chapter 1), on the basis of the average XRD intensity of the CDHA's peaks <hkl>= <002;300;211;112> of the modified cements as compared to the control.

2.2.4. Microstructural characterisation

The cement microstructure was analysed by Scanning Electron Microscopy (SEM; *JEOL JSM-6400*) after 5 days of cement's setting. Several CS-samples were broken

diametrically. Samples were quenched in acetone before fracture to stop further setting. The fracture surfaces were gold-covered previous to SEM observation.

2.3. Results

2.3.1. Compressive strength

Fig. 2.1 shows the evolution of the CS attained after 5 days of setting for the three studied experimental series S1 (i.e. L/P=0.32 mL/g; SP=0.5 *vol%*), S2 (i.e. L/P=0.32 mL/g; SP=5 *vol%*) and S3 (i.e. L/P=0.256 mL/g; SP=50 *vol%*), and as compared to the control (i.e. *Biocement-H*© without SP). The results showed, in general, similar trends for all the series. Series S1 shows, as an example, that the CS of the control (35 ±7 MPa) increased significantly ($p<0.05$) with *V5-700* (46 ±4 MPa), *S500* (57 ±8 MPa) and *S500-HE* (60 ±3 MPa) but not ($p>0.05$) with the *S300* additive (37 ±7 MPa). In this sense, the results were SP-type dependent (different chemical affinity). For example, 0.5 *vol%* of *S500-HE* addition let in series S1 to 71% CS improvement (as compare to the control), while 0.5 *vol%* of *V5-700* only resulted in 31% CS increase.

Fig. 2.1 also shows that the *S500-HE* additive (i.e. vinilic modified copolymer with organic-mineral agents) allowed suitable combinations of both the L/P ratio and the amount of SP, while maintaining optimum cement workability (as compare to the control). This was not the general tendency observed for the other SPs for who the CS diminished slightly/gradually (*V5-700*/*S500*) or drastically (*S300*) as the L/P ratio decreased. These general trends were confirmed by statistic analysis (Dunnett's multiple comparison tests).

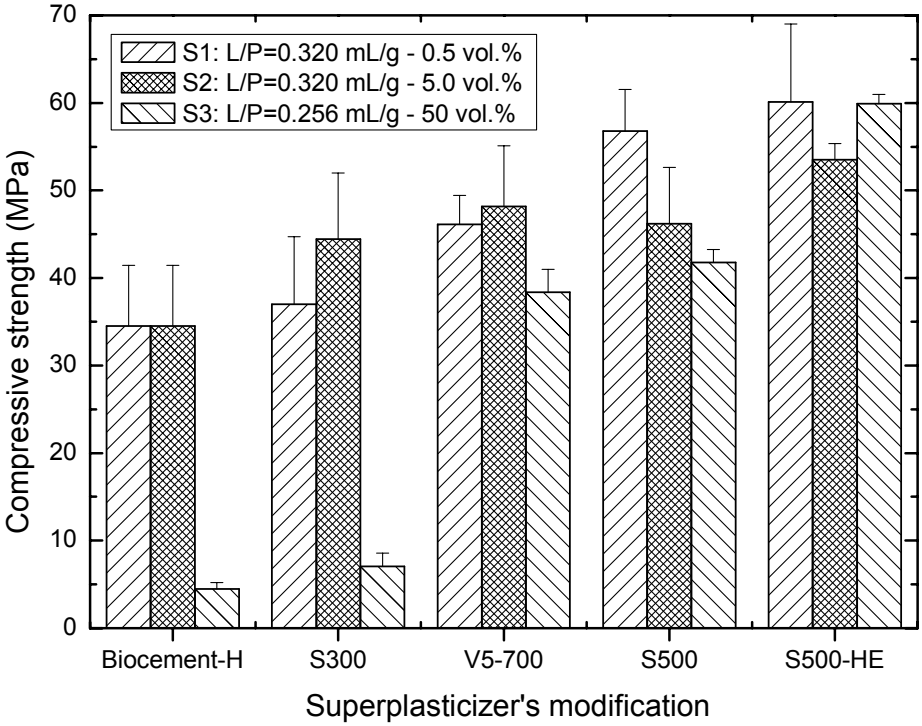

Figure 2.1. Compressive strength (after 5 days of setting) vs. Superplasticizer's modification, as a function of the L/P ratio and the amount of the additive. (*Note: Despite the same patterns as the other groups, note that Biocement-H© contains no superplasticizers)

2.3.2. X-ray diffraction

Figs. 2.2-2.5 show the crystalline phases which are present after 5 days of setting for samples *S300*, *V5-700*, *S500* and *S500-HE*, respectively, at the different *vol%* additions and compared to the control before (*Biocement-H(0D)*) and after setting (*Biocement-H(5D)*). These figures also show the extent of conversion, R(%), of the α-TCP into CDHA as compared to full conversion of α-TCP, in sample *Biocement-H(0D)* (i.e., control before setting), into CDHA crystals, in sample *Biocement-H(5D)* (i.e. control after 5 days of setting).

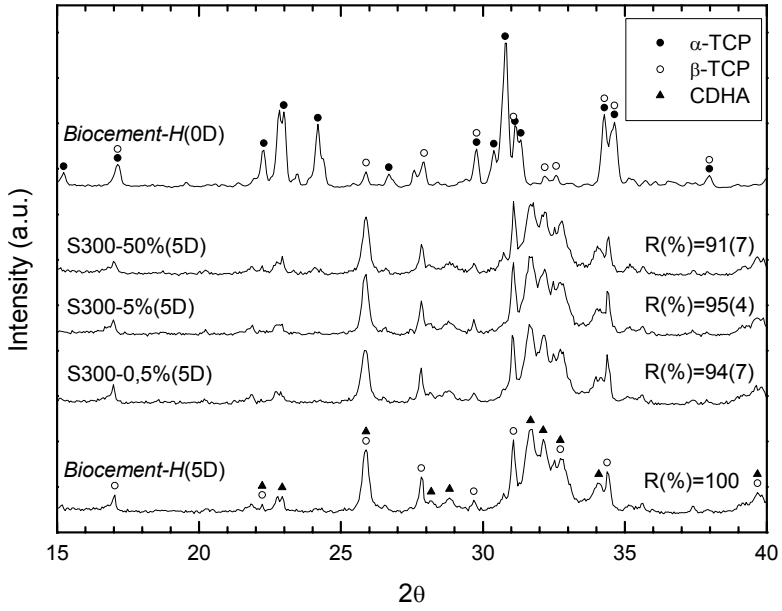

Figure 2.2. XRD patterns of *Biocement-H©*'s modification, before and after setting, with *Sikament-300®* SP (L/P and *vol%* as in Fig. 2.1).

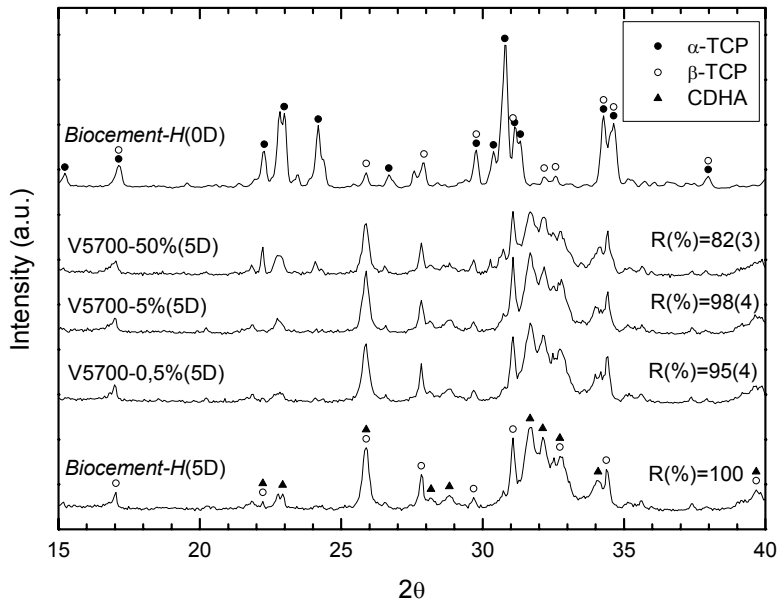

Figure 2.3. XRD patterns of *Biocement-H©*'s modification, before and after setting, with *ViscoCrete-5-700®* SP (L/P and *vol%* as in Fig. 2.1).

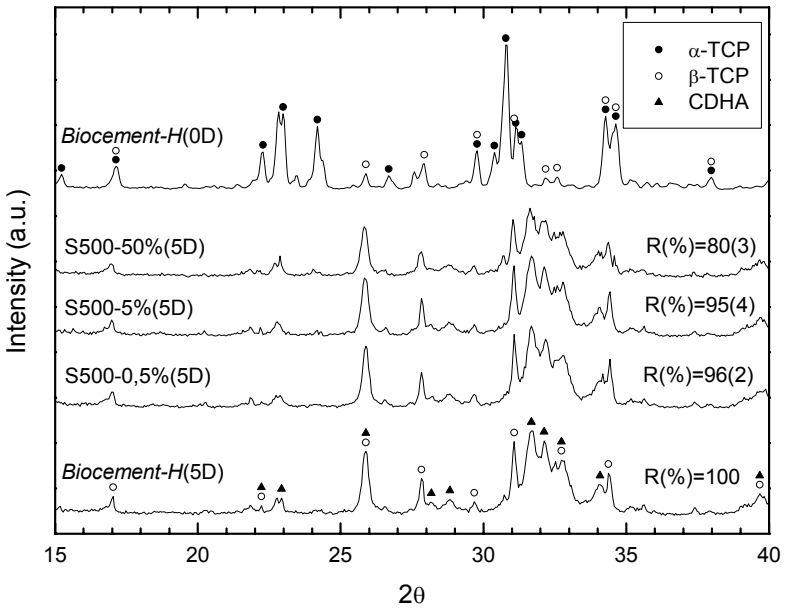

Figure 2.4. XRD patterns of *Biocement-H*©'s modification, before and after setting, with *Sikament-500*® SP (L/P and *vol%* as in Fig. 2.1).

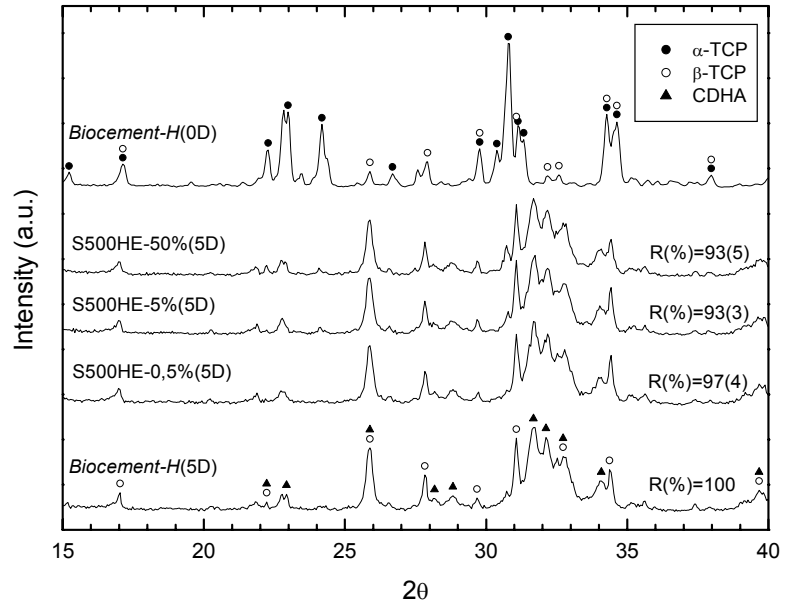

Figure 2.5. XRD patterns of *Biocement-H*©'s modification, before and after setting, with *Sikament-500-HE*® SP (L/P and *vol%* as in Fig. 2.1).

On the other hand, all samples in Figs. 2.2-2.5 contained after setting ≈15 *wt%* of β-TCP. This β-TCP is formed during the quenching process of the α-TCP high-temperature production and does not react during the whole setting process [24,25]. In general, only samples *V5-700* (see Fig. 2.3) and *S500* (see Fig. 2.4) did show a significant retard of the setting reaction when the additive was increased from 5 to 50 *vol%*, i.e. from R(%)=98(±4) to R(%)=82(±3) for sample *V5-700* and from R(%)=95(±4) to R(%)=80(±3) for sample *S500*, respectively. Moreover, none of the additives did affect the setting with second phases or compounds; only CDHA crystals were precipitated.

2.3.3. Scanning electron microscopy

Figs. 2.6 and 2.7 show different characteristics of the microstructure evolved during the setting of modified cements. Fig. 2.6 shows (x6000; from top to bottom: *S300*, *V5-700*, *S500* and *S500-HE*) different pictures of the specific microstructures developed after 5 days of setting for the series S1 (left hand) and S2 (right hand). Fig. 2.7 shows a low (x100; left hand) and a high (x6000; right hand) magnification of the microstructure observed for each additive (same order as in Fig. 2.6 from top to bottom) for cements of series S3 (i.e. L/P=0.256 mL/g and 50 *vol%* addition). The right-hand photos of Fig. 2.7 show, in general, the presence of minor amounts (see arrows) of unreacted α-TCP particles (also present in Fig. 2.6), in agreement to XRD analysis (see Figs. 2.2 to 2.5). The left-hand photos of Fig. 2.7 show that additives have an intrinsic hydrophilic/hydrophobic behaviour acting, in a certain degree, as air-entraining agents (see the presence of air-bubbles) [13] and probably having, jointly with the specific microstructure developed in each cement, a direct effect on the mechanical properties (see Fig. 2.1). Despite some differences can be highlighted between Figs. 2.6 and 2.7 it is not possible, at this stage, to argue any direct correlation between these microstructures and the mechanical properties observed in Fig. 2.1.

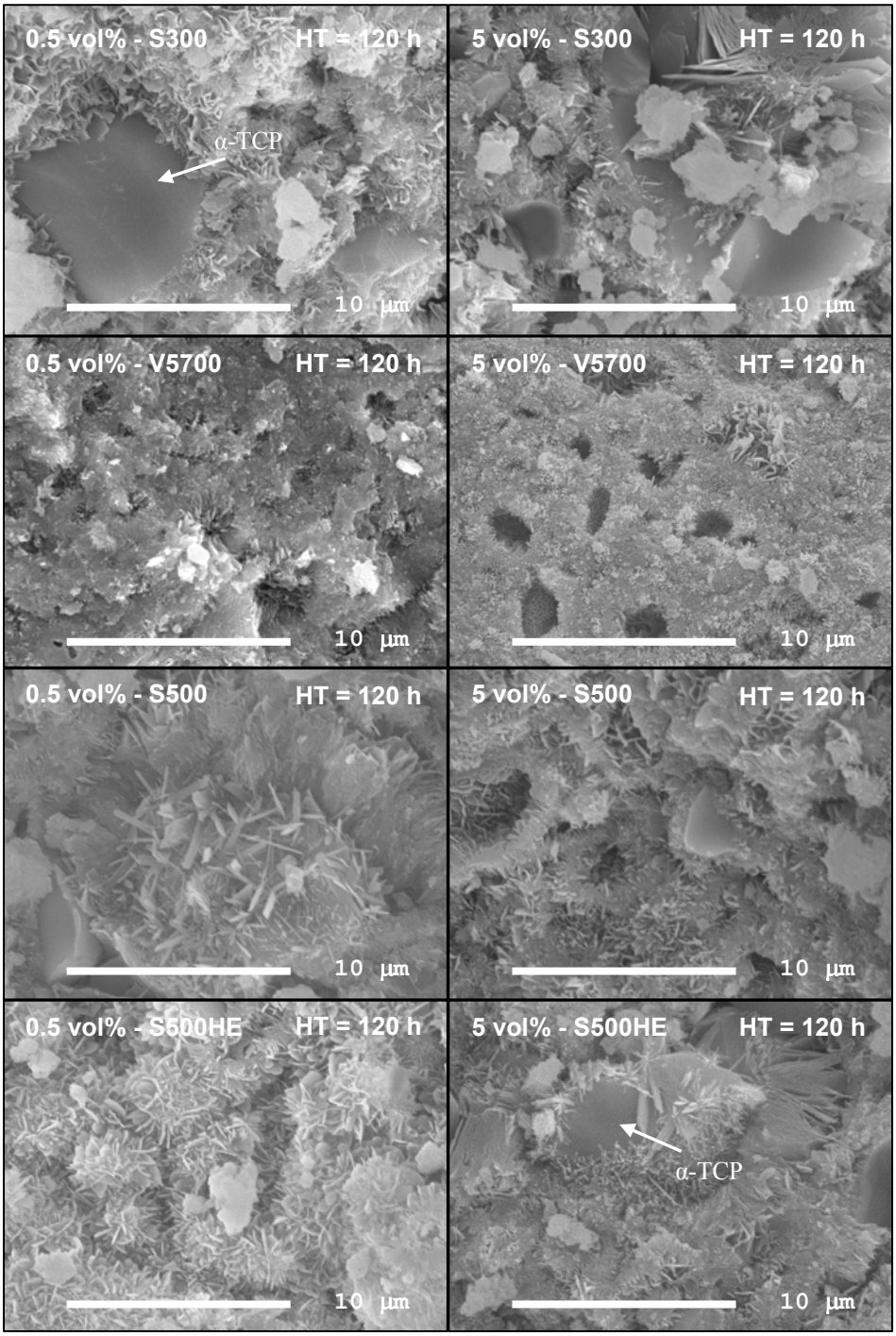

Figure 2.6. SEM microstructures, after 5 days of setting, for the 0.5 *vol.%* (left) and 5 *vol.%* (right) superplasticizers' addition (L/P=0.320 mL/g).

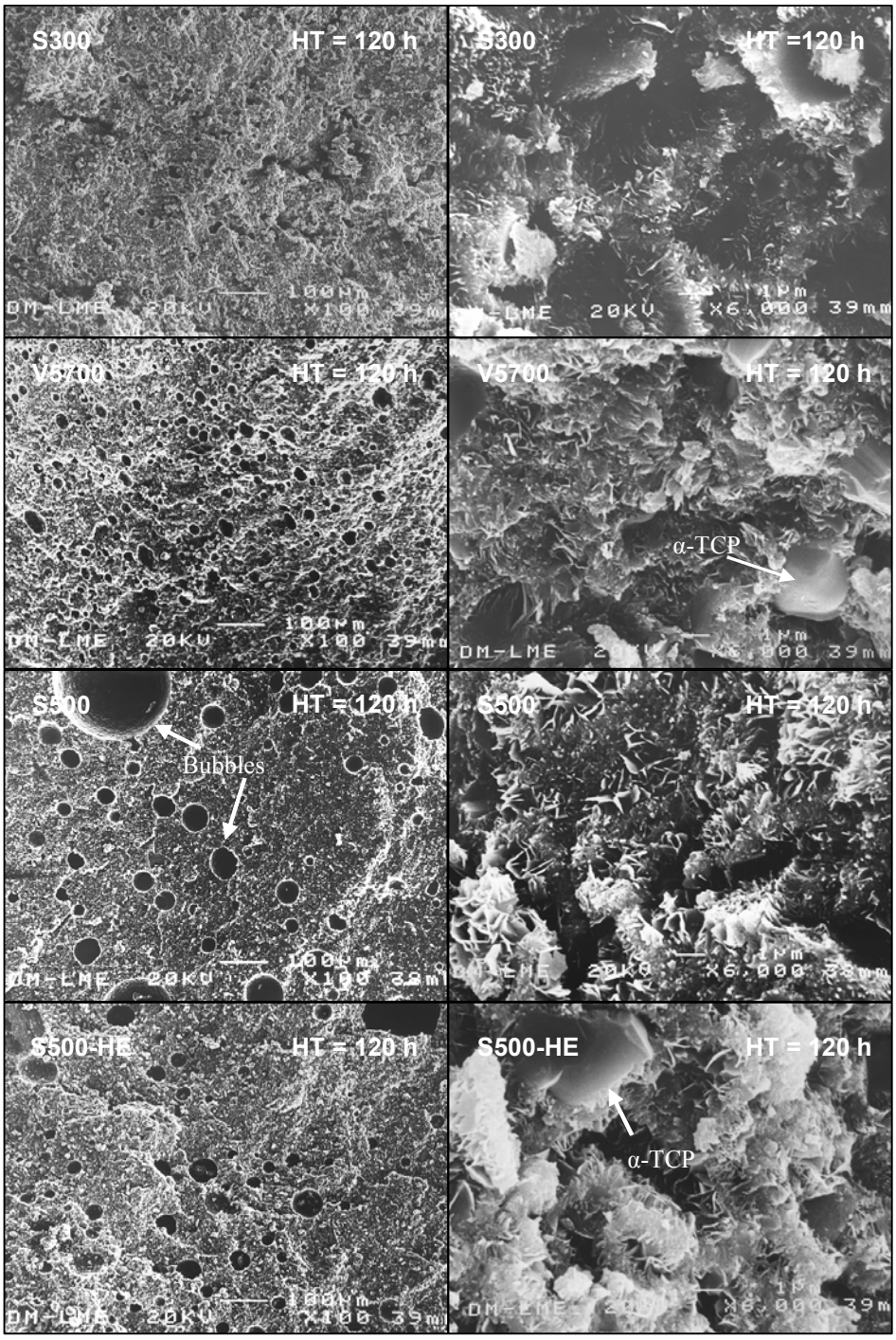

Figure 2.7. SEM microstructures, after 5 days of setting, for the 50 vol.% superplasticizers' addition (left: x100; right: x6000; L/P=0.256 mL/g).

On the other hand, all modified cements displayed well-known entangled structures of apatitic crystals (whatever the SP's concentration used) similar as those observed during the setting of α-TCP based cements [6,22,24,25] and as those obtained for the control at its main setting step processes (see Fig. 2.8; top-left hand=dissolution; top-right hand=nucleation; bottom-left hand=surface control precipitation; bottom-right hand=shell diffusion control precipitation).

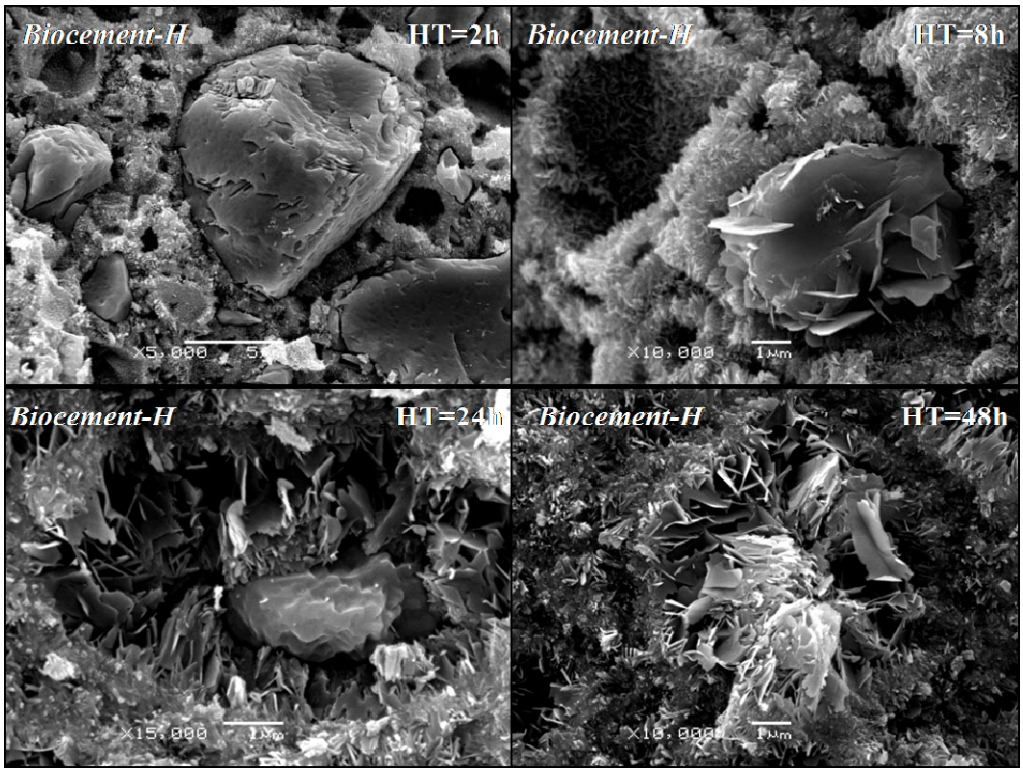

Figure 2.8. SEM microstructures showing different stages of *Biocement-H*®'s setting and hardening processes (left-top: dissolution of α-TCP particles after 2h of setting; right-top: nucleation and growth of apatite crystals after 8h; left-bottom: further surface-control growth after 24h; right-bottom: further diffusion-control growth after 48h).

2.4. Discussion

The main objective of using water-reducing admixtures and/or superplasticizers during the manufacture of calcium phosphate bone cements is to decrease the L/P ratio (while retaining the desired workability) and consequently to increase the mechanical properties (alternatively, to improve workability at a fixed L/P ratio).

In this study we have used different commercial SPs, which are classified as high range water reducers in the concrete industry, to test that the mechanical properties of apatitic bone cements can be also improved in a similar way. This study showed that minor amounts of all of the additives improved cement hydration efficiency (and so, workability) of *Biocement-H©* at its standard L/P ratio (L/P=0.32 mL/g), so increasing its maximum compressive strength at saturation (see Fig. 2.1). On the other hand, at constant L/P ratio, the observed improvement of cement's workability was followed by longer cement setting times. For this reason, the setting times need to be controlled (if needed) by lowering the L/P ratio [27]. In this study, the L/P ratio was reduced up to L/P=0.256 mL/g (20 *vol.%* water reduction) without losing mechanical properties. In fact, it is expected that in the future (for certain applications) this 20 *vol.%* of water reduction will be further approached to the maximum theoretical reduction allowed (≈94 *vol.%*) for the stoichiometrically transformation of α-TCP into CDHA. In this sense, an improvement of the hydration efficiency of the α-TCP particles is needed.

As it is known, particles tend to agglomerate due to *Van der Waals* forces and the presence of electric charges onto their surfaces which also entrap some water into the clusters and avoids complete surface particle hydration. The main action of the SPs molecules is to wrap themselves around the cement particles as to give them a highly negative charge so that they repel each other. This results in deflocculation and dispersion of the cement particles, so exposing a greater surface area for cement

hydration, which will progress at a higher rate in the early stages, resulting in an increase of its mechanical strength. Although water-reducing admixtures affect the rate of hydration of cement and its micro-architecture (see Figs. 2.6 and 2.7), the nature of the products of hydration is unchanged (see Figs. 2.2-2.5). Moreover, SPs do not significantly affect the surface tension of water and so, they do not entrain large amounts of air (see Fig. 2.7, left-hand) and can therefore be used at high concentration [26].

The present study shows that some SPs used for the concrete industry act as high-range water reducing agents for apatitic bone cements; at a given L/P ratio and at low level of addition (0.5 *vol.%*), their dispersion action increased cement's workability and strength (see Fig. 2.1). It is relevant to comment on the 71% strength's increment that was observed when the control (C=35 ± 7 MPa; L/P=0.32 mL/g) was modified with 0.5 *vol.%* S500-HE (C=60 ± 3 MPa; L/P=0.32 mL/g). There is no reason to support any considerable variation of the density of the modified materials as compared to the control at those low liquid-phase modifications. In fact, the experimental density of these cements was the same (1.74 ± 0.05 g/cm3) and so the expected porosity. This means that the observed differences are intrinsic to the materials and so to their developed microstructure due to SPs. It is also relevant to note (see Fig. 2.1) that sample S500-HE showed the same compressive strength at L/P=0.32 mL/g (0.5 *vol.%*) and at L/P=0.256 mL/g (50 *vol.%*). If we look at Fig. 2.7, it is observed that sample S500-HE showed entrained air-bubbles at L/P=0.256 mL/g. These bubbles should be acting as pores and so it should be expected a decrease in the compressive strength. However, this did not happen and again the recovery of the strength should be explained by the general decrease of the porosity as due to the lower L/P ratio used. These both effects support the idea that S500-HE superplasticizer has an intrinsic effect on the micro- and/or nano- crystal structure. Thus, a comprehensive and congruent explanation of the compressive strength's increase can not be found with the present data and for that a complete kinetic analysis, as those done

in the literature [6,22,24,25], should be performed. In this sense, it is important to consider that *Biocement-H©* sets due to the hydration reaction of α-TCP into CDHA ($3\ \alpha\text{-}Ca_3(PO_4)_2 + H_2O \rightarrow Ca_9(HPO_4)(PO_4)_5OH$) following a series of reaction steps (see Fig. 2.8): (a) the dissolution reaction of the α-TCP particles; (b) the nucleation of apatite crystals onto their surfaces; (c) a linear growth of apatite crystals (surface control process); and (d) a potential growth of apatite crystals (diffusion control process). After all these reaction processes an entangled network of apatite crystals, responsible for the mechanical properties, results. However, when setting reaction is complete the extent of conversion of α-TCP into CDHA should not be changed in agreement with data (see values for R(%) in Figs. 2.2-2.5). For these reasons, what can be anticipated and concluded from data are the different time effects on the setting step processes due to the nature and molecular mass of the organic additives. In this sense, the results showed (see Fig. 2.1) that vinylic modified copolymers (S500 and S500-HE) displayed better water reducing action than synthetic modified melamine (S300) and modified policarboxilate (V5-700).

2.5. Summary conclusion

This study shows that mechanical properties of apatitic calcium phosphate bone cements can be further improved through the modification of its liquid phase with minor amounts of superplasticizers. In this study, the main effect of the commercial additives resulted in better dispersion and hydration of the cement particles. The setting and hardening processes of *Biocement-H©* were plasticizer-type dependent. In particular, 0.5 *vol.%* of the additive *Sikament-500-HE®* (vinylic modified copolymer) allowed for 20% water reduction and 71% compressive strength increase. Thus, it is expected that if suitable biocompatible superplasticizers can be developed then new high-strength calcium phosphate bone cements will be developed while still being injectable and useful for MIST applications.

References

1. Troczynski T. Bioceramics: A concrete solution. Nature Materials 2004;3:13-14.

2. Bohner M. Physical and chemical aspects of calcium phosphates used in spinal surgery. Eur Spine J 2001;10:S114-21.

3. Barralet JE, Hoffman M, Grover LM, Gbureck U. High-strength apatitic cement by modification with α-hydroxy acid salts. Adv Mater 2003;15;24:2091-94.

4. Watts NB, Harris ST, Genant HK. Treatment of painful osteoporotic vertebral fractures with percutaneous vertebroplasty or kyphoplasty. Osteoporosis International 2001;12:429-37.

5. Mathis JM, Barr JD, Belkoff SM, Barr MS, Jensen ME, Deramond H. Percutaneous vertebroplasty: A developing standard of care for vertebral compression fractures. American Journal of Neuroradiology 2001;22:373-81.

6. Sarda S, Fernández E, Nilsson M, Planell JA. Kinetic study of citric acid influence on calcium phosphate bone cements as water-reducing agent. J Biomed Mat Res 2002;61;4:653-59.

7. Sarda S, Fernández E, Llorens J, Martínez S, Nilsson M, Planell JA. Rheological properties of an apatitic bone cement during initial setting. J Mater Sci: Mater Med 2001;12:905-9.

8. Friberg J, Fernández E, Sarda S, Nilsson M, Ginebra MP, Martínez S, Planell JA. An experimental approach to the study of the rheology behaviour of synthetic bone calcium phosphate cements. Key Eng Mat 2000;192-5:777-80.

9. Carlson J, Nilsson M, Fernández E, Planell JA. An ultrasonic pulse-echo technique for monitoring the setting of $CaSO_4$-based bone cement. Biomaterials 2003;24:71-77.

10. Nilsson M, Carlson J, Fernández E, Planell JA. Monitoring the setting of calcium-based bone cements using pulse-echo ultrasound. J Mater Sci: Mater Med 2002;13:1135-41.

11. Standard Test Method for Time of Setting of Hydraulic Cement Paste by the Gillmore Needles, ASTM C266-89, Annual Book of ASTM Standards, Vol. 04.01: Cement, Lime, Gypsum. Philadelphia, 1993:189-91.

12. Almirall A, Larrecq G, Delgado JA, Martínez S, Planell JA, Ginebra MP. Fabrication of low temperature macroporous hydroxyapatite scaffolds by foaming and hydrolysis of an α-TCP paste. Biomaterials 2004;25:3671-80.

13. Sarda S, Fernández E, Nilsson M, Planell JA. Influence of surfactant molecules as air-entraining agent on bone cement macroporosity. J Biomed Mater Res 2003;65A:215-21.

14. Del Real RP, Wolke JGC, Vallet-Regí M, Jansen JA. A new method to produce macropores in calcium phosphate cements. Biomaterials 2002;23:3673-80.

15. Barralet JE, Grover L, Gaunt T, Wright AJ, Gibson IR. Preparation of macroporous calcium phosphate cement tissue engineering scaffold. Biomaterials 2002;23:3063-72.

16. Takagi S, Chow LC. Formation of macropores in calcium phosphate cement implants. J Mater Sci: Mater Med 2001;12(2):135-9.

17. Markovic M, Takagi S, Chow LC. Formation of macropores in calcium phosphate cements through the use of mannitol crystals. Key Eng Mat 2000;192-1:773-6.

18. Hankermeyer CR, Ohashi KL, Delaney DC, Ross J, Constantz BR. Dissolution rates of carbonated hydroxyapatite in hydrochloric acid. Biomaterials 2002;23:743-50.

19. Fulmer MT, Ison IC, Hankermayer CR, Constantz BR, Ross J. Measurements of the solubilities and dissolution rates of several hydroxyapatites. Biomaterials 2002;23:751-55.

20. Xu HHK, Quinn JB, Takagi S, Chow LC, Eichmiller FC. Strong and macroporous calcium phosphate cement: effects of porosity and fiber reinforcement on mechanical properties. J Biomed Mater Res 2001;57;3:457-66.

21. Khairoun I, Driessens FCM, Boltong MG, Planell JA, Wenz R. Addition of cohesion promotors to calcium phosphate cements. Biomaterials 1999;20:393-8.

22. Ginebra MP, Driessens FCM, Planell JA. Effect of the particle size on the micro and nanostructural features of a calcium phosphate cement: a kinetic analysis. Biomaterials 2004;25:3453-62.

23. Safety Data Sheet. Available at: <http://www.sika.es> or <http://www.sika.co.uk>.

24. Fernández E, Ginebra MP, Boltong MG, Driessens FCM, Ginebra J, De Maeyer EAP, Verbeeck RMH, Planell JA. Kinetic study of the setting reaction of a calcium phosphate bone cement. J Biomed Mater Res 1996;32:367-74.

25. Ginebra MP, Fernández E, Driessens FCM, Planell JA. Modeling of the hydrolysis of α-tricalcium phosphate. J Am Ceram Soc 1999;82(10):2808-12.

26. Neville AM. In: Properties of concrete. 4th Edition. Harlow, Essex, Longman. 1995;252-55.

Chapter 3

Effect of calcium sulphate on the setting properties of alpha-tricalcium phosphate bone cements

3.0. Structured abstract

Mini Abstract. In this study, a new method to modulate the porosity (and so the strength) of α-tricalcium phosphate (α-TCP) bone cements has been investigated. This method consists in the modification of the cement's powder phase with calcium sulphate dihydrate (CSD). The resulting mechanical properties of the new biphasic cements are a combination between the progressive hardening due to the main α-TCP reactant and the passive *in vitro* dissolution of the CSD phase, which render a porous material.
Study Design. Experimental study to characterise the setting and hardening properties of biphasic α-TCP-CSD bone cements.
Objective. To investigate the setting and hardening properties of biphasic α-TCP-CSD bone cements.
Summary of Background Data. Calcium phosphate bone cements are injectable biomaterials that are being used in dental and orthopaedic applications through minimally invasive surgery techniques. Nowadays, apatitic bone cements based on α-TCP are of special interest due to their self-setting behaviour when mixed with an aqueous liquid phase. Apatitic cements have shown excellent biocompatibility and adequate mechanical properties but have slow resorption in the human body. To assure new bone aposition and faster *in vivo* cement resorption it is necessary then to improve cement porosity. In this study, a new method to improve the porosity (and so the *in vivo* osteointegration) of α-TCP based cements is presented.
Methods. *Biocement-H©*, an α-TCP based cement, was used as control. The powder phase was modified with CSD and the resulting biphasic CSD-α-TCP cements were prepared according to literature. The evolution of the compressive strength accounted for the cement hardening process. Scanning Electron Microscopy followed the evolution of the

cement microstructure during hardening. X-ray diffraction analysis confirmed the evolution of the crystalline phases controlling the setting and the hardening processes.

Results. It was observed that the maximum compressive strength attained for *Biocement-H*© (45 MPa) decreased with CSD addition (≈30 MPa for 25 *wt.%* of CSD). Moreover, SEM and XRD analysis showed that CSD particles dissolved passively with time while the main α-TCP reactant transformed into an entangled matrix of apatite-like crystals. The plain effect was a porous apatitic structure still suitable for cancellous bone applications (strength ≈10 MPa).

Conclusions. It has been shown that CSD-α-TCP biphasic bone cements evolved with time into a porous entangled matrix of calcium-deficient apatite crystals within the strength optimum limits of trabecular bone applications.

Key Points.

- The addition of CSD into the powder phase of alpha-tricalcium phosphate based bone cement significantly enhanced the porosity of the resulting apatitic matrix.
- The additive did not modify the setting reactions and the evolved apatitic microstructure produced cements with compressive strength within the limits of cancellous bone applications.
- The new CSD-α-TCP biphasic cements can be further improved to adjust the rate of porosity creation (as due to the passive dissolution of CSD particles) with the rate of new bone apposition after implantation *in vivo*.

3.1. Introduction

It is generally accepted that calcium phosphate bone cements need further improvements to broad their potential clinical applications [1]. In fact, recent publications highlight the efforts made to improve the injectability [2], of use in spinal surgery applications [3,4], and/or the strength of these materials [5-8]. Unfortunately, these improvements are not enough for apatitic (i.e. the end setting product being hydroxyapatite ($Ca_{10}(PO_4)_6(OH)_2$; HA) and/or calcium deficient hydroxyapatite ($Ca_9HPO_4(PO_4)_5OH$; CDHA) bone cements, which are so stable *in vivo* that bone cement's resorption takes a long time, i.e. 1-2 years [9,10]. In order to accelerate bone tissue colonisation and resorption of the cement implant, several authors have improved macroporosity, i.e. more and larger pores, of apatitic bone cements in several ways [11-17].

Sarda et al. [12] achieved a good compromise between suitable mechanical strength (porosity) and injectability by using surfactants in the cement's liquid phase as compare to other studies using oxygen peroxide [11] in the liquid phase and/or ice [14], sugar [15] and/or mannitol [16] crystals, as porogenic agents, in the cement's powder phase, and/or oil liquid-phase emulsions [17].

Barralet et al. [14], have applied pressure to mixtures of cement powder and ice crystals to form compacts with setting properties. Xu et al. [18], have tried to improve the strength by reinforcing the porous apatitic cement matrix with aramide fibres. However, none of these approaches are useful for minimally invasive surgery applications where the main problem is still to assure cement's injectability [2].

In this study, we propose a new method to modulate the porosity (and so the strength) of an α-tricalcium phosphate (α-TCP; α-$Ca_3(PO_4)_2$) bone cement during hardening in a Ringer's solution. For that purpose, calcium sulphate dihydrate (CSD; $CaSO_4.2H_2O$) particles are added into the cement paste. This method is related to that

proposed by Fernández et al. [19] (later on by Lidgren et al. [20]), where α-TCP and calcium sulphate hemihydrate (CSH; $CaSO_4.½H_2O$) were mixed together to form a biphasic cement that sets due to the hydration reactions of both main reactants, i.e. α-TCP into CDHA and CSH into CSD. Unfortunately, CSH crystals, which stayed partially unreacted within the cement matrix, increased the setting times and reduced as well the strength of the cement [21,22]. Recently, Bohner et al. [23] showed interesting effects with various CSD amounts added to the liquid phase, such as better setting time control (faster setting times with more CSD) but more α-TCP left after 24 h of reaction, suggesting a complex effect of sulphate ions on the setting reaction. The present study adds more data for the whole comprehension of the setting of α-TCP and CSD cement mixtures.

3.2. Materials and methods

3.2.1. Cement preparation

Biocement-H© (by *Merck GmbH*; inlab preparation) [24], served as a basis for all experiments. The plain cement was used as control, whereas the experimental groups had variable amounts of CSD as addition. *Biocement-H©* is made of 98 *wt.%* α-TCP (minor contents of β-TCP) and 2 *wt.%* precipitated hydroxyapatite (PHA; *Merck-2143*), added as a seed in the powder phase. Its liquid phase is an aqueous solution of 2.5 *wt.%* disodium hydrogen phosphate Na_2HPO_4 (DHP; *Panreac-131679*). The liquid to powder (L/P) ratio was 0.32 mL/g, which is its minimum L/P ratio to assure suitable mouldability and cohesive property [24]. This control cement presented the same setting properties as published in the literature [24,25], i.e. around 8 and 20 minutes for the *Gillmore* initial and final setting times, respectively. *Biocement-H©* was selected because it is ≈100 *wt.%* α-TCP (up to 15 *wt.%* of β-TCP). Thus, its modification with CSD should be of interest to other commercial α-TCP cements [25].

In this study, the powder phase of *Biocement-H©* was modified (α-TCP, by *Mathys Medical, Switzerland*) with 5, 10, 20 and 25 *wt.%* CSD (*Sigma-C3771*). Samples were coded as BioCSD-5, BioCSD-10, BioCSD-20 and BioCSD-25, respectively. In addition, the liquid phase of all BioCSD samples was reduced from 2.5 *wt.%* to 2.0 *wt.%* of DHP. This adjustment was necessary to keep the mouldability of BioCSD samples as similar to that of the control. In a previous study, Bohner [23] showed that CSD and DHP interact in the liquid phase as to control the cement setting (and so the workability) of α-TCP and CSD mixtures. In particular, the addition of CSD powder to α-TCP-water cement mixtures strongly decreased their setting time, particularly when the phosphate concentration was high [23]. For the same reason, in this study, it is expected that the DHP reduction was also dependent on the CSD content and could be further optimised. All the cements were mixed by hand in a mortar with a spatula.

3.2.2. Cement hardening

Biocement-H© and BioCSD samples were made at an aspect ratio of 2:1 (10 mm length x 5 mm diameter). The specimens, immersed in 200 mL Ringer's solution at 37°C, were removed from the moulds after 30 min and stored again for 1, 2, 4, 8, 16 h and 1, 3, 5 and 14 days prior to testing. Moreover, BioCSD-20 and BioCSD-25 were kept in the Ringer's solution for 28 and 35 days (in the 35 days group, the solution was renewed every day). The compressive strength C(MPa) ($n \geq 8$) was measured at the hardening times (HT) specified above at a crosshead speed of 1 mm/min using a mechanical testing machine Bionix-858 (*MTS, Eden Prairie, MN, USA)* with a 100 kN load cell.

3.2.3. Microstructural characterisation

The evolution of the cement microstructure was analysed, at different hardening times, by Scanning Electron Microscopy (SEM; *JEOL JSM-6400*) on the surface of two cylinders

kept to this end and broken diametrically. These samples were quenched in acetone before fracture to stop the setting reaction. The fracture surfaces were gold-covered previous to SEM observation.

3.2.4. Chemical characterisation

Immediately after the compressive strength testing, the broken samples were quenched in acetone, to stop the setting, dried and ground for X-Ray Diffraction (XRD; *Siemens-D500, Germany*). XRD data were collected from 2θ=4-45° with a step size of 0.05° and a count time of 3 s/step. The phase composition was checked by means of JCPDS (Joint Committee on Powder Diffraction Standards) reference patterns (9-348 for α-TCP, 9-169 for β-TCP, 06-0046 for CSD and 9-432 for CDHA). The dissolution of the α-TCP and CSD phases as well as the precipitation of the new CDHA phase were recorded against time as described in a previous paper [26] following the evolution of the XRD intensity of several selected peaks (for α-TCP, <hkl> = <201;161;261;034>; for β-TCP, <hkl> = <217;214>; for CSD, <hkl> = <020;12-1;14-1>; and for CDHA, <hkl> = <002;300;211;112>). Details about these peaks are summarised in Table 3.1.

3.3. Results and discussion

3.3.1. Mechanical strength

Fig. 3.1 shows the compressive strength, C, attained at different hardening times, HT, by samples BioCSD-10 (B-10), BioCSD-20 (B-20) and BioCSD-25 (B-25) as compared to the control (*Biocement-H©*; B-H). In Fig. 3.1, only the results obtained for HT<120 h were fitted (see Table 3.2) to an exponential function such as $C=C_1+C_2*\exp(-t/\tau_c)$. The points obtained at longer times belonged to other experimental series, and hence were not included. The

experiments at 14 days were programmed after the results of the first series to check if samples modified with CSD still fit well to the same exponential growth.

The hypothesis was to suppose that CSD did not affect the setting and hardening reactions of the apatitic cements and so their strength. This was at first not valid because passive dissolution of CSD occurring at the same time as the dissolution of the α-TCP phase should be acting negatively on the maximum compressive strength attainable at saturation. In fact, continuous dissolution of the CSD phase should not lead to a saturation but to a maximum strength at certain hardening time from which, the compressive strength should further decrease in agreement to the amount of porosity formed into the cement as a result of the dissolution of the CSD powder phase (i.e. 1 pore=1 dissolved CSD particle). However, to check the validity of the above hypothesis it was further necessary to test BioCSD-20 sample at 28 days in the same ageing conditions as the other data (ageing in a Ringer's solution at 37°C) and to test BioCSD-25 sample after 35 days of setting in modified ageing conditions (same as before but with the Ringer's solution renewed every day). All these data are also represented in Fig. 3.1.

From the analysis of Fig. 3.1, it is observed that compressive strength increased linearly during the setting period 1h<HT<10 h no matter the relative amount of CSD contained into the α-TCP control sample. However, the rate of strengthening (slope of linear fits for HT<10 h) decreased as the amount of CSD increased into the cement's samples. This shows that CSD delayed the hardening reactions in agreement to the study of Bohner [23]. Moreover, Fig. 3.1 also shows that maximum compressive strength decreased as CSD increased. This is an indication that passive dissolution of CSD particles contributes to the amount of porosity of the cement. However, the dissolution of CSD particles seems to be blocked after 10 h of setting because the maximum compressive strength attained at this time was maintained later on even after 28 days of setting. Only, when the liquid phase of BioCSD-25 sample was renewed every day it was

observed that effectively the compressive strength at saturation (≈30 MPa) continued to decrease until very low values (≈10 MPa). This result shows that further dissolution of CSD particles continues because the chemical equilibrium was broken when sulphate ions were washed away during Ringer's solution change every day. All these cause-effect relationships were further analysed by looking at the evolution of the cement microstructure as it is reported in the next section.

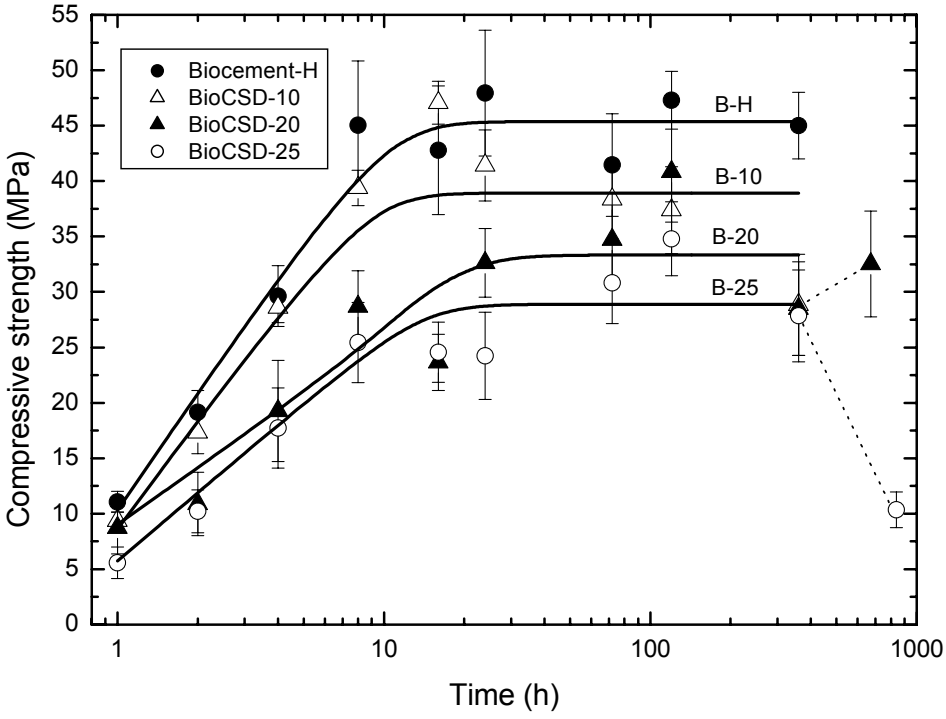

Figure 3.1. Evolution of the compressive strength against the hardening time for the control and the modified cements. (Note1: the fittings are only for HT<120h (see details in Table 3.2); Note2: the Ringer's solution of cement BioCSD25 for 35 days was renewed every day).

Table 3.1.
Summary of the main XRD intensity peaks used for calculations in Fig. 3.6

Characteristics of XRD peaks (Data from JCPDS cards)				**XRD analysis of BioCSD-25 (see Fig. 3.6) $R=R_1 + R_2*\exp(-t/\tau_r)$**		
Phase	**<hkl>**	**I/I_{100}**	**2θ**	**R_1**	**R_2**	**τ_r (days)**
α-TCP	201	24	22.20	0.10 ± 0.02	0.86 ± 0.04	4.3 ± 0.5
α-TCP	161,-331	33	24.10	0.07 ± 0.03	0.91 ± 0.07	2.7 ± 0.5
α-TCP	-361,261	17	29.64	0.07 ± 0.04	0.82 ± 0.07	5.1 ± 1.2
α-TCP	034,-434	100	30.74	0.11 ± 0.03	0.82 ± 0.07	3.2 ± 0.7
CDHA	002	40	25.80	0.91 ± 0.04	-0.81 ± 0.09	2.1 ± 0.5
CDHA	300	60	32.90	0.88 ± 0.04	-0.78 ± 0.09	1.4 ± 0.4
CDHA	211	100	31.76	0.90 ± 0.04	-0.76 ± 0.10	2.0 ± 0.6
CDHA	112	60	32.20	0.88 ± 0.03	-0.75 ± 0.09	1.3 ± 0.3
CSD	020	100	11.60	0.21 ± 0.02	0.80 ± 0.06	0.9 ± 0.2
CSD	12-1	50	20.70	0.42 ± 0.01	0.58 ± 0.04	0.6 ± 0.1
CSD	14-1	50	29.10	0.31 ± 0.01	0.69 ± 0.04	1.1 ± 0.1

Table 3.2.
Summary of the main calculations used in Figs. 3.1 and 3.7

Compressive strength *vs.* Hardening time (see Fig. 3.1) $C=C_1 + C_2*\exp(-t/\tau_c)$			
Sample	**C_1**	**C_2**	**τ_c (hours)**
B-H	45.4 ± 1.3	-47.8 ± 5.5	3.2 ± 0.7
B-10	38.9 ± 2.4	-44.7 ± 13.2	2.6 ± 1.2
B-20	33.3 ± 2.2	-28.2 ± 5.5	6.7 ±3.2
B-25	28.9 ± 1.7	-29.1 ± 5.4	4.4 ±1.7
Compressive Strength vs. Extent of reaction (see Fig. 3.7) $C=C_1 + C_2*R$			
Phase	**C_1**	**C_2**	**r-value**
α-TCP	-7.7 ± 2.2	41.0 ± 3.6	0.97147
CDHA	-28.6 ± 3.9	63.8 ± 5.5	0.97739

3.3.2. Scanning Electron Microscopy

Figs. 3.2 and 3.3 show a collection of SEM pictures taken at different hardening times, between 1 h and 5 days, for both the control (*Biocement-H©*) and its modification with 25 *wt.%* CSD crystals (BioCSD-25). In general terms, the microstructure of both samples evolved as expected for α-TCP based cements, such that α-TCP particles dissolved and CDHA crystals precipitated (see also Chapter 2). The main difference was the presence of perfectly elongated CSD crystals and/or CSD-holes, due to their dissolution, in the BioCSD-25 sample. Figs. 3.2 and 3.3 also show that the microstructure evolved faster during the hardening period 1h ≤ HT ≤ 16h and stabilised during the period 16h ≤ HT ≤ 120h, both in agreement to the linear growth and the saturation stage observed in Fig. 3.1 for the compressive strength.

To further understand the saturation stage in Fig. 3.1, observed for all the samples during the hardening period between 16h ≤ HT ≤ 120h, sample BioCSD-20 was analysed for the compressive strength (see Fig. 3.1) and the microstructure at longer times, i.e. 14 and 28 days. Fig. 3.4 summarises the SEM results and shows a collection of pictures taken at different magnifications. There was no difference between the microstructure observed at short times and after 14 or 28 days. This is in agreement to the similar mechanical strength obtained at 14 and 28 days, as reported in Fig. 3.1, and in line to the previous saturation stage level (≈35 MPa). However, at both 14 and 28 days a high amount of CSD crystals were observed intact and completely integrated into a matrix of small apatite-like crystals.

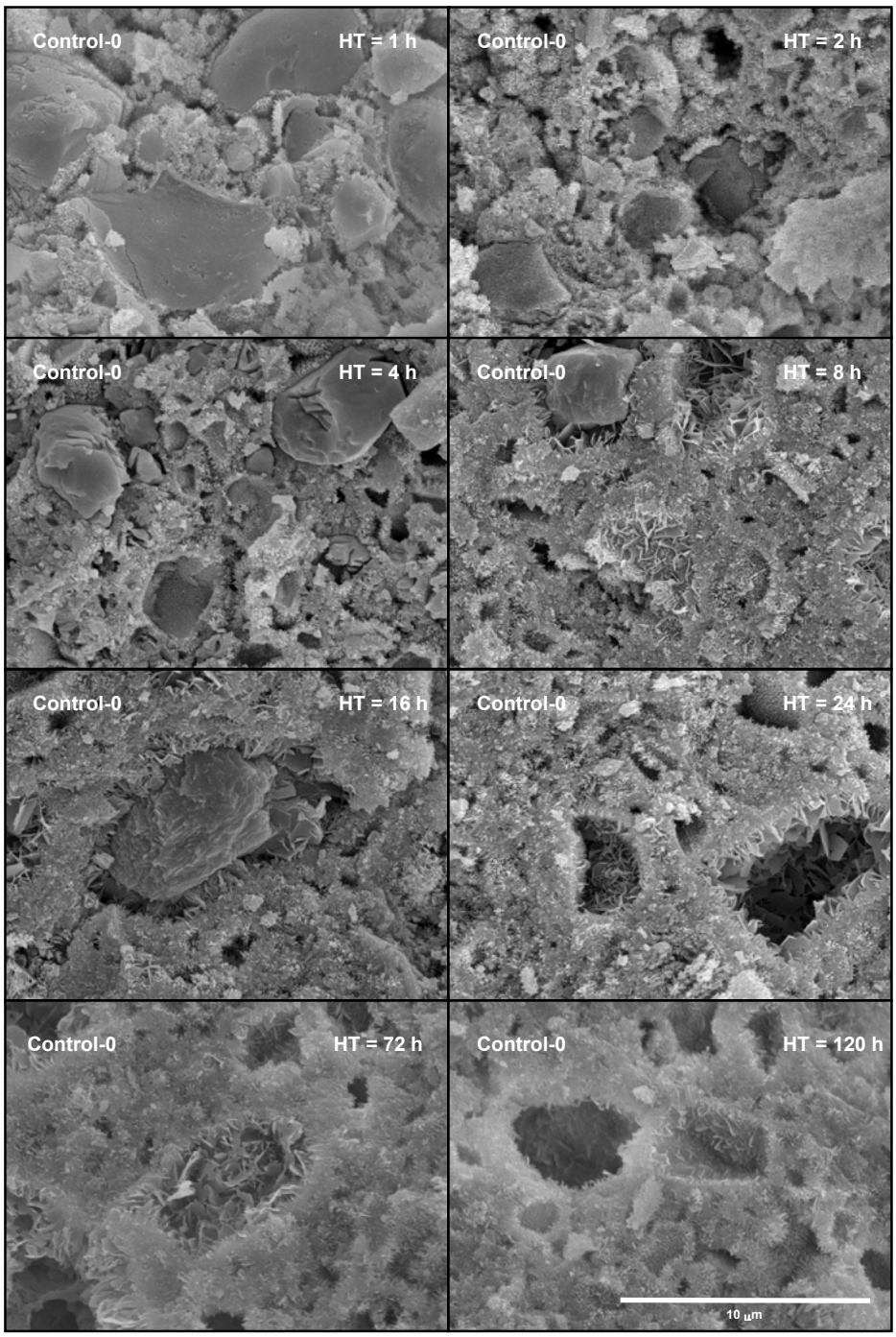

Figure 3.2. SEM pictures at different hardening times for the control (Biocement-H©) cement. (x6000)

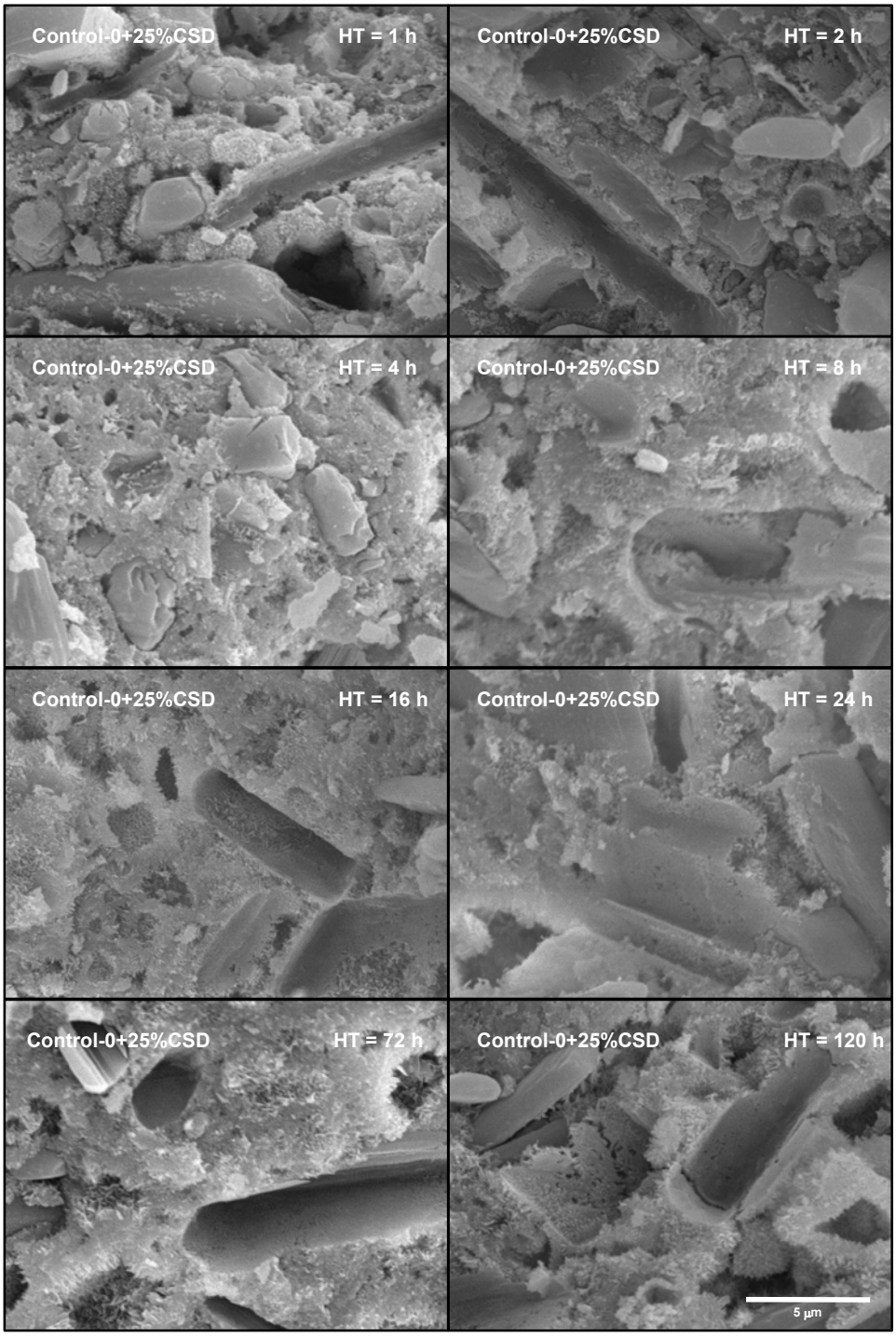

Figure 3.3. SEM pictures at different hardening times for the cement BioCSD25 (*Biocement-H*© modified with 25 *wt.%*-CSD). (x5000)

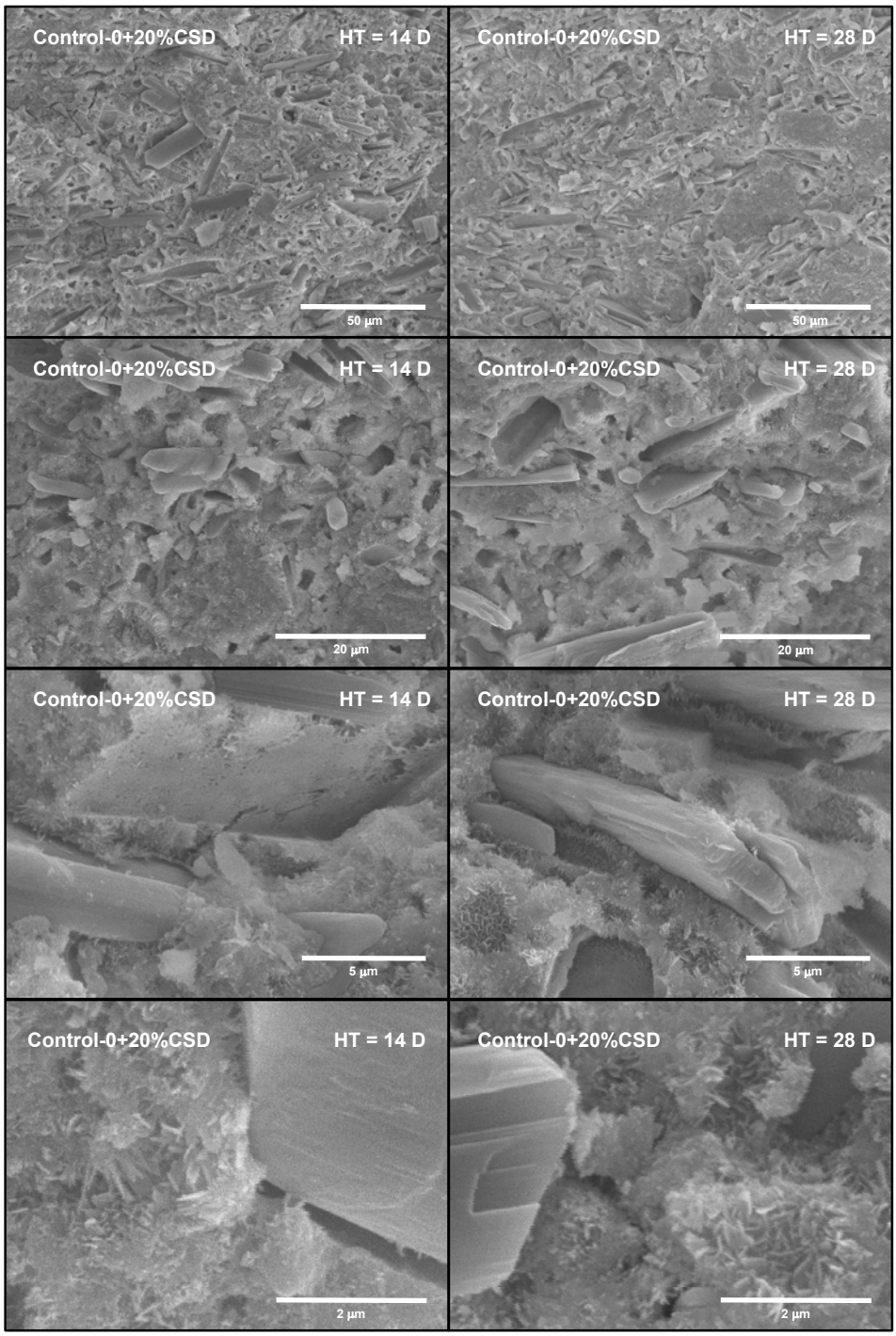

Figure 3.4. SEM pictures at 14 days (left) and 28 days (right) of setting for the cement BioCSD20 (*Biocement-H*© modified with 20 *wt.*%-CSD). (By raws: x500, x1500, x5000, x15000).

This was a clear indication that an equilibrium chemical reaction resulted between CSD crystals and their surroundings due to the Ringer's solution being supersaturated with sulphate ions. This indication was confirmed by comparing the microstructure of sample BioCSD-25 after 14 days of setting in a non-renewable Ringer's solution (see Fig. 3.5; left hand) to the one set during 35 days in a every day renewed Ringer's solution (see Fig. 3.5; right hand). When Ringer's solution was renewed every day CSD crystals disappeared completely leaving behind a CSD-like shape macroporous structure in agreement to the low value of the compressive strength obtained for this sample (see Fig. 3.1). In general terms, similar results have been published for α-TCP and CSH mixtures [21,22]. To clarify these observations, following similar literature studies [26], next section contains the detailed XRD study done on BioCSD-25 sample.

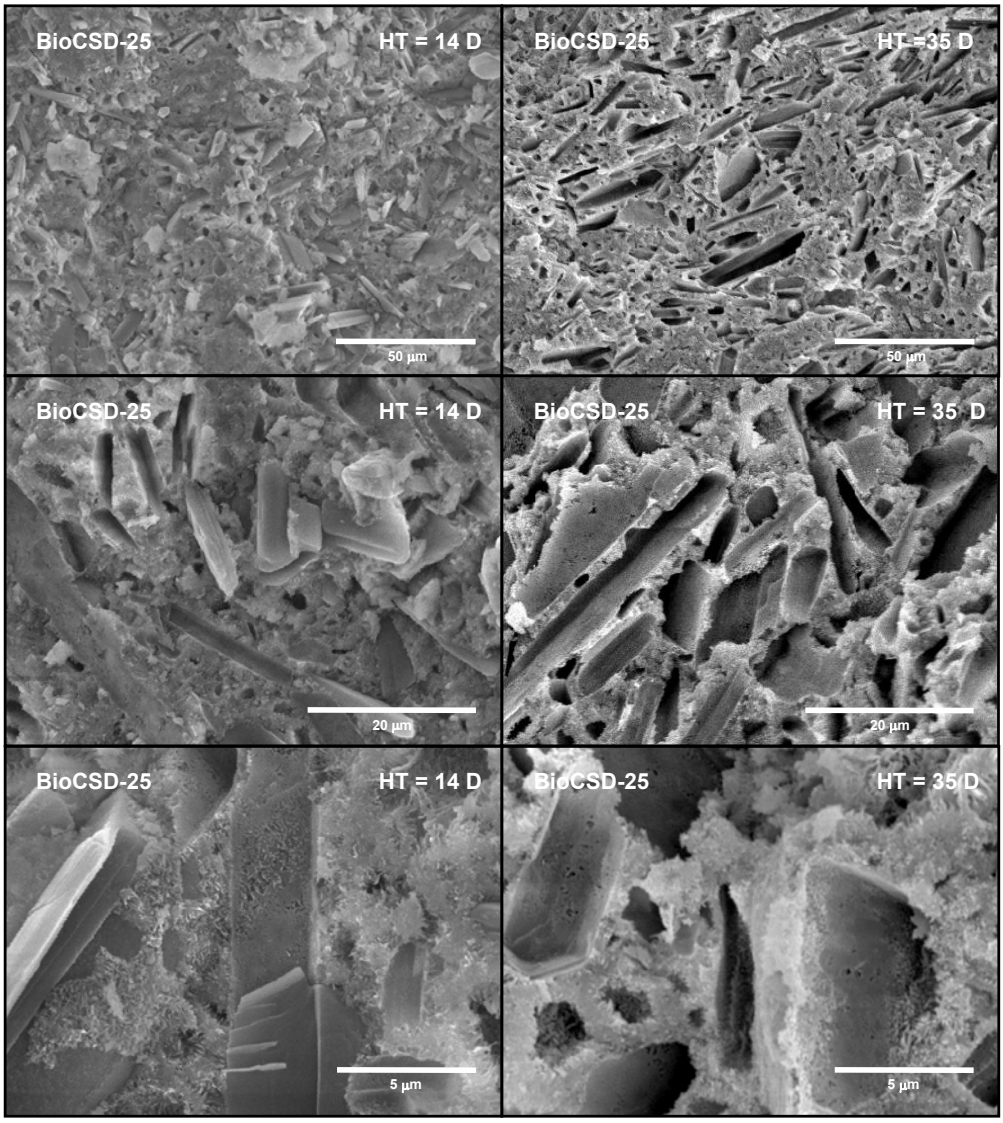

Figure 3.5. SEM pictures at 14 days (left) and 35 days (right) of setting for the BioCSD25 sample (*Biocement-H*© modified with 25 wt%-CSD). (By raws: x500, x1500, x5000)

3.3.3. X-ray diffraction

Fig. 3.6 summarises the results obtained from the XRD analysis of the evolution of the main crystalline reactive cement phases for the BioCSD-25 sample. Data points in Fig. 3.6 are the average vale of the extent of the dissolution (or precipitation) reaction, R, of the α-TCP and CSD phases (or of the CDHA phase) obtained from data of individual peaks (see Table 3.2). Despite 10-15 *wt.*% β-TCP was formed during the quenching process of the α-TCP phase, its presence did not influence the setting of the bone cements. This phase did not react against the time and for this reason, it has not been represented (not considered) in Fig. 3.6 (in Table 3.1). On the other hand, the dissolution of the α-TCP and the CSD phases, as well as the precipitation of the new CDHA phase, fit well to the exponential functions (see details in Table 3.1).

One of the main observations in Fig. 3.6 is to see that between 1 and 14 days of setting the three present phases (i.e. α-TCP, CSD and CDHA) showed a constant behaviour (saturation). The XRD intensity of the α-TCP peaks decreased with time mainly during the first 24 h of setting indicating dissolution of this phase and giving a saturation value for the extent of this reaction of 10%. Similarly, the XRD intensity of the CDHA peaks increased with time up to a saturation value of 90%. Meanwhile, the fast initial dissolution of the CSD phase stopped and was kept constant at around 30%. However, when the Ringer's solution was renewed daily the average intensity observed for the CSD phase after 35 days of setting was not detected, indicating complete dissolution of this phase. This was in agreement to the SEM observations made in Fig. 3.5 where no CSD-crystals but CSD-holes were observed into the apatitic cement matrix.

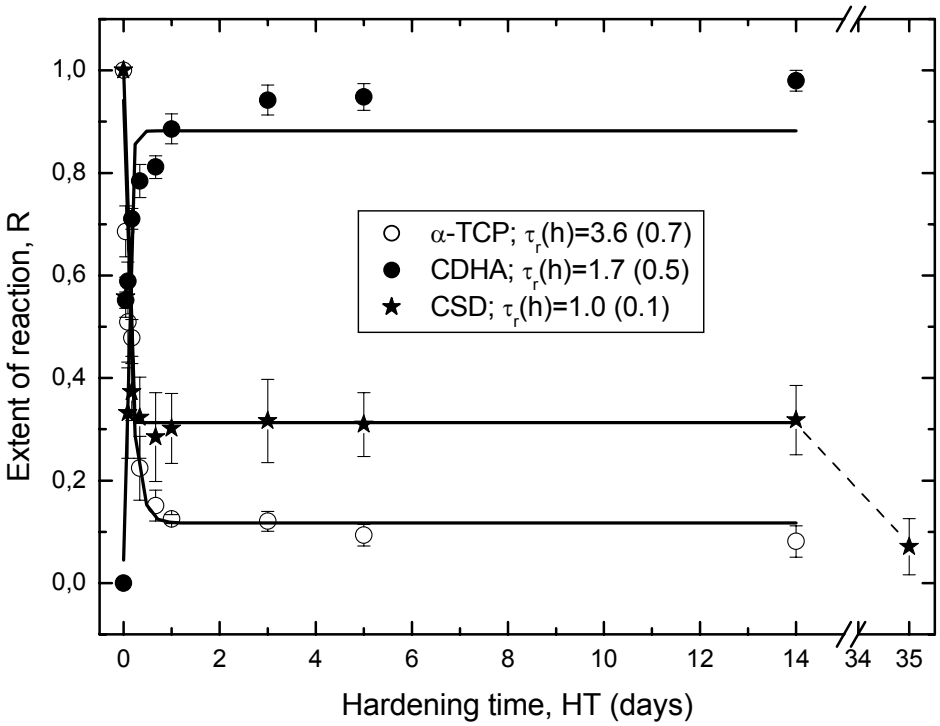

Figure 3.6. Evolution of the extent of reaction, R, against the hardening time for the cement BioCSD25. (Note1: the fittings are only for HT<120h (see details in Table 3.1); Note2: the R-value for CSD at 35 days results from the every day change of the Ringer's solution).

If we look at the lifetime constant, τ of the exponential fittings (see Table 3.1) of BioCSD-25 sample there are some comments to be made. For example, the average τ-value obtained for the extent of the dissolution reaction of the α-TCP phase (see Fig. 3.6) was $\tau_d^{\alpha\text{-TCP}}(h)=3.6\pm0.7$ This means that after 3.6 h of setting the α-TCP phase has dissolved ≈63%. In the same period of time the compressive strength of BioCSD-25 sample (see Fig. 3.1 and Table 3.1; $\tau_c(h)=4.4\pm1.7$) has attained ≈63% of its maximum value. This indicates a direct relation between the dissolution of the α-TCP phase and the mechanical strength development of these bone cements. However, it is well known that when α-TCP dissolves a CDHA phase precipitates [6,23,26]. This means that under normal conditions

(3 α-TCP + H_2O → CDHA) the average τ-value obtained for the precipitation of the CDHA phase should accomplish that $\tau_p^{CDHA} \geq \tau_d^{\alpha\text{-}TCP}$, which was not the case in this study ($\tau_d^{\alpha\text{-}TCP} \approx 2*\tau_p^{CDHA}$). With our data after only 1.7 h of setting ≈63% of CDHA was precipitated (≈88% after 3.6 h). This means that α-TCP dissolution does not account itself for the precipitation of the apatitic matrix. For this reason it is assumed that during fast dissolution of CSD (τ_d^{CSD}=1.0±0.1), calcium ions interact with phosphate ions from the liquid phase (2.5 wt.% Na_2HPO_4) to form hydroxyapatite (HA; $Ca_5(PO_4)_3OH$) and/or calcium deficient apatite (CDHA; $Ca_9(HPO_4)(PO_4)_5OH$), as proposed also by Bohner et al. [23]. However, this apatitic phase formed from the interaction between the CSD and the phosphate liquid phase does not seem to affect the mechanical strength ($\tau_d^{CSD} < \tau_p^{CDHA} < \tau_h$(h)=4.4±1.7). In the next section a deeper analysis is done.

3.3.4. Mechanical strength versus chemical reaction

In order to clarify the above observations the compressive strength data were further analysed against the data of the extent of reaction. The results are summarised in Fig. 3.7. The main observation is that whatever the compressive strength analysis is done against the dissolution of the α-TCP and/or the precipitation of the CDHA a linear relation between the strength and the chemical reactivity is found (see also Table 3.2). This means, as expected, that the mechanical strength of bone cement is directly correlated to the dissolution of the reactants and the precipitation and further entanglement of the new apatitic crystal phase. However, as it is seen in Fig. 3.7, the slope of the fits were different, being higher for the precipitation data (XRD intensity of CDHA phase) as compared to the dissolution data (XRD intensity of the α-TCP phase). Theoretically, as has been commented before, the slope in Fig. 3.7 should be the same under the supposition that the extent of the dissolution ($R_d \approx \exp(-t/\tau_d)$) and the extent of the precipitation ($R_p \approx 1 - \exp(-t/\tau_p)$) take place at the same time ($\tau_d \approx \tau_p$). However, in Fig. 3.7, despite the extent of

reaction of the dissolution data R_d are represented as $R \equiv (1-R_d)$, it was seen that precipitation of CDHA was faster than the dissolution of the α-TCP. The follow up of the dissolution process of the CSD phase seems to help to understand these differences.

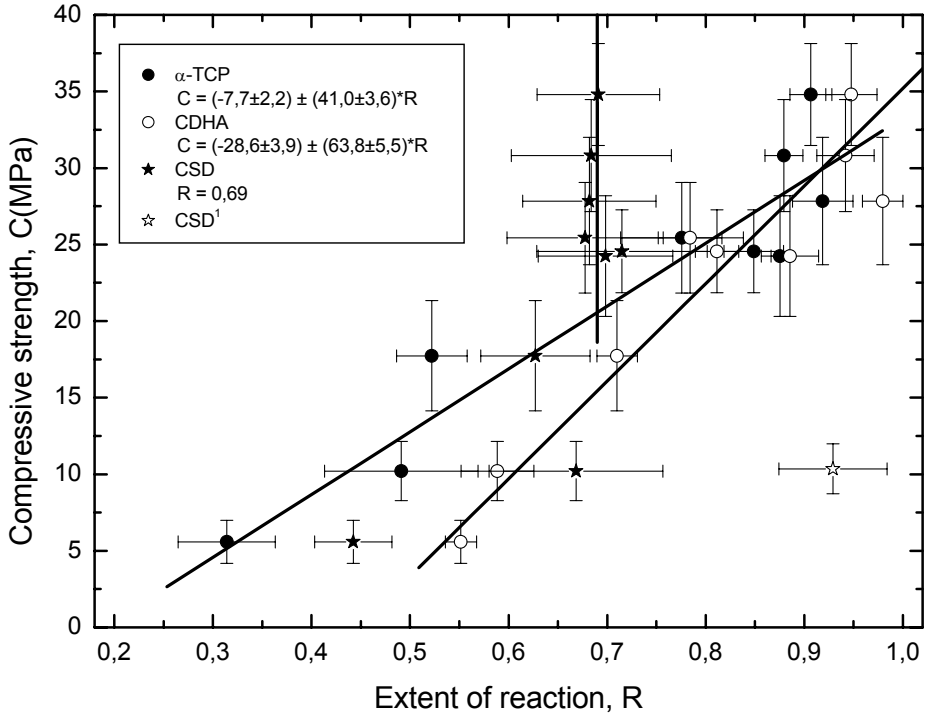

Figure 3.7. Comparison between the compressive strength and the extent of reaction for the cement BioCSD25. (Note 1: Data marked ❶ correspond to the sample set during 35 days in an every day changed Ringer's solution).

If we look at Fig. 3.7, ≈69% of CSD dissolved and then stopped (vertical fit). This means that this phase did not contribute to any further gain of the compressive strength after its blockage, something that occurred at a time lower than 2 h (see fit in Fig. 3.6). This seems again to indicate that this fast dissolution of the CSD phase together with the presence of phosphate ions from the liquid phase (2.5 *wt.*% Na_2HPO_4) were in fact responsible of the high XRD signal observed for the CDHA phase as compared to the

expected one from the dissolution of the main α-TCP reactant. This means that in this new α-TCP-CSD bone cement the amount of the phosphate accelerator used in the cement liquid should also be optimised jointly with the two phases. This interaction between CSD and DHP was also observed by Bohner et al. [23].

Finally, it should be noted in Fig. 3.7 that when the Ringer's solution was renewed every day the compressive strength attained (≈10MPa) was in agreement to the high value of dissolution observed for the CSD phase (≈93%). This means that if a new study is done under this condition, the new data in Fig. 3.7 will not be fitted to any unique linear relation. Instead, a real maximum will appear in Fig. 3.7, being explained by the positive effect on the strength due to entanglement of the new precipitated CDHA crystals going against the negative effect of the passive dissolution of the CSD phase, which increases the porosity of the cement itself. Obviously, this combined effect is of great interest in an *in vivo* application because if both processes are optimised, the macroporosity (i.e. the total of all CSD-holes) which is let down by the passive dissolution of the CSD powder phase will favour bone tissue osteointegration of the implant.

3.4. Summary conclusion

In this study, biphasic bone cement made of alpha-tricalcium phosphate and calcium sulphate dihydrate was studied. The α-TCP phase transformed during the setting into an entangled matrix of calcium deficient apatite crystals while the CSD phase dissolved passively during time. This composite material evolved gradually into a porous material within the strength optimum limits of trabecular bone applications. As porosity appeared gradually, due to the dissolution of the CSD phase, this composite material could have the advantage of being useful as a CSD-drug delivery system. Moreover, bone tissue cells could use the increasing porosity to improve the osteointegration of the implant as well

as to accelerate its complete transformation into real bone tissue. This material could be used, for example, in spinal surgery (*vertebro* and/or *kyphoplasties*) and periodontology applications (*sinus-lifting*).

References

1. Troczynski T. Bioceramics: A concrete solution. Nature Materials 2004;3:13-14.

2. Bohner M, Baroud G. Injectability of calcium phosphate pastes. Biomaterials 2005;26(13):1553-63.

3. Watts NB, Harris ST, Genant HK. Treatment of painful osteoporotic vertebral fractures with percutaneous vertebroplasty or kyphoplasty. Osteoporosis International 2001;12:429-37.

4. Mathis JM, Barr JD, Belkoff SM, Barr MS, Jensen ME, Deramond H. Percutaneous vertebroplasty: A developing standard of care for vertebral compression fractures. American Journal of Neuroradiology 2001;22:373-81.

5. Gbureck U, Barralet JE, Spatz K, Grover LM, Thull R. Ionic modification of calcium phosphate cement viscosity. Part I: hypodermic injection and strength improvement of apatitic cement. Biomaterials 2004;25:2187-95.

6. Barralet JE, Grover LM, Gbureck U. Ionic modification of calcium phosphate cement viscosity. Part II: hypodermic injection and strength improvement of brushite cement. Biomaterials 2004;25:2197-03.

7. Barralet JE, Hoffman M, Grover LM, Gbureck U. High-strength apatitic cement by modification with α-hydroxy acid salts. Adv Mater 2003;15;24:2091-94.

8. Sarda S, Fernández E, Nilsson M, Planell JA. Kinetic study of citric acid influence on calcium phosphate bone cements as water-reducing agent. J Biomed Mat Res 2002;61;4:653-59.

9. Hankermeyer CR, Ohashi KL, Delaney DC, Ross J, Constantz BR. Dissolution rates of carbonated hydroxyapatite in hydrochloric acid. Biomaterials 2002;23:743-50.

10. Fulmer MT, Ison IC, Hankermayer CR, Constantz BR, Ross J. Measurements of the solubilities and dissolution rates of several hydroxyapatites. Biomaterials 2002;23:751-55.

11. Almirall A, Larrecq G, Delgado JA, Martínez S, Planell JA, Ginebra MP. Fabrication of low temperature macroporous hydroxyapatite scaffolds by foaming and hydrolysis of an α-TCP paste. Biomaterials 2004;25:3671-80.

12. Sarda S, Fernández E, Nilsson M, Planell JA. Influence of surfactant molecules as air-entraining agent on bone cement macroporosity. J Biomed Mater Res 2003;65A:215-21.

13. Del Real RP, Wolke JGC, Vallet-Regí M, Jansen JA. A new method to produce macropores in calcium phosphate cements. Biomaterials 2002;23:3673-80.

14. Barralet JE, Grover L, Gaunt T, Wright AJ, Gibson IR. Preparation of macroporous calcium phosphate cement tissue engineering scaffold. Biomaterials 2002;23:3063-72.

15. Takagi S, Chow LC. Formation of macropores in calcium phosphate cement implants. J Mater Sci: Mater Med 2001;12(2):135-9.

16. Markovic M, Takagi S, Chow LC. Formation of macropores in calcium phosphate cements through the use of mannitol crystals. Key Eng Mat 2000;192-1:773-6.

17. Bohner M. Calcium phosphate emulsions: possible applications. Key Engineering Materials 2001;192-195:765-8.

18. Xu HHK, Quinn JB, Takagi S, Chow LC, Eichmiller FC. Strong and macroporous calcium phosphate cement: effects of porosity and fiber reinforcement on mechanical properties. J Biomed Mater Res 2001;57(3):457-66.

19. Fernández E, Ginebra MP, Lidgren L, Nilsson M, Planell JA. Cemento de sulfato de calcio con biodegradación controlada. Spanish Patent: ES2178556. Priority Data: 30-06-2000.

20. Lidgren L, Nilsson M. Composition for an injectable bone mineral substitute material. US Patent No. US2004048947. Foreign Application Priority Data: 16-07-2000.

21. Nilsson M, Fernández E, Sarda S, Lidgren L, Planell JA. Characterisation of a novel calcium phosphate/sulphate bone cement. J Biomed Mater Res 2002;61(4):600-7.

22. Nilsson M, Fernández E, Planell JA, McCarthy I, Lidgren L. The effect of ageing an injectable bone graft substitute in simulated body fluid. Key Eng Mat 2003;240-42:403-6.

23. Bohner M. New hydraulic cements based on α-tricalcium phosphate-calcium sulfate dihydrate mixtures. Biomaterials 2004;25:741-9.

24. Ginebra MP, Fernández E, Driessens FCM, Planell JA. Modeling of the hydrolysis of α-tricalcium phosphate. J Am Ceram Soc 1999;82(10):2808-12.

25. Bohner M. Physical and chemical aspects of calcium phosphates used in spinal surgery. Eur Spine J 2001;10:S114-21.

26. Fernández E, Ginebra MP, Boltong MG, Driessens FCM, Ginebra J, De Maeyer EAP, Verbeeck RMH, Planell JA. Kinetic study of the setting reaction of a calcium phosphate bone cement. J Biomed Mater Res 1996;32(3):367-74.

Chapter 4

Effect of calcium/phosphorus ratio on the setting properties of calcium phosphate bone cements

4.0. Structured abstract

Mini Abstract. In this study, biphasic calcium phosphate bone cements (BCPCs) were obtained and characterized in terms of setting, hardening, microstructure and crystal phase evolution. The powder cement phases were obtained by sintering appropriate mixtures of monetite and calcium carbonate at different calcium-to-phosphorus ratio (Ca/P). The results showed that when Ca/P ratio deviated from 1.5, the setting and hardening properties of the resulting cements were negatively affected.

Study Design. Experimental study to characterise the setting and the hardening properties of calcium phosphate bone cements (CPBCs) with different Ca/P ratio.

Objective. To investigate the potential effects on the setting properties of alpha-tricalcium phosphate (α-TPC) based bone cements as due to uncontrolled variations of the Ca/P ratio of the α-TCP (i.e. on its purity; Ca/P=1.5) during its fabrication.

Summary of Background Data. BCPCs are made by mixing different proportions of several calcium phosphate reactants. Currently, BCPCs are considered better than single phase cements because of better control of cement's setting and resorption *in vivo*. However, the presence of several phases can let to interactions during dissolution-precipitation reactions that affect end cement properties. On the other hand, specific impurities may often be present either as deliberate additions (i.e. magnesium or iron ions) or as second minor calcium phosphate phases produced during sintering as due to unbalanced Ca/P ratio of the starting reagents. Among the wide range of available calcium phosphates with potential use in cement formulation, the α-TCP has became the main reactant of most experimental and commercial bone cements. For these reasons, it is important to investigate the potential effect that uncontrolled deviations of the Ca/P ratio of the α-TCP (i.e. its purity; Ca/P=1.5) can have on their cements' setting and hardening.

Methods. Setting times were measured by the *Gillmore* needles standard. The compressive strength accounted for the cement hardening. pH gave information on solution chemistry. Scanning Electron Microscopy followed the cement microstructure. X-ray diffraction confirmed the evolution of the crystalline phases.

Results. Optimum setting times and compressive strength were obtained for Ca/P=1.50 (i.e. pure α-TCP), for which pH≈9. Setting proceed slowly as Ca/P deviated from Ca/P=1.5. In fact, for Ca/P=1.29 setting did not occur. In general, the results agreed with the microstructure evolved during setting.

Conclusions. The results showed that: (a) there is a strong correlation between cement's reactivity and the Ca/P ratio of the starting powder phase; (b) when α-TCP was the main reactant, its hydration into CDHA was responsible for the setting of the cement; (c) the cement's compressive strength was lower when Ca/P deviated more from Ca/P=1.5 (i.e. pure α-TCP); and (d) the microstructure of the cements was also Ca/P ratio dependent.

Key Points.

- A method to optimise the setting properties of α-TCP cements has been showed; it is particularly useful when the α-TCP has low reactivity as due to uncontrolled ionic contamination or unbalanced Ca/P ratio of the starting batch-reactants.
- The study points to new search for controlling the "ionic-contamination" in order to stabilize the α-TCP phase and so recover the setting and hardening properties of non-reactive cements (if so).
- The study indicates that BCPCs should be made by mixing mechanically two pure calcium phosphate reactant phases (with exact control of both proportion and particle sizes) and not by direct sintering and subsequent milling of biphasic calcium phosphate ceramics (even if this contains the same proportion of the two calcium phosphate phases).

4.1. Introduction

Bioactive calcium phosphate biomaterials made of biphasic mixtures (both as sintered ceramics or as cements) or so called binary eutectic ceramic structures have been widely studied for use in specific clinical applications, due to their ability to assure new bone apposition after implantation *in vivo* [1-8]. However, calcium phosphate bone cements (CPBCs) have the advantage over the bioceramics that they do not need to be delivered in prefabricated forms, because of their self-setting properties and facilities to be handled by the clinician in paste form and injected into bone defects.

CPBCs have been increasingly employed in dental and orthopaedic applications [9-11] in recent years and are now being use in minimally invasive surgery such as vertebro- or kyphoplasty [12-16]. Since the first CPBC proposed by Brown and Chow [10] many formulations have been studied and several commercial calcium phosphate cements are available [13,17] as combination of calcium phosphate compounds. Currently, biphasic calcium phosphate cements (BCPCs), comprising specific mixtures of two calcium phosphate compounds, are better considered than single phase cements due to the possibility of positive combination of the dissolution behaviour of the two phases (synergies) that, at the end, influences the setting properties as well as the resorption mechanism of the cement after implantation *in vivo* [18,19].

However, phase-reactants purity is a well-recognized but not always well-understood variable affecting the dissolution-precipitation processes (and so the cement properties) during the setting of apatitic CPBCs. In fact, minor amounts of specific relevant impurities may often be present either as deliberate additions (i.e. magnesium or iron ions) or as second minor phases resulting from decomposition during main reactants sintering or as due to unbalanced Ca/P ratio's deviation of the starting reagents (i.e. unwanted contamination due to uncontrolled deviations of the stoichiometry of the

starting reagents) [20-22]. In this sense, it has been observed after inlab main reactant's production, that sometimes (in coincidence with batch-reagent changes, i.e. change of the "batch's serial number") there are enormous differences between theoretical "identical α-TCP based cements" (both at the level of initial setting and hardening properties) [22]. It is important to know that reactants' Ca/P ratio is closely related to its acidity and solubility [23-26]; for this reason, the Ca/P ratio is a very useful parameter of control for scientists working in this field. Among the wide range of available calcium phosphates with potential use in cement formulation, the α-TCP has became the main reactant of most experimental and commercial bone cements. Thus, at this stage, new approaches are needed for the whole comprehension of the potential effect that uncontrolled deviations of the Ca/P ratio of the α-TCP (i.e. its purity; Ca/P=1.5) can have on its cements' setting and hardening.

Therefore, the justification of this study was based on experimental observations that indicated that if α-TCP contained (after sintering) hydroxyapatite (HA) as a second phase (i.e. potential deviation of the Ca/P ratio of the initial reactants' powder mixture in the interval 1.5<Ca/P<1.67) then the cements simply did not set (unpublished data). Thus, the objective of this study was to investigate in a controlled manner the potential effect that uncontrolled variations of the α-TCP's Ca/P ratio can have on the setting and hardening cement's properties.

4.2. Materials and methods

4.2.1. Biphasic calcium phosphate cements

4.2.1.1. Cements' powder production

Powder cement's phases were prepared as follows: calcium hydrogen phosphate $CaHPO_4$ (DCP; Ref. C-7263; *Sigma, Spain*) and calcium carbonate $CaCO_3$ (CC; Ref. C-4830;

Sigma, Spain) were homogenously mixed into appropriate Ca/P molar ratios (i.e. 1.29, 1.50, 1.51, 1.58, 1.67 and 1.77). Then, powder mixtures were identically sintered at 1400°C for 2h and quenched in air to room temperature. The resulting ceramic materials were identically milled in a planetary ball mill (PM-100; *Retsch GmbH, Germany*) up to medium particle size of 6.63 μm (d_{10}=0.56 μm, d_{50}=2.47 μm, d_{90}=16.86 μm).

4.2.1.2. Cements' preparation

Six calcium phosphate cements (CPC) were prepared and coded as $CPC^{1.29}$, $CPC^{1.50}$, $CPC^{1.51}$, $CPC^{1.58}$, $CPC^{1.67}$, $CPC^{1.77}$ (i.e. cement powder phases of Ca/P=1.29, 1.50, 1.51, 1.58, 1.67 and 1.77, respectively). All powder's phases contained 2 *wt%* of precipitated hydroxyapatite setting accelerator (PHA; Ref. 2143; *Merck, Spain*). The aqueous liquid phase also contained 2.5 *wt%* of di-sodium hydrogenphosphate accelerator (Na_2HPO_4; Ref. 131679; *Panreac Química S.A., Spain*). The cement's liquid-to-powder ratio (L/P) was 0.32 mL/g. Homogeneous cement slurries were obtained by mixing the powder and the liquid phases for 1 minute, in a mortar with a pestle. Then after, cement pastes were molded into cylindrical samples (5 mm diameter by 10 mm height) and immersed in Saline Physiological solution (0.9 *wt%* NaCl; Ref. 610667; *Grifols, Spain*) at 37°C for 30 min; then after, samples were unmolded and stored again for fixed hardening times (HT; i.e. 4 and 24h) under the same conditions. After completion of HTs, the samples were investigated for phase composition, microstructure and compressive strength.

4.2.2. Setting times

The Initial and the Final Setting Time (IST and FST) were measured with the Gillmore needles standard (i.e. ASTM-C266-89) [27].

4.2.3. Mechanical strength testing

Cylindrical hardened (i.e. for 4 and 24h) samples were tested until fracture under compression using a Universal Testing Machine (*MTS Insight-5*) at a crosshead speed of 1mm/min. Each compressive strength *C* value was an average of at least eight samples (n≥8). The results were fitted to a Gaussian function of the form $C_R=C_M*exp[-[(x-R_2)/R_3]^2]$, where C_R is the compressive strength measured for each cement (i.e. for each Ca/P ratio), C_M is the maximum compressive strength (i.e. the height of the Gaussian peak), R_2 is the Ca/P ratio corresponding to the maximum compressive strength C_M, (i.e. R_2 is the position of the center of the peak) and R_3 is a parameter meaning a statistical dispersion, averaging the squared distance between possible and expected values, (i.e. the Ca/P ratio parameter controlling the width of the bell curve).

4.2.4. pH measurements

Cement slurries were recorded for pH at L/P ratio of 200 mL/g under continuous stirring using a computer-controlled pH-meter (SevenMulti™ S80; *Mettler-Toledo, Spain*). Data were collected every minute during 24h.

4.2.5. Chemical characterization

Tested compressive strength samples were immediately quenched in acetone to stop further setting reactions, dried and ground for X-ray diffraction (XRD) analysis. Data were recorded with a *PANalytical X'Pert PRO alpha1* diffractometer (PANalytical, *Holland*) equipped with an *X'Celerator* detector working with the CuKα_1 radiation (1.5406 Å) in the 2θ range 20-40° with a scan step size of 0.017° and a step-time of 200s. The phase composition was checked by indexing the diffraction peaks according to JCPDS (*Joint Committee on Powder Diffraction Standards*) cards (9-348 for α-TCP (i.e. alpha-$Ca_3(PO_4)_2$;

alpha tricalcium phosphate), 9-169 for β-TCP (i.e. beta-$Ca_3(PO_4)_2$; beta tricalcium phosphate), 9-432 for CDHA (i.e. $Ca_9(HPO_4)(PO_4)_5OH$; calcium deficient hydroxyapatite), 9-346 for CPP, (i.e. $Ca_2P_2O_7$; β-calcium pyrophosphate) and 25-1137 for TTCP (i.e. $Ca_4O(PO_4)_2$; tetracalcium phosphate).

4.2.6. Microstructural characterization

Scanning Electron Microscopy (SEM; *JEOL JSM-5610, Hitachi, Japan*) was used to characterize the cement microstructure developed after 4 and 24h of setting. Two cylindrical samples were quenched in acetone and fractured diametrically. The resulting surfaces were gold covered before SEM observations.

4.3. Results

4.3.1. Setting times

Fig. 4.1 accounts for the evolution of the IST and the FST of the experimental CPCs as a function of the Ca/P ratio of the powder cement phases. The results show that for Ca/P=1.29 the IST and the FST were too large (cement did not set, properly), while in the range of 1.5≤Ca/P≤1.77 the setting reactions were much faster and the optimum setting times (minimum values) were found for Ca/P = 1.50 (i.e. pure α-TCP).

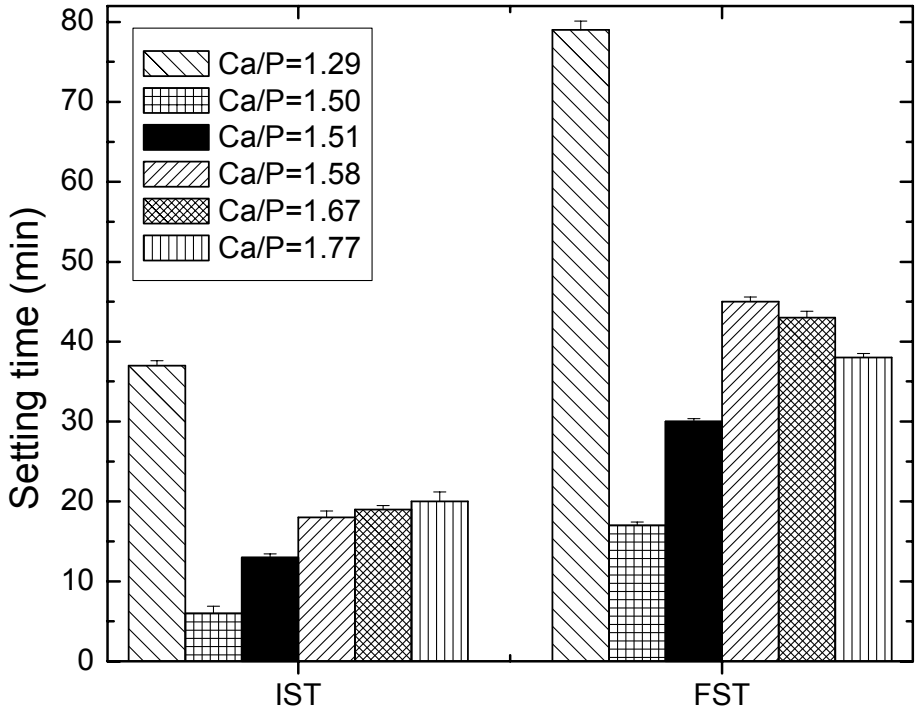

Figure 4.1. Characteristic setting times (IST and FST) as a function of the Ca/P ratio of the experimental cements (i.e. CPC$^{1.29;1.50;1.51;1.58;1.67;\text{ and }1.77}$).

4.3.2. Compressive strength

Fig. 4.2 shows the compressive strength values obtained after 4 and 24h of hardening for the experimental cements studied (i.e. 1.29≤Ca/P≤1.77). The results have been fitted to a Gaussian curve just for clarity in order to show a general tendency. It is observed that the maximum compressive strength was again obtained near the Ca/P=1.5, i.e. when only the main reactive cement phase was α-TCP. The hardening rate and so the compressive strength decreased from this Ca/P ratio in both directions, i.e. for Ca/P<1.5 (i.e. presence of CPP; see XRD results) and for Ca/P>1.5 (i.e. presence of HA and TTCP; see XRD results). However, the compressive strength was more affected with the presence of CPP

(i.e. Ca/P<1.5) than with the presence of HA and/or TTCP (i.e. Ca/P>1.5) as second phases. In fact, for Ca/P=1.29 the "cement" did not hard (C=0 MPa). On the other hand for Ca/P=1.77 the compressive strength was too low, around 5 MPa, which is the equivalent static pressure corresponding to the FST (as measured by the Gillmore needles), after both 4 and 24h of setting, which means that setting did not further evolve. Strictly speaking, fitting in Fig. 4.2 should be only considered for Ca/P≥1.5.

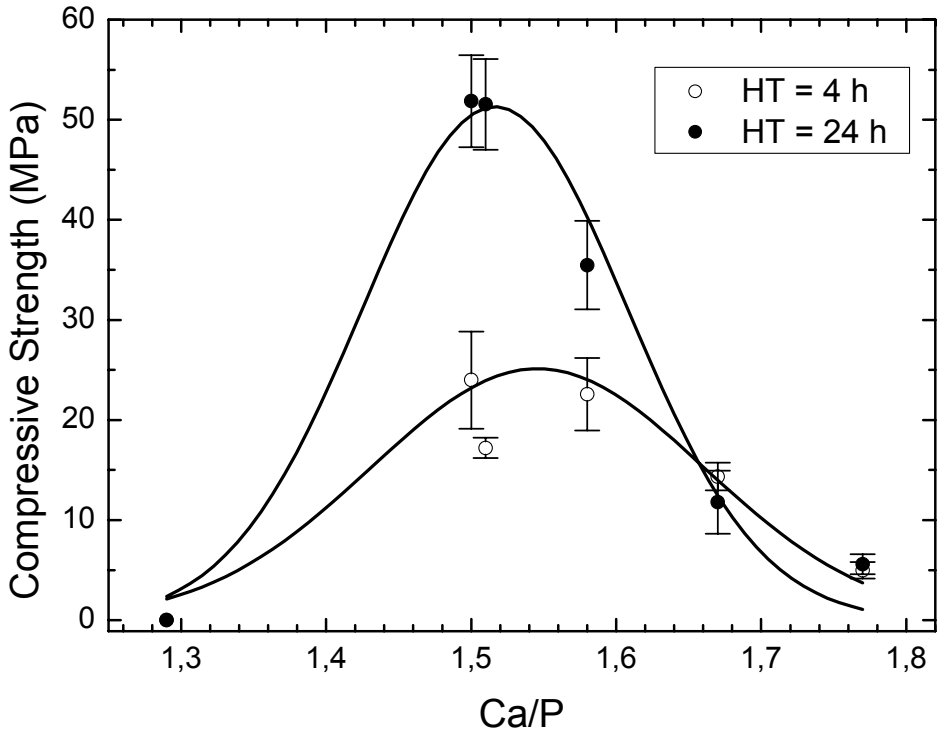

Figure 4.2. Evolution of the compressive strength, C(MPa), as a function of the Ca/P ratio and hardening time (4 and 24h) for the cements *CPC*$^{1.29}$, *CPC*$^{1.50}$, *CPC*$^{1.51}$, *CPC*$^{1.58}$, *CPC*$^{1.67}$ and *CPC*$^{1.77}$.

4.3.3. pH measurements

Fig. 4.3 presents the pH-Time evolution for the studied cements. Measurements were performed in diluted systems (1g powder for 200 mL liquid phase). In general, the pH-Time curves moved to lower pH values (more acid cements) when the Ca/P ratio was decreased. The time trend was, except for Ca/P=1.29, as follows: first, the pH increased with time until a maximum or a plateau was reached; then, at some specific time t_d, the pH continuously decreased. Moreover, t_d was Ca/P ratio's dependent and it increased for higher Ca/P ratios (more basic cements).

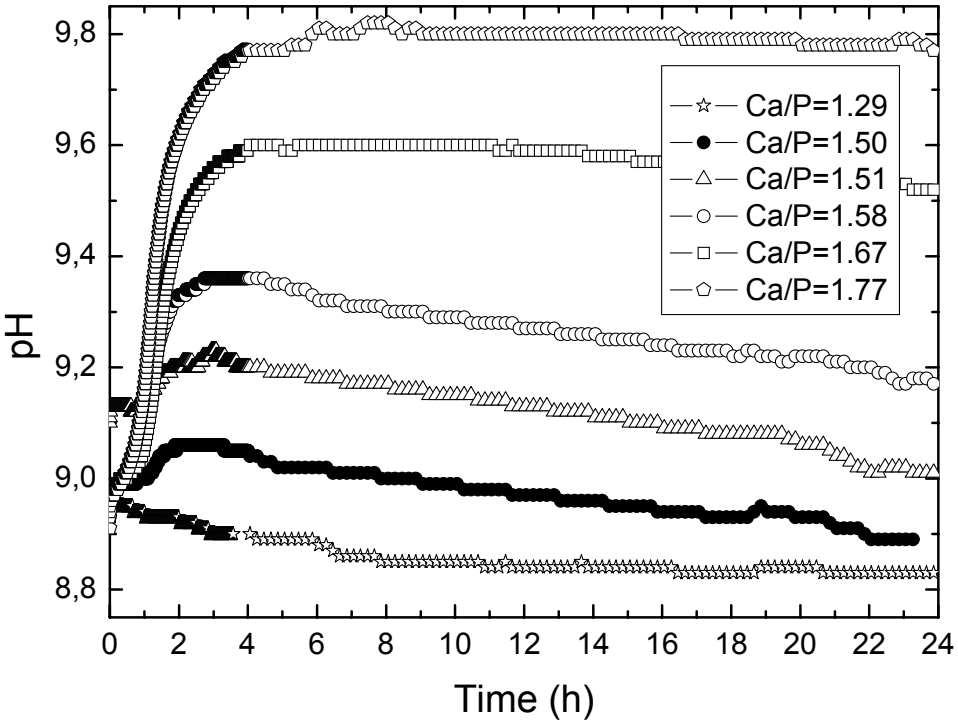

Figure 4.3. Evolution of pH against time for the different Ca/P ratio cement slurries (L/P=200 mL/g).

4.3.4. X-ray diffraction

Figs. 4.4-4.6 show the XRD patterns obtained for powdered cements at different hardening times (i.e. HT=0, 4 and 24h). At HT=0h (i.e. starting cement powder phase; Fig. 4.4.), the peaks detected were: for Ca/P=1.29, α-TCP, β-TCP and CPP; for 1.5<Ca/P≤1.77, α-TCP, TTCP and HA; and for Ca/P=1.5, only α-TCP. In general, the peak intensities of α-TCP, β-TCP and TTCP decreased with time while the intensity of a new precipitated HA phase increased accordingly (Fig. 4.5 and 4.6). This was the normal trend for all the cements, except for Ca/P=1.29, for which both α-TCP and CPP peaks remained practically stable after 4h of setting (Fig. 4.5), and even after 24h of setting the presence of new precipitated HA was minimum, i.e. negligible crystallization during setting (Fig. 4.6).

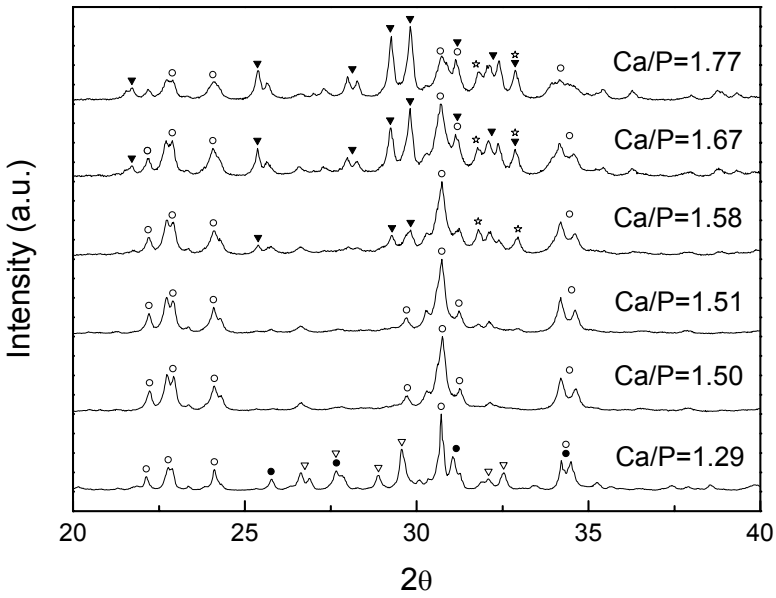

Figure 4.4. XRD patterns of *CPC*$^{1.29}$, *CPC*$^{1.50}$, *CPC*$^{1.51}$, *CPC*$^{1.58}$, *CPC*$^{1.67}$ and *CPC*$^{1.77}$ before setting. (○) α-TCP; (☆) CDHA; (●) β-TCP; (▽) CPP; (▼) TTCP.

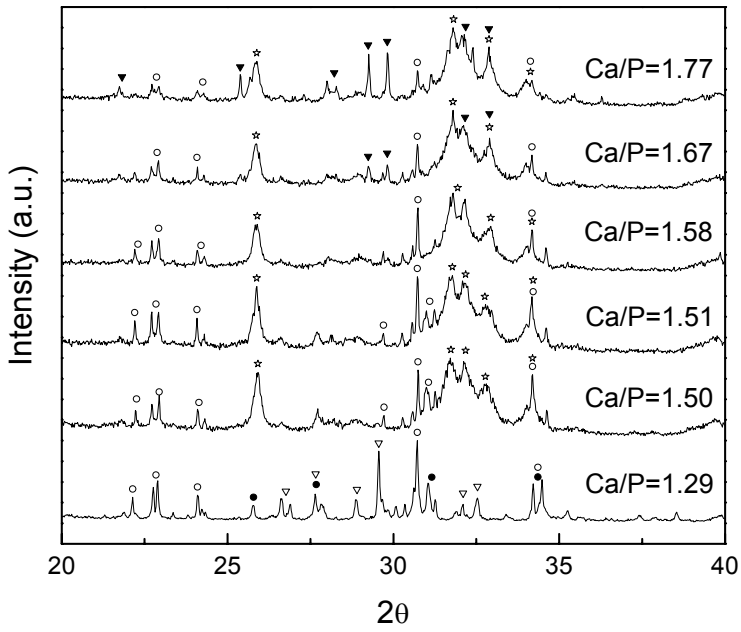

Figure 4.5. XRD patterns of *CPC*$^{1.29}$, *CPC*$^{1.50}$, *CPC*$^{1.51}$, *CPC*$^{1.58}$, *CPC*$^{1.67}$ and *CPC*$^{1.77}$ after 4h of hardening. (○) α-TCP; (☆) CDHA; (●) β-TCP; (▽) CPP; (▼) TTCP.

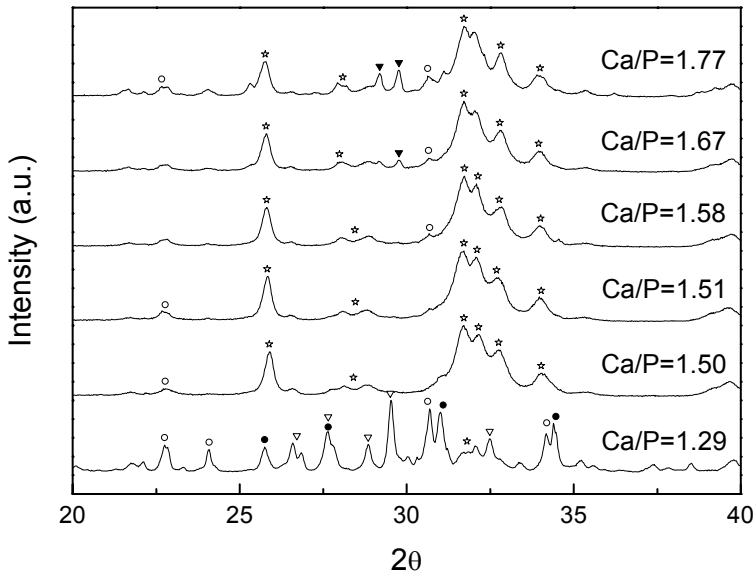

Figure 4.6. XRD patterns of *CPC*$^{1.29}$, *CPC*$^{1.50}$, *CPC*$^{1.51}$, *CPC*$^{1.58}$, *CPC*$^{1.67}$ and *CPC*$^{1.77}$ after 24h of hardening. (○) α-TCP; (☆) CDHA; (●) β-TCP; (▽) CPP; (▼) TTCP.

4.3.5. Scanning electron microscopy

Figs. 4.7 and 4.8 show at different magnification (x5000 and x15000, respectively) some representative SEM pictures taken on different cement's fracture surfaces after 4 and 24h of hardening. It is observed that the cement $CPC^{1.29}$ (i.e. Ca/P=1.29) shows most unreacted α-TCP particles even after 24h of setting, in agreement to XRD (see Fig. 4.6). In general, the surface aspect was sandy and detached, also in agreement to the observed compressive strength values (see Fig. 4.2).

On the other hand, cement $CPC^{1.50}$ (i.e. Ca/P=1.50) and $CPC^{1.58}$ (i.e. Ca/P=1.58), shows that after 4h of setting the α-TCP particles were surrounded by a shell layer of very small, acicular CDHA crystals (Fig. 4.7). Moreover, after 24h of setting, only a small amount of undissolved α-TCP particles can be found, while now also laminar bigger crystals of CDHA have grown in place of the α-TCP particles previously surrounded by the CDHA crystalline shells (Fig. 4.8); the surface aspect was more compact and entangled, and the observations are in agreement to both compressive strength and XRD results (see Figs. 4.2 and 4.6).

Finally, for cements $CPC^{1.67}$ (i.e. Ca/P=1.67) and $CPC^{1.77}$ (i.e. Ca/P=1.77), it is observed that the microstructure has now distinctive features, i.e. the precipitated CDHA crystals are smaller than those in $CPC^{1.50}$, and they are grouped into crystal colonies regularly space distributed, seemingly to a cauliflower, but less entangled between them; these features also agree with the compressive results in Fig. 4.2.

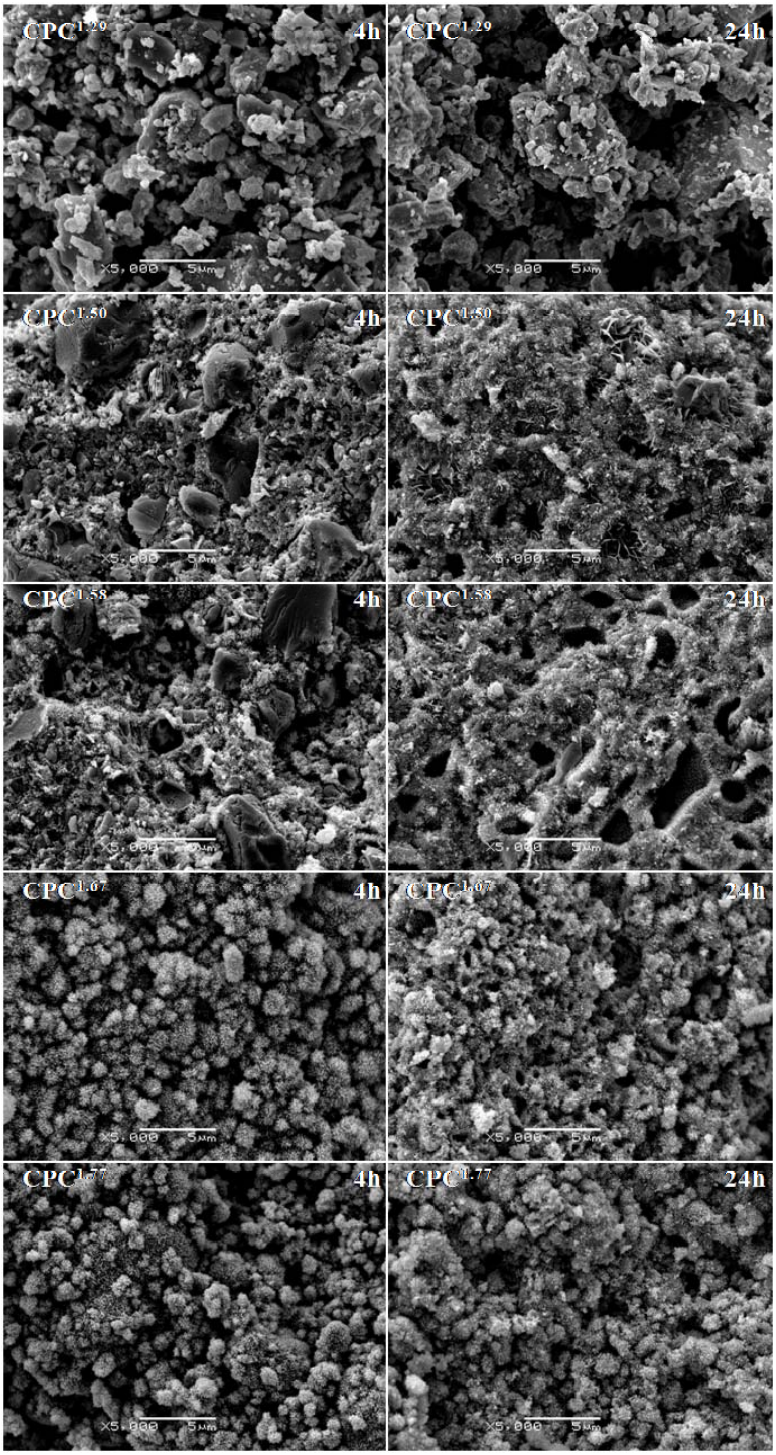

Figure 4.7. SEM pictures after 4 and 24h of hardening for $CPC^{1.29}$, $CPC^{1.50}$, $CPC^{1.51}$, $CPC^{1.58}$, $CPC^{1.67}$ and $CPC^{1.77}$ (x5000).

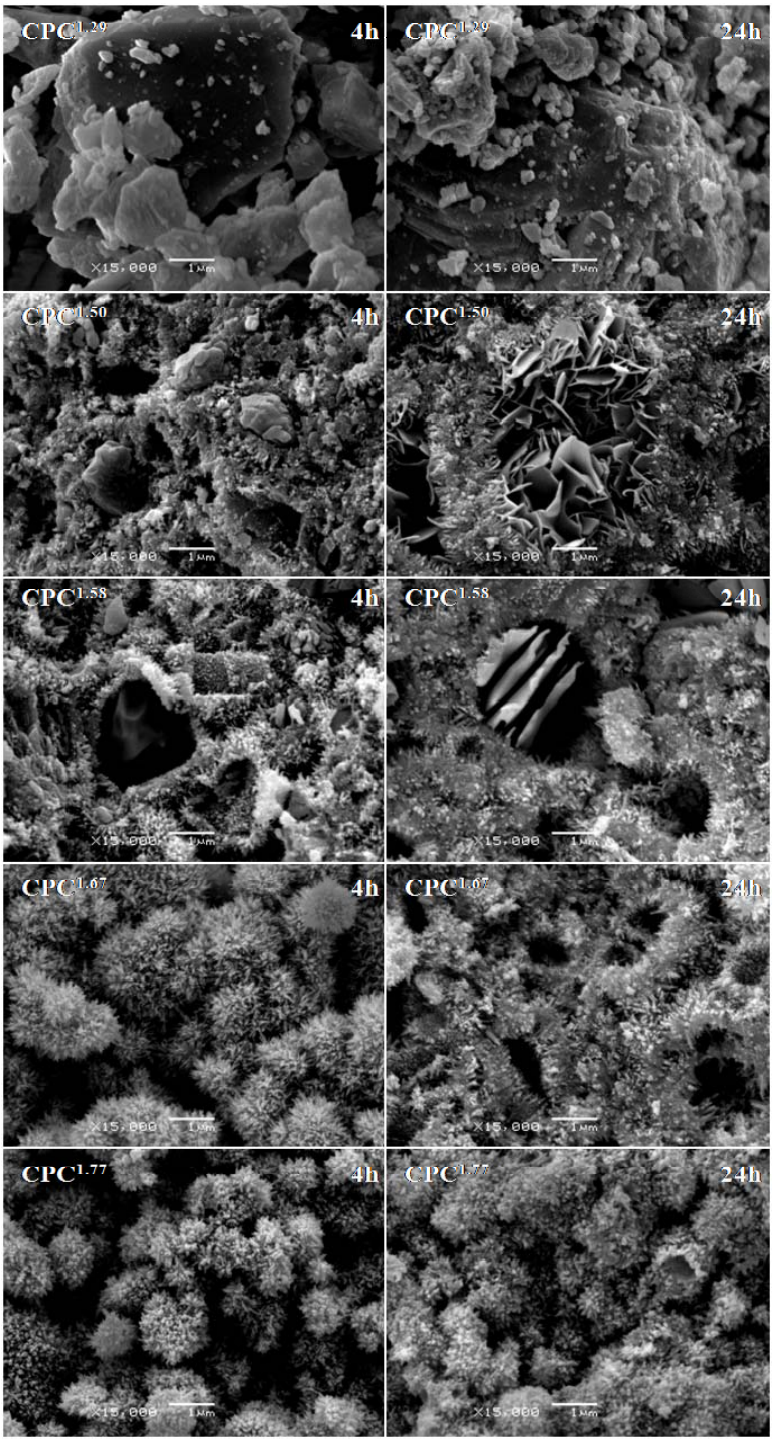

Figure 4.8. SEM pictures after 4 and 24h of hardening for *CPC*$^{1.29}$, *CPC*$^{1.50}$, *CPC*$^{1.51}$, *CPC*$^{1.58}$, *CPC*$^{1.67}$ and *CPC*$^{1.77}$ (x15000).

4.4. Discussion

In this study, the proportions of the reagents (i.e. the Ca/P ratio of the powder reagent's mixture) normally used (i.e. monetite and calcium carbonate) for α-TCP production were appropriately changed in order to obtain after sintering (using the same sintering protocol as for standard α-TCP fabrication) different biphasic ceramic materials of use for cement powder production. When the reagents mixture was adjusted in the range of $1.29 \leq Ca/P < 1.5$, the biphasic ceramic was made of CPP and α-TCP; while for $1.5 \leq Ca/P < 1.77$, the ceramic was mainly α-TCP and TTCP (see Fig. 4.4.), in agreement to the phase diagram of the binary system $CaO\text{-}P_2O_5$ [28].

The first observations of this study showed that setting times: a) were minimum for the cement with Ca/P=1.50; b) drastically increased for the cement with Ca/P=1.29; and c) gradually increased for the cements with Ca/P>1.50 (see Fig. 4.1). It is evident from Fig. 4.3 (pH measurements) that Ca/P ratio controls the basicity or acidity of the resulting biphasic cement powder phase. In fact, it is known that basicity of calcium phosphates are ordered as CPP<α-TCP<HA<TTCP. For this reason, Ca/P ratio controls also the solution supersaturation's degree against the solubility isotherm of HA, and according to solubility diagrams the supersaturation is maximum (precipitation is favoured) around pH≈9 and, it decreases for other pHs [30,31]; this can explain why the best results (optimum setting times and compressive strength) were found for the cement with Ca/P=1.50, i.e. when only α-TCP was the main cement reactant (see Figs. 4.1 and 4.2).

The microstructural features (Figs. 4.7 and 4.8) showed, jointly with the XRD results (Figs. 4.4-4.6), that CPCs' self-setting property was mainly related to the progressive hydration reaction of α-TCP (when this was the main reactant phase) into CDHA. This process started with the nucleation of CDHA crystallites onto the surface of α-TCP particles (surface control process, i.e. fast rate process), when the solution supersaturation

was the driving force. However, as it is clear from the SEM pictures, further dissolution of α-TCP and growth of CDHA crystals was a diffusion control process (slow rate process) through the initial precipitated CDHA crystal-shells surrounding the α-TCP particles. This diffusion process influences the formation of the entangled framework of crystals and it has been related to the end hardening cement properties [29]. In this sense, as has been commented before, the maximum compressive strength (i.e. optimum development of the entangled framework of CDHA crystals) was found on the Gaussian curve (see Fig. 4.2) for the cement with Ca/P=1.50, which also agrees with the pH measurements and the supersaturation conditions controlling the dissolution and the precipitacion reactions in this cement (see Fig. 4.3) [30,31].

It is obvious, from the knowledge of the binary ceramic phase diagram $CaO\text{-}P_2O_5$ [28], that when the Ca/P ratio of the cement reactants is changed then, after sintering at 1400 °C, at least biphasic ceramic materials should result with different weight proportions of two stable phases. However, as sintering is followed by quenching to air, it was also expected [28] to obtain eutectic-like complex structures (containing α/β CPP and α/β-TCP) for $1.29 \leq Ca/P < 1.5$ and mixtures of α-TCP, HA and TTCP for $1.5 \leq Ca/P < 1.77$. In fact, XRD analysis confirmed the presence of β-CPP, α-TCP, β-TCP, HA and TTCP into the ceramic powder phases (see Fig. 4.4.).

In conclusion, the present study shows that the setting and hardening properties of α-TCP based cements are negatively affected when for whatever reason the Ca/P ratio of the main reactant (i.e. the α-TCP) suffers uncontrolled deviations from its theroretical value, i.e. Ca/P=1.50. As the Ca/P ratio affects the basicity of the cements (see Fig. 4.3.), it also influences (according to the solubility diagrams) the reaction rates of dissolution, nucleation and precipitation. In fact, it influences the crystal size, its spatial configuration (as observed by SEM; see Figs. 4.7. and 4.8.), and consequently, the mechanical strength of the entire structure of the cement (see Fig. 4.2). Moreover, the results showed that the

negative effect is more important if the deviation occurs at Ca/P<1.5 (i.e. when CPP is present) than at Ca/P>1.5 (i.e. when TTCP is formed). However, the present study do not explain why when the α-TCP contains HA (instead of TTCP) after sintering (i.e. deviation on the interval 1.5<Ca/P<1.67), the resulting cements do not set. In this case, setting times are large and the compressive strength practically null (data not shown). According to our experience this happens sometimes coinciding whith changes of weather conditions (summer, winter, rain, etc.) affecting the humidity (water vapeur pressure) of the environment in the lab.

4.5. Summary conclusion

It is concluded that the present study: (a) shows a method to optimize the fabrication process of α-TCP, particularly when the resulting cements show low reactivity during setting as due to uncontrolled ionic contamination or unbalanced Ca/P ratio of the main reactant; (b) opens the search for new "controlled ionic-contamination" processing routes to stabilize the α-TCP phase and its properties, specially when small Ca/P ratio deviations produce HA as second phase, and the resulting cements are not reactive, i.e. do not set; and (c) establish that the powder phase of biphasic cements (i.e. the majority of commercial brands; α-TCP + HA or TTCP [9,13,17]) should be made by mechanical mixing of pure phases, at selected adecuate proportions and particle size distributions, and not by direct sintering and subsequent milling of the resulted biphasic ceramic material containing the same proportion of phases.

References

1. Vallet-Regí M, Gonzáles-Calbet JM. Calcium phosphates as substitution for bone tissues. Progress in Solid Stare Chemistry 2004;32:1-31.

2. Vallet-Regí M. Ceramic for medical applications. J Chem Soc 2001;97-108.

3. Fernández E. Bioactive Bone Cements. In: Wiley Encyclopedia of Biomedical Engineering, 6-Volume Set, ISBN: 0-471-24967-X, John Wiley & Sons, Inc. (USA), Metin Akay (Ed.), June 2006, pp. 1-9.

4. De Aza PN, Guititi F, De Aza S. Bioeutectic: a new ceramic material for human bone replacement. Biomoterials 1997;18:1285-91.

5. Alemany MI, Velasquez P, de la Casa-Lillo MA, De Aza PN. Effect of materials' processing methods on the 'in vitro' bioactivity of wollastonite glass-ceramic materials. Journal of Non-Crystalline Solids 2005;351:1716-26.

6. Dorozhkin SV. A review on the dissolution models of calcium apatites. Progress in Crystal Growth and Characterization of Materials 2002; pp.45-61

7. Petrov OE, Dyulgerova E, Petrov L, Popova R. Characterization of calcium phosphate phases obtained during the preparation of sintered biphase Ca-P ceramics. Materials Letters 2001;48:162-67.

8. Dorozhkina EI, Dorozhkin SV. Mechanism of the solid-state transformation of a calcium-deficient hydroxyapatite (CDHA) into biphasic calcium phosphate (BCP) at elevated temperatures. Chem Mater 2002;14:4267-72.

9. Bohner M. Calcium orthophosphates in medicine: from ceramics to calcium phosphate cements. Injury 2000;31(S4):D37-D47.

10. Brown WE, Chow LC. Dental restorative cement pastes. US Patent No. 4518430, 1985.

11. Tyllianakis M, Giannikas D, Panagopoulos A, et al. Use of injectable calcium phosphate in the treatment of intra-articular distal radius fractures. Orthopedics 2002;25(3):311-315.

12. Takegami K, Sano T, Wakabayashi H, et al. New ferromagnetic bone cement for local hyperthermia. J Biomed Mater Res: Appl Biomat 1998;43:210-214.

13. Heini PF, Berlemann U. Bone substitutes in vertebroplasty. Eur Spine J 2001;10:S203-215.

14. Phillips FM. Minimally invasive treatments of osteoporotic vertebral compression fractures. Spine 2003;28:S45-S53.

15. Lewis G. Injectable bone cements for use in vertebroplasty and kyphoplasty: state of the art review. J Biomed Mater Res: Appl Biomat 2005;76B(2):456-468.

16. Belkoff SM, Mathis JM, Jasper LE. Ex vivo biomechanical comparison of hydroxyapatite and polymethylmetacrylate cements for use with vertebroplasty. Am J Neuroradiol 2002;23:1647-51.

17. Bohner M. Physical and chemical aspects of calcium phosphates used in spinal surgery. Eur Spine J 2001;10:S114-S121.

18. Fernández E, Vlad MD, Gel MM, López J, Torres R, Cauich JV, Bohner M. Modulation of porosity in apatitic cements by the use of α-tricalcium phosphate–calcium sulphate dehydrate mixtures. Biomaterials 2005;26:3395-04.

19. Gisep A, Wieling R, Bohner M, Matter S, Schneider E, Rahn B. Resorption patterns of calcium-phosphate cements in bone. J Biomed Mater Res 2003;66:532-40.

20. Driessens FCM. Formation and stability of calcium phosphates in relation to the phase composition of the mineral in calcified tissues. In: De Groot K, editor. Bioceramics of Calcium Phosphate, CRC Press, Inc., Boca Raton, Florida, 1993, p. 1-32.

21. Bohner M, Gbureck U, Barralet JE. Technological issues for the development of more efficient calcium phosphate bone cements: a critical assessment. Biomaterials 2005;26:6423-29.

22. Fernández E, Vlad MD, Hamcerencu M, Darie A, Torres R, López J. Effect of iron on the setting properties of α-TCP bone cements. J Mater Sci 2005;40:3677-82.

23. Kannan S, Rocha JHG, Ventura JMG, Lemos AF, Ferreira JMF. Effect of Ca/P ratio of precursors on the formation of different calcium apatitic ceramics-An X-ray diffraction study. Scripta Materialia 2005;53:1259-62.

24. Lilley KJ, Gburech U, Wright AJ, Farrar DF, Barralet JE. Cement from nanocrystalline hydroxyapatite: Effect of calcium phosphate ratio. J Mater Sci Mater Med 2005;16:1185-90.

25. Wang H, Lee J-K, Moursi A, Lannutti JJ. Ca/P ratio effects on the degradation of hydroxyapatite in vitro. J Biomed Mater Res 2003;67A:599-08.

26. Burguera EF, Guitian F, Chow LC. Effect of the calcium to phosphate ratio of tetracalcium phosphate on the properties of calcium phosphate bone cement. J Biomed Mater Res 2008;85A:674-83.

27. Standard Test Method: ASTM C266-89. Time of setting of hydraulic cement paste by Gillmore needles. In: Annual book of ASTM standards, vol. 04.01. Cement, lime, Gypsum. Philadelphia, PA: ASTM. 1993;444-72.

28. Kreidler ER, Hummel FA. Phase relationships in the system SrO-P_2O_5 and the influence of ware vapour on the formation of $Sr_4P_2O_9$. Inorg Chem 1967;6:884-91.

29. Fernández E, Ginebra MP, Boltong MG, Driesens FCM, Ginebra J, De Maeyer EA, Verbeek RM, Planell JA. Kinetic study of the setting reaction of calcium phosphate bone cements. J Biomed Mater Res 1996;32:367-74.

30. Fernández E, Gil FJ, Ginebra MP, Driessens FCM, Planell JA, Best SM. Calcium phosphate bone cements for clinical applications. I: Solution chemistry. J Mater Sci Mater Med 1999;10:169-76.

31. Fernández E, Gil FJ, Ginebra MP, Driessens FCM, Planell JA, Best SM. Best. Calciumphosphate bone cements for clinical applications. II: Precipitate formation during setting reactions. J Mater Sci Mater Med 1999;10:177-83.

Chapter 5

Effect of iron on the setting properties of alpha-tricalcium phosphate bone cements

5.0. Structured abstract

Mini Abstract. This study reports on the setting and hardening properties of iron modified alpha-tricalcium phosphate (α-TCP) solid like solutions $(3.CaO\text{-}1.P_2O_5)_{1-x}(FeO)_x$. The results show that it is possible to obtain new ceramic materials from the ternary system «$CaO\text{-}P_2O_5\text{-}FeO$» with the ability to set as cement like materials when mixing a powder phase made of one and/or several of these new reactants, and an aqueous liquid phase. Moreover, these new cement reactants showed to be magnetic and the resulting cements too, even during the whole hydration process of the iron-modified α-TCP into iron-modified calcium deficient hydroxyapatite during hardening.

Study Design. Experimental study to characterize the setting and hardening properties of iron-modified alpha-tricalcium phosphate based cements.

Objective. To characterize the setting and hardening properties of iron-modified alpha-tricalcium phosphate based bone cements.

Summary of Background Data. Calcium phosphate bone cements (CPBCs) are biocompatible, bioactive (osteoclastic and osteoblastic activity) and versatile biomaterials used in a wide range of dental and orthopaedic applications. Recent research has proven that these materials could be of use after further optimization to spinal surgery too (*kypho-* and *vertebro-plasty*). However, most experimental and commercial CPBCs are based on α-TCP and experience shows that the cement properties of this reactant are very sensible to uncontrolled minor ion contamination during its production at high temperature. For this reason, in this study the iron-modification of α-TCP has been proposed as a way to control and stabilize the setting properties of this reactant.

Methods. Two different protocols were followed to sinter the iron-modified α-TCP ceramic phase, i.e. $\alpha\text{-}(3.CaO\text{-}1.P_2O_5)_{1-x}(FeO)_x$. Cement setting times were measured by the *Gillmore* needles method. The evolution of the compressive strength accounted for the

cement hardening process. The magnetic properties were evaluated with a standard Cobalt-Nickel magnet by visual inspection.

Results. The main results show that α-TCP production tailored in advance with small amounts of "iron-contaminants" proved to be a useful method to assure standard setting properties even in the case the main cement reactants could come negatively contaminated. In this sense, 0.3 *wt%* of iron-α-TCP contamination proved to be enough to recover the properties of unsetting cements. On the other hand, controlled iron-contamination showed synergies, i.e. both the cement's compressive and magnetic strengths increased with the iron addition. Finally, the α-TCP sintering route also showed to affect the setting and hardening properties of the resulting cements.

Conclusions. It is concluded that iron citrate modification of α-TCP's reactant is a good solution to improve setting, hardening and magnetic properties of α-TCP based bone cements. In general, the results could be further exploited by designing improved magnetic apatitic cements with suitable mechanical properties for use in dental, orthopaedic and spinal applications.

Key Points.

- New ceramic reactants with the ability to set as cement like materials can be sintered from the ternary system «CaO-P_2O_5-FeO».
- These new reactants are magnetic and the cements obtained from them, too.
- Small iron additions during the α-TCP sintering showed to stabilize the setting and hardening properties of α-TCP based cements.
- The setting, the hardening and the magnetic properties of iron-modified α-TCP cements improved with the iron addition.

5.1. Introduction

As has been commented in previous chapters, the main idea behind calcium phosphate bone cements (CPBCs) consists in making use of the different acidity of calcium phosphates to precipitate, after mixing a powder of at least two different calcium phosphates with a liquid phase, an apatitic mineral phase similar to that in bone tissues [1-9]. In such situation, the precipitated apatitic crystals evolve, due to the chemical reactions controlling the setting, into a mechanically stable microstructure of entangled crystals of hydroxyapatite [10,11]. This apatitic structure could be then reabsorbed *in vivo* by osteoclastic and osteoblastic activity [12-14]. In fact, due to the apatitic nature of the products of the setting reactions, these CPBCs have osteoconductive property [15]. Moreover, depending on the degree of crystallinity and porosity, CPBCs can be made to be more or less stable after implantation [15-19]. All these advantages support the new clinical research trials of CPBCs in spinal surgery applications (*kypho-* and *vertebro-plasties*) [20].

However, Chapter 4 came up with the problem of CPBCs' reproducibility setting properties as due to uncontrolled ionic contaminations affecting the true calcium-to-phosphorous (Ca/P) ratio of the cement. For this reason, the present research was planned with the objective of study the effect of controlled iron additions on the setting and hardening properties of alpha-tricalcium phosphate (α-TCP) bone cements, as a possible way to stabilize its setting properties. Iron ion was selected because, according to literature, there is also interest to extent the use of CPBCs to the treatment of certain types of bone cancer thorugh *hyperthermia therapies*.

Thus, the ternary system «CaO-P_2O_5-FeO» was investigated in order to obtain new ceramic reactants with the ability to set as cement like material when mixing a powder phase, made of one and/or several of these new reactants, and an aqueous liquid phase.

In this chapter, we report specifically on the setting and hardening properties of solid solutions like $(3.CaO\text{-}1.P_2O_5)_{1-x}(FeO)_x$. This is the first approach to the magnetic modification of α-TCP ($3.CaO\text{-}1.P_2O_5$) based cements.

5.2. Materials and methods

5.2.1. Preparation of α-TCP

In this study, two different protocols were followed to sinter the iron-modified α-TCP ceramic phase, i.e. $\alpha\text{-}(3.CaO\text{-}1.P_2O_5)_{1-x}(FeO)_x$. This approach was important to assure the stability of the properties of the end product. The manufacture protocols were as follow:

a) Protocol "A": Calcium hydrogen phosphate $CaHPO_4$ (DCP; *Sigma-Ref. C-7263*) and calcium carbonate $CaCO_3$ (CC; *Sigma-Ref. C-4830*) were mixed in a 2:1 molar ratio. Then, iron citrate $Fe(C_6H_5O_7)$ (IC; *Sigma-Ref. 22897-4*) was added at different weight proportions (1, 4, 8, 16 and 24 *wt%*) in respect of the theoretic weight of α-TCP produced. The whole mixture was homogenised by mixing in a planetary rotary mill (Pulverisette 6, by *Fritsch GmbH*) at low speed. Then, it was sintered at 1400°C for 2 h and quenched in air to room temperature («(T_0=20°C→T_1=300°C); r=2°C/min; d=1h», «(T_1=300°C→T_2=1100°C); r=2°C/min; d=2h», «(T_2=1100°C→T_3=1400°C); r=2°C/min; d=2h». The resulting ceramic material was powdered to an appropriate particle size (d_{50}=10 μm) for cement production.

b) Protocol "B": In this case, α-TCP was first sintered by a 2:1 molar ratio of a mixture of DCP and CC, following the same sintering program as that in P1. The resulting ceramic material was powdered following the same milling protocol as that in P1 and then, different amounts of IC (1, 4, 8, 16 and 24 *wt%*) were added to the α-TCP phase. The

resulting mixture was homogenised and sintered again to 1400°C during 2 h and then, quenched in air to room temperature («(T_0=20°C→T_3=1400°C); r=20°C/min; d=2h»). The final ceramic was powdered as in P1.

5.2.2. Preparation of cement

In this study, it was decided to produce *Biocement-H* [21], which is made of 98 *wt%* of α-TCP and 2 *wt%* of precipitated hydroxyapatite (PHA; *Merck-2143*), added as a seed in the powder phase. The liquid phase is an aqueous solution of 2.5 *wt%* of disodium hydrogen phosphate Na_2HPO_4 (DHP; *Merck-6586*). The liquid to powder (L/P) ratio was initially selected as 0.32 mL/g, which is the minimum ratio that assures suitable workability and cohesive properties, for *Biocement-H* [21]. However, for the new iron-modified cements the minimum L/P ratio was 0.30 mL/g. This L/P ratio's difference was maintained throughout the study. *Biocement-H* was selected mainly because it is ≈100 *wt%* α-TCP. In this sense, magnetic modification of *Biocement-H* should be of interest to other commercial α-TCP cements [20].

5.2.3. Preparation of controls

A positive and a negative control (+/-Control) of *Biocement-H* were produced. "+Control" behaved as expected from the point of view of the setting and hardening data reported in the literature [22]. However, "-Control" did not show hardening properties with time. The main difference between the controls was the lot number of the DCP ("+Control"=Sigma-Lot.11k0303; "-Control"=Sigma-Lot.122k0127) used to manufacture the α-TCP. This was studied to highlight the problem of scaling up production of α-TCP, which affects commercial and experimental α-TCP based cements, and especially reproducibility of data between different scientists.

5.2.4. Compressive strength measurements

Cylindrical (5 mm of diameter and 10 mm of height) cement samples (n=10 for statistics) were moulded in a stainless steel mould and immersed in Ringer's solution at 37°C for different hardening times. After completion they were unmoulded and tested in compression at a crosshead speed of 1 mm/min in an Electromechanical Testing Machine.

5.2.5. Setting times measurements

Initial (I) and Final (F) setting times were measured with the *Gillmore* needles [22,23]. Each measurement was repeated three times for statistic analysis.

5.2.6. Magnetic evaluation

The new iron-modified α-TCP based cements were evaluated for magnetic properties with a standard Cobalt-Nickel magnet by visual inspection of the effect of movement of compressive strength samples at different reaction times. Iron-modified α-TCP in both powder and granule form was tested similarly before cement sample preparation. A proper magnetic characterization is under way but is not presented in this PhD Thesis.

5.3. Results

5.3.1. Effects on the compressive strength

Figs. 5.1 and 5.2 show the results of the evolution of the compressive strength, C(MPa), *versus* the amount of the iron citrate, IC(*wt*%), for the "-Control" (L/P=0.30 mL/g) and for the manufacturing protocols "A" and "B", respectively. The figures contain data at two different hardening times, 4 and 24 h.

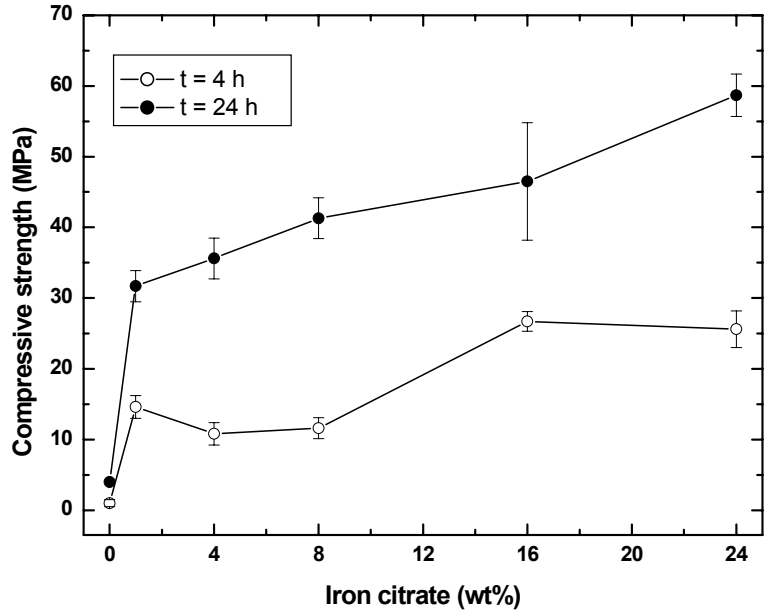

Figure 5.1. Evolution of the compressive strength, C(MPa), as a function of the iron citrate, IC(*wt*%), for the "-Control" (L/P=0.30 mL/g) and the protocol "A".

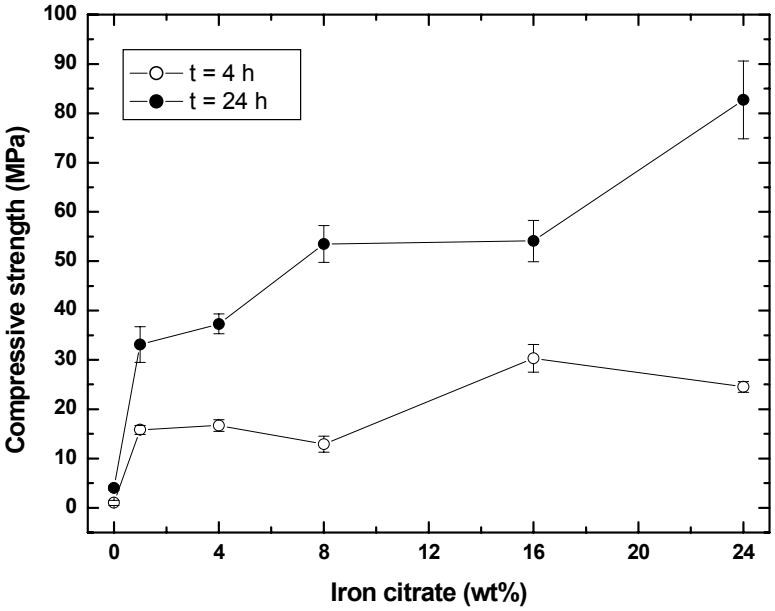

Figure 5.2. Evolution of the compressive strength, C(MPa), as a function of the iron citrate, IC(*wt*%), for the "-Control" (L/P=0.30 mL/g) and the protocol "B".

Fig. 5.3 shows the evolution of the compressive strength, at two different hardening times, 4 and 24 h, for the positive ("+Control"; L/P=0.32 mL/g), the negative ("-Control"; L/P=0.30 mL/g) and the recovered ("-Control+24 *wt*%IC"; L/P=0.30 mL/g) control. In this figure data correspond to cements made with the manufacture protocol "A".

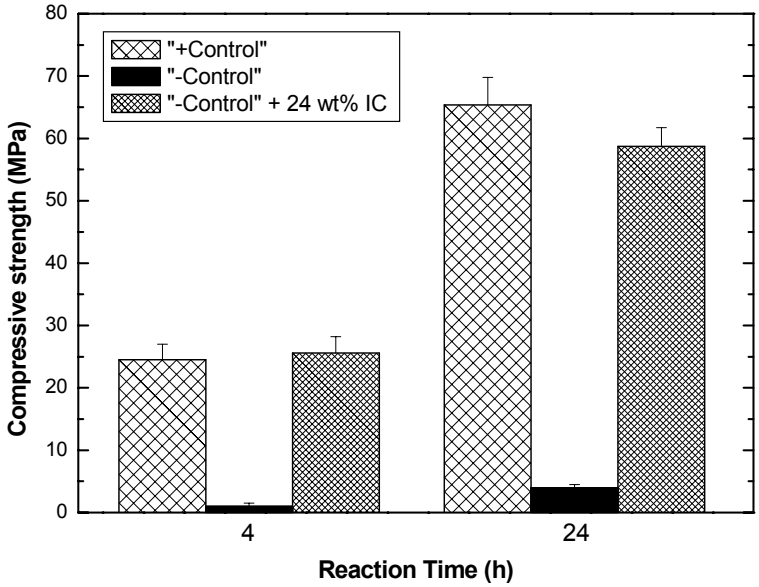

Figure 5.3. Compressive strength, C(MPa), at 4 and 24h of reaction time, for "+Control" (L/P=0.32 mL/g), "-Control" (L/P=0.30 mL/g) and the recovered "-Control+24 *wt*%IC" (L/P=0.30 mL/g), all of them made with the protocol "A".

Figs. 5.4 and 5.5 show the effect of the manufacture protocols, "A" and "B", for a 4 *wt*% IC-modified "+Control" (L/P=0.30 mL/g) cement sample, on the compressive strength, after 4 and 24 h of hardening, and on the setting times, respectively.

Figs. 5.6 and 5.7 show the evolution of the compressive strength *versus* the reaction time (hardening curves) as a function of the iron citrate, IC(*wt*%), for "-Control" (L/P=0.30 mL/g) made with the manufacture protocol "A" and "B", respectively.

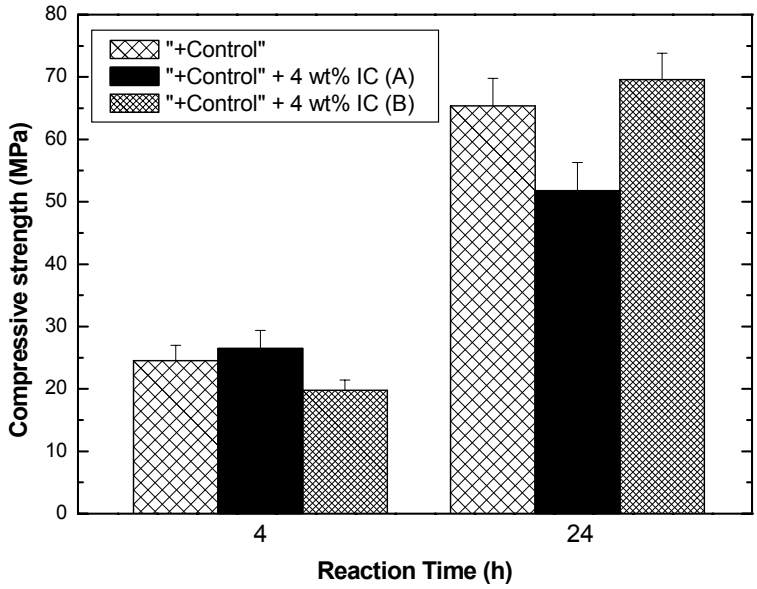

Figure 5.4. Compressive strength, C(MPa), at 4 and 24 h of reaction time, for a 4 *wt%* IC-modified "+Control" (L/P=0.30 mL/g): Effect of protocols "A" and "B".

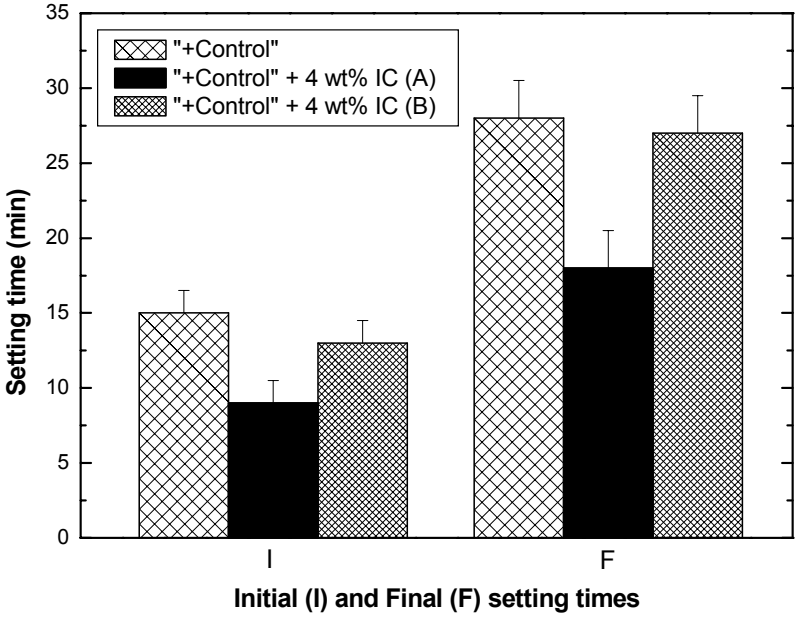

Figure 5.5. Setting times, I(min) and F(min), for a 4 *wt%* IC-modified "+Control" (L/P=0.30 mL/g): Effect of protocols "A" and "B".

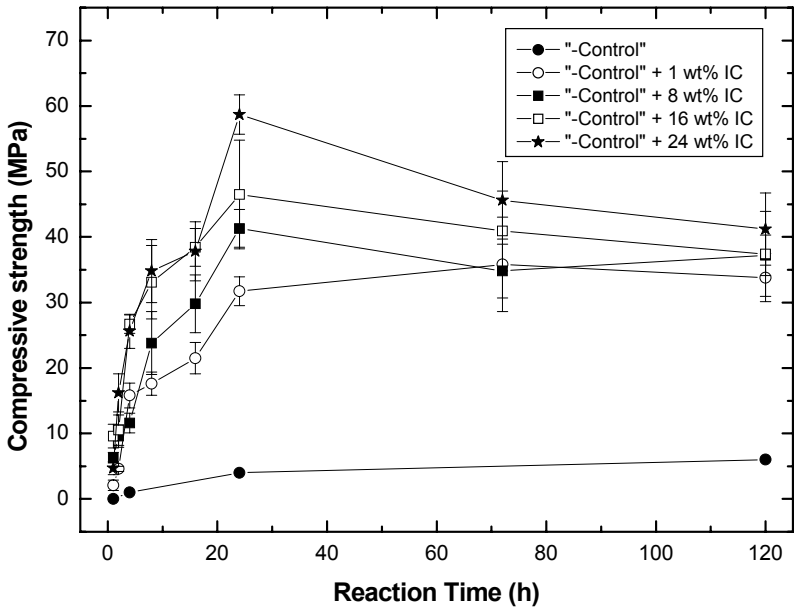

Figure 5.6. Hardening curves as a function of the iron citrate, IC(*wt%*), for "-Control" (L/P=0.30 mL/g) made with the protocol "A".

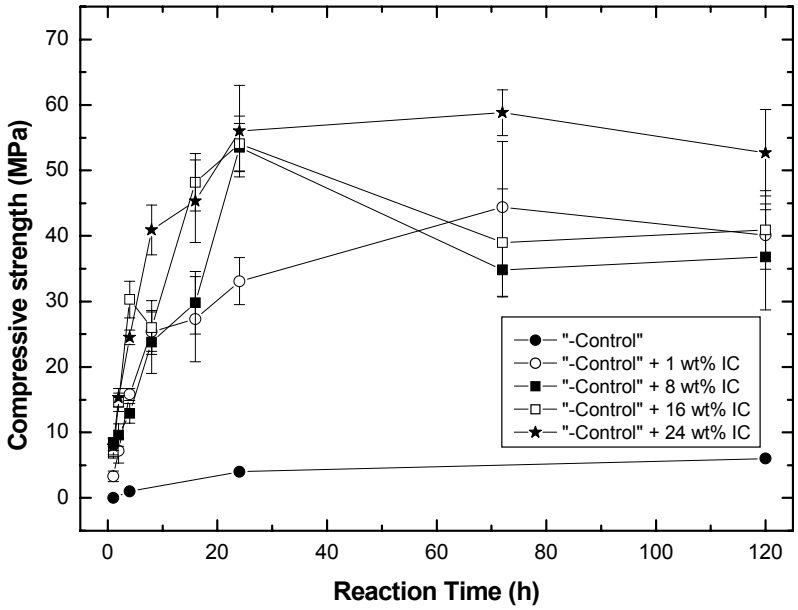

Figure 5.7. Hardening curves as a function of the iron citrate, IC(*wt%*), for "-Control" (L/P=0.30 mL/g) made with the protocol "B".

5.3.2. Effects on the setting times

Finally, Fig. 5.8 shows the evolution of the setting times, I(min) and F(min), *versus* the amount of the iron citrate, IC(*wt%*), for "-Control" (L/P=0.30 mL/g), as a function of the manufacture protocols "A" and "B".

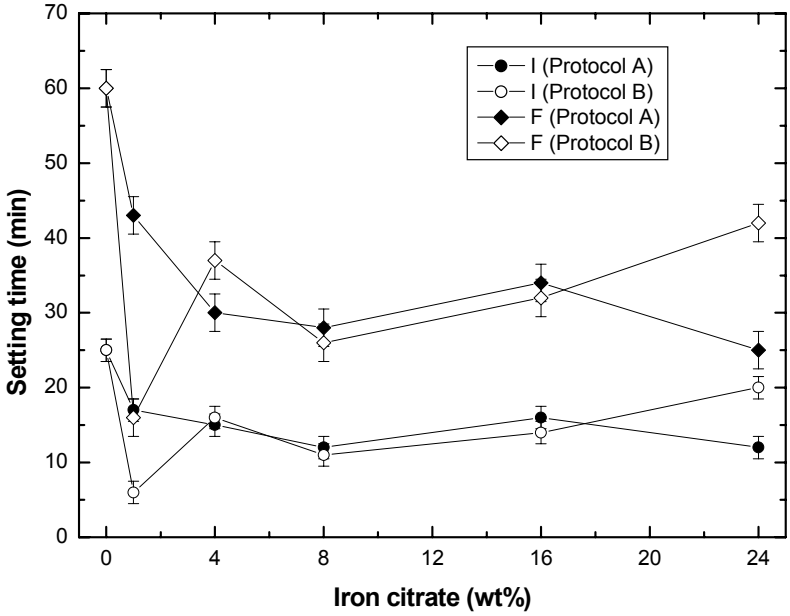

Figure 5.8. Setting times, I(min) and F(min), for "-Control" (L/P=0.30 mL/g) as a function of the iron citrate, IC(*wt%*): Effect of protocols "A" and "B".

5.4. Discussion

Probably, one of the most practical and important results of this study is found in Figs. 5.1 and 5.2. No matter the protocol used to manufacture the α-TCP, i.e. "A" and "B", those figures show that to recover the normal setting and hardening properties of a negative control of *Biocement-H* (in this case, "-Control"), it is just enough to modify the standard α-TCP production with less than 0.3 *wt%* of iron (i.e. 1.57 mol%-Fe over 99.43 mol%-α-

TCP). Obviously, no one working in bone cements makes negative controls of his experimental and commercial formulations; this is something that simply occurs, and scientists working on this field know the headache produced every time this happens. At the moment there is not in the literature any study focussing on the deleterious or the beneficial effect of very small amounts of certain ionic elements on the hydration properties of the α-TCP. Sometimes, it has been reported that magnesium contamination of the reactants used during the fabrication of the α-TCP, and specially that of the monetite ($CaHPO_4$), is the cause for not having setting and hardening properties on α-TCP based cements. This has sense because, as it is known, the hardening of α-TCP cements is due to nucleation, precipitation and growth of calcium deficient hydroxyapatite crystals (CDHA; $Ca_9(HPO_4)(PO_4)_5OH$), [24,25] and nucleation of apatite crystals is blocked by magnesium ions [26]. Unfortunately, chemical analysis of positive and negative α-TCP batches do not ever show any significant difference in the minor ionic contaminants. For this reason, α-TCP production tailored in advance with small amounts of "iron-contaminants" seems a novel and useful method to assure standard properties even in the case the main reactants could come negatively contaminated. It should be noted that the maximum amount of iron addition (i.e. 24 *wt%*IC) used in this study during the α-TCP modification was too small as to not detect by X-ray diffraction other chemical phases than α-TCP (data not shown).

Moreover, Figs. 5.1 and 5.2 show the same increasing tendency for "-Control" (no matter the protocol used to fabricate the α-TCP, i.e. "A" in Fig. 5.1 or "B" in Fig. 5.2) of the compressive strength, attained at 4 and/or 24 h of hardening, as the amount of iron citrate was increased during the α-TCP manufacturing protocols.

In fact, Fig. 5.3 shows how relevant iron-modification could be to recover the standard properties of a positive control of *Biocement-H* (+Control). In this case, the compressive strength of "+Control", after 4 and 24 h of hardening, was around 25(±3) and 65(±4) MPa,

respectively. In comparison, "-Control" showed 1(±0.5) and 4(±0.5) MPa in the same conditions. If we consider that the static strength supported by the cement at its final setting time, F, as measured by the *Gillmore* needles, is the equivalent to 5 MPa [23] then, "-Control" simply did not set and so it was easily deformed under the pressure of two fingers. However, when "-Control" was modified with 24 *wt%*-IC, under the protocol "A", the values encountered for the compressive strength were statistically the same ($p>0.05$) as those reported for the "+Control".

Whether or not the different protocols "A" and "B" had significant effects on the hardening and the initial setting of *Biocement-H* (in this case, "+Control") is analysed from Figs. 5.4 and 5.5. Fig. 5.4 shows no significant differences ($p>0.05$) after 4 h of hardening between the "+Control" and the same control modified with 4 *wt%*-IC, no matter the protocol. However, after 24 h of hardening, the protocol "B" showed better compressive strength results (and statistically significant, i.e. $p<0.05$), as compared to the protocol "A" and in agreement with the values of "+Control". If we consider, at the same time, what happened with the initial setting properties (see Fig. 5.5 for the setting times) then, the protocol "B" also agreed to the data of "+Control" but the protocol "A" showed statistically better results (i.e. lower I and F setting times). This means that with protocol "A" the chemical reactions controlling the initial setting of *Biocement-H* (i.e. dissolution of α-TCP particles, nucleation and precipitation of apatite-like crystals) are faster than with protocol "B". This is in agreement with the results in Fig. 5.4 where in fact it is known, experimentally, that higher setting times (i.e. slow chemical reactions) are directly correlated to also higher values of compressive strength (i.e. more develop and compact crystalline microstructure). A possible explanation could be related to a more significant presence of iron (both, in the form of α-TCP iron solid solutions and/or stable iron phases) on and/or around the surface of the α-TCP particles in protocol "B" rather than a more favoured volume diffusion and/or precipitation of phases of iron in protocol "A".

This has been corroborated by pH analysis, where α-TCP manufactured with protocol "B" showed less basic values (pH≈8.7) than both the one with "A" (pH≈9.2) and the "+Control" (pH≈9.7). This is in agreement to a higher iron protonation in the solution. This chemical reaction should be lowering the supersaturation of the solution and so retarding the precipitation of apatite-like crystals. A further study is on its way to understand exactly what is happening.

If we look at the hardening curves, Figs. 5.6 and 5.7 also show interesting results. For example, when the negative control of *Biocement-H* (-Control) was modified with IC, from 1 *wt%*-IC to 24 *wt%*-IC, the hardening curves of modified *Biocement-H*'s cements graduated in average to higher values as the amount of IC increased. This is a noticeable result because thanks to the iron-modification of the α-TCP, which is also applicable to tetracalcium phosphate and α-TCP, we have a way to increase at the same time the mechanical and the magnetic strength (as confirmed by the Cobalt-Nickel magnet; see *5.2.6. Magnetic evaluation*) of both experimental and commercial new bone cements.

Moreover, this synergetic effect had also its influence on the setting times. The I and the F setting time for the "-Control" were 25(±1) min and ≥24 h, respectively (note that in Fig. 5.8 the F-time has been represented for clarity as F≡60 min). However, with just 1 *wt%*-IC the I-time was reduced to ≈6(±1) min and the F-time to ≈16(±2) min when the protocol "B" was used. In this case, i.e. 1 *wt%*-IC, protocol "A" showed higher values for the setting times, I≈17(±1) min and F≈44(±2), but for the rest of the IC values the differences between protocols were not significant ($p>0.05$) until 24 *wt%*-IC, where protocol "B" did show higher values than protocol "A". Despite the individual differences between values, which are difficult to explain, the most important result is the fact that the setting times of *Biocement-H* are not drastically affected by the IC modification. On the other hand, they are controlled into an appropriate range of values that could be even

further optimised to the present medical applications, for example, by using increasing amounts of accelerators such as DHP.

These results in conjunction with the results obtained for the hardening curves in Figs. 5.6 and 5.7 and the fact that IC modification gives *Biocement-H* magnetic properties, as an added value, are the most relevant results both from the scientific and the commercial point of view.

5.5. Summary conclusion

In this study, it is reported that a new family of iron modified calcium phosphates, whose chemical compositions can be written, in general, as α/β-$(3.CaO\text{-}1.P_2O_5)_{1-x}(FeO)_x$, $(4.CaO\text{-}1.P_2O_5)_{1-x}(FeO)_x$, $(10.CaO\text{-}3.P_2O_5)_{1-x}(FeO)_x$, show magnetic properties and, at the same time, they present intrinsic different acidities. Thus, these new reactants show cement-like properties when mixed together into a cement powder phase while being magnetic throughout the whole setting. These new magnetic cements could be of use after further optimisation: a) to stabilise bone fractures and/or to fill bone cavities; b) to treat osteosarcoma; c) as new thermal and magnetic activated drug delivery systems; and d) as new scaffolds to bone tissue engineering, among others [27].

References

1. Brown WE, Chow LC. Dental restorative cement pastes. US Patent No.: 4,518,430. Priority Data: May 21, 1985.

2. Brown WE, Chow LC. A new calcium phosphate water-setting cement. In: Brown PW, editor. Cements Research Progress. Westerville, Ohio. American Ceramic Society; 1986, p. 351-79.

3. Lemaitre J, Mirtchi A, Mortier A. Calcium phosphate cements for medical use: state of the art and perspectives of development. Sil Ind Ceram Sci Tech 1987;52:141-6.

4. Chow LC, Takagi S, Constantino PD, Friedman CD. Self-setting calcium phosphate cements. Mat Res Soc Symp Proc 1991;179:3-24.

5. Chow LC. Development of self-setting calcium phosphate cements. J Ceram Soc Japan (International Edition) 1992;99:927-36.

6. Sugama T, Allan M. Calcium phosphate cements prepared by acid-base reaction. J Am Ceram Soc 1992;75(8):2076-87.

7. Lemaitre J. Injectable calcium phosphate hydraulic cements: new developments and potential applications. Innov Tech Biol Med 1995;16(1):109-20.

8. Fernández E, Gil FJ, Best SM, Ginebra MP, Driessens FCM, Planell JA. Calcium phosphate bone cements for clinical applications: I. Solution chemistry. J Mater Sci Mater Med 1999;10:169-76.

9. Fernández E, Gil FJ, Best SM, Ginebra MP, Driessens FCM, Planell JA. Calcium phosphate bone cements for clinical applications: II. Precipitate formation during setting reactions. J Mater Sci Mater Med 1999;10:177-83.

10. Nilsson M, Fernández E, Sarda S, Lidgren L, Planell JA. Characterisation of a novel calcium phosphate/sulphate bone cement. J Biomed Mater Res 2002;61(4):600-7.

11. Fernández E, Gil FJ, Best SM, Ginebra MP, Driessens FCM, Planell JA. Improvement of the mechanical properties of new calcium phosphate bone cements in the $CaHPO_4$-α-$Ca_3(PO_4)_2$ system: Compressive strength and microstructural development. J Biomed Mater Res 1998;41:560-67.

12. Knabe C, Driessens FCM, Planell JA, Gildenhaar R, Berger G, Reif D, Fitzner R, Radlanski RJ, Gross U. Evaluation of calcium phosphates and experimental calcium phosphate bone cements using osteogenic cultures. J Biomed Mater Res 2000;52:498-08.

13. Ohura K, Bohner M, Hardouin P, Lemaitre J, Pasquier G, Flautre B, Blary MC. Resorption and bone formation of new α-tricalcium phosphate-monocalcium phosphate cements: an in vivo study. J Biomed Mater Res 1996;30:193-200.

14. Oreffo ROC, Driessens FCM, Planell JA, Triffitt JT. Growth and differentiation of human bone marrow osteoprogenitors on novel calcium phosphate cements. Biomaterials 1998;19:1845-54.

15. Driessens FCM, Planell JA, Boltong MG, Khairoun I, Ginebra MP. Osteotransductive bone cements. Proc Instn Mech Engrs 1998;212H:427-35.

16. Charrière E, Lemaitre J, Zysset Ph. Hydroxyapatite cement scaffolds with controlled macroporosity: fabrication protocol and mechanical properties. Biomaterials 2003;24:809-17.

17. Sarda S, Nilsson M, Balcells M, Fernández E. Influence of surfactant molecules as air-entraining agent on bone cement macroporosity. J Biomed Mater Res 2003;65A:215-21.

18. Barralet JE, Grover L, Gaunt T, Wright AJ, Gibson IR. Preparation of macroporous calcium phosphate cement tissue engineering scaffold. Biomaterials 2002;23:3063-72.

19. Bohner M. Calcium phosphate emulsions: possible applications. Key Eng Mater 2001;192-195:765-8.

20. Bohner M. Physical and chemical aspects of calcium phosphates used in spinal surgery. Eur Spine J 2001;10:S114-21.

21. Khairoun I, Driessens FCM, Boltong MG, Planell JA, Wenz R. Addition of cohesion promotors to calcium phosphate cements. Biomaterials 1999;20:393-8.

22. Ginebra MP, Driessens FCM, Planell JA. Effect of the particle size on the micro and nanostructural features of a calcium phosphate cement: a kinetic analysis. Biomaterials 2004;25:3453-62.

23. Standard Test Method: ASTM C266-89. Time of setting of hydraulic cement paste by Gillmore needles. In: Annual book of ASTM standards, vol. 04.01. Cement, lime, Gypsum. Philadelphia, PA: ASTM. 1993;444-72.

24. Ginebra MP, Fernández E, De Maeyer EAP, Verbeeck RMH, Boltong MG, Ginebra J, Driessens FCM, Planell JA. Setting reaction and hardening of an apatitic calcium phosphate cement. J Dent Res 1997;76(4):905-12.

25. Fernández E, Ginebra MP, Boltong MG, Driessens FCM, Ginebra J, De Maeyer EAP, Verbeeck RMH, Planell JA. Kinetic study of the setting reaction of a calcium phosphate bone cement. J Biomed Mater Res 1996;32:367-74.

26. Driessens FCM. Formation and stability of calcium phosphates in relation to the phase composition of the mineral in calcified tissues. In: De Groot K, editor. Bioceramics of Calcium Phosphate, CRC Press, Inc., Boca Raton, Florida, 1993, p. 1-32.

27. Fernández E. Fosfatos de calcio modificados con hierro. Spanish Patent No. ES2257131 (A1). Universidad Politécnica de Cataluña. Priority Date: 01/10/2003.

Chapter 6

Cytocompatibility study of novel iron-modified apatitic bone cement

6.0. Structured abstract

Mini Abstract. In this study, the cytocompatibility of human ephitelial (HEp-2) cells cultured on new iron-modified calcium phosphate cements (IM-CPCs) was investigated in terms of cell adhesion, cell proliferation and morphology. Quantitative MTT-assay and scanning electron microscopy (SEM) showed that cell adhesion and viability were not affected with culturing time by iron concentration in a dose-dependent manner. SEM-cell morphology showed that HEp-2 cells, seeded on IM-CPCs, were able to adhere, spread and attain normal morphology. These results showed that IM-CPCs have cytocompatible features of interest to spinal applications for the treatment of osteoporotic vertebral compression fractures.

Study Design. Experimental study to characterise the cytocompatibility properties of apatitic bone cement.

Objective. To investigate the cytocompatibility properties of new iron-modified calcium phosphate bone cements.

Summary of Background Data. In the last years, a large number of studies have been conducted to prove the biomedical applicability of iron-modified biomaterials. Calcium phosphate bone cements (CPBCs) are clinically used in a wide range of applications for bone repair in dental and orthopaedic pathologies (to stabilize bone fractures, bone tumours and osteoporosis). In Chapter 5, it was shown that iron modification improves the setting, hardening and magnetic properties of α-TCP based bone cements, which is of interest to certain clinical applications. However, despite iron is required from eukaryotic cells for survival and proliferation, requirements of clearance of iron from the body often arise, because in extreme case, an excess of "free" reactive iron might promote oxidative damage. For this reason, the cytocompatibility of the new IM-CPCs was approached in

this chapter by analyzing and quantifying the response (adhesion, morphology, viability) of HEp-2 cells seeded on different IM-CPCs substrates.

Methods. The cytocompatibility was analysed by culturing human ephitelial cells onto iron-modified cements and controls and evaluating both the relative cell viability and the adhesion cell density. SEM followed the morphological features of cell adhesion and proliferation processes.

Results. Direct-contact cellular cultures onto iron-modified "non-active α-TCP" (see Chapter 5) based cement substrates showed that the cellular viability of the IM-CPCs increased with the iron-amount addition. The results clearly demonstrated that the IM-CPCs showed similar initial cell attachment and viability profiles as the "active α-TCP" cement control. Moreover, they had higher ability to enhance adhesion and proliferation of HEp-2 cells as compared with the "non-active α-TCP" control cement. This confirms that α-TCP iron modification is an improved way to recover not only the setting and hardening properties of α-TCP based cements (see Chapter 5), but also to recover their *in vitro* cytocompatibility.

Conclusions. It has been shown that iron-modified α-TCP based bone cements have the ability to support cellular colonization. Both quantitative and morphologic evaluations showed that adhesion, proliferation and viability of HEp-2 cells were not negatively influenced by iron concentration in a dose-dependent manner.

Key Points.

- The iron citrate modification of the α-TCP's reactant significantly enhanced the cytocompatibility of the resulting α-TCP based bone cements.
- The iron modification of α-TCP did not show negative dose-dependent effects on HEp-2 cell's adhesion, viability and morphology.
- The new resulting IM-CPCs showed to be non cytotoxic.

6.1. Introduction

In the last years, a large number of studies have been conducted to prove the biomedical applicability of iron-modified biomaterials in thermotherapy procedures [1-3], drug targeting [4] or as contrast agents in magnetic resonance imaging [5]. However, requirements of clearance of iron from the body often arise.

Iron is required from eukaryotic cells for survival and proliferation. The cellular iron metabolism is apparently *sine qua non* for cell replication; particularly, when cells are subjected to acute grow conditions [6]. The biological importance of iron is largely attributable to its chemical properties as a transition metal [7]. The most intracellular free iron is in the ferric state (Fe^{3+}) and during the intracellular events is reduced in a ferrous form (Fe^{2+}), which catalyzes free radical formation in the Fenton reaction [8]. However, in extreme case, an excess of "free" reactive iron might exceed the cell homeostatic capacity, thus compromising its integrity [6-8].

Calcium phosphate bone cements (CPBC) are clinically used in a wide range of applications, due to their ease of use, conformability, excellent plastic behaviour before hardening and high biocompatibility after being implanted *in vivo* [9]. Apatitic calcium phosphate cements set *in situ* by forming a net of entangled crystals of bone-like hydroxyapatite [10,11] that has demonstrated to show good osteointegration [12,13]. These characteristics make CPBCs promising materials for bone repair in dental and orthopaedic applications (to stabilize bone fractures, bone tumours and osteoporosis) [14-17]. Despite all these advantages, CPBCs lack of mechanical strength and this limits their applications to non-load bone bearing situations [18]. Moreover, with the advent of minimally spinal invasive surgery techniques (vertebroplasty and kyphoplasty) it has been put forward that apatitic cements are difficult to inject into the compression fractured osteoporotic vertebras [18-20].

However, it has been showed recently that iron modification improves the mechanical strength and the injectability of apatitic bone cements [21,22], which is of interest to spinal applications. Taking into account the comments given earlier, it is necessary to show at this stage that iron-modified calcium phosphate cements (IM-CPCs) are cytocompatible. For this reason, the cytocompatibility of the new IM-CPCs has been approached in this study by analyzing and quantifying the response (adhesion, morphology, viability) of human epithelial HEp-2 cells seeded on different IM-CPCs substrates.

6.2. Materials and methods

6.2.1. Cement substrates

Cement powder's phase was made of 70 *wt%* alpha-tricalcium phosphate (α-TCP; α-$Ca_3(PO_4)_2$ and 30 *wt%* of calcium sulphate dihydrate (CSD; $CaSO_4 \cdot 2H_2O$; *Sigma-C3771*) used as a porosity control agent (see Chapter 3) to improve further *in vivo* cellular colonization [23]. The α-TCP used was of two types: a) a fast hydration rate α-TCP (*CemContr*; by *Mathys Medical, Switzerland*); and b) a slow hydration rate α-TCP (*Cem-N*; inlab preparation). Moreover, the slow hydration rate α-TCP was modified by sintering it again with 1, 8 and 24 *wt%* of iron citrate (*CemIC1*, *CemIC8* and *CemIC24*). Details have been explained in Chapter 5. On the other hand, the aqueous cement liquid phase was modified with 2.5 *wt%* disodium hydrogen phosphate (DHP; Na_2HPO_4; *Panreac-131679*). The liquid to powder (L/P) ratio was 0.32 mL/g. After mixing, the cement paste was immediately placed into disk moulds to ensure standardized shapes (10 mm diameter by 2 mm height). The cement disks were removed from the moulds after setting for 30 min in Ringers solution at 37°C. Immediately after, the disks were sterilized by UV-irradiation for 30 min and then used as substrates for cell culture.

6.2.2. Cytocompatibility testing

6.2.2.1. Cell culture

HEp-2 cells (epithelial cells derived from a human laryngeal carcinoma) were cultured in Dulbecco's modified Eagle medium (DMEM) supplemented with 10% foetal bovine serum, 1% penicillin/streptomycin/L-glutamine (*Sigma Chemical Co., USA*) in humidified atmosphere of 95% air, 5% carbon dioxide at 37°C. The medium was changed every 2 days. Cultures of 90% confluent cells were rinsed with phosphate buffered saline (PBS) and detached by incubating with trypsin/ethylenediaminetetraacetic acid (EDTA) (*Sigma Chemical Co., USA*). The detached cells were resuspended in fresh media and counted using a hemocytometer and 4% trypan blue as dye vital. The HEp-2 cells were seeded on top of cement samples at a density of $5x10^4$ cells/well. Each cement disk was placed on the assigned well (24-well polystyrene-treated standard culture plate); before cell seeding, 200 μl of the culture medium was added into each well in order to minimize the number of cells attaching to the side and bottom's well or under the surface's disk. The wells containing cell culture medium without cement sample were used as controls (*Control-wells*).

6.2.2.2. Cell viability

To determine cell viability, the cells cultured on the cement substrates were evaluated after 1 and 6 days (1D and 6D) of incubation, using a quantitative MTT-assay. For this purpose, the medium in the wells was replaced with fresh medium and then 40 μl of MTT (3-(4,5-dimethyltiazol-2-yl)-2,5-diphenyltetrazolium bromide) dye solution (3 mg/ml in PBS) was added on each well. After 3 h of incubation at 37°C, the medium was removed and formazan crystals (i.e. dark-blue insoluble product formed inside the viable

cells, due to activity of mitochondria dehydrogenases) were solubilised with 500 μl of dimethylsulphoxide (DMSO) under continuous agitation (*Mini Rocker MRI; Boeco, Germany*) for 15 min, to facilitate the dissolution of the reacted dye. The liquid of each sample was removed for assay, which was performed in a 96-well plate. The absorbance of each well (i.e. the colour intensity directly related to the number of viable cells) was read on a microplate reader (*Anthos 2020 Microplate Reader; ASYS Hitech, Austria*) at wavelength of 540 nm. The background absorbance produced by wells containing no liquid was subtracted from all the samples. The number of cells was determined using a linear equation obtained from a calibration curve containing absorbance values against different counts of cells. *Cell relative viability (%)* was calculated by $N_{test}/N_{control}$ x 100; where N_{test} is the number of cells corresponding to the tested sample and $N_{control}$ is the number of cells corresponding to the Control-wells.

6.2.2.3. Cell adhesion

The effect of the five experimental cement substrates on HEp-2 cells adhesion was determined as follows: the cells were cultured onto the cement disks for 1 and 6 days; the samples were washed with PBS to eliminate unattached or dead cells; cement disks were placed in new 24-well plate and evaluated by the MTT-assay following the experimental conditions described in the above sections. The *Adhesion profile (cells/cm²)* was obtained by normalizing the number of cells adhered onto the cements to the disk-cement area available for cell's attachment.

6.2.3. Morphological study

Cells cultured for 1 and 9 days onto the experimental cement substrates and *Thermanox* coverslips (as positive cytocompatible control, *TMX*; *Nunc, Sigma, Spain*) were rinsed with PBS, fixed with 2.5% glutaraldehyde and subjected to graded alcohol dehydrations,

and then sputter coated with gold. A scanning electron microscope (SEM, *JEOL JSM-5610; Hitachi, Japan*) was used to examine the cells onto disk-cements.

6.2.4. Statistical analysis

Each experiment was done in quadruplicate. The results were expressed as mean ± standard deviation (mean ± SD). A one-way ANOVA test was used to analyze the mean variance of the data. Turkey's multiple comparison was used to compare the data at a family confidence coefficient of 0.95. Statistical significance was accepted at a level of p-value < 0.05.

6.3. Results

6.3.1. Cytocompatibility

Fig. 6.1 shows the *Cell relative viability (%)* of HEp-2 cells after 1 and 6 days of culture on iron-modified calcium phosphate cements (*CemIC1, CemIC8, CemIC24*), *CemContr* and *Cem-N* substrates, which was quantitatively evaluated using the MTT-assay (see 6.*2.2. Cytocompatibility testing*). After 1 day of culture, all the cements showed similar level of viability, ($p>0.05$). The growth and proliferation on all the cements tested increased with the increase of culturing time. After 6 days of culture the viability of the cells cultured on *CemContr* was statistically significant ($p<0.05$) as compared to *Cem-N* and *CemIC1*. Significant differences were also found among the IM-CPCs, i.e. *CemIC1* showed lower level of viability than *CemIC24* ($p<0.05$).

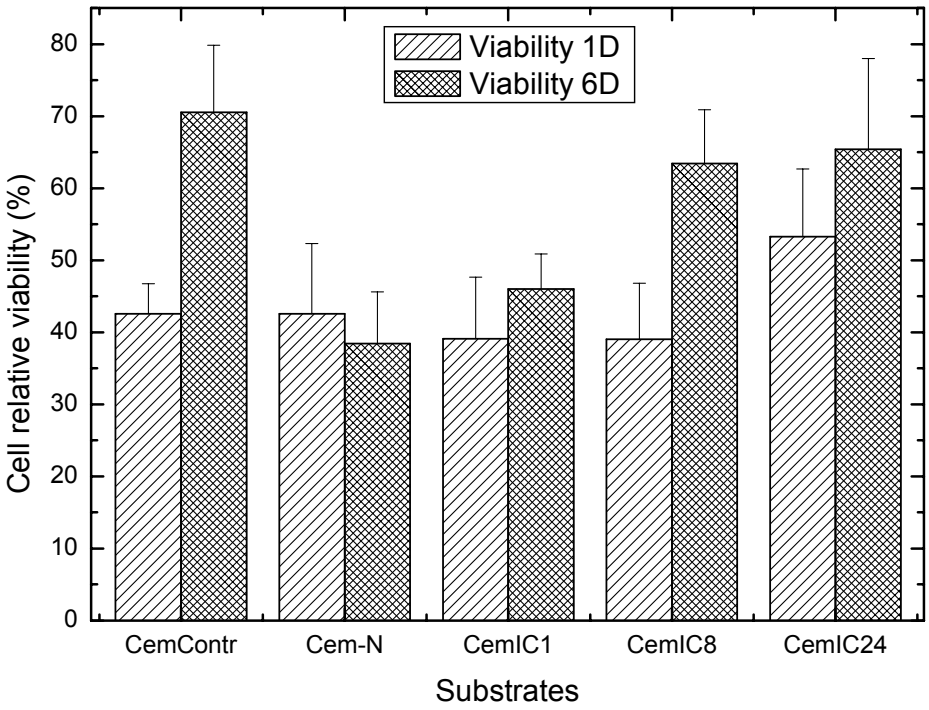

Figure 6.1. Cell relative viability *vs.* cement formulations: Effect of iron-modified cements on cells viability after 1 and 6 days of culturing (i.e. 1D and 6D).

Fig. 6.2 shows the *Adhesion profile (cells/cm²)* of HEp-2 cells onto *CemContr*, *Cem-N*, *CemIC1*, *CemIC8* and *CemIC24* substrates after cellular culture for 1 and 6 days. All the cements developed similar adhesion profiles after 1 day ($p>0.05$). However, after 6 days, it was observed that the adhesion rate increased with the culture time with no significant differences among the iron-modified and the control (i.e. *CemContr*) substrates ($p>0.05$). On the other hand, the non-active α-TCP control (i.e. *Cem-N*) showed no significant adhesion and proliferation results with the increase of the culture time ($p<0.05$).

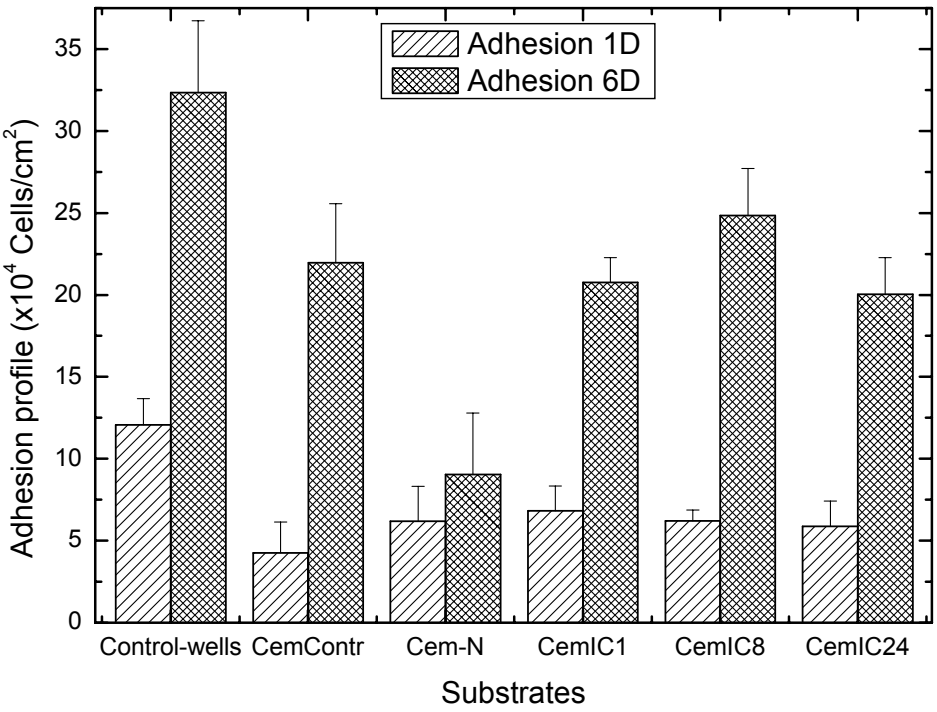

Figure 6.2. Adhesion profile *vs.* cement formulations: Effect of iron-modified cements on cells adhesion during 1 and 6 days of culturing (i.e. 1D and 6D).

6.3.2. Cellular morphology

Figs. 6.3 to 6.5 show the morphology of HEp-2 cells cultured onto *CemContr*, *CemIC1*, *CemIC8*, *CemIC24* and *TMX* respectively, for 1 and 9 days. Cells cultured for 1 day had proliferated and the tendency to form a confluent cell monolayer was observed on all the cements, as shown in Fig. 6.3 (see left column). The cellular density qualitatively appeared similar on *CemContr* and *CemIC24*. These observations are in correspondence with the quantitative data in Fig. 6.2.

Fig. 6.3 (see right column) and Fig. 6.4 show that cells attached and spread in a comparable manner on all the substrates, i.e. the cells developed many filopodia and

large lamellipodia. After 1 day, the cells onto cements' surfaces had a flat appearance and showed similar bipolar and/or tripolar spindle-like morphology, seeming to attach on specific surface's structural sites like sharp or ridge reliefs. A higher magnification is shown in Fig. 6.4, where cytoplasmic processes are observed attaching to the cement's surface. On the other hand, picture B in Fig. 6.4 (see top-right) shows cell-cell interactions on the cement's surface.

Fig. 6.5 shows the results of cells cultured on *TMX* and *CemIC8* for 9 days. It was observed that some small areas were not covered by a confluent cell monolayer. This is characteristic for carcinogenic cells; i.e. after reaching maxima confluence some cells spontaneously detach. Fig. 6.5-D shows HEp-2 cells in the process of dividing. A higher magnification of cytoplasmic processes of HEp-2 cells anchored to the hydroxyapatite crystals of *CemIC8* surface is also shown in Fig. 6.5 (see pictures E-H).

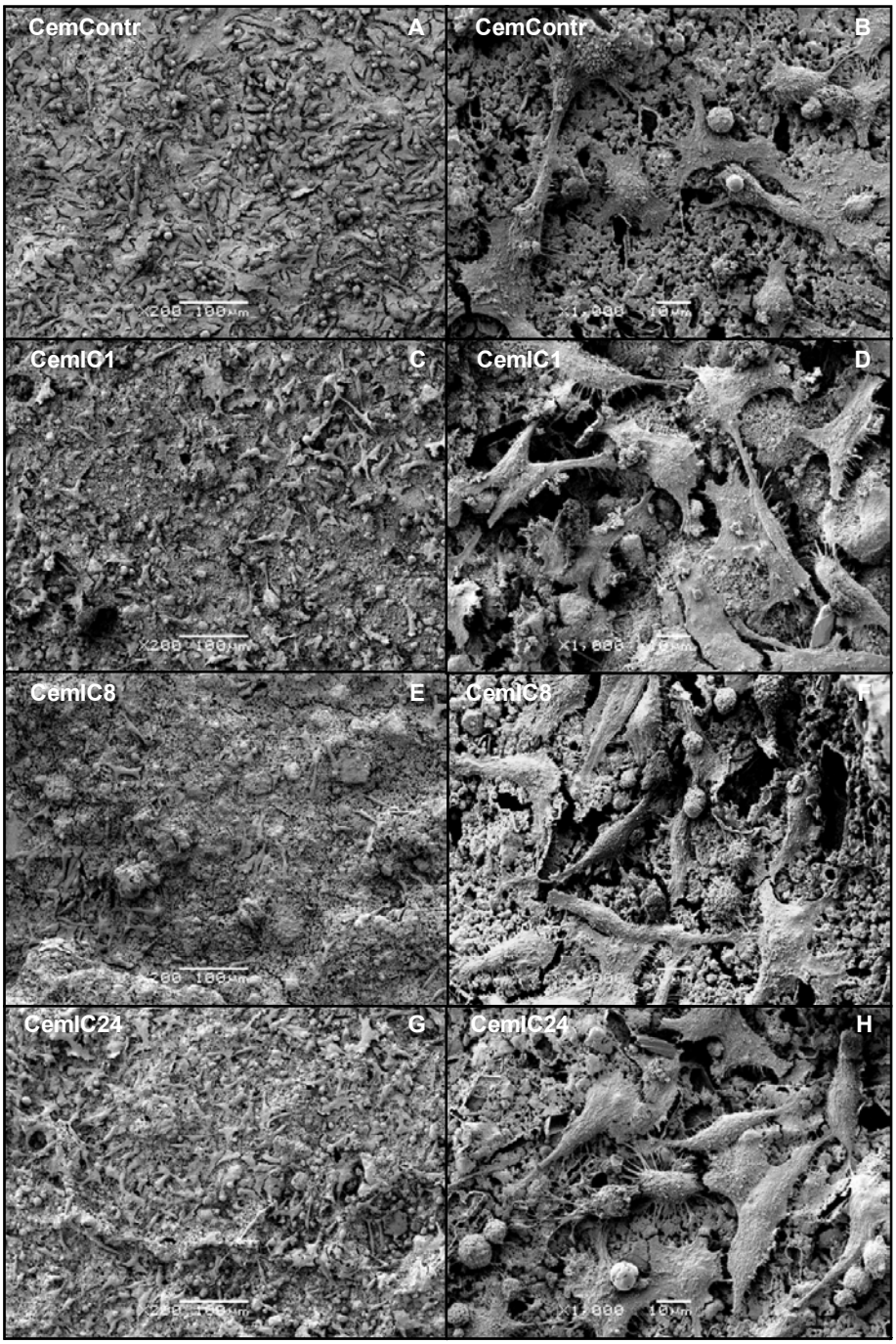

Figure 6.3. SEM pictures of HEp-2 cells cultured for 1 day onto the experimental bone cements (see details on the text; left: x200; right: x1000).

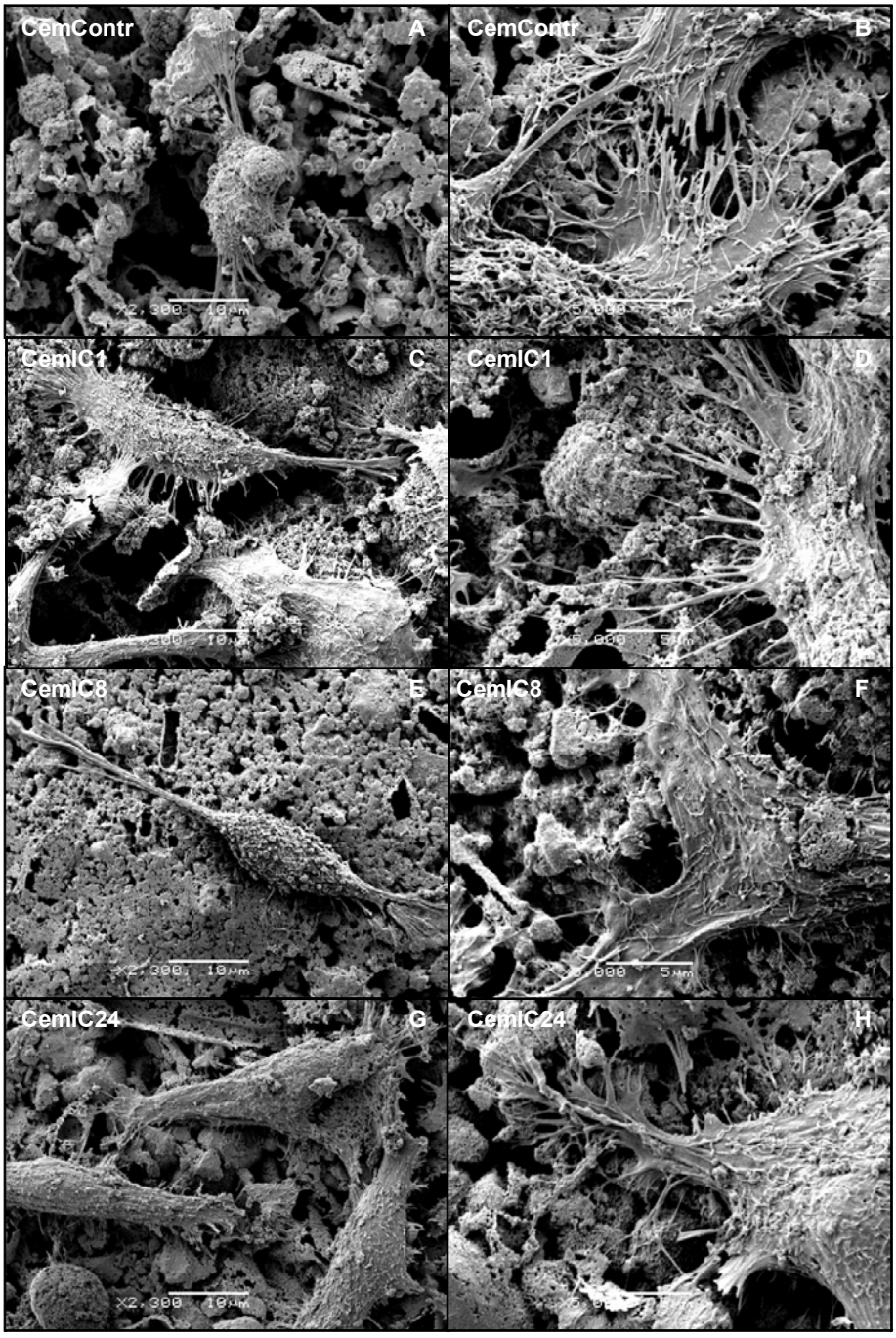

Figure 6.4. SEM pictures of HEp-2 cells attached to the surface of the experimental bone cements after 1 day of culture (left: x2300; right: x5000). Image B shows cell-cell interactions (see details on the text).

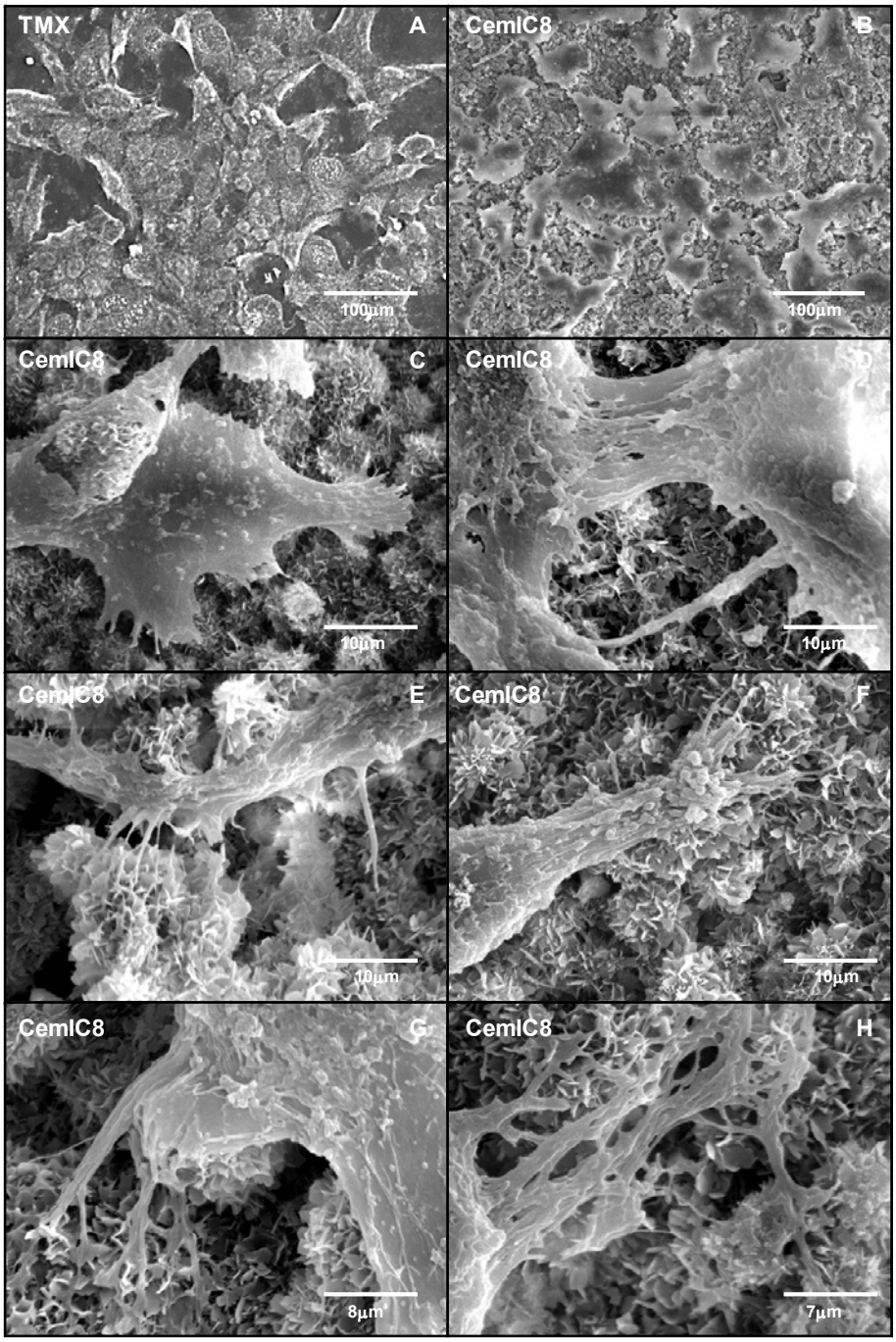

Figure 6.5. SEM pictures of HEp-2 cells cultured after 9 days on *TMX* (A) and *CemIC8* (B-H). Images E-H show the cytoplasmic process anchored to the hydroxyapatite crystals (see details on the text; A: x370; B: x350; C: x3500; D: x4500; E: x5500; F: x6000; G: x7000; H: x8500).

6.4. Discussion

First of all, it should be highlighted that α-TCP is the main powder component of most commercial calcium phosphate bone cements [12,20] because it hydrates naturally into calcium deficient hydroxyapatite (CDHA; $Ca_9(HPO_4)(PO_4)_5OH$) during setting [11]. However, the hydration reaction of α-TCP into CDHA sometimes is limited (i.e. very slow rate-transformation) depending on uncontrollable ion impurities contained by the commercial reactants used during α-TCP high-temperature manufacturing (see Chapter 5). For this reason, in this study, a cement control made with an "active α-TCP" (i.e. *CemContr*) and a cement control made with a "non-active α-TCP" (i.e. *Cem-N*) were used. As referred in Chapter 5, the resulting "non-active α-TCP" was modified by sintering it again with IC in order to recover further α-TCP cement's setting properties. In fact, IC minor additions did not change the α-TCP purity according to X-ray diffraction analysis (XRD; data not shown).

Taking into account these previous considerations, the results from Fig. 6.1 showed that the cellular viability of the iron-modified cements increased with the *wt%*-IC, i.e. iron modification of α-TCP did not show negative dose-dependent effects on HEp-2 cell's viability. On the other hand, the evaluation of the total iron liberated from the cements during curing time (data not shown) showed no iron-ion liberation phenomenon. This could be related to some stable fixation of iron into the structure of the α-TCP phase (as indicated by XRD) as well as to the favoured entrapment of iron into the apatitic phase formed during setting [24]. In fact, the setting and the hardening properties of α-TCP based bone cements are due to the progressive dissolution of the α-TCP particles, process which is followed by the nucleation of apatite crystals that growth until a stable mechanical structure of entangled apatite-crystals is formed [11,25]. Moreover, the viability results of Fig. 6.1 agree with the general delay of cells' growth observed as a

consequence of initial failure of cells' attachment [26,27] to the cements (as shown in Fig. 6.2), due to their surface's reactivity [28,29] (i.e. continuous dissolution and precipitation reactions that affect calcium and phosphate ion concentrations during the cement setting). In addition, it should be point out that the cements used in this study contained also 30 *wt%* of CSD crystals, which after 5 days of cement incubation [23] can lead to interfacial supersaturated conditions due to their passive dissolution. In general, the behaviour of the cells seeded on all the cements fit into hypothesis, except for cement *Cem-N*. In this case, both the cell attachment and the subsequent viability were lower than that observed for the other cements. It is thought that, in this case, the weak structural integrity of its surface (due to the slow hydration reaction of α-TCP into CDHA as confirmed by XRD analysis; data not shown) led to enough particle debridement as to favour cellular endocytosis. This ingestion process could adversely affect the calcium and phosphate homeostatic mechanism and cellular function. The chemical changes undergone by the cytosol and the subsequently accumulation of calcium into mitochondria could have promoted cell's death [30]. Moreover, actin cytoskeleton is molecularly linked to endocytosis [31] and the reorganisation of actin filaments could have negatively affected the cellular functions [32-34].

The results obtained from this study clearly demonstrated that the iron-modified apatitic cements showed similar initial cell attachment and viability profiles as the active α-TCP cement control (i.e. *CemContr*). Moreover, they had higher ability to enhance adhesion and proliferation of HEp-2 cells as compared with the non-active α-TCP cement control (i.e. *Cem-N*). This confirms that α-TCP iron modification is an improved way to recover not only the setting and hardening properties of α-TCP based cements [20] (see also Chapter 5), but also to recover their *in vitro* cytocompatibility. In fact, Fig. 6.2 shows, for the adhesion profiles after 1 day of culture, the same increasing tendency for both the all iron-modified cements and the control (i.e. *CemContr*). Moreover, if we look at the

adhesion profiles attained after 1 day of culture, these were slightly similar ($p>0.05$) for all the substrates (i.e. around 48.61%) as compared to positive controls (i.e. *Control-wells*; considered as 100%). On the other hand, Fig. 6.2 also shows that the adhesion profile observed for *CemContr* after 6 days of culture was 87.35% of that of *Control-wells*. This difference on the initial cellular adhesion of cements as compared to controls could be attributed to the activity of the cement's surfaces (differences in pH and ion concentrations) as well as to differences in surface's morphology between the cements (i.e. rough crystalline surface) and the control wells (i.e. smooth surface) [26]. In fact, it is known that the surface properties play an essential role on the first phase of cell-material interactions, including cell's attachment, adhesion and spreading on the biomaterial surface [35,36]. The quality of this first phase depends on adhesion proteins [37], such as vitronectin and fibronectin, and will influence cell's ability to proliferate and subsequent viability. Despite the proliferative character generally exhibited by the neoplastic cells, the present *in vitro* cytocompatibility study was less favoured by this feature because HEp-2 cells lack of production of fibronectin (adhesion protein) and tenascin-C (glycoprotein closely associated with cell proliferation and migration) [38].

Fig. 6.3 also indicates that *CemContr* and IM-CPCs had similar initial cell's attachment onto their surfaces; i.e. most of them adopt a rather polygonal shape, which is a cellular feature indicative of better adhesion. Furthermore, the cell polarized morphologies sustain the locomotion phenomenon on cements' surface, which favoured the colonisation of the surface, confirming the short-term biocompatibility of the experimental cements. Moreover, SEM pictures also show that the IM-CPCs substrates provided favourable conditions for further increase of cell's attachment (see Figs. 6.3-6.4). In fact, cement hydroxyapatite crystals provided anchorage for HEp-2 cells (see Fig. 6.5, pictures C-H) showing, as expected, that the microgeometry of a substrate plays a significant role in the whole process of cell's attachment and migration [36]. In this case,

cytoplasmic processes allowed the movement of the migrating cells along the cement-like substratum and the tension generated by the forward movement explains the taut appearance of the cells (see Fig. 6.3-right column and Fig. 6.5), as observed also in other studies [39-41]. It should be noted that the surface's microgeometry of the IM-CPCs also provided favourable conditions for a rich network of cell-to-cell contact formation in the early stage of cell proliferation.

The results obtained in this study related to IM-CPCs and *Cem-N* were consistent with our previous results in Chapter 5. This confirms that iron-modification of α-TCP is a useful approach to stabilize the mechanical properties of α-TCP based bone cements after setting without affecting its cytocompatility. Moreover, it is an interesting approach to look for some apatitic thermotherapeutic cements.

A final comment is needed to justify the use of epithelial cells instead of osteogenic cells in this early study. The main reactant of the bone cement used in this research was α-TCP. As stated at the beginning of this chapter, the α-TCP was modified during sintering with minor amounts of IC. It was not the objective of this first research to study the osteogenic behavior of the new iron-modified bone cement which, on the other hand, is well known for α-TCP [9]. The interest was focused on the possible negative effect of the iron ion solubility (oxidative damage) [6,8] on the general mechanism of cellular adhesion and viability.

6.5. Summary conclusion

The present study showed that iron-modified α-TCP based bone cements have cytocompatible features. Both quantitative and morphologic evaluations showed that adhesion, proliferation and viability of HEp-2 cells were not negatively influenced by iron concentration in a dose-dependent manner. In fact, proliferation and cellular

viability improved at the level of cement's surface and cement's environment. The results obtained show that iron-modified cements have the ability to support cellular colonization. The results might provide new insights into the development of new thermotherapy apatitic calcium phosphate bone cements. However, further *in vitro* and *in vivo* studies are required to confirm the possible application for bone repair/substitution. In fact, the positive effects observed in this study should be evaluated in detail with osteogenic cells in order to determine the levels of specific markers of the cellular function. These key points are dealed with in next chapters.

References

1. Takegami K, Sano T, Wakabayashi H, Sonoda J, Yamazaki T, Morita S, Shibuya T, Uchida A. New ferromagnetic bone cement for local hyperthermia. J Biomed Mater Res Part B: Appl Biomater 1998;43B:210-14.

2. Arcos D, del Real RP, Vallet-Regi M. Biphasic materials for bone grafting and hyperthermia treatment of cancer. J Biomed Mater Res 2003;65A:71-78.

3. Kawashita M, Domi S, Saito Y, Aoki M, Ebisawa Y, Kokubo T, Saito T, Takano M, Araki N, Hiraoka M. In vitro heat generation by ferromagnetic maghemite microspheres for hyperthermia treatment of cancer under an alternating magnetic field. J Mater Sci: Mater Med 2008;19:1897-03.

4. Berry CC, Wells S, Charles S, Curtis ASG. Dextran and albumin derivatised iron oxide nanoparticles: influence on fibroblast in vitro. Biomaterials 2003; 24:4551-57.

5. Kim EH, Lee HS, Kwak BK, Kim BK. Synthesis of ferrofluid with magnetic nanoparticles by sonochemical method for MRI contrast agent. Journal of Magnetism and Magnetic Materials 2005;289:328-30.

6. Kakhlon O, Cabantchik ZI. The labile iron pool: characterisation, measurement, and participation in cellular processes. Free Radical Biology & Medicine 2002;33(8):1037-46.

7. Henze MW, Muckenthaler MU, Andrews NC. Balancing acts: molecular control of mamalian iron metabolism. Cell 2004;117:285-97.

8. Cotran R, Kumar V, Abbas AK, Fausto N. In: Robbins & Cotran, ed. Pathologic Basis of Disease, 7th edition, WB Saunders Co, 2004, chapter 1, pp. 14-17.

9. Dorozhkin SV. Calcium orthophosphate cements for biomedical application. J Mater Sci 2008;43:3028-57.

10. Fernández E, Gil FJ, Best SM, Ginebra MP, Driessens FCM, Planell JA. Improvement of the mechanical properties of new calcium phosphate bone cements in the CaHPO4-α-Ca3(PO4)2 system: Compressive strength and microstructural development. J Biomed Mater Res 1998;41:560-67.

11. Fernández E. Bioactive Bone Cements. In: Wiley Encyclopedia of Biomedical Engineering, 6-Volume Set. ISBN: 0-471-24967-X, John Wiley & Sons, Inc. (USA), Metin Akay (Ed.), 2006:1-9.

12. Gisep A, Wieling R, Bohner M, Matter S, Schneider E, Rahn B. Resorption patterns of calcium-phosphate cements in bone. J Biomed Mater Res 2003;66(3):532-40.

13. Apelt D, Theiss F, El-Warrak AO, Zlinszky K, Wolfisberger RB, Bohner M, Matter S, Auer JA, von Rechenberg B. In vitro behavior of three different injectable hydraulic calcium phosphate cements. Biomaterials 2004;25:1439-51.

14. Bohner M. Physical and chemical aspects of calcium phosphates used in spinal surgery. Eur Spine J 2001;10:S114-S121.

15. Deb S, Giri J, Dasgupta S, Datta D, Bahadur D. Synthesis and characterisation of biocompatible hydroxyapatite coated ferrite. Bull Mater Sci 2003;26(7):655-60.

16. Arcos D, del Real RP, Vallet-Regi M. A novel bioactive and magnetic biphasic material. Biomaterials 2002;23:2151-58.

17. Tyllianakis M, Giannikas D, Panagopoulos A, Panagiotopoulos E, Lambiris E. Use of injectable calcium phosphate in the treatment of intra-articular distal radius fractures. Orthopedics 2002;25(3):311-15.

18. Bohner M, Gbureck U, Barralet JE. Technological issues for the development of more efficient calcium phosphate bone cements: a critical assessment. Biomaterials 2005;26:6423-29.

19. Lewis G. Percutaneous vertebroplaty and kyphoplasty for the stand-alone augmentation of osteoporosis-induced vertebral compression fractures: present status and future directions. J Biomed Mater Res Part B: Appl Biomater 2007;81B:371-86.

20. Lewis G. Injectable bone cements for use in vertebroplasty and kyphoplasty: state of the art review. J Biomed Mater Res Part B: Appl Biomater 2005;76B:456-68.

21. Fernández E, Vlad MD, Hamcerencu M, Darie A, Torres R, López J. Effect of iron on the setting properties of α-TCP bone cements. J Mater Sci 2005;40:3677-82.

22. Vlad MD, del Valle LJ, Barracó M, Torres R, López J, Fernández E. Iron oxide nanoparticles significantly enhances the injectability of apatitic bone cement for vertebroplasty. Spine 2008;33(21): 2290-2298.

23. Fernández E, Vlad MD, Gel MM, López J, Torres R, Cauich JV, Bohner M. Modulation of porosity in apatitic cements by the use of α-tricalcium phosphate-calcium sulphate dehydrate mixtures. Biomaterials 2005;26:3395-04.

24. Jiang M, Terra J, Rossi AM, Morales MA, Saitovitch EMB, Ellis DE. Fe^{2+}/Fe^{3+} substitution in hydroxyapatite: theory and experiment. Phys Rev B 2002; 66(22):224107-1/15.

25. Fernández E, Ginebra MP, Boltong MG, Driessens FCM, Planell JA, Ginebra J, De Maeyer EAP, Verbeeck RMH. Kinetic study of the setting reaction of calcium phosphate bone cements. J Biomed Mater Res 1996;32:367-74.

26. Anselme K, Bigerelle M, Noel B, Dufresne E, Judas D, Iost A, Hardouin P. Qualitative and quantitative of human osteoblast adhesion on materials with various surface roughness. J Biomed Mater Res 2000;49:155-66.

27. Ignjatovic N, Ninkov P, Kojic V, Bokurov M, Srdic V, Krnojelac D, Selakovic S, Uskokovic D. Cytotoxicity and fibroblast properties during in vitro test of biphasic calcium phosphate/poly-di-lactide-co-glycolide biocomposites and different phosphate materials. Microscopy Research and Technique 2006;69:976-82.

28. Suzuki T, Ohashi R, Yokogawa Y, Nishizawa K, Nagata F, Kawamoto Y, Kameyama T, Toriyama M. Initial anchoring and proliferation of fibroblast L-929 cells on unstable surface of calcium phosphate ceramics. Journal of Bioscience and Bioengineering 1999;87(3):320-27.

29. Simon CG, Guthrie WF, Wang FW. Cell seeding into calcium phosphate cement. J Biomed Mater Res 2004;68A:628-39.

30. Juin P, Pelletier M, Oliver L, Tremblais K, Gregoire M, Meflah K, Vallette FM. Induction of a caspase-3-like activity by calcium in normal cytosolic extracts triggers nuclear apoptosis in a cell-free system. The Journal of Biological Chemistry 1998;273(28):17559-64.

31. Qualmann B, Kessels MM, Kelly RB. Molecular links between endocytosis and the actin cytoskeleton. The Journal of Cell Biology 2000;150(5):F111-16.

32. Chen CS, Mrksich M, Huang S, Whitesides GM, Ingber DE. Geometric control of cell life and death. Science 1997;276:1425-28.

33. Ninomiya JT, Struve JA, Stelloh CT, Toth JM, Crosby KE. Effects of hydroxyapatite particulate debris on the production of cytokines and proteases in human fibroblasts. Journal of Orthopaedic Research 2001;19:621-28.

34. Pioletti DP, Takei H, Lin T, Van Landuyt P, Ma QJ, Kwon SY, Sung KLP. The effects of calcium phosphate cement particles on osteoblast functions. Biomaterials 2000;21:1103-14.

35. Anselme K. Osteoblast adhesion on biomaterials. Biomaterials 2000;21:667-81.

36. Berry CC, Campbell G, Spadiccino A, Robertson M, Curtis ASG. The influence of microscale topography on fibroblast attachment and mobility. Biomaterials 2004;25:5781-88.

37. Harnett EM, Alderman J, Wood T. The surface energy of various biomaterials coated with adhesion molecules used in cell culture. Colloids and Surfaces B: Biointerfaces 2007;55:90-97.

38. Yoshida T, Yoshimura E, Numata H, Sakakura Y, Sakakura T. Involvement of tenascin-C in proliferation and migration of laryngeal carcinoma cells. Virchows Archiv 1999;435:496-500.

39. In: Bruce Alberts, Alexander Johnson, Julian Lewis, Martin Raff, Keith Roberts, Peter Walter. Molecular Biology of the cell. Fourth edition, pp. 907-1080. Garland Science, NY, 2002.

40. Safiejko-Mroczka B, Bell PB. Reorganization of the actin cytoscheleton in the protruding lamellae of human fibroblasts. Cell Motility and the Cytoskeleton 2001;50:13-32.

41. Lefaix H, Asselin A, Vermaut P, Sautier JM, Berdal A, Portier R, Prima F. On the biocompatibility of a novel Ti-based amorphouos composite: structural characterisation and in vitro osteoblasts response. J Mater Sci: Mater Med 2008;19:1861-69.

Chapter 7

Effect of iron oxide nanoparticles on the setting and hardening properties of bone cement

7.0. Structured abstract

Mini Abstract. In this chapter a new approach to improve the injectability of alpha-tricalcium phosphate (α-TCP) based bone cements for vertebroplasty (VP) and kyphoplasty (KP) was followed. This study was based on previous observations performed in Chapters 5 and 6. In the present research, it is shown that iron oxide (IO) cement modification produced better injectable cements with better mechanical properties after hardening. Moreover, the resulting cements were also non cytotoxic.

Study Design. Experimental study to characterise the setting and the cytocompatibility properties of α-TCP based bone cement.

Objective. To investigate the setting, flowing and biocompatibility properties of new iron oxide modified α-TCP based bone cement.

Summary of Background Data. VP and KP are efficient procedures for the treatment of painful vertebral compression fractures. Nowadays, calcium phosphate cements (CPCs) are used to treat these fractures mainly due to the similar bone apatitic phase formed after setting. However, clinicians have reported great difficulties in filling the vertebral bodies due to the high pressures needed to inject these materials. Accordingly, there is a need for new approaches to improve the initial flowing properties of these cements without affecting or even improving their short-term mechanical stability and their long-term *in vivo* cement transformation into bone tissue.

Methods. Setting times were measured by the *Gillmore* needles. The compressive strength accounted for the cement hardening. Scanning Electron Microscopy and X-ray diffraction followed the cement microstructure and the crystalline phases during setting. Injectability was approached by recording the injection force needed to empty filled cement syringes. Finally, the cytocompatibility was evaluated by studying the viability and the adhesion profiles of human ephitelial cells cultured onto the cements.

Results. The addition of IO nanoparticles into the powder phase of α-TCP based cement significantly enhanced its injectability by lowering the extrusion force required for its delivery. For example, 24 *wt%* IO addition resulted in 83% of cement injected with an extrusion force lower than 25 N. Moreover, the setting and the working times of the cements increased with IO addition. Also, the new cements showed improved compressive strength in agreement with the crystalline microstructure evolved during hardening. On the other hand, IO modification did not produced cytotoxic cements.

Conclusions. It has been shown that the addition of IO nanoparticles into the powder phase of α-TCP based cement improved both, the initial injectability and the maximum compressive strength without affecting its physico-chemical setting reactions and its cytocompatibility. These results could be further exploited by designing improved strength and injectable apatitic cements with suitable *in vivo* transformation ratios into bone tissue by incorporating phases creating porosity (see Chapter 3).

Key Points.

- The addition of IO nanoparticles into the cement powder phase of α-TCP based bone cement significantly enhanced the injectability of the resulting pastes.
- The new IO-modified bone cements had longer working and setting times.
- The IO additive did not modify the setting reactions and the evolved apatitic microstructure produced cements with higher compressive strength at saturation.
- The new IO modified cements showed to be non cytotoxic.
- Further research is needed to adjust the porosity of the cements to improve vertebral bone tissue regeneration.

7.1. Introduction

Calcium phosphate bone cements (CPBC) have been used in dental and orthopaedic applications (bone fractures, bone tumours, osteoporosis and craniofacial affections), mainly due to the similar bone-like apatite structure evolved during their setting, their high biocompatibility and their good osteointegration after being implanted *in vivo* [1-8]. Moreover, with the advent of minimally invasive surgery techniques, CPBC have been also applied to spinal management (*vertebro-* and *kyphoplasty*) associated with vertebral compression fracture due to osteoporosis [9-13]. In these applications, bone cement has been injected under pressure through a cannula by hand or gun injection into the porous structure of cancellous bone. However, surgeons have reported great difficulties in filling the vertebral bodies (i.e. bad injectability, filter-pressing phenomena and cement decohesion) observed during vertebral body injection, which have resulted in bone instability due to low mechanical strength [14]. In view of these observations, the study of the injectability of CPBC has been approached by different methods [15-19]. However, as these materials have progressive setting [20], it is not clear what rheological properties are needed to maintain the injectability during cement application and before their setting, without any further detrimental mechanical effect [21]. For these reasons, in this study, it has been investigated the influence of iron oxide (IO) addition on the setting, mechanical, injectability and biocompatibility properties of an experimental CPBC as a way to improve its flowing properties without affecting the strength or the cytocompatibility [22].

7.2. Materials and methods

7.2.1. Calcium phosphate bone cement

The experimental CPBC, used as control (*CemContr*), was made of a powder phase of *alpha*-tricalcium phosphate (α-TCP; α-$Ca_3(PO_4)_2$; *Robert Mathys Foundation, Mathys Medical, Switzerland*) and an aqueous phase of 2.5 *wt%* of disodium hydrogen phosphate (Na_2HPO_4; Ref. 131679; *Panreac Química, S.A., Spain*). α-TCP was milled in a planetary ball mill (PM-100; *Retsch GmbH, Germany*) up to a medium particle size of 7 μm (d_{10}=0,7 μm; d_{50}=3.4 μm; d_{90}=16,5 μm). The powder phase of this control was modified with 8 *wt%* (*Cem8IO*) and 24 *wt%* (*Cem24IO*) of iron oxide (α-Fe_2O_3; $d_{50}\approx$150 nm; Ref. 212375; *Panreac Química, S.A., Spain*) addition. Cement powder and liquid phases were mixed together by hand, for 1 minute, in a mortar with a spatula at a liquid-to-powder ratio (L/P) of 0.32 mL/g. Immediately after, the slurries thus obtained were placed into appropriate moulds to obtain cylindrical and disc samples for compressive strength and cytocompatibility testing, respectively.

7.2.2. Setting times

Initial and Final Setting Times (IST and FST) were measured following the *Gillmore* needles standard method [23].

7.2.3. Mechanical strength testing

Cylindrical (5 mm diameter by 10 mm height) compressive strength samples were unmoulded after setting into water solution of pharmaceutical quality (H_2O; Ref. 253054; *Grifols, Spain*) at 37°C for fixed hardening times (HT; i.e. 1, 2, 4, 8, 16, 24 and 48 hours). After completion of these HT, samples were tested until fracture under compression in a

universal testing machine (*MTS Insight-5*) at a crosshead speed of 1 mm/min in order to follow the evolution of mechanical strength with time. Each measurement was an average of eight samples. The experimental values were fitted to an exponential function of the form $C_t=C_s*(1-\exp(-t/\tau))$, where t is time, C_t is the compressive strength measured at time t, C_s means the compressive strength at saturation and τ is a parameter meaning an *average hardening lifetime* for the cement, i.e. for $t=\tau$, C_t attains 63% of C_s [1].

7.2.4. Injectability testing

Cement injectability was assessed, similarly as in the literature [15], by extruding syringes of 5 mL (equivalent capacity of 40 mm) filled with cement using an *MTS Insight-5* universal testing machine, at a crosshead speed of 50 mm/min (i.e. equivalent time to empty the syringe of 48 s) and up to a maximum load of 300 N.

7.2.5. Chemical characterization

Compressive strength tested samples were immediately quenched in acetone to stop further setting, dried for several days, grounded to powder and characterized by X-ray diffraction (XRD; *Siemens-D500, Germany*) for chemical phase analysis. The XRD range was from 20 to 40 degrees (2θ) with a step size of 0.05° and a counting time of 3 s/step. The phase composition was checked by indexing the diffraction peaks according to JCPDS (*Joint Committee on Powder Diffraction Standards*) cards (9-348 for α-TCP, 9-432 for CDHA (i.e. $Ca_9(HPO_4)(PO_4)_5OH$; calcium deficient hydroxyapatite) and 33-664 for IO).

7.2.6. Microstructural characterization

Scanning Electron Microscopy (SEM; *JEOL JSM-5610, Hitachi, Japan*) was used to characterize the evolution of the cement microstructure. Observations of the fracture

surfaces of dried cylindrical samples broken diametrically were performed at the hardening times specified above (see *7.2.1. Calcium phosphate bone cement*). Prior to SEM observation, the fracture surfaces were gold covered.

7.2.7. Cytocompatibility testing

Cytocompatibility disc samples (10 mm in diameter and 2 mm in height) were unmoulded after setting for 1 h at 37°C into the water solution of pharmaceutical quality. Immediately after, they were sterilized by UV-irradiation and used as cement substrates for *in vitro* cell culture. The cytocompatibility of the IO-modified bone cements was approached by quantifying both the *Cell relative viability (%)* and the *Adhesion density* (*cells/cm*^{2}) of *HEp-2* cells (epithelial cells derived from a human laryngeal carcinoma) cultured on cement discs and control wells not containing cement samples. The cells were seeded at 5x10^4 cells/well, in a 24 well plate, and incubated for 1 and 6 days (1D and 6D) at 37°C in humidified atmosphere of 95% air and 5% carbon dioxide. The medium used was Dulbecco's modified Eagle medium (DMEM) supplemented with 10% foetal bovine serum, 1% penicillin/streptomycin/L-glutamine (*Sigma Chemical Co., USA*) and it was changed every two days.

Cement cytocompatibility was assessed, similarly as in the literature, by the *MTT-assay* [24]. After incubation, the culture was removed and 3-(4,5-dimethyltiazol-2-yl)-2,5-diphenyl tetrazolium bromide (*MTT*) dye solution in culture medium was added on each well. As it is known, viable cells have the ability to convert *MTT* reagent into dark blue insoluble *formazan* crystals due to the activity of mitochondria dehydrogenases. These crystals were solubilised with dimethylsulphoxide (*DMSO*) and the characteristic absorbance was read on a microplate reader (*Anthos 2020 Microplate Reader; ASYS Hitech, Austria*) at 540 nm wavelenght. This absorbance is directly related to the number of viable cells, i.e. to cell proliferation activity *in vitro*. The number of cells was determined using a

linear equation obtained from a calibration curve containing absorbance values against different counts of cells.

Cell relative viability was calculated by $N_{test}/N_{control}$ x 100; where N_{test} is the number of cells corresponding to the tested sample and $N_{control}$ is the number of cells corresponding to control wells. The *Adhesion density* was obtained by normalizing the number of cells adhered onto the cements to the area available for cell's attachment. The results were expressed as mean ± standard deviation (mean±SD; n=4). Groups were compared by one-way ANOVA and statistical significance was accepted at p-value<0.05 by Tukey's multiple comparison method.

7.3. Results and discussion

7.3.1. Setting times

Fig. 7.1 shows that the addition of IO increases both the IST and the FST of *CemContr* sample, thus producing cements with longer workability and better fluidity. This improvement depends on the quantity of the IO, i.e. setting times increase as the *wt%* of IO increases and was more noticeable for the IST than for the FST. For example, 8 *wt%*-IO (*Cem8IO*) and 24 *wt%*-IO (*Cem24IO*) let to an IST of 19 min and 23 min, which means 90% and ≈100% of IST's *CemContr* delay, respectively.

On the other hand, the increase of setting times should not have any clinical issue because injection of cement is performed well before the IST. It should be remembered that the setting times have been measured at room temperature. In clinical practice, the cement will set after injection into the bone cavity at body temperature and consequently the cement will set faster [21].

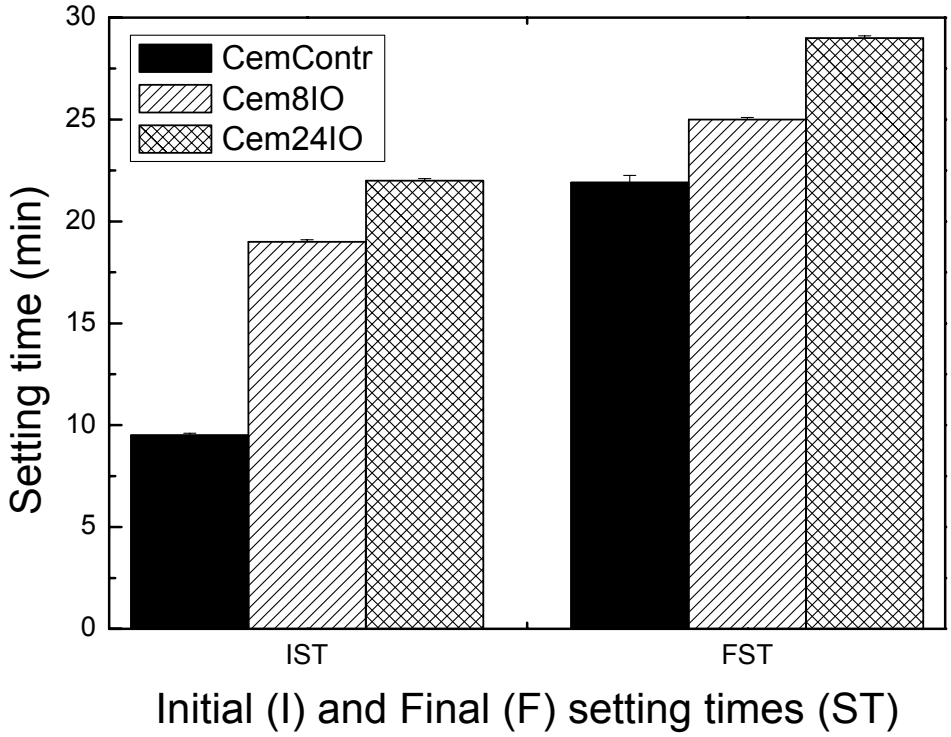

Figure 7.1. Effect of iron oxide addition on the initial and final setting times of control cement.

7.3.2. Compressive strength

Fig. 7.2 shows the evolution of the compressive strength with the hardening time for the control (*CemContr;* $C_s^{0IO}(MPa)=49\pm3$; $\tau_{0IO}(h)=7.8\pm1.5$) and the IO modified cements. It is observed that maximum compressive strength at saturation, i.e. C_s, evolved as the amount of IO increased in a dependent concentration manner. For example, 8 *wt%*-IO (*Cem8IO;* $C_s^{8IO}(MPa)=68\pm7$; $\tau_{8IO}(h)=12.3\pm3.4$) let to 68 MPa of compressive strength at saturation, which means 39% of *CemContr*'s strength improvement. In fact, $\tau_{8IO}>\tau_{0IO}$, indicating (according to experience [1,25]) that α-TCP setting reactions proceed faster in the unmodified cement so expecting a network of bigger entangled calcium deficient

apatite (CDHA; $Ca_9(HPO_4)(PO_4)_5OH$) crystals [1,25] (for further details see *7.3.5. Scanning Electron Microscopy*).

On the other hand, 24 *wt%*-IO (*Cem24IO; C_s^{24IO}(MPa)=53±4; τ_{24IO}(h)=8.4±1.6*) did not modify appreciably *CemContr*'s strength at saturation (only 8% improvement), not the whole compressive strength curve according to fitting (i.e. $\tau_{24IO} \approx \tau_{0IO}$). This tendency (i.e. $\tau_{8IO} > \tau_{24IO} \approx \tau_{0IO}$) means that the compressive strength of *CemContr* can be maximized for an optimum amount of IO addition.

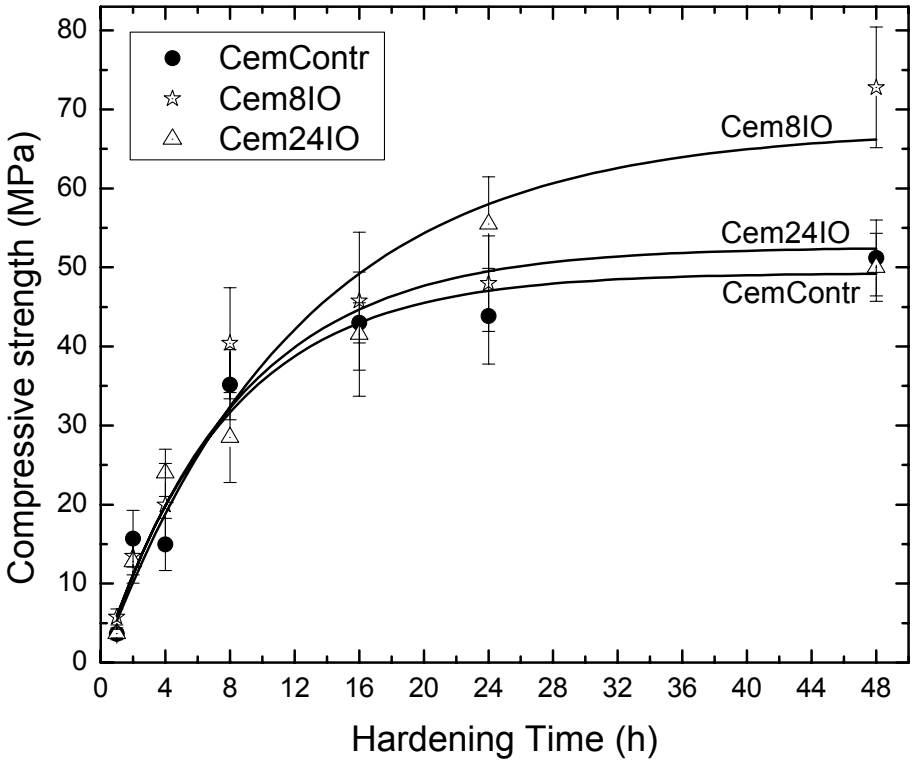

Figure 7.2. Effect of iron oxide addition on the evolution of the compressive strength of control cement.

It should be highlighted that the results obtained after 48 h of setting have a high weight on fitting (see Fig. 7.2). In particular, the compressive strength obtained for *Cem24IO* was lower enough (statistically significant) as compare to *Cem8IO* (i.e. ≈50 MPa *vs.* ≈72 MPa, respectively) as to have a statistically significant influence on fitting. It should be noted, for comparison, that the individual strength value obtained after 24 h of setting was higher (statistically significant) for *Cem24IO* than the one obtained for *Cem8IO* (≈56 MPa *vs.* ≈48 MPa, respectively). For this reason, data observed at 48 h can not be explained at this stage. There is no apparent reason why compressive strength at 48 h of setting should be low for *Cem24IO* (high amount of IO, i.e. 24 *wt%*) as compare to *Cem8IO* (low amount of IO, i.e. 8 *wt%*). In fact, continuous pH measurements performed at L/P=200 mL/g (data not shown) showed no appreciably differences between cements *Cem8IO* and *Cem24IO*, being both a bit more basic («average pH/over 24 h of setting» ≈ 9) than *CemContr* («average pH/over 24 h of setting» ≈ 8.7). A possible explanation of the different effect of IO addition (as it increases) on the evolution of mechanical properties of *CemContr* is commented later on (see *7.3.5. Scanning Electron Microscopy*).

Despite the above apparent inconsistency of data, the results in Fig. 7.2 show that (for this α-TCP experimental cement) IO modification maximizes (for 24 *wt%*-IO addition) both the initial workability (i.e. longer setting times; see Fig. 7.1) and flowing cement properties (see *7.3.3. Injectability*) of *CemContr* without disturbing its mechanical properties.

7.3.3. Injectability

Fig. 7.3 shows the evolution of the extrusion force recorded against the time for the control cement and the IO-modified cements let to set inside the 5 mL syringe during 10 min (*CemContr-10*; *Cem8IO-10*; *Cem24IO-10*), i.e. up to completion of the IST of *CemContr* (see Fig. 7.1). Injection tests performed on a syringe filled only with water (*Water*) and on

control cement let to set for 20 min (*CemContr-20*), i.e. up to completion of its characteristic FST, has been included for comparison. It is observed that "no-force" was needed to extrude all the water inside the syringe at the crosshead speed of 50 mm/min (i.e. equivalent extrusion time of 48 s). On the other hand, *CemContr-20* attained 300 N during extrusion in only 5 s, i.e. only the equivalent of 4,2 mm of cement was extruded outside the syringe, which means that *CemContr* was only 10% injectable after its FST. Similarly, *CemContr-10* was 58% injectable at its IST, under the same experimental conditions. The relevant observation is that 8 and 24 *wt%*-IO modification let, under the same testing conditions (*Cem8IO-10* and *Cem24IO-10*), to 69% and 100% cement injectability, respectively.

Moreover, *Cem24IO-10* shows that more than 83% of this cement was injectable with an extrusion force lower than 25 N. These results, jointly with those in Fig. 7.2, show clearly that, for the experimental cement analysed (*CemContr*), it is possible to attain 100% injectability (see Fig. 7.3, sample *Cem24IO-10*) without affecting the compressive strength (possibly improving it after further optimization) during the entire setting (see Fig. 7.2, samples *CemContr* and *Cem24IO*) if control cement is modified with 24 *wt%*-IO. This new possibility (i.e. improving initial cement injectability without losing (or even improving) mechanical stability after setting due to IO cement modification) should be of interest for certain clinical procedures and applications (*vertebro-* and *kypho-plasty*).

However, the present data are not avoided of discussion. For example, one important concern with vertebroplasty is the risk of neurological damage from leakage into the spinal canal. It therefore appears that the reduction in viscosity afforded by the iron oxide nanoparticles increases the risk of leakage. In the present study, the viscosity of our cements varied between 1000-3000 Pa.s (unpublished data) in the time interval 2-10 min. This viscosity is comparable to the one reported for an acrylic bone cement tested at a shear rate of 0,4 s^{-1} (initial setting time=3-5 min) [17]. However, it is still high comparing

with the ideal range reported to be for vertebroplasty procedure between 100-200 Pa.s at a shear rate of 40 s^{-1} [17]. For these reasons, leakage should not be a problem if clinical practice is properly done.

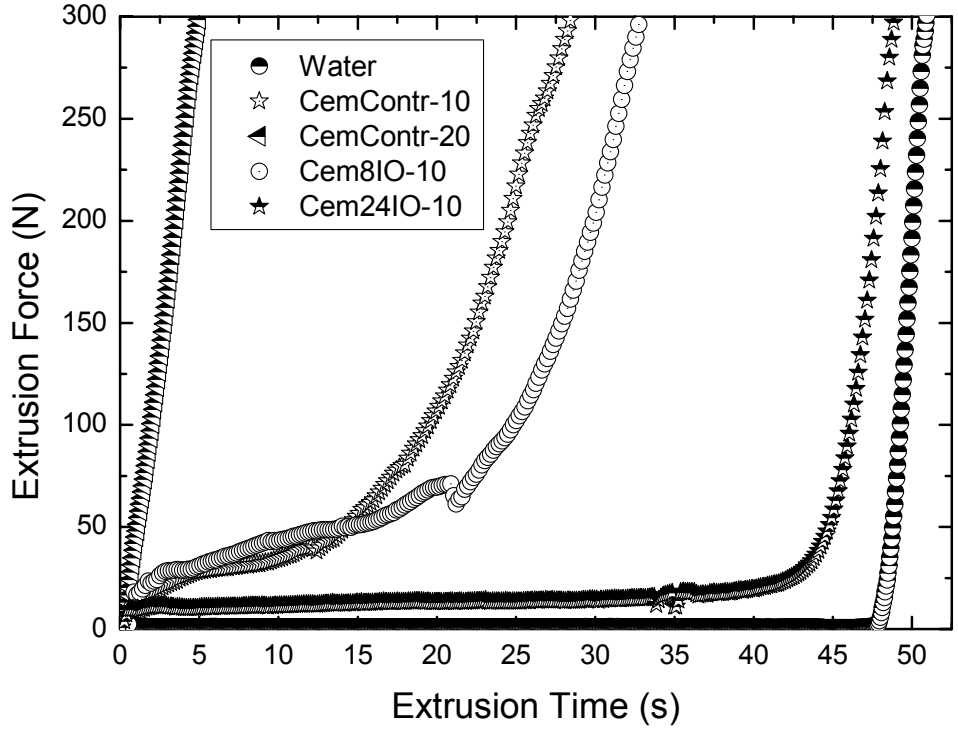

Figure 7.3. Effect of iron oxide addition on the injectability of cements previously set during 10 min, i.e. before the IST of control cement. Injectability tests performed on water and on control cement set for 20 min, i.e. before the FST of control cement, are included for comparison.

Another point of discussion is related to the possible artefacts that IO particles can produce during magnetic resonance imaging (MRI) follow up after injection. It is expected that, in this particular case, the used IO phase (i.e. α-hematite) should not produce any artefact during MRI follow up. There are some data in the literature that

indicates this fact. For example, it is well known that superparamagnetic IO nanoparticles are used as MRI contrast agents to differentiate pathologic and physiologic tissues, being the main contrast phase's magnetite (Fe_3O_4) and maghemite (γ-Fe_2O_3) [26,27]. However, α-hematite (α-Fe_2O_3) has antiferromagnetic properties in normal conditions. Some studies have indicated that α-hematite nanoparticles dispersed in a non-magnetic polymeric matrix (to avoid chemical and structural changes) show some magnetic particle's interaction for high particle's concentration [28]. However, in the present study, low particle's concentrations were used (i.e. high interparticle distance). Moreover, the particles were fixed into an entangled net of hydroxyapatite crystals.

7.3.4. X-ray diffraction

Figs. 7.4 and 7.5 show the XRD patterns observed at different hardening times HT for cements *Cem8IO* and *Cem24IO*, respectively. At HT=0h (i.e. initial powder phase before mixing with liquid phase) the main peaks of α-TCP (*JCPDS-9-348*) and IO (*JCPDS-33-664*) phases can be detected. As expected, IO peaks were higher in *Cem24IO* (see Fig. 7.5) than in *Cem8IO* (see Fig. 7.4) due to the higher content of IO additive in that sample (24 *wt% vs.* 8 *wt%*, respectively). It is important to notice that IO peaks did not evolve during setting in both cements, i.e. peak intensity was nearly constant with hardening time. This was not the case for α-TCP and CDHA *(JCPDS-9-432)* phases where peaks evolved as expected [1,25], i.e. α-TCP intensities decreased progressively and the CDHA peaks gradually increased. These data supported the idea that α-TCP transformed totally into CDHA, in the presence of a practically non-reactive phase (i.e. IO) according to the known setting reaction 3α-TCP + $H_2O \rightarrow$ CDHA [1,25]. As a consequence, these results suggested at first that no direct negative effect should be found on the cytocompatibility of these cements due to the presence of the IO additive (for data confirmation, see *7.3.6. MTT-assay*). Moreover, it is known that iron ions, when present in solution, can be

incorporated into stable apatitic phases due to the cation-exchange property of hydroxyapatite [29].

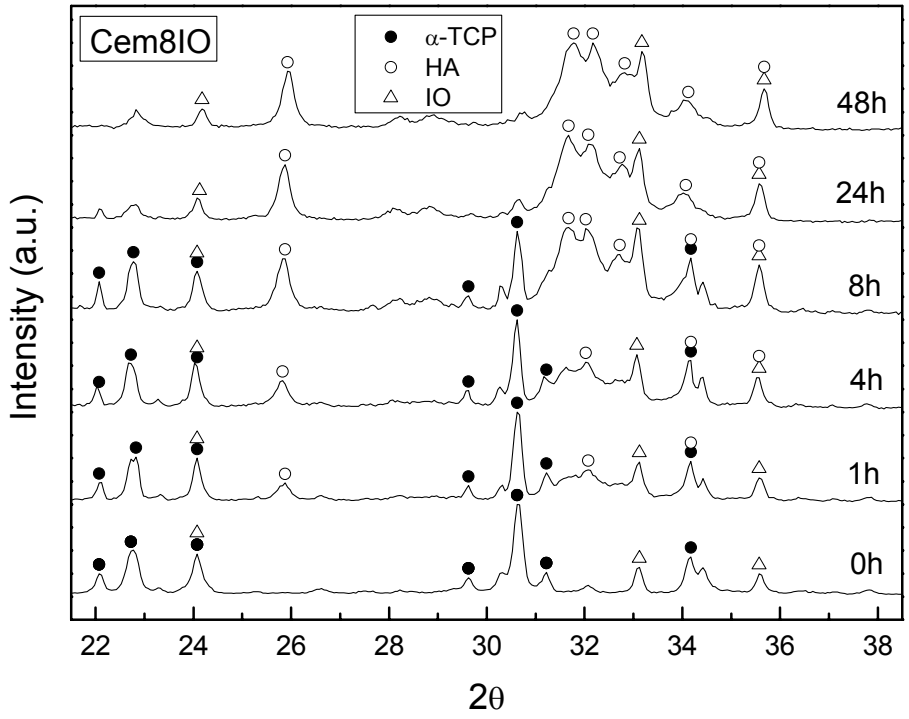

Figure 7.4. XRD patterns of Cem8IO after different hardening times. The observation is that α-TCP phase transformed with time into CDHA in the presence of a non-reactive IO additive.

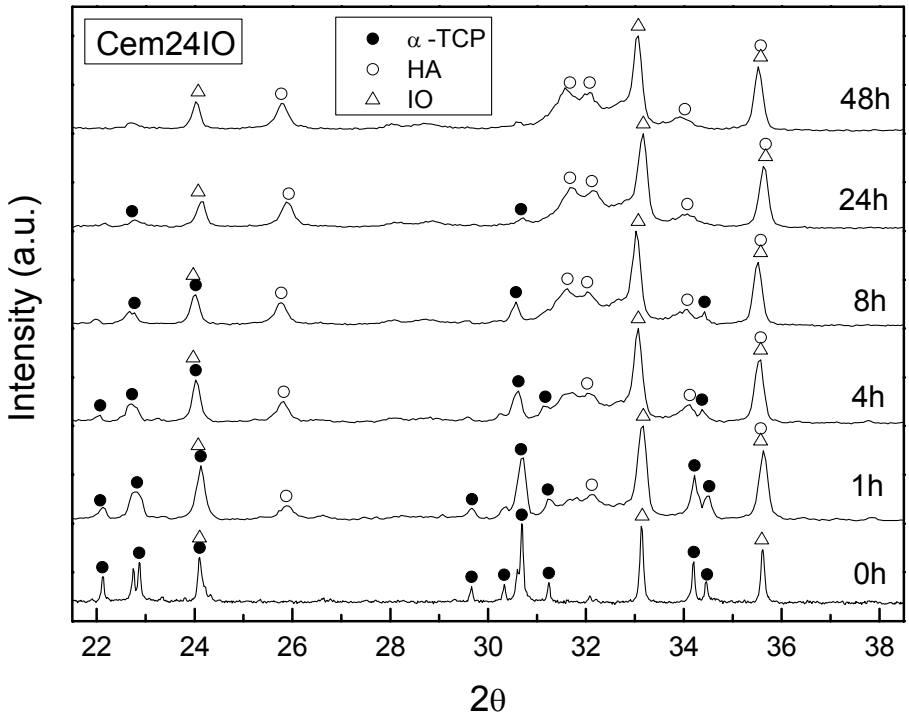

Figure 7.5. XRD patterns of *Cem24IO* after different hardening times. The observation is that α-TCP phase transformed with time into CDHA in the presence of a non-reactive IO additive.

7.3.5. Scanning electron microscopy

Figs. 7.6 and 7.7 show representative SEM pictures taken at different hardening times HT from fracture surfaces of the cement samples. The general observation is that the microstructure of the IO-modified cements (i.e. *Cem8IO* and *Cem24IO*; see Fig. 7.7, left and right, respectively) evolved similarly as for the control (i.e. *CemContr*; see Fig. 7.6, right) and as expected for α-TCP-based cements [1,25], i.e. initial dissolution of α-TCP particles (by surface control process [1]), later nucleation, precipitation and formation of egg-like shells of entangled CDHA crystals surrounding the α-TCP particles (see pictures

at 1 and 4 h), and further inner-shell transformation of α-TCP particles (into CDHA crystals) and inner CDHA crystal growth (by diffusion control process [1]; see pictures at 8 and 48 h; see also Chapter 1).

In general, SEM pictures (see Fig. 7.6 and 7.7) did not show noticeable differences between cement microstructures as to explain differences in mechanical properties (see Fig. 7.2). In fact, the only observation that could explain why *Cem24IO* developed lower strength than *Cem8IO* was related to IO particles agglomeration as that showed in Fig. 7.8. This lack of homogenization, produced during the initial powder and liquid cement mixture, results in local concentration (also local pH variations) of non-reactive (see *7.3.4. X-ray diffraction*) IO-particles; as these particles do not entangle between them or with the CDHA entangled crystal matrix (see Fig. 7.8, top-right), these local points are weaker zones to propagate a crack. This conclusion also indicates that proper homogenization could further increase the observed strength of *Cem24IO* (similarly as *Cem8IO*) as compare to *CemContr*.

Fig. 7.8 is also important because it shows a possible explanation for the observed improvement at short times of initial cement injectability as IO increases (see Fig. 7.3). It is hypothesized that rounded IO particles of nanometer size (see Fig. 7.8, bottom-left (for *Cem24IO*) and bottom-right (for IO-raw material)) can be acting as nanometer rollers between contacting α-TCP particles with the net effect of particle-particle interaction's friction decrease. In this sense, the addition of IO-particles lubricated the hydrodynamic interaction between the bigger α-TCP particles. It should be noted that IO-particles have been observed at different hardening times as allocated onto the surface of α-TCP particles (see for example Fig. 7.7, *Cem8IO* at 4 h) so supporting the above hypothesis.

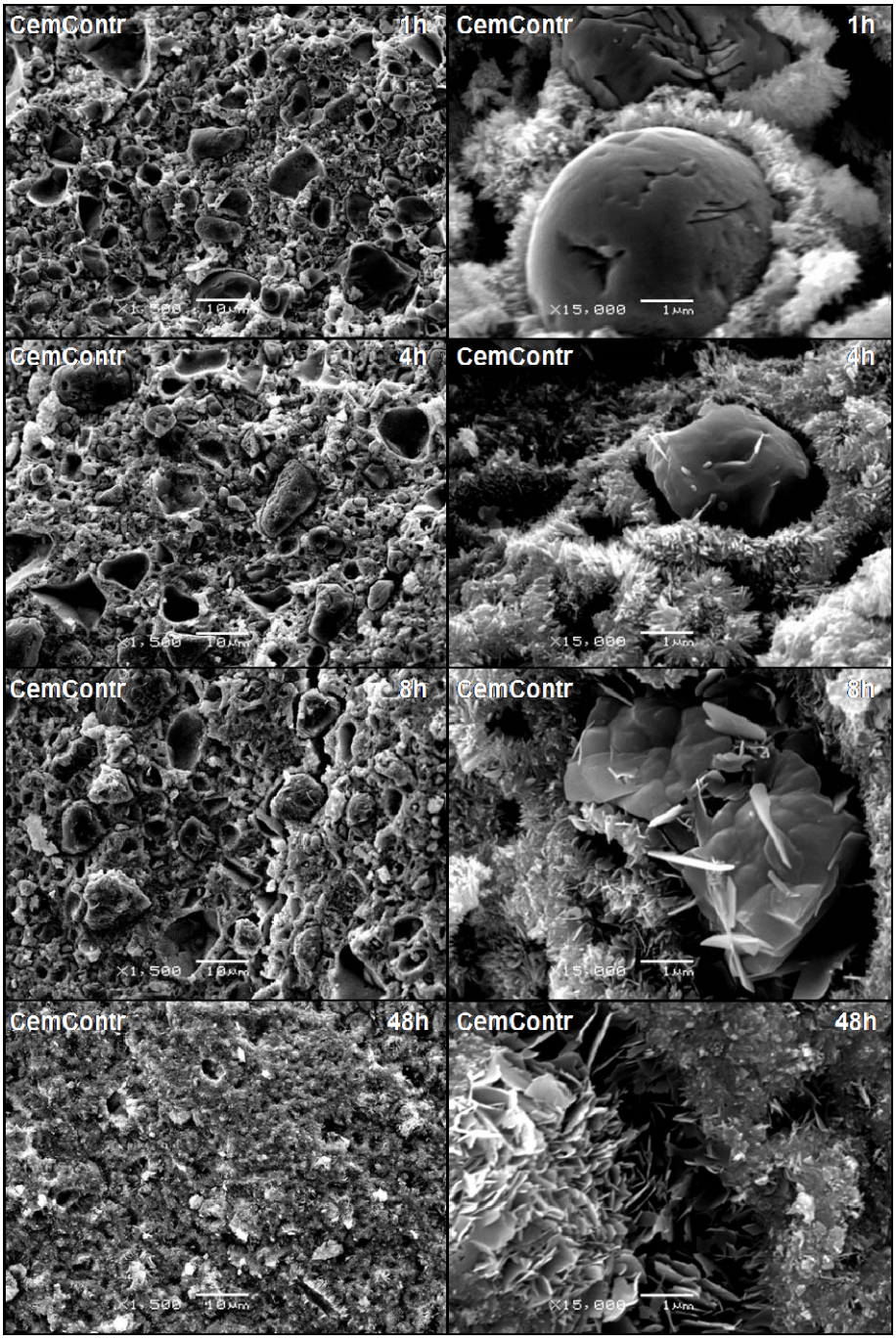

Figure 7.6. SEM pictures at different hardening times for *CemContr* (left: ×1500; right: x15000). Egg-like shells of CDHA crystals surrounding α-TCP articles and its further inner transformation into bigger CDHA crystals can be observed.

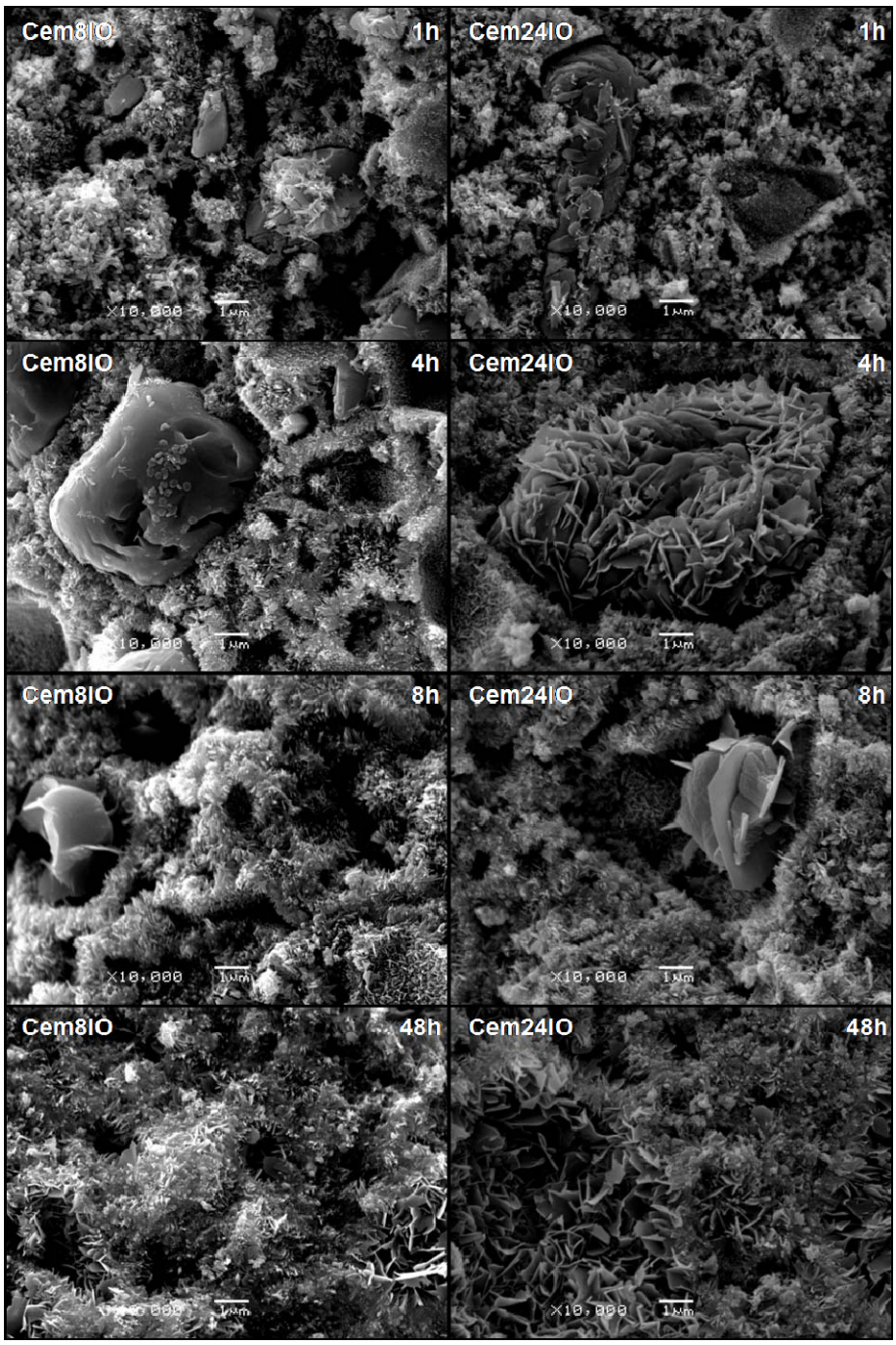

Figure 7.7. SEM pictures at different hardening times for *Cem8IO* and *Cem24IO* (i.e. *CemContr* modified with 8 and 24 *wt%*-IO) (×10000). The microstructure evolved similarly as for the control cement.

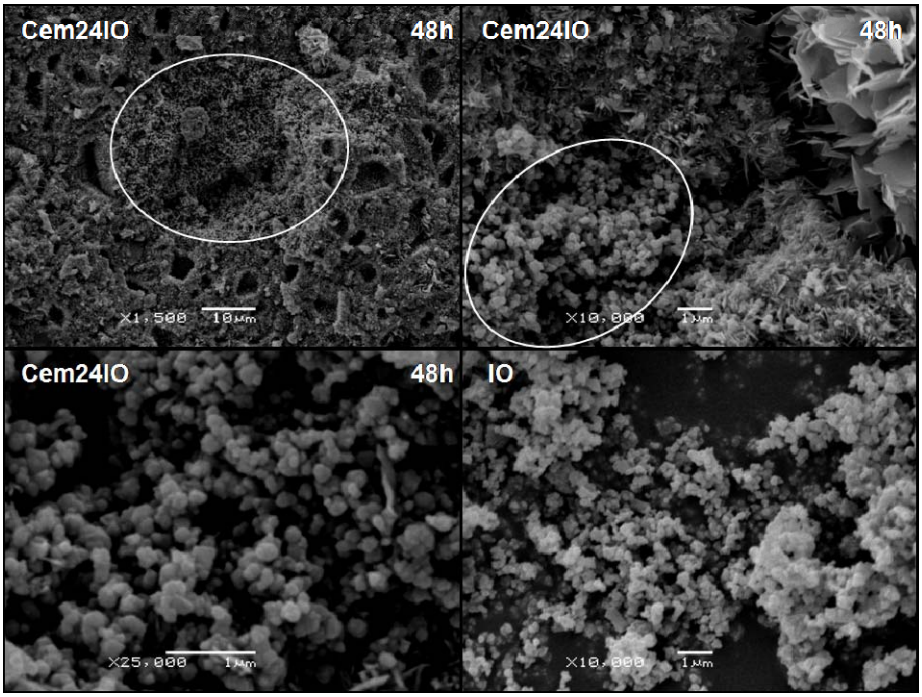

Figure 7.8. Top: Agglomerated IO-particles have been found in the cement matrix (left). As these particles does not react with the apatitic matrix (right) they act as weaker zones to propagate cracks. Bottom: Agglomerated IO particles found into the cement matrix (left) can be compared to the IO particles as received (right).

7.3.6. MTT-assay

Fig. 7.9 shows that *Cell relative viability (%)* of *HEp*-2 cells, co-cultured for 1 and 6 days with cements, was not significantly affected, i.e. all cements showed similar levels of cell viability at both incubation times. This indicates that differences in cement composition (i.e. *wt%* of IO addition) were not statistically significant ($p>0.05$) to the cellular viability. Moreover, after 6 days of incubation the cellular viability for all the cements was similar to that observed at 1 and 6 days for the control wells without cement. The only noticeable difference was the retard in cellular proliferation activity as deduced from Fig. 7.9 when

comparing the cement samples to the control-well after 1 day of incubation. In fact, cells were seeded at an initial density ρ_{0D} of $5x10^4$ cells/well (i.e. $\rho_{0D}\approx22000$ cells/cm^2) and Fig. 7.10 supports this observation.

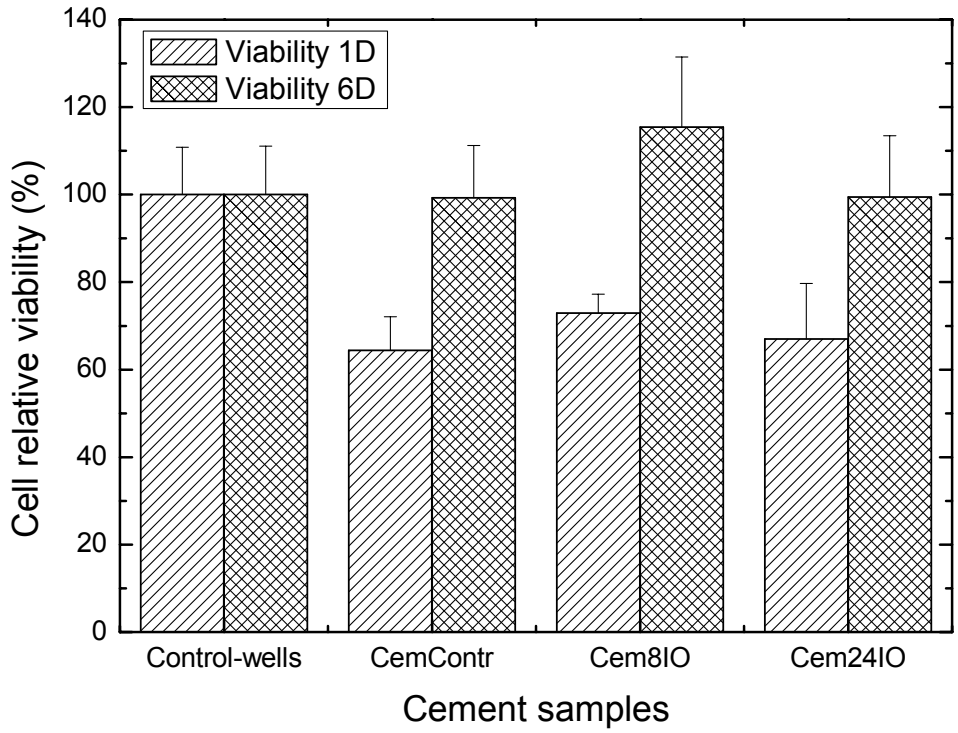

Figure 7.9. Effect of iron oxide on the relative cell viability after 1 and 6 days of culture *in vitro*.

Fig. 7.10 shows the *Adhesion density (cells/cm²)* measured for the different samples. It is observed that after 1 day of incubation samples *Cem8IO* ($\rho_{1D}\approx3.0x\rho_{0D}$) and *Cem24IO* ($\rho_{1D}\approx3.6x\rho_{0D}$) did not show significant difference between them ($p>0.05$) but with the controls ($p<0.05$), i.e. *CemContr* ($\rho_{1D}\approx2.1x\rho_{0D}$) and *Control-well* ($\rho_{1D}\approx5.5x\rho_{0D}$). In this sense, *Cem24IO* had higher ability to enhance adhesion of *HEp-2* proliferated cells as compared to *CemContr* ($p<0.05$), showing no-dose dependent effects of iron oxide on *HEp-2* cell's

function. Moreover, this data showed that the number of cells initially adhered onto the smooth surface of *Control-well* was statistically significant ($p<0.05$) as compare to the ones adhered onto the rough surfaces of the cements (i.e. *CemContr*, *Cem8IO* and *Cem24IO)*. However, Fig. 7.10 also shows that the adhesion density increased with the incubation time. In this sense, it is observed that after 6 days of culture there were not significant differences among the experimental bone cements and the controls ($p>0.05$). These results suggest that, despite cell viability and cell adhesion were similar on *Cem8IO* and *Cem24IO* so indicating a no-dose IO effect, the proliferation and growth of *HEp-2* cells were initially affected by the rough characteristics of the disk-cement surfaces [30,31]. However, this effect was not significant at longer incubating times.

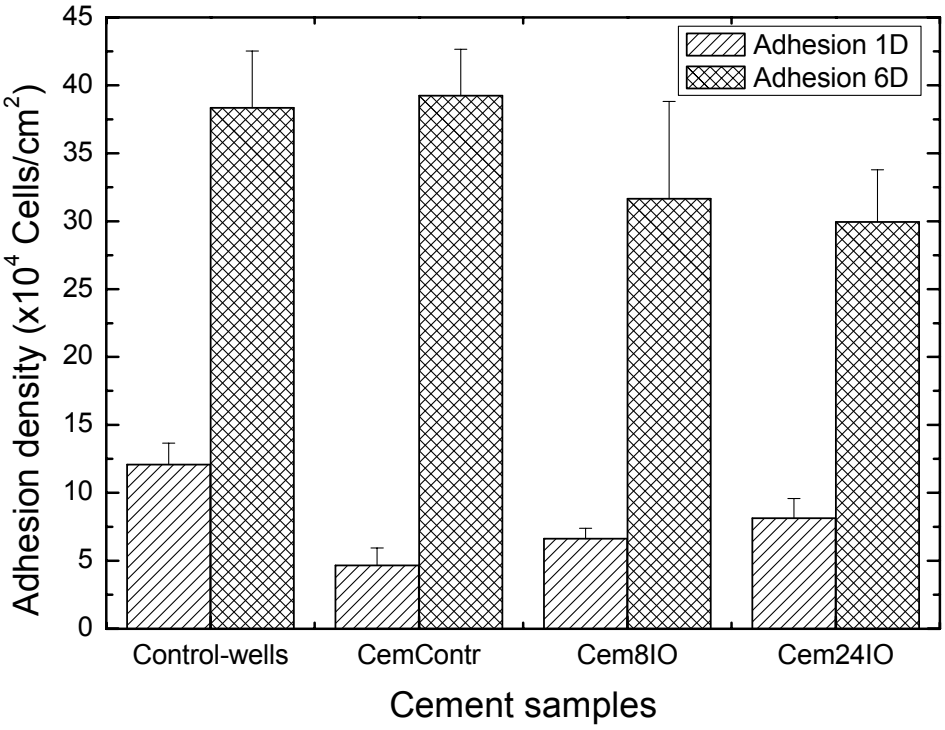

Figure 7.10. Effect of iron oxide on cells adhesion after 1 and 6 days of culture *in vitro*.

A final comment is needed to justify the use of epithelial cells instead of osteogenic cells in this study. The main reactant of the bone cement used in this research was alpha-tricalcium phosphate (α-TCP). As stated at the beginning of this chapter, the α-TCP-based bone cement was modified with different amounts of iron oxide particles. It was not the objective of this research to study the osteogenic behavior of the new iron-modified bone cement (this will be approach in next chapter) which, on the other hand, is well known for α-TCP. The interest was focused on the possible negative effect of the iron additive (oxidative damage) on the general mechanism of cellular adhesion and viability. A similar approach was followed in Chapter 6. The approach took into account that all eukaryotic cells need iron to survive and proliferate [32]. However, despite iron is essential for cellular replication, when iron is in excess the homeostatic cellular capacity can be exceeded, and consequently the cellular integrity affected [32-34].

7.4. Summary conclusion

In this study, it has been investigated the effect of iron oxide (IO) addition (8 and 24 *wt*%-IO) on the mechanical, injectability and biocompatibility properties of an experimental alpha-tricalcium phosphate cement (CPC). The results showed that the addition of IO nanoparticles: a) improved the maximum compressive strength of CPC after hardening; b) improved also both the initial workability (longer setting times) and the injectability of CPC before the initial setting; and c) did not have any detrimental effect on cement cytocompatibility. The conclusion is that IO-cement modification could be a suitable way to improve the initial cement's flowing properties, without affecting further hardening processes, of this or other similar bone calcium phosphate cement systems. These results open up new possibilities for the development of new injectable CPBCs for spinal surgery applications. However, attention should be given to the fact that the major limitation of

the present study is the lack of evaluation of the modified cement in actual osteoporotic vertebrae. In this sense, the advantages of the new cement may not hold true in an acute vertebral body. This issue should be addressed in the future.

References

1. Fernández E. Bioactive Bone Cements. In: Wiley Encyclopedia of Biomedical Engineering, 6-Volume Set, ISBN: 0-471-24967-X, John Wiley & Sons, Inc. (USA), Metin Akay (Ed.), June 2006, pp. 1-9.

2. Bohner M. Calcium orthophosphates in medicine: from ceramics to calcium phosphate cements. Injury 2000;31(S4):D37-D47.

3. Brown WE, Chow LC. Dental restorative cement pastes. US Patent No. 4518430, 1985.

4. Tyllianakis M, Giannikas D, Panagopoulos A, Panagiotopoulos E, Lambiris E. Use of injectable calcium phosphate in the treatment of intra-articular distal radius fractures. Orthopedics 2002;25(3):311-15.

5. Takegami K, Sano T, Wakabayashi H, Sonoda J, Yamazaki T, Morita S, Shibuya T, Uchida A. New ferromagnetic bone cement for local hyperthermia. J Biomed Mater Res: Appl Biomat 1998;43:210-14.

6. Heini PF, Berlemann U. Bone substitutes in vertebroplasty. Eur Spine J 2001;10:S203-215.

7. Gisep A, Wieling R, Bohner M, Matter S, Schneider E, Rahn B. Resorption patterns of calcium-phosphate cements in bone. J Biomed Mater Res 2003;66(3):532-40.

8. Apelt D, Theiss F, El-Warrak AO, Zlinszky K, Bettschart-Wolfisberger R, Bohner M, Matter S, Auer JA, von Rechenberg B. In vitro behavior of three different injectable hydraulic calcium phosphate cements. Biomaterials 2004;25:1439-51.

9. Phillips FM. Minimally invasive treatments of osteoporotic vertebral compression fractures. Spine 2003;28:S45-S53.

10. Truumees E, Hilibrand A, Vaccaro AR. Percutaneous vertebral augmentation. Spine J 2004;4:218-29.

11. Lewis G. Injectable bone cements for use in vertebroplasty and kyphoplasty: state of the art review. J Biomed Mater Res: Appl Biomat 2005;76B(2):456-68.

12. Belkoff SM, Mathis JM, Jasper LE. Ex vivo biomechanical comparison of hydroxyapatite and polymethylmetacrylate cements for use with vertebroplasty. Am J Neuroradiol 2002;23:1647-51.

13. Rotter R, Pflugmacher R, Kandziora F, Ewert A, Duda G, Mittlmeier T. Biomechanical in vitro testing of human osteoporotic lumbar vertebrae following prophylactic kyphoplasty with different candidate materials. Spine 2007;13:1400-5.

14. Bohner M, Gbureck U, Barralet JE. Technological issues for the development of more efficient calcium phosphate bone cements: a critical assessment. Biomaterials 2005;26:6423-29.

15. Khairoun I, Boltong MG, Driessens FCM, Planell JA. Some factors controlling the injectability of calcium phosphate bone cements. J Mater Sci: Mater Med 1998;9:425-28.

16. Bohner M, Baroud G. Injectability of calcium phosphate pastes. Biomaterials 2005;26:1553-63.

17. Baroud G, Bohner M, Heini P, Steffen T. Injection biomechanics of bone cements used in vertebroplasty. Bio-medical Materials and Engineering 2004;14(4):487-04.

18. Baround G, Vant C, Giannitsios D, Bohner M, Steffen T. Vertebral shell on injection pressure and intravertebral pressure in vertebroplasty. Spine 2004;30:68-74.

19. Krebs J, Ferguson SJ, Bohner M, Baroud G, Steffen T, Heini PF. Clinical measurements of cement injection pressure during vertebroplasty. Spine 2005;30:188-22.

20. Vlad MD, Torres R, López J, Barracó M, Moreno JA, Fernández E. Does mixing affect the setting of injectable bone cement? An ultrasound study. J Mater Sci: Mater Med 2007;18:347-52.

21. Sarda S, Fernández E, Llorens J, Martínez S, Nilsson M, Planell JA. Rheological properties of an apatitic bone cement during initial setting. J Mater Sci: Mater Med 2001;12:905-09.

22. Fernández E. Iron-modified calcium phosphates. Spanish Patent No. ES2257131, 2003.

23. ASTM C191-92, Annual Book of ASTM Standards, vol. 04.01: Cement, Lime, Gypsum. Philadelphia: ASTM 1993;189-91.

24. Gupta AK, Gupta M. Cytotoxicity suppression and cellular uptake enhancement of surface modified magnetic nanoparticles. Biomaterials 2005;26:1565-73.

25. Sarda S, Fernández E, Nilsson M, Balcells M, Planell JA. Kinetic study of citric acid influence on calcium phosphate bone cements as water-reducing agent. J Biomed Mater Res 2002;61:653-59.

26. Kim DK, Zhang Y, Kehr J, Klason T, Bjelke B, Muhammed M. Characterization and MRI study of surfactant-coated superparamagnetic nanoparticles administered into the rat brain. Journal of Magnetism and Magnetic Materials 2001;225:256-61.

27. Corti M, Lascialfari A, Micotti E, Castellano A, Donativi M, Quarta A, Cozzoli PD, Manna L, Pellegrino T, Sangregorio C. Magnetic properties of novel superparamagnetic MRI contrast agents based on colloidal nanocrystals. Journal of Magnetism and Magnetic Materials 2008;320(14):320-33.

28. Vasquez-Mansilla M, Zysler RD, Arciprete C, Dimitrijewits MI, Saragovi C, Greneche JM. Magnetic interaction evidence in α-Fe_2O_3 nanoparticles by magnetization and Mössbauer measurements. Journal of Magnetism and Magnetic Materials 1999;204(1-2):29-35

29. Jiang M, Terra J, Rossi AM, Morales MA, Baggio Saitovitch EM, Ellis DE. Fe^{2+}/Fe^{3+} substitution in hydroxyapatite: theory and experiment. Physical Review B 2002;66:224107.

30. Anselme K, Bigerelle M, Noel B, Dufresne E, Judas D, Iost A, Hardouin P. Qualitative and quantitative of human osteoblast adhesion on materials with various surface roughness. J Biomed Mater Res 2000;49:155-66.

31. Suzuki T, Ohashi R, Yokogawa Y, Nishizawa K, Nagata F, Kawamoto Y, Kameyama T, Toriyama M. Initial anchoring and proliferation of fibroblast L-929 cells on

unstable surface of calcium phosphate ceramics. Journal of Bioscience and Bioengineering 1999;87(3):320-27.

32. Kakhlon O, Cabantchik ZI. The labile iron pool: characterisation, measurement, and participation in cellular processes. Free Radical Biology & Medicine 2002;33(8):1037-46.

33. Henze MW, Muckenthaler MU, Andrews NC. Balancing acts: molecular control of mamalian iron metabolism. Cell 2004;117:285-97.

34. Cotran R, Kumar V, Abbas AK, Fausto N. In: Robbins & Cotran, ed. Pathologic Basis of Disease, 7th edition, Philadelphia: Elsevier Saunders, 2005, chapter 1, pp. 14-17. ISBN:0-7216-0187-1.

Chapter 8

Osteogenic features of biphasic calcium sulphate dihydrate/iron-modified alpha-tricalcium phosphate bone cements: in vitro and in vivo study

8.0. Structured abstract

Mini Abstract. The cytocompatibility, the biocompatibility and the osteogenic character of new "iron-modified alpha-tricalcium phosphate (IM/α-TCP) and calcium sulphate dihydrate (CSD)" byphasic cements (IM/α-TCP/CSD-BC) has been investigated in terms of MG-63 *in vitro* cell adhesion, proliferation, morphology and cytoskeleton organization and in terms of the *in vivo* cement resorption, bone formation and host tissue response on animal model. The results showed that the new cements have cyto- and biocompatible features of interest as possible spinal cancellous bone replacement biomaterial.

Study Design. Experimental study to characterise the cytocompatibility (through direct-contact osteoblast-like cells culture) and the biocompatibility (by implantation on sheep animal model) of the new IM/α-TCP/CSD-BC.

Objective. To investigate the cytocompatibility properties and the biocompatibility features with special interest on cement resorption (i.e. cement decomposition and cell-mediated resorption).

Summary of Background Data. Calcium phosphate cements (CPCs) are used in a wide range of clinical applications due to their suitable biocompatibility and osteointegration after implantation. However, apatitic cements have slow resorption *in vivo*. In adition, CPCs' mechanical strength limits their applications to nonload bone bearing situations. However, the present Thesis has approached new methods for improving both the osteointegration (see Chapter 3) and the cement strength (see Chapters 5 and 7) of apatitic CPCs. Thus, this chapter is a combination of the ideas of previous chapters and is focussed on the *in vitro* and *in vivo* behaviour of the new porous iron-modified CPCs.

Methods. The cytocompatibility was analysed by culturing MG-63 osteoblast-like cells onto the new cements and the controls and by evaluating both the relative cell viability and the adhesion cell density. Scanning Electron Microscopy (SEM) followed the

morphological features of cell adhesion and proliferation. Confocal microscopy was used to examine the cytoskeleton organization of the fluorescently-labeled cells seeded onto the cements-like substratum. Sheep animal model was used to study the biocompatibility. Histological evaluation performed on un-decalcified cement-bone specimens assessed the *in vivo* behaviour.

Results. Quantitative MTT-assay and SEM showed that cell adhesion and viability were not affected with culturing time by compositional or surfaces' geometric factors. SEM-cell morphology and cytoskeleton observations showed that MG-63 cells (seeded on the new cements) were able to adhere, to spread and to attain normal morphology. On the other hand, the *in vivo* study proved the biocompatibility and the osteogenic features of the new cements (i.e. osteoconductivity and macrophage-mediated resorption).

Conclusions. It has been shown that IM/α-TCP/CSD-BC has the ability to support cellular colonization *in vitro* and lead firm bone binding *in vivo*. Both, quantitative and morphologic evaluations showed that adhesion, proliferation and viability of MG-63 cells were not negatively influenced by the presence of iron into the cements. Qualitative histology proved cement biocompatibility, osteocoduction and favorable resorption.

Key Points.

- Byphasic cement made of iron-modified α-TCP (the main reactant of apatitic cements) and calcium sulphate dihidrate (CSD) showed favorable substratum properties for osteoblast-like cells proliferation and differentiation *in vitro*.
- Iron-modification did not affect negatively the known-proved biocompatibility of calcium phosphate cements.
- The new biphasic cements showed osteoconductive features and good resorption, mainly through a macrophage-mediated mechanism.

8.1. Introduction

Since the first calcium phosphate bone cement (CPBC) synthesized by Brown and Chow [1] many different formulations have been studied and have resulted in various commercial products (i.e. *Norian SRS©*, *Cementek©*, *Biocement-D©*, *α-BSM©*, *BoneSource©* and/or *Biopex©*) [2,3] used in a wide range of clinical applications (bone fractures, bone tumours, osteoporosis and craniofacial affections) [4-9], mainly due to the similar bone-like apatite structure evolved during their setting [10-19], their high biocompatibility and their good osteointegration after being implanted *in vivo* [20-23].

Despite these advantages, it is generally accepted that CPBCs need further improvements to broad their potential clinical applications [24] due to the fact that apatitic (i.e. the end setting product being hydroxyapatite ($Ca_{10}(PO_4)_6(OH)_2$; HA) and/or calcium deficient hydroxyapatite ($Ca_9HPO_4(PO_4)_5OH$; CDHA) [25-27]) bone cements are so stable *in vivo* that bone cement's resorption takes a long time, i.e. months to years [28-31]. In order to accelerate new bone aposition and resorption of the cement implant, several authors have improved macroporosity, i.e. more and larger pores, of apatitic bone cements in several ways [32-38]. Moreover, depending on the degree of crystallinity and porosity, CPBCs can be made to be more or less stable after implantation [21,30,39-41]. It should be remembered that in previous Chapter 3, it has been presented a method to improve the osteointegration of α-tricalcium phosphate (α-TCP) based cements by the modification of the cement's powder phase with different amounts of calcium sulphate dihydrate (CSD) [42]. The resulting hardening properties of the new biphasic cements were a combination between the progressive hardening due to the main α-TCP reactant and the progressive dissolution of the CSD phase, which render a porous material (see Chapter 3). In fact, CSD (first implanted by Dreesmann [43]) has been of the interest of many scientists that have used it as a filler material and/or as a replacement for

cancellous bone graf due to its widely proved biocompatibility and rapid resorption [44-48]. Even, Bohner et al. [49] has showed that small amounts of CSD added to the liquid phase can have interesting effects on the cement setting reactions, suggesting a complex effect of sulphate ions on it.

In addition to the above comments, it should be noted that CPBCs lack of high mechanical strength and this limits their applications to nonload bone bearing situations [24]. Moreover, with the advent of minimally spinal invasive surgery techniques (vertebro- and kyphoplasty) it has been put forward that apatitic cements are difficult to inject into the compression fractured osteoporotic vertebras [24,50,51]. However, the present Thesis has approached new methods for improving the osteointegration (see Chapter 3) and the injectability and the cement strength (see Chapters 5 and 7) of apatitic CPCs [52-54], which is of interest to spinal applications (see also Chapter 6). Thus, the present chapter/study is a combination of the ideas of previous chapters and adds new data for the whole comprehension of the *in vitro* and *in vivo* behaviour of new "iron-modified alpha-tricalcium phosphate (IM/α-TCP) and calcium sulphate dihydrate (CSD)" byphasic cements (IM/α-TCP/CSD-BC). Thus, the objective of this research was to investigate the cytocompatibility properties of the new IM/α-TCP/CSD-BC through direct-contact osteoblast-like cells cultures, as well as to study their biocompatibility features and their bioactivity (in the sense of osteoconduction and resorption) after implantation on sheep animal model.

8.2. Materials and methods

8.2.1. Cement substrates

In this study, the main ceramic reactive used for cement production, i.e. the α-TCP, was of two types: a) high-purity α-TCP (according to XRD data) for control cement's

productiont (coded as *CemContr* in Chapter 6 and now coded as *CemC* for convenience; by *Mathys Medical, Switzerland*); and b) iron-modified α-TCP (*IM/α-TCP*; inlab preparation). This *IM/α-TCP* was prepared by sintering together calcium hydrogen phosphate (DCP; $CaHPO_4$; *Sigma-C7263*) and calcium carbonate (CC; $CaCO_3$; *Sigma-C4830*), at 2:1 molar ratio, with 8 *wt%* of iron oxide (IO; α-Fe_2O_3; *Panreac-212375*), added in respect to the theoretic amount of α-TCP obtained from the 2:1 DCP/CC mixture. Other details concerning the sintering protocol can be found in Chapter 5 where this sintering protocol was named as Protocol-A. The resulting *IM/α-TCP* was coded for this study as *8IM/α-TCP* and according to XRD (data not shown) only α-TCP peaks were detected (i.e. no individual iron phases seemed to be present).

Once the main reactives were obtained, biphasic cement formulations were produced containing 70 *wt%* α-TCP (non-iron or iron-modified) and 30 *wt%* calcium sulphate dihydrate (CSD; $CaSO_4 \bullet 2H_2O$; *Sigma-C3771*). The resulted cements were codes as *CemC-CSD* and *8IM-CSD*, respectively. CSD was used as a porosity control agent to improve further *in vivo* cellular colonization [42], following the ideas and results obtained previously in Chapter 3.

Moreover, as no iron-phases (i.e. sintered by-products) were detected by XRD in the new sintered *IM/α-TCP* reactive, a second cement control, proved to be non-cytotoxic in Chapter 7 (code: *Cem8IO*; now renamed for convenience as *CemC-8IO*), was also used to clear whatever new doubt on the potential negative *in vitro* behaviour of cells [53,54], as due to the presence of iron into the crystalline structure of the *IM/α-TCP* reactive (possibly forming stable solid solutions). Thus, according to the data of Chapter 7, it should be remembered that cement *CemC-8IO* was a mixture of 92 *wt%* pure α-TCP (by *Mathys Medical*) and 8 *wt%* IO particles (by *Panreac*).

Thus, the cement-like substrates used for the *in vitro* study were prepared as follows. *CemC*, *CemC-CSD*, *8IM-CSD* and *CemC-8IO* cement's powder phases were mixed with an

aqueous cement phase containing 2.5 *wt%* of disodium hydrogen phosphate (DHP; Na_2HPO_4; *Panreac-131679*) setting accelerator. The cement mixing liquid to powder (L/P) ratio was set to 0.32 mL/g. Then, the liquid and powder phases were mixed for 1 min up to homogeneisation. The resulting cement paste was immediately placed into appropriate disk moulds to ensure standardized shapes (10 mm diameter by 2 mm height). The cement disks were removed from the moulds after setting for 30 min in Ringers solution at 37°C. Immediately after, the disks were sterilized by UV-irradiation for 30 min and then used as substrates for the *in vitro* cell culture.

8.2.2. Cytocompatibility testing

8.2.2.1. Cell culture

The *in vitro* cell culture protocol used in this study was identical to that described in Chapter 6 (see *6.2.2.1. Cell culture*). In that chapter HEp-2 cells (epithelial cells derived from a human laryngeal carcinoma) were used while in this one MG-63 osteoblast-like cells line (cell line derived from human osteosarcoma; *American Type Culture Collection, USA*) were used. This cell line (the prototype for osteoblastic cells) is well characterized and has been used as validated model to test the biocompatibility of various biomaterials [55-58]. In this study, glass disks coverslips (*Knittel Glaser, Germany*) were used as positive cytocompatible controls (*Coverslips*).

8.2.2.2. Cell viability

The viability of MG-63 cells, seeded onto the cement substrates and incubated for 1 and 7 days (1D and 7D), was evaluated using quantitative MTT-assay [59]. The applied protocol was exactly the same as that described in Chapter 6 (see *6.2.2.2. Cell viability*). However, some different experimental equipment was used this time. For example, the

solubilization of formazan crystals was done under continuous agitation in a different orbital shaking platform (*Grant-bio POS-300; Grant Instruments Ltd., England*). Also, the absorbance was read on a different microplate reader (*Synergy 2; BioTek Instruments, USA*). Finally, the *Cell relative viability (%)* was calculated as explained in Chapter 6.

8.2.2.3. Cell adhesion

The *Adhesion profile (cells/cm²)* of MG-63 cells, cultured onto the experimental cement substrates for 1 and 7 days, was obtained by following the same protocol explained in Chapter 6 (see *6.2.2.3. Cell adhesion*). It should be remember that the *Adhesion profile* is the ratio between the cells adhered onto the substrates and the disk-cement area available for cell's attachment.

8.2.3. Morphological study

This study was performed by Scanning Electron Microscopy (*SEM, JEOL JSM-5610; Hitachi, Japan*) on MG-63 cells cultured onto the experimental substrates for 7 and 14 days. Before SEM observations, the substrates were rinsed with PBS, fixed with 2.5% paraformaldehyde (*Electron Microscopy Science-Ref. 1571*), subjected to graded alcohol dehydrations and sputter coated with gold (see also *Chapter 6; 6.2.3. Morphological study*).

8.2.4. Immunocytochemical study

8.2.4.1. Immunofluorescence staining

The protocol for the immunofluorescence staining's study was as follow. MG-63 cells cultured onto cement disks for 7 days were fixed in 4% paraformaldehyde/PBS during 15 min. Then, the samples were washed with PBS, and a permeabilising buffer (0.1% Triton X-100 in 1% Bovine Serum Albumin (BSA)/PBS) was added for 5 min. Then after, the

samples were incubated for 5 min in 1% BSA/PBS and washed with 0.1% BSA/PBS for other 5 min. After this, it followed the simultaneous addition of monoclonal anti-α-tubulin-FITC antibody (1:100 in 0.1% BSA/PBS; *Sigma Chemical-F2168*) and Phalloidin-TRITC (for F-actin staining; 1:100 in 0.1% BSA/PBS; *Sigma Chemical-P1951*) for 1 h. Then after, samples were washed twice in 0.1% BSA/PBS for 5 min, and Hoechst 33342 (1:2000 in 0.1% BSA/PBS; *Sigma Chemical*) was added for 10 min to stain the cells' nucleus. A final wash was given before mounting the samples for 24 h in *ProLong Gold* mountant (*Molecular Probes, England*). After the mountant's curing process the samples were ready for confocal microscopy observations. The entire immunofluorescent staining protocol was done at room temperature.

8.2.4.2. Cytoskeleton observation

Leica TCS SP5 laser scanning confocal microscope (*Leica Microsystem Heidelberg GmbH, Germany*) equipped with DMI6000 inverted microscope, Argon laser and 63x oil immersion objective lens (NA 1.4), was used to examine the fluorescently-labeled cells present onto the cement-like substrates. Hoechst 33342, FITC and TRITC images were acquired sequentially using 405, 488 and 561 nm laser lines thanks to an acousto optical beam splitter (AOBS) device with emission detection ranges of 415-450, 500-535 and 570-650 nm, and confocal pinhole set at 1 airy units. The final analysis of the deconvolved images was performed using proprietary Image J software.

8.2.5. Statistical analysis

The *in vitro* experiments were done in triplicate. The numeric results have been expressed as mean ± standard deviation (mean ± SD). A one-way ANOVA test was used to analyze the mean variance of the data. Tukey`s multiple comparison was used to compare the

data at a family confidence coefficient of 0.95. Statistical significance was accepted at a level of p-value < 0.05.

8.2.6. In vivo experimental study

8.2.6.1. Animal model

Four adult (age 3-5 years), female, Romanian Alpine sheep with mean body weight of 41 kg were included in this study (permission granted by the Animal Care and Ethical Committee of the Faculty of Veterinary Medicine, Iasi, Romania). The experimental animals were divided into two groups with two animals each. The study period until euthanasia was 3 and 6 month. Animals were clinically examined and accommodated to new environments 2 weeks prior surgery. They had free access to food and water, throughout the entire study, except before anesthesia, i.e. food was withdrawn 24 h prior surgery but water was permitted ad libitum.

8.2.6.2. Bone cement implants: design of the experiment

The apatitic bone cements used in this study were *CemC*, *CemC-CSD* and *8IM-CSD* (see details in *8.2.1. Cement substrates*). The powder and the liquid cement phases were mixed at the operation theatre for 1 min, in a mortar with a pestle. After homogeneisation, the cement pastes were placed in 5 mL syringes and injected into the previously prepared cylindrical sheep bone defects (see next section), at least 3 min later than the start of mixing; the initial setting time IST at room temperature was 20-25±2 min (Gillmore needles method; [60]). The implantation sites were distributed such that none of the cements were placed twice in the same location at the same time (see Table 8.1). On the other hand, biphasic bone cements (i.e. *CemC-CSD* and *8IM-CSD*) were implanted three times more than control-cement (CemC) or control-defects (i.e. empty holes) because of

the interest of CSD as a controlling porosity agent during bone remodeling (see Chapter 3). Note that empty control holes (8mm diameter by 13mm depth) were drilled in the distal epiphysis and proximal metaphysis of the right and left humerus and femur to model mechanically unloaded bone defects [23].

Table 8.1. Implant sites, animal codes and observation periods of planned *in vivo* study.

Implant site	**3 months**		**6 months**	
	RO105	**RO106**	**RO105**	**RO106**
Humerus right proximal	CemC-CSD	8IM-CSD	8IM-CSD	CemC-CSD
Humerus right distal	8IM-CSD	CemC-CSD	CemC-CSD	8IM-CSD
Femur right proximal	CemC-CSD	8IM-CSD	CemC	CemC-CSD
Femur right distal	8IM-CSD	CemC	Control	CemC-CSD
Humerus left proximal	Control	CemC-CSD	CemC-CSD	8IM-CSD
Humerus left distal	CemC-CSD	8IM-CSD	8IM-CSD	CemC
Femur left proximal	CemC	CemC-CSD	8IM-CSD	Control
Femur left distal	8IM-CSD	Control	CemC-CSD	8IM-CSD

8.2.6.3. Surgical and postoperative protocol

All surgical interventions were performed under general anesthesia in aseptic conditions. Before induction of anesthesia the sheep were premedicated with atropine (0.02 mg/kg s.c; *Atropina, Pasteur Institute, Romania*). Anesthesia was induced with xylazine (0.1 mg/Kg i.m.; *Xylazine® Bio 2%, Bioveta, Czech Republic*) and ketamine (10 mg/kg i.m.; *Ketaminol® 10, Intervet International GmbH, Germany*). The animals were placed for surgery in lateral recumbency and were rotated to the other side during the surgical protocol. The preoperative preparation of the surgical sites was routinely done by cleaning with 96% alcohol and antiseptic solutions (Videne; *Adams Healthcare Ltd., England*). Lateral surgical

approaches of the proximal and distal extremities of the humerus and femur were performed routinely. A total of 4 drill holes were done on one side using an 8 mm drill burr. The resulting bone cavities were carefully washed to eliminate bone debris and dried with gauze before being filled with the apatitic bone cements; the filling was carefully done from the bottom of the cylindrical deffect to ensure both minimal inclusion of air bubbles and direct cement-bone contact. Then after, implanted cements were granted with 30 min of hardening before routine closure of the wounds. This was done to assure suitable cement strength as to properly suture the fascias and the subcutaneous tissue without damaging the implanted cement integrity and the cement-bone contact area. Closure of fasciae and subcutaneous tissue was routinely done using resorbable material (Vicryl 3/0; *Ethicon, Germany*) in a continuous fashion. The skin was closed by means of mattress sutures. The surgery procedure was identical on both animal sides. Each animal received peri- and postoperative analgesia (carprofen 4.4 mg/kg s.c.; *Rimadyl®, Pfizer, UK*). Antibiosis consisted in 7.5 mg/kg amoxicillin (*VEYX® YL LA 200; Veyx-Pharma GmbH, Germany*). Analgesia and antibiosis were continued for 3 days after surgery. After recovery, sheep were kept confined in small stalls for 3-4 weeks before they were allowed unrestricted mobility; during this period, sheep were checked dayly for clinical lameness or other complications.

8.2.6.4. Radiographic and macroscopic analysis

To assess both, bone and cement density, as well as the amount of cement filling, conventional X-rays radiographs (*Sirescop CX, Siemens, Germany*) were done following medio-lateral (m-l) and craniocaudal (a-p) views. The radiographs were done postoperatively and post-euthanasia at 46 kV and 4 mA for m-l view, and at 45 kV and 3.2 mA for a-p view, using a focus-film distance of 1.2 m (*Kodak Diagnostic Film*). The implanted bones were harvested immediately post-euthanasia and the experimental

defects were macroscopically evaluated by considering the tissue reaction adjacent to the cement, the visibility of the cement, the amount of cement filling, the quality of the cement integration as well as the level of cement resorption and new bone formation.

8.2.6.5. Microscopic evaluation

Qualitative histology was done to account for cement resorption, bone formation and cellular events involved during the cement degradation (including either inflammatory or immune reactions); special interest was placed on the adjacent host tissue. For this, histology sections of undecalcified cement-bone specimens were prepared [61]. Briefly, after euthanasia, all cement-bone specimens were fixed in 10% buffered formalin, dehydrated in increasing grades of ethanol (50-100%), and embedded in methyl methacrylate (MMA). Sections of 10 μm thickness were obtained with a microtome (*Leica 22550, Leica Instruments GmbH, Germany*) and specimens' sections were deplasticized with methyl-acetate and stained by the Von Kossa's (VK) and the Goldner's trichrome (TRI) techniques. The sections were taken in all cases from the middle of the implants (cement-bone specimens were cutted sagittally or transversally). A total of 4 sections per block were VK and TRI stained (i.e. two sections for each stain) for conventional light microscopy. The qualitative histology was performed from stained sections using a microscope (*Olympus BX51, Germany*) with attached digital camera (*DP70, Olympus, Germany*). It should be remembered that VK stains the osteoid in red and the mineralized bone in black, while TRI stains the osteoid in red, the mineralized bone in green and the cell nucleus in blue.

8.3. Results

8.3.1. Cytocompatibility

Fig. 8.1 shows the MTT-assay results. This figure accounts for the *Cell relative viability (%)* of MG-63 cells after 1 and 7 days (i.e. 1D and 7D) of culture onto the experimental cements (i.e. *CemC-CSD*, *8IM-CSD*) and the controls (*Coverslip*, *CemC* and *CemC-8IO*). First of all, it is observed that cell growth and proliferation increased with time for all the cements but in different amounts. For example, CSD-modified cements (i.e. *CemC-CSD*, *8IM-CSD*) showed similar levels of vialibility between them at both 1D (lower) and 7D (higher). However, at 1D, these cements showed lower (statistically significant, $p<0.05$) viability than the controls. Moreover, at 7D, the viability of these cements was still a bit lower (statistically significant) than that observed for the controls.

Fig. 8.2 shows the *Adhesion profile (cells/cm^2)* of MG-63 cells for all the tested substrates at 1D and 7D of cell culture. All the substrates developed similar adhesion profiles at 1D ($p>0.05$). However, at 7D, despite it is observed that the adhesion rate increased with the time for all the substrates, the CSD-modified cements (i.e. *CemC-CSD* and *8IM-CSD*) showed lower significant values ($p<0.05$) as compare to the controls (i.e. *Coverslip*, *CemC* and *CemC-8IO*) but similar values between them.

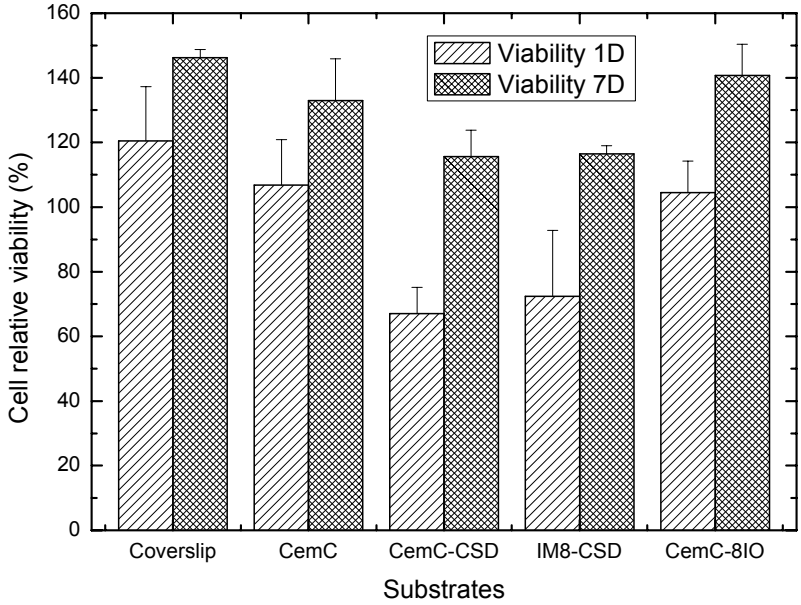

Figure 8.1. Cell relative viability *vs.* cement substrates: effect of CSD and iron on MG-63 cells' viability after 1 & 7 days of culture (i.e. 1D and 7D).

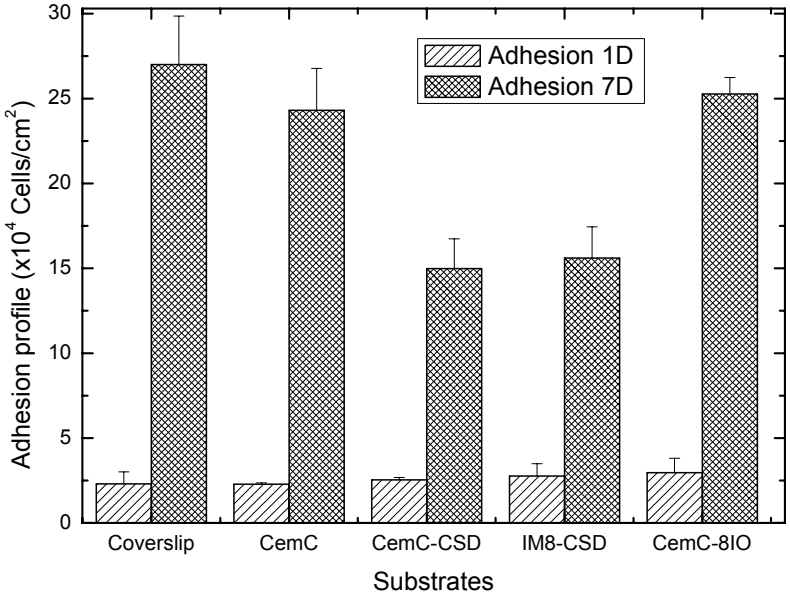

Figure 8.2. Adhesion profile *vs.* cement substrates: effect of CSD and iron on MG-63 cells adhesion after 1 & 7 days of culture (i.e. 1D and 7D).

8.3.2. Cellular morphology

Fig. 8.3 and Fig. 8.4 show the morphology of MG-63 cells cultured onto *CemC-CSD* and *8IM-CSD* for 7 and 14 days (14D), respectively. In general, it was observed that cells cultured for 7D proliferated and formed confluent cell monolayers on both cements. However, some small areas were observed to be not covered by the confluent cell monolayer, as shown in Fig. 8.3 (see top row). Broadly speaking, Fig. 8.3 shows that cells attached and spread in a comparable manner onto the both substrates. In this sense, cells developed many large lamellipodia and some long filopodia, as noted in Fig. 8.3.c and Fig. 8.3.d at a higher magnification; these figures show cytoplasmic processes attaching to the cement's surface. Moreover, after 7D, cells had flat appearance and showed similar bipolar and/or tripolar spindle-like morphology, attaching on specific surface's structural sites like sharp or ridge reliefs. On the other hand, pictures A-D in Fig. 8.3 show cell-cell interactions onto the cement's surface.

Similarly, Fig. 8.4 shows some pictures of cells cultured onto *CemC-CSD* and *8IM-CSD* for 14 days. The appearance of the cells onto the substrates seemingly varied with its surface topography (see top row). The cells grown on both substrates were well spread and formed continuous monolayer. At higher magnification, it was observed that the cells grown on *CemC-CSD* had similar morphology to those on *8IM-CSD* and exhibited greater activity (as compared to 7D) onto their surface (see pictures D and E), forming clump-like structures at random spots (i.e. mineralised nodules formation occurred; see picture G and picture J, which is a higher magnification of picture G). Moreover, some cells seem to be embedded into extracellular matrix (ECM) while others developed many thin filopodia anchored to the ECM or contacting with adjacent cells. In addition, they appeared to form multiple layers onto the both cements' surfaces. On the other hand, it

was observed that many cells were in the process of cell division (a detail is shown in picture H; K is a higher magnification of H, showing the anchorage process).

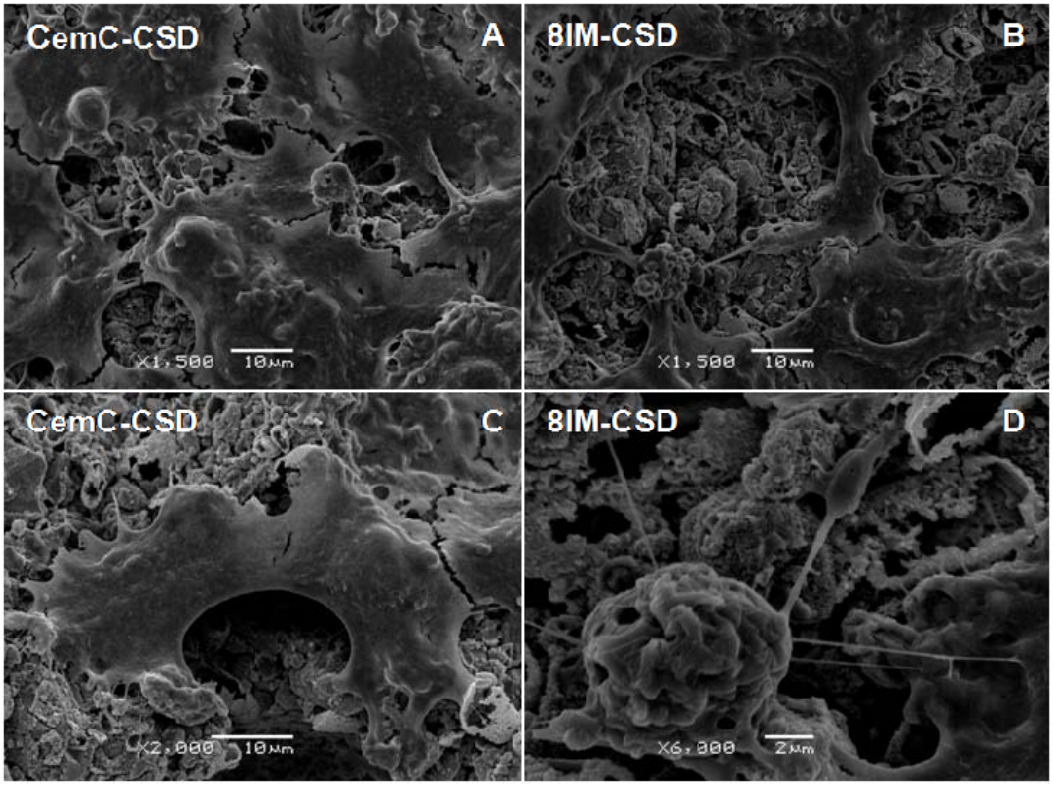

Figure 8.3. SEM pictures of MG-63 cells attached to the surface of *CemC-CSD* and *8IM-CSD* bone cements after 7 days of culture (top: 1500x; bottom-left: 2000x; bottom-right: 6000x). Images show cell–cell and cell-material interactions (see details on the text).

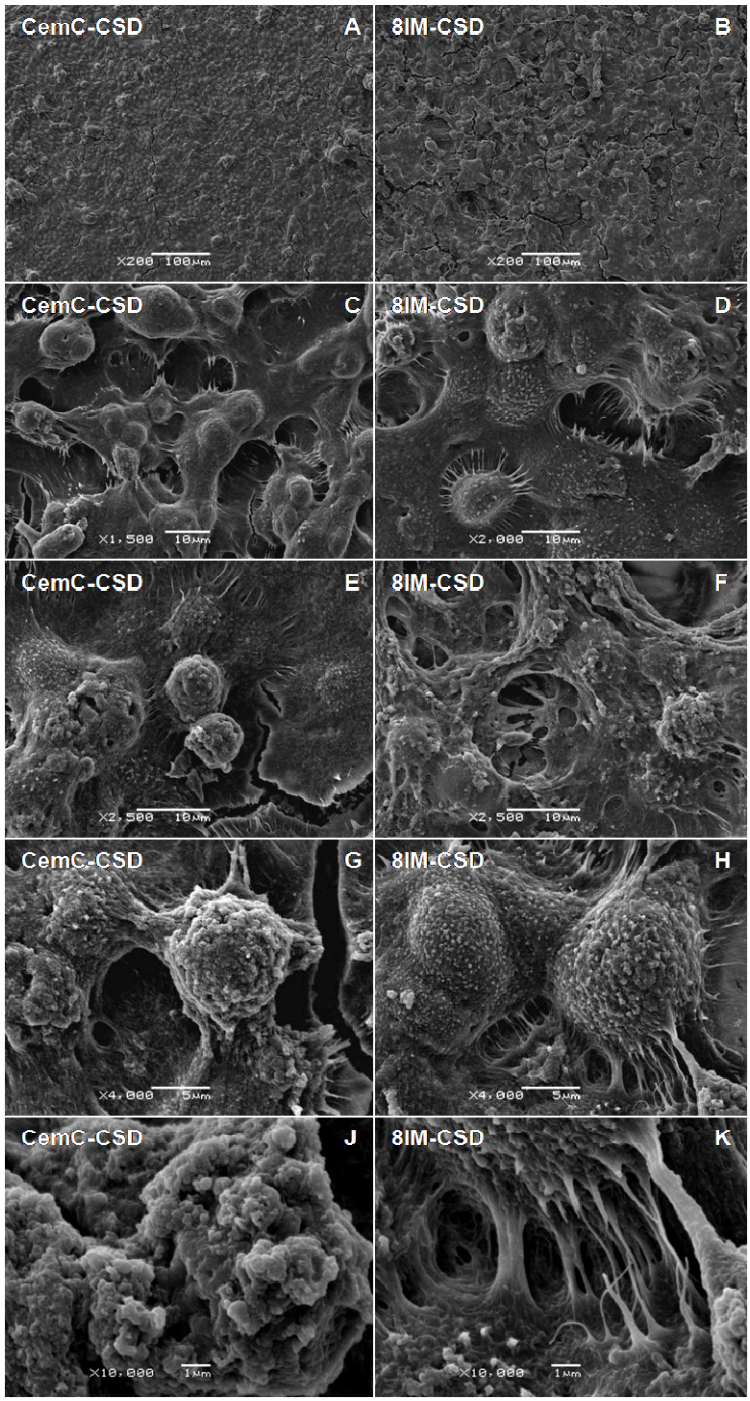

Figure 8.4. SEM pictures of MG-63 cells cultured for 14 days onto *CemC-CSD* and *8IM-CSD* showing the later stage of the osteoblastic cell function. (a-b) 200x; (c) 1500x; (d) 2000x; (e-f) 2500x; (g-h) 4000x; (j-k) 10000x).

8.3.3. Cytoskeleton organisation

Figs. 8.5-8.7 show the observations performed by confocal microscopy on the cytoskeleton organization of MG-63 cells, cultured onto the different substrates, for 7 days. It is observed that actin filaments were visible within the cells for all the substrates. Processes containing distinct parallel bundles were also noted. F-actin cytoskeleton (Fig. 8.5, left column) appeared well defined and organised for the control cells (i.e. *Coverslip* substrates) with parallel bundles observed throughout the cytoplasm. However, the actin cytoskeleton showed distinct distribution (like gel-like network) within the cells for the experimental cement substrates, with microfilaments inside the cytoplasm and exhibiting strong peripheral F-actin along the cell edge, which is indicative of cortical actin fibres. Also, the microfilaments were organised in a few thick bundles forming stress fibres. On the other hand, for α-tubulin (Fig. 8.5, middle column), the microtubules formed a dense network equally distributed around the nucleus of the cells. However, the CSD-modified cements showed better developed microtubules towards the border of the cells. Moreover, the observed cellular density (see Fig. 8.6) of *CemC* and *8IM-CSD* was qualitatively in agreement with the quantitative data in Fig. 8.2. Furthermore, it was founded that cells established a rich net of cell-to-cell contact, like gap junctions, onto the cements' surface (see Fig. 8.6). In addition, it was observed that many of the cells were in the process of cell division (see Fig. 8.6 and Fig. 8.7 for higher magnification). In fact, Fig. 8.7 shows cells undergoing mitosis (first row), with the condensed genetic material in blue and the mitotic spindle in green during the telophase of mitosis (see the second row) and a cell that has almost completed the cytokinesis where microtubules still join the two daughter cells (see the third row).

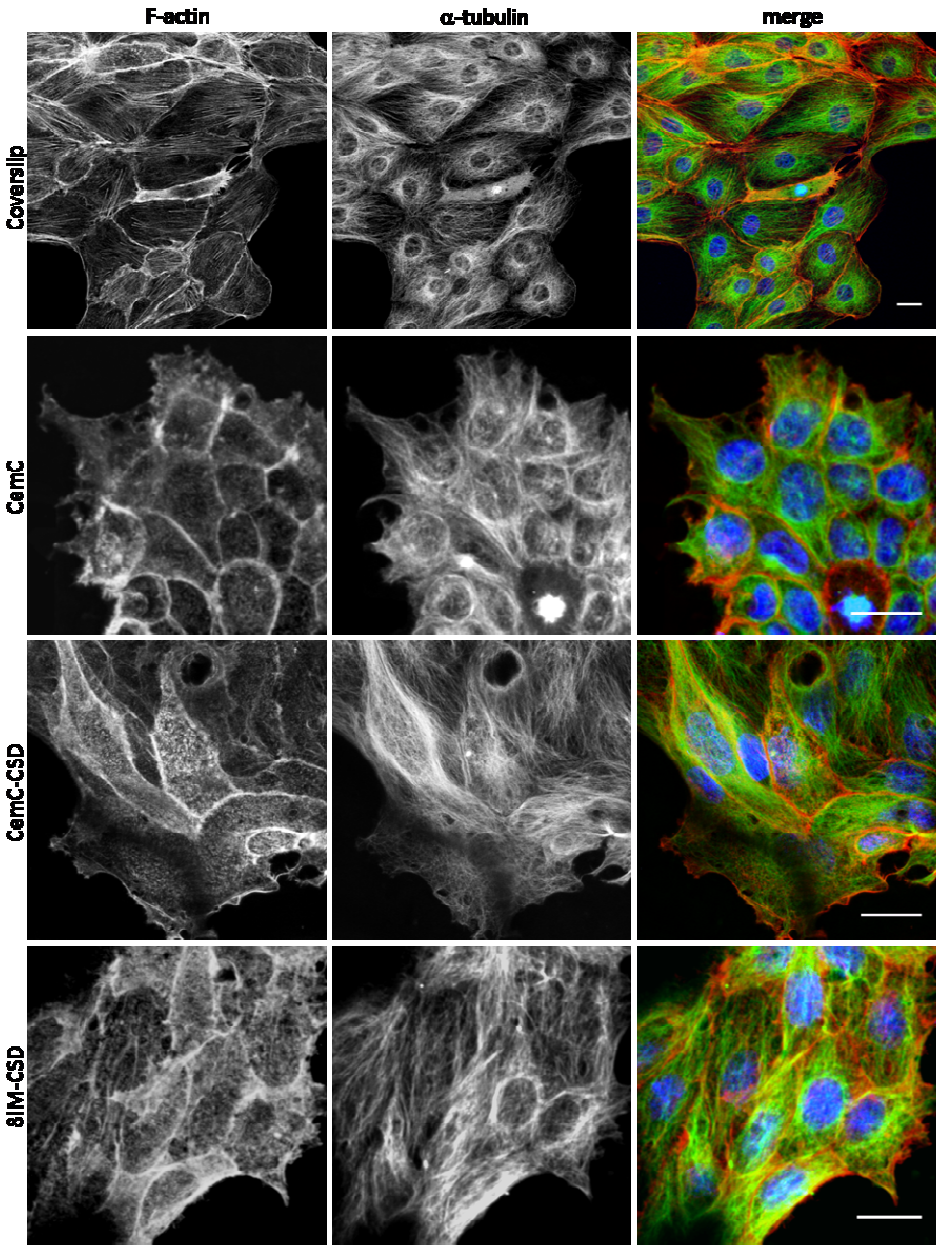

Figure 8.5. Confocal microscopy images of MG-63 cells' cytoskeleton after 7 days of culture onto the different materials. F-actin, α-tubulin and nucleus stain are shown. Third column is the colocalized immunofluorescent picture showing F-actin (red), α-tubulin (green) and nucleus (blue). Bar, 20μm.

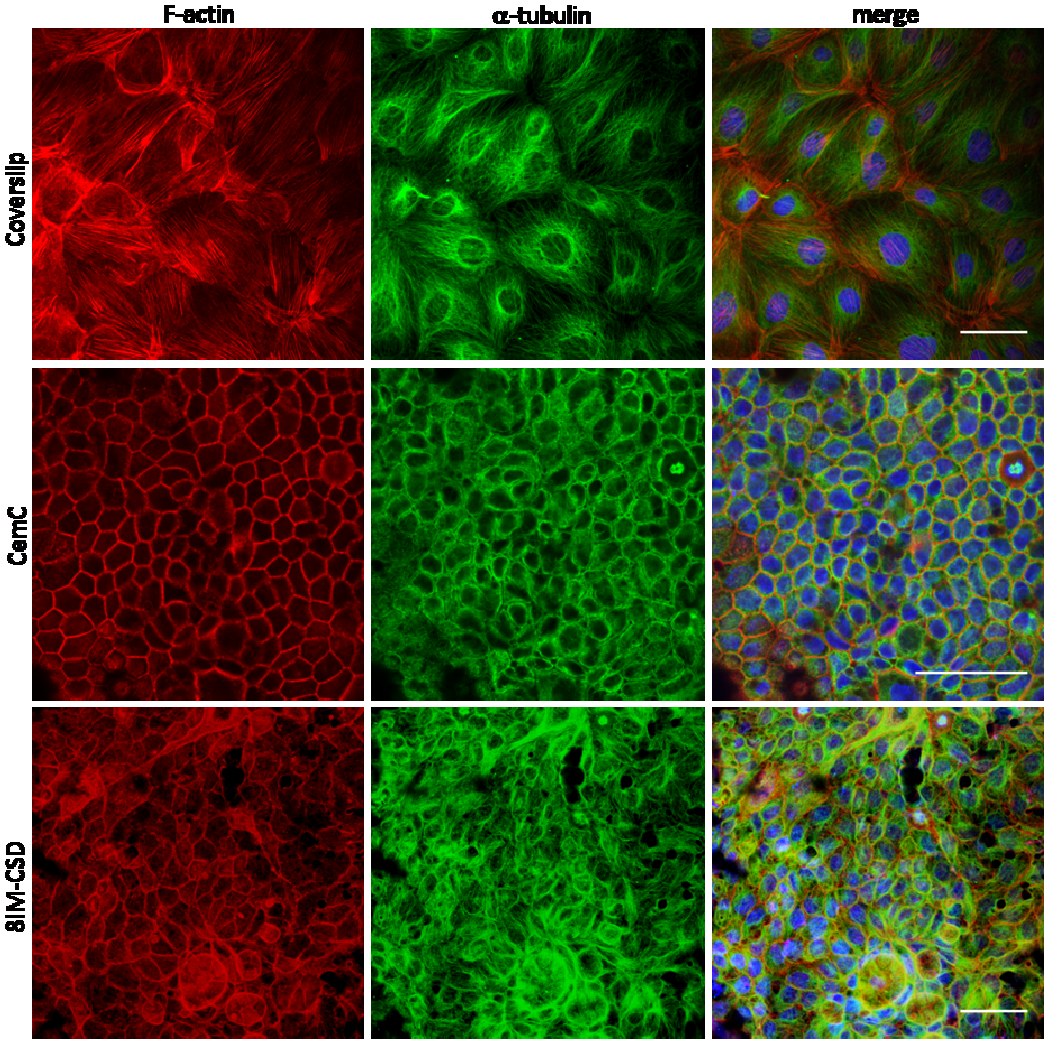

Figure 8.6. Confocal microscopy images of MG-63 cells adhered onto the surface of *CemC* and *8IM-CSD* experimental bone cements and control *Coverslip* after 7 days of culture (see details on the text). F-actin (red), α-tubulin (green) and nucleus (blue) stains are shown. Bar, 20μm.

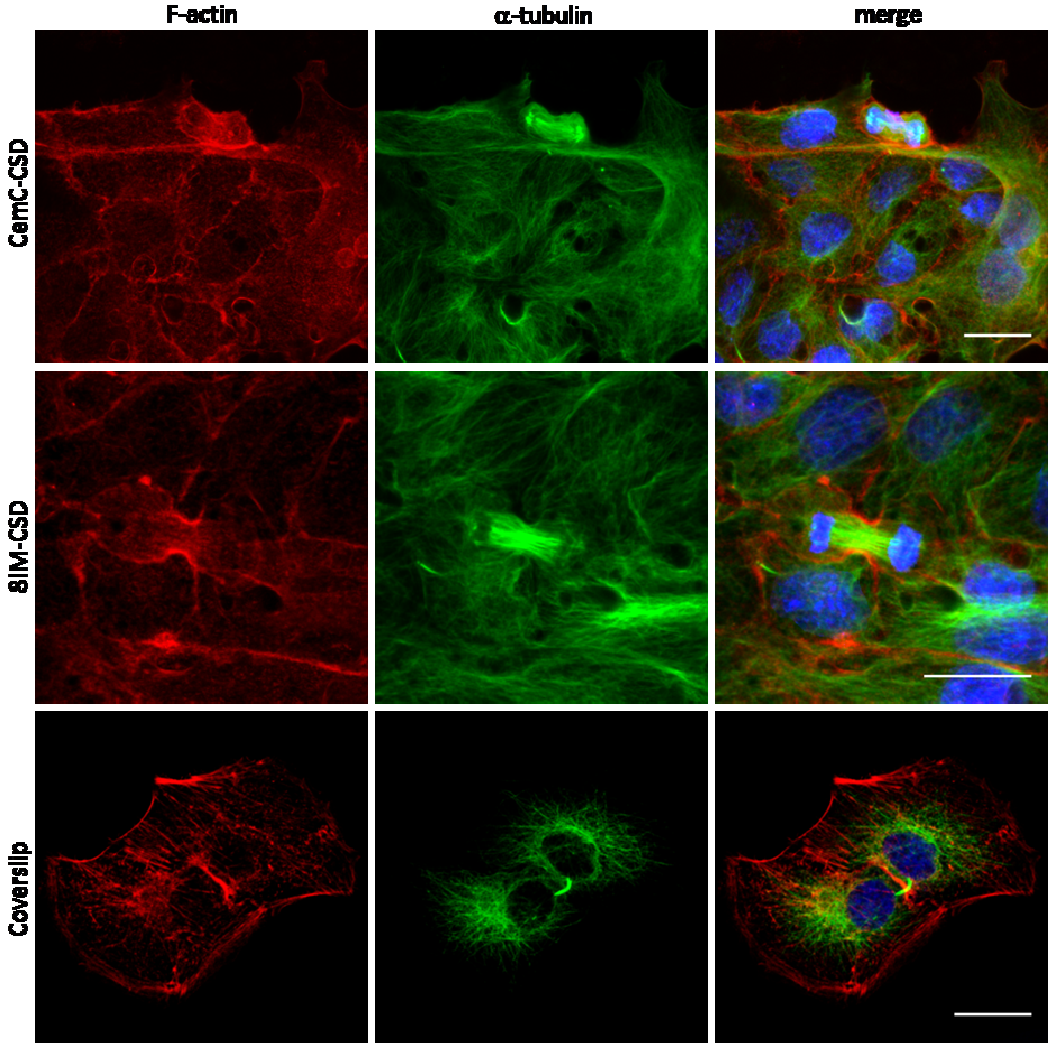

Figure 8.7. Confocal microscopy images of MG-63 cells cultured for 7 days onto the experimental CSD-modified bone cements. These pictures show cells in the process of dividing (see details on the text). Bar, 0.20μm.

8.3.4. Surgeries

All surgical interventions were performed without complications. The postoperative healing was uneventful in all sheep; the experimental animals recovered well and fast, and never showed any signs of discomfort or lameness. The postoperative treatment also proved to be reasonable and safe; infections were never encountered in all surgical procedures. All wounds from the humeral and femoral defects healed uneventfully. In the osseous defects no problems occurred during surgeries and healing; i.e. no failure of any bone defect was observed during the course of the experiment. All three types of cements hardened enough after application. Moreover, after the allowed setting time, overfilled cement was removed from the edge of the bone defect without problem. The setting of the cement was never disturbed due to capillary bleeding, since occasionally haemorrhages occurred from the bone defect surface.

8.3.5. Radiographic and macroscopic evaluation

The experimental bone cements were clearly distinguished from the surrounding cortical and trabecular bone on the postoperative and post-euthanasia radiographs because of its higher radio density. All defects were completely filled with cement and were detected as white round spots (m-l view) in the proximal and distal part of the humerus and femur. When the bones were radiographied after euthanasia, the cement implants were still visible mainly in the original defect. Overall, the radiodensity of the drill holes filled with cement was different compared to the adjacent host bone.

Macroscopically, all experimental bone cements seemed to be nicely incorporated and did not elicit an obvious inflammatory reaction in the adjacent soft tissue. No bone formation within the muscles or outside of the original drill hole was observed at any study's period at the time of euthanasia. The original bone defect and the implanted

cement were visible in all locations. All the cements were well integrated within the bone and covered by fibrous tissue at the level of drill-hole insertion. In some cases, after cement-bone specimens sectioning, perpendicular to the original drill-hole axis, a slight grayish-brown area adjacent to the implantation site was observed. These specimens corresponded to those locations were haemorrhages occurred during the implantation protocol. However, this did not seem to affect the overall results. In the rest of cement-bone specimens, this was never the case. In another two cases, the cement bulk greatly differed in size from the considered osseous defect, due to the trabecular bone destruction during drill-hole formation. These cement-bone specimens were excluded from the study.

8.3.6. Qualitative histology

Intensive bone remodelling was noticed with the biphasic bone cements (i.e. *CemC-CSD* and *8IM-CSD*); i.e. the CSD-modified cements were resorbed faster compared to the pure α-TCP control cement (i.e. *CemC*), showing more osteoid as well as new bone formation and higher number of cells. Throughout the observation periods, the amount of the remaining cement decreased; instead, new bone formation did not always occur parallel to cement resorption. The woven bone, often connected to the trabecular bone of the defect margins, was mostly surrounded with osteoid-synthesizing cells. Newly formed bone in direct contact with still intact or already resorbing cement fragments was also observed repeatedly at 3 months, and more frequently at 6 months. However, in the cement control defect (i.e. *CemC*) the presence of newly formed islets of osteoid in direct contact with the remaining cement was occasional after 3 months. In addition, many multinuclear cells, most likely osteoclasts, were found mainly in the area of the original bone defect.

Sections at 3 months of biphasic cement-bone specimens (i.e. *CemC-CSD* and *8IM-CSD*) showed that the resorption and new bone formation front was dominated by osteoblasts, osteoclasts, macrophages and new blood vessels (see arrows in Figs. 8.8-8.10). In general, the presence of the following relevant events were noticed: a) the cytoplasm of macrophages was filled with *8IM-CSD* cement particles, in this cement (see Fig. 8.8.b,c); b) palisades of active osteoblasts lining the newly formed bone and the old calcified bone matrix (Fig. 8.8.e); c) intensive new osteoid production (Fig. 8.8.a-e); d) new trabecula within the fibrovascular stroma (Fig. 8.8.c); and, e) presence of osteoclasts on the *CemC-CSD* cement border (Fig. 8.8.f, Fig. 8.9.c). Moreover, Fig. 8.9.a shows osteoid deposition inside the cement's porosity.

For the 6 months group, a great area of the original cement was replaced with osteoid and new bone. The cell types observed primarily in both biphasic cement-bone specimens, at 3 months, were again osteoprogenitor cells, osteoblasts, osteoclasts and macrophages which phagocytosed cement particles (Fig. 8.11.a,c). A great number of osteoblasts as well as osteoid were found on the bone surface at the defect margins (Fig. 8.11.b,d). Osteoclasts, starting to remodel the newly formed woven bone were first found in the drill-hole defect close to the old defect margins (Fig. 8.11.b).

The resorption zone (i.e. the area between the original osseous defect margin and the still existing residual cement) of the *8IM-CSD* appeared to be somewhat richer in cells and events compared to the *CemC-CSD*. In this observation interval, the resorption zone enclosed accumulations of both adipocytes and macrophages containing cement particles, as well as, intact or only partially preserved cement (see Fig. 8.10). In one case, in the middle of the resorption zone a great infiltration of adipose cells was found (see Fig. 8.10.c). The resorption zone near the cement presented enclosed newly formed woven bone and islets of not yet mineralized osteoid in direct contact with the residual cement (Fig. 8.10.a,b).

Histological sections of *CemC* specimens (Fig. 8.12) demonstrated somewhat different findings. Cement resorption rarely occurred in the 3 months, and only marginally in the 6 months group. In addition, the cell population was different compared to the biphasic cements at all times; i.e. only few macrophages-like cells were visible around the original bone defect at 3 months, while osteoclasts were not found on the outside edge, and also, osteoblasts were less active producing new osteoid and bone. However, both osteoblasts and osteoclast-like cells were mainly visible within the remodeling lacunae, formed in the cement crevices, where they penetrate and grew in from the edge of the bone defect (Fig. 8.12.a).

The control-defects (i.e. empty holes) were partially filled with new bone along the original shape (Fig. 8.13). The residual cavity was mostly filled by dense fibrous tissue in the cortical edge and fibro-connective tissues in the cancellous site (Fig. 8.13.e). Newly formed osteoid was occasionally found as islets of osteoid contacting with the old trabecula (Fig. 8.13.c). At the 6 month period, the newly grown bone seemed to be denser than the original cancellous structures surrounding the implantation site (Fig. 8.13.d). Also, woven bone trabeculas were found at the defect margin in cancellous sites (Fig. 8.13.f). In the histological sections of the empty controls no macrophages were noticed. In two experimental animals, adipocytes (as encountered in the bone marrow sections adjacent to the defect) appeared at 3 and 6 months in the entire control-defect or at the bottom edge of the original cavity, respectively (see pictures C and E in Fig. 8.13).

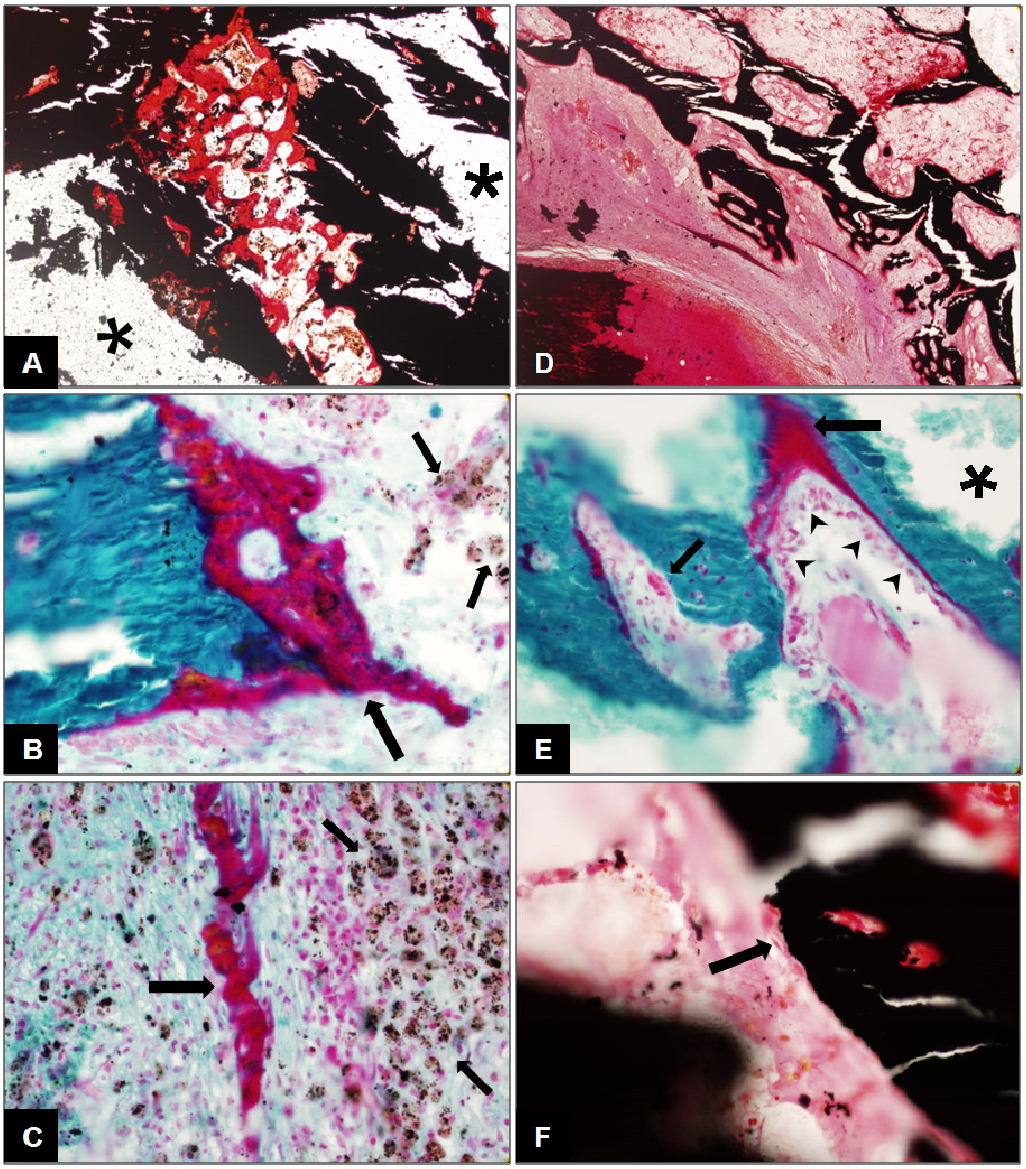

Figure 8.8. Histological pictures of *8IM-CSD* (left) and *CemC-CSD* (right) specimens evaluated after 3 months of implantation. Images show osteoid and new bone formation, bone remodeling, cement resorption, and the dominant cells involved (see details on text; (a) 60x; (b-c,e-f) 400x; (d) 40x). Stains: von Kossa (a,d,f); Goldner trichrome (b-c,e). * indicates an artifact of histologic processing (white), located on the residual cement's zone.

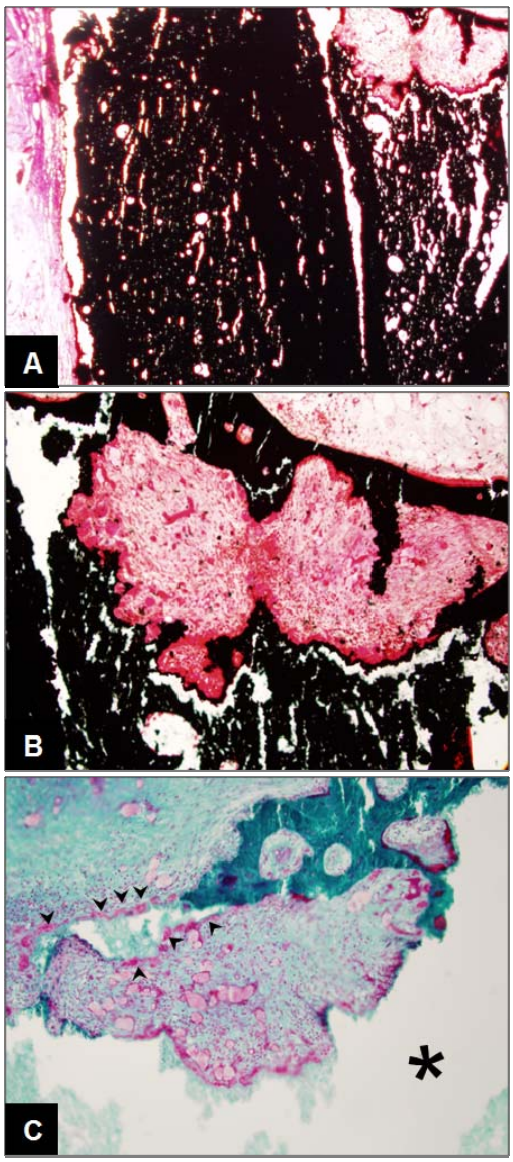

Figure 8.9. Histological sections of *CemC-CSD* at 3 months, showing cement porosity infiltrated by osteoid (a), remodelling lacunae (b), and the rim of osteoclast-like cells (c), mediating cement resorption (see details on text; (a) 60x; (b,c) 100x). Stains: von Kossa (a,b); Goldner trichrome (c). * indicates an artifact of histologic processing (white), located on the residual cement's zone (light green).

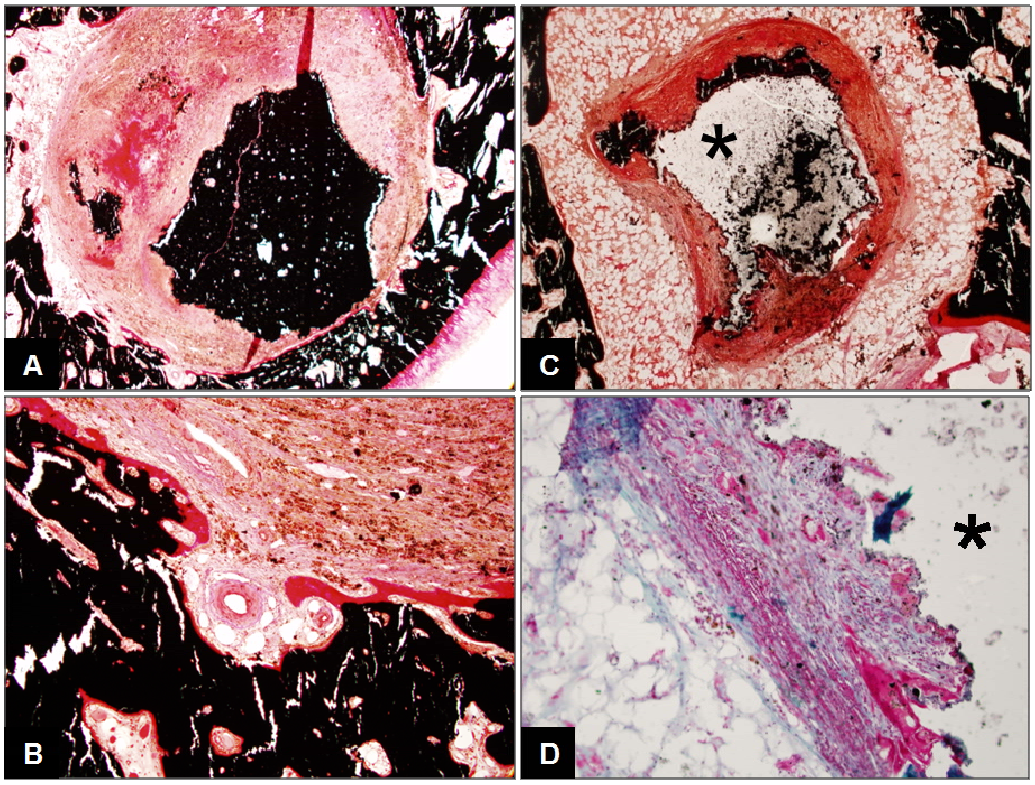

Figure 8.10. Histological sections of *8IM-CSD* specimens at 3 (a,b) and 6 month (c,d) showing the resorption zone (a-b) and bone-cement interface highly infiltrated by blood vessels and osteoid (see details on text; (a,c) 20x; (b,d) 100x). Stain: von Kossa (a-c), Goldner trichrome (d). * indicates an artifact of histologic processing located on the residual cement's area.

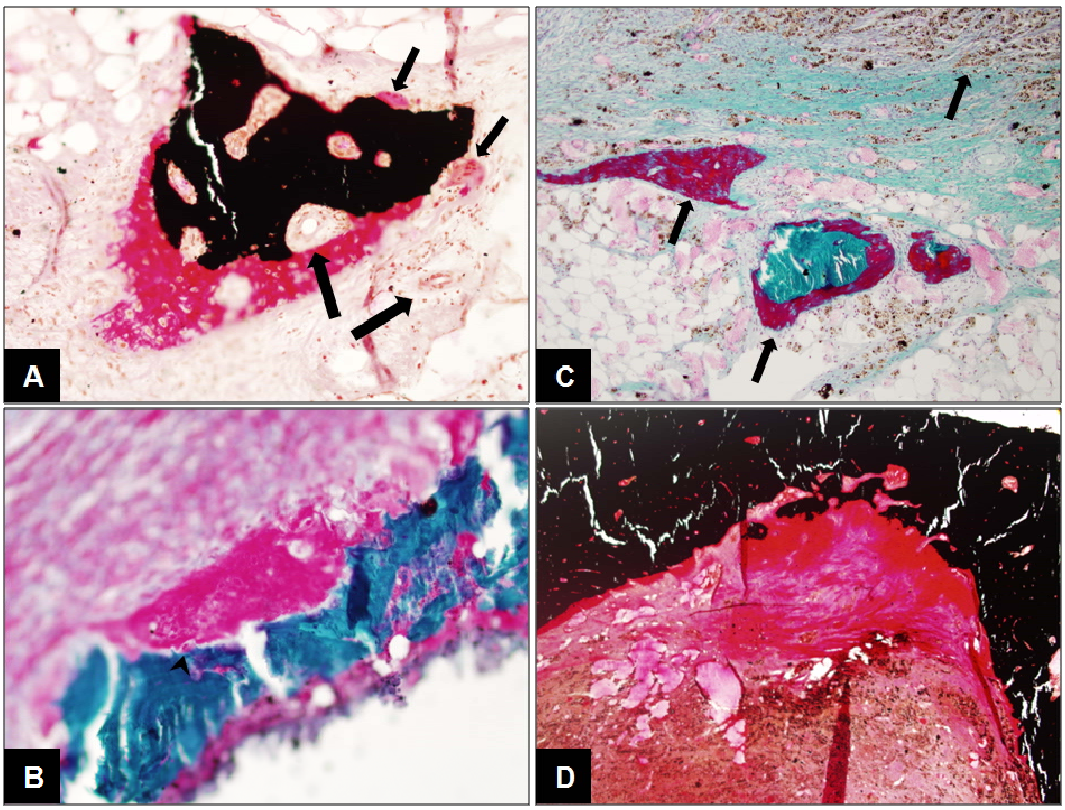

Figure 8.11. Histological sections of *CemC-CSD* (left) and *8IM-CSD* (right) specimens at 6 months showing cement resorption and new bone formation (see details on text; (a,b) 200x; (c) 100x; (d) 40x). Stains: von Kossa (a,d); Goldner's trichrome (b,c).

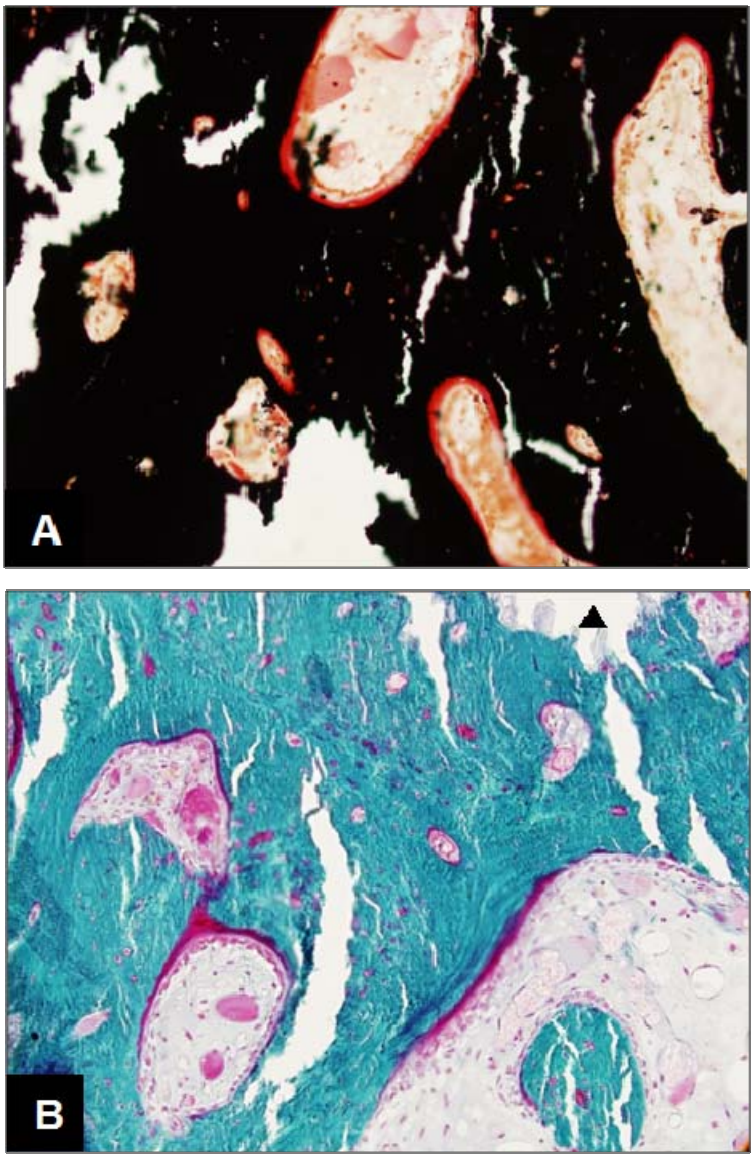

Figure 8.12. Histological pictures resulted for the control-cement (i.e. *CemC*) corresponding to a study period of 3 months, showing numerous remodelling lacunae at the interface between cement (a) and bone (b) (see details on text; (a,b) 200x. Stains: von Kossa (a) and Goldner trichrome (b). ▲ indicates the location of residual cement's area.

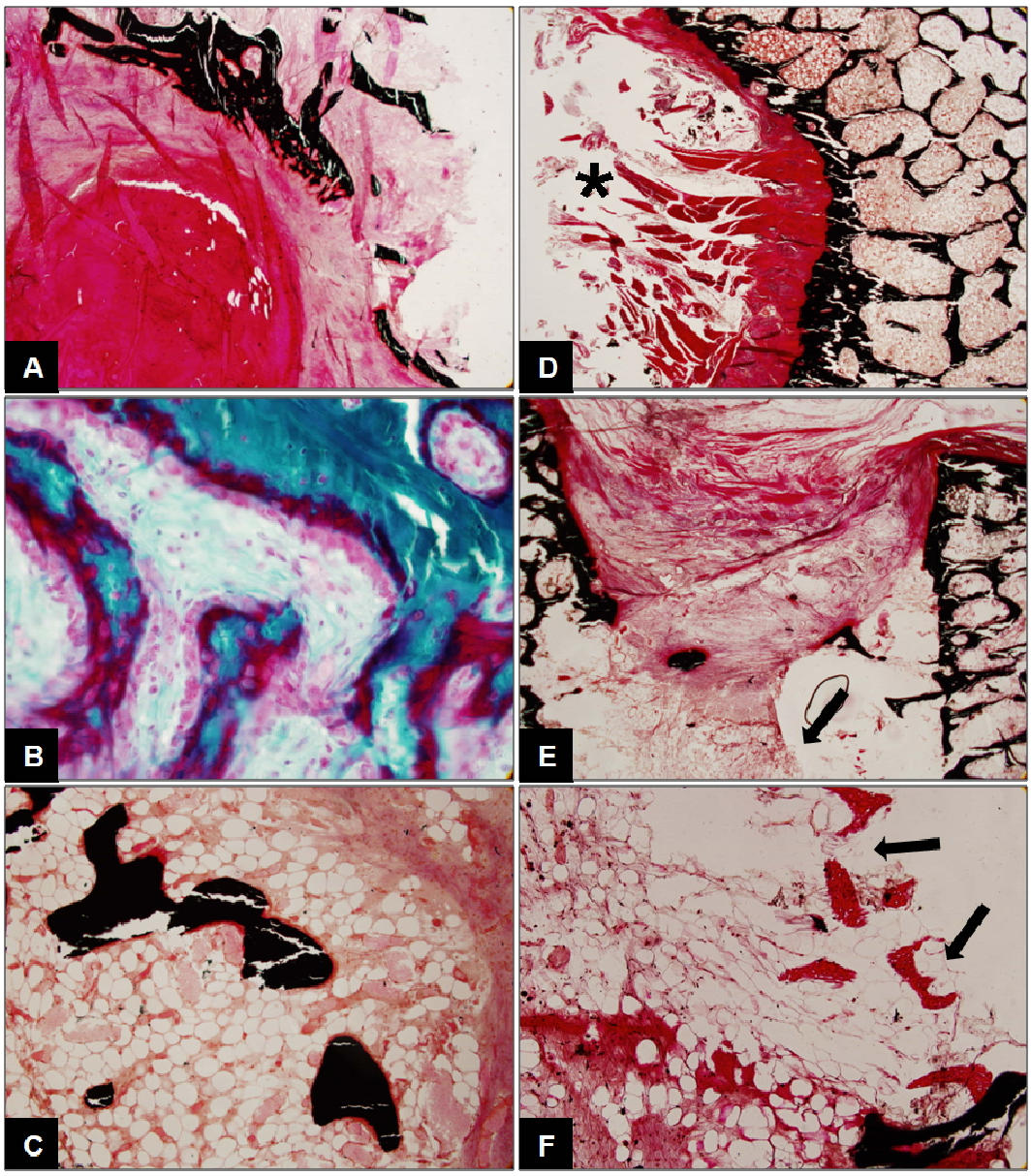

Figure 8.13. Histological pictures resulted for the control-defect (i.e. empty hole) corresponding to a study period of 3 months (left) and 6 months (right), respectively (see details on text; (a,d,e) 20x; (c) 40x; (b) 400x; (f) 100x). Stains: Goldner trichrome (b) and von Kossa. * indicates an artifact of histologic processing.

8.4. Discussion

The cytocompatibilty study (see Figs. 8.1-8.2) showed that osteoblastic-like cells can adhere, grow and proliferate onto the experimental cement-like substrates. The adhesion profiles attained at 1D of culture were slightly similar ($p>0.05$) for all the substrates (see Fig. 8.1); this could be explained by the high affinity of serum protein components for the apatitic surfaces [62-65]. Thus, it should be concluded that the early osteoblast-like cells attachment stage was similar for the four cement surfaces (despite the expected different evolutionary setting crystalinity). However, Fig. 8.2 showed that cell viability was lower for *CemC-CSD* and *8IM-CSD* as compared to the control substrates (i.e. *CemC*, *CemC-8IO* and *Coverslip*) after both 1D and 7D.

The importance of the initial cell's attachment for further cellular proliferation and subsequent viability is widely recognized. In fact, it is known that surface properties (such as topography, charge, chemistry) play an essential role on the first phase of cell-material interactions [66,67]. In this sense, the differences on the cellular viability, after 1D and 7D, for *CemC-CSD* and *8IM-CSD* as compared to the control group ($p<0.05$; as shown in Fig. 8.2) agree with the general delay of cells' growth and proliferation, observed as a consequence of failure or labile cells' attachment [68,69] to the cements' surface due to different interfacial supersaturated conditions [70,71] (probably due to passive dissolution of CSD [42]). In the same way, the evolution of the adhesion profiles and the cellular viability for *CemC* and *Cem-8IO* was attributed to surface stability [64,72,73], and was consistent with the minimal cement dissolution rate as a result of total transformation of α-TCP into calcium deficient hydroxyapatite (CDHA) during the first 24 h of setting (as confirmed by SEM and XRD analysis) [53].

On the other hand, it is widely reported that biomaterials' performance depends on how cells and proteins interact with their surface [66,65]. Early interactions established

between cells and materials' surface, mediated by adhesion proteins, control most aspects of subsequent cell behavior such as morphology, migration, proliferation and differentiation [66,67,74,75]. Regarding the MG-63 cells' morphology, it should be noted that most of them adopted a rather polygonal shape (see Figs. 8.3, 8.5-8.6), which is an osteoblast feature indicative of better adhesion [66]. However, some cells cultured onto the cement substrates also showed distinctive shapes. For example, the cells cultured onto CSD-modified cements (i.e. *CemC-CSD* and *8IM-CSD*) showed spindle-like morphology, while the cells cultured onto control-cement (i.e. pure α-TCP cement; *CemC*) adopted an intermediate morphology between control-cells (i.e. cultured on *Coverslip*) and those cultured on CSD-modified cements (see Fig. 8.5). In fact, it is known that the general morphologic aspects of MG-63 cells can vary depending on the substrate microgeometry due to the ability of cells to modify their shape in response to mechanical stresses, as has been demonstrated in other studies [76,77]. Furthermore, the observed cell polarized morphologies sustain the locomotion phenomenon onto the cements' surface, which favoured the colonisation of the surface, confirming the biocompatibility of the experimental cements.

Cell migration requires a dynamic interaction between the cell, its substrate and its cytoskeleton [66,67,77]. From the results of the cytoskeleton organisation study (Figs. 8.5-8.6), it was observed that the apatitic cements-like substrates induced different changes in the cytoskeleton organisation of MG-63 osteoblast-like cells as compared to the control *Coverslip* substrate. The observation that cells' cytoskeleton migrated onto *CemC*, *CemC-CSD* and *8IM-CSD* behaved differently from those cells migrated onto *Coverslip* led to the conclusion, as expected, that the surface topography of the experimental cements significantly affected the cytoskeleton organization of the osteoblastic cells [67]. In fact, it is known, that the cytoskeleton plays a major role not only on mobility but also on cell

shape, division, adhesion and many connexions between the cells and their environment [78].

The increase expression of actin, as a major structural element of the cytoskeleton, involved in a range of cell functions including cell shape, mechanical stability and locomotion [79], is indicative of better cell-substrate contact. Culturing the cells onto *CemC-CSD* (i.e. high textured/porous substrate; Fig. 8.5 third row) resulted in an enormous lamelipodium formation that extented from a great circumference-part of the cells. Actin filaments fill (as dense microfilamentous core; stained in red) the large lamellipodium, generally, responsible for the cell rapid movement onto the surface by crawling (highly complex integrated process, dependent on the actin-rich cortex beneath the plasma membrane) [80]. Also, the cells' microtubules on the textured/porous surfaces (i.e. *CemC-CSD* and *8IM-CSD*, in Fig. 8.5) appeared more distinct and better developed than those on the smooth substrate (i.e. *Coverslip*); this could be due to the cells attachment and spreading onto surface structural sites like sharp or ridge reliefs. Cell spreading is an indicator of non-cytotoxicity of the experimental bone cements. In addition, it should be noted that the nucleus deformation observed within the cells cultured onto the more textured/porous surfaces (see *CemC-CSD* and *8IM-CSD* in Fig. 8.5-third and fourth rows) suggest that the tensile force causing cell's elongation can also be impaired to the nucleus, causing its deformation [76,81]. In fact, it has been reported that changes in gene expression caused by constraining the nuclear shape can promote osteoblasts expressing the osteocalcin *in vitro* [76].

Also, it should be noted that up to 14 days, the chronological events (adhesion, proliferation, differentiation) concerning the MG-63 behaviour onto *CemC-CSD* and *8IM-CSD* (see Fig. 8.4) were not negatively affected by the passive calcium-ion dissolution of the CSD phase, present into the CSD-modified cement-like substrates, as also observed in a preliminary study [54]. Furthermore, previous studies have reported that an increased

extracellular ionized calcium concentration promoted the osteoblastic differentiation, enhanced the alkaline phosphatase activity and induced mineralization *in vitro* [63,83-85]. These results are supported by a recent report on MG-63 cells where it is showed that the extracellular calcium sensing-receptor (CaR) is not only expressed but functionally active, contributing to the regulation of the osteoblast function by the calcium-ion [86]. Consequently, the compositional factors of the experimental cements can be acting as to favour the differentiation of the osteoblasts [63].

In adition, after 14 days of direct-contact cell culture onto *Cem-CSD* and *8IM-CSD*, the random clump-like structures observed in the cell layer (see Fig. 8.4) were assigned to the occurrence of mineralization, evidence of normal osteoblasts development [76,87], and may be positively correlated with the later stage bone cell differentiation behaviour (i.e. mineralization). The formation of mineralized matrix is of great importance as an evidence of favourable cement-like substratum for bone deposition [76]. In addition, the dorsal surface activity of the cells was associated to matrix vesicles formation since osteoblastic cells have the ability to synthesize the extracellular matrix [88].

A final observation is that the surface microgeometry of the experimental cements also provided favourable conditions for both the rich network of cell-to-cell contact formation (see Fig. 8.6), i.e. occurrence of intercellular communication through direct exchange of ions via gap junctions [66], and the cellular division (see Fig. 8.7), which is indicative of favourable substrates for cell proliferation.

The main results of the *in vitro* study concerning adhesion, viability, morphology and cytoskeleton organisation of MG-63 osteoblast-like cells demonstrate the biocompatible/non-cytotoxic character of all the experimental cements studied, despite their modification with CSD and/or iron. In fact, calcium sulphate and calcium phosphate based cements have been used for a long time in clinical application and their non-cytotoxic and biocompatible character has been extensively proved [44-48]. In addition,

the non-cytotoxic character of iron-modified apatitic bone cements has also been proved [53,54] (see also Chapter 6). All these results confirm the ability of the experimental bone cements (porous iron-modified) to support the growth, proliferation and metabolic activity of MG-63 osteoblasts-like cells *in vitro*; i.e. their optimum osteogenic character.

In the present study, the biocompatibility and the resorption of three apatitic bone cements was also investigated in a sheep animal model over an observation period of 3 and 6 months. The study was focused on the new porous iron-modified cement (i.e. *8IM-CSD*) as candidate cancellous bone-filling biomaterial for spinal surgery. The results showed differences in cement resorption and new bone formation between the different evaluated cement formulations. While both biphasic cements (i.e. *CemC-CSD* and *8IM-CSD*) showed good resorption, the pure apatite cement (i.e. *CemC*) remained almost unchanged throughout the study period of 6 months. Biphasic cements' resorption occurred through dissolution and a cell-mediated process which in the case of *CemC-CSD* was due to osteoclast-like cells, whereas in the case of *8IM-CSD* macrophages were also involved. Although osteoclasts were rarely at the cement's surface in the case of *CemC* (i.e. pure apatitic cement), cement resorption and its replacement by new bone are suggested to occur in similar manner to bone remodeling.

A great number of studies have been devoted to understand the mechanisms of biodegradation of calcium phosphates biomaterials, in order to identify the key factors controlling the process (depending on material formulation) [89-100], which, in fact, are still not completely elucidated [89]. However, it is generally assumed that the resorption of calcium phosphate biomaterials is due to dissolution and cell-mediated decomposition; i.e. it may be promoted *in vivo* by a dissolution process in the extracellular liquid, followed by disintegration into small particles that are either intracellularly digested or transported to lymphatic nodes [20,89-91].

The resorption rate of calcium phosphate biomaterials is related to its chemical composition, crystallinity and porosity [89,90], while dissolution depends on its solubility product. Thus, after implantation, the α-TCP phase of the studied cements transformed during the setting into an entangled matrix of calcium deficient apatite crystals (CDHA) while the CSD phase dissolved passively during time. The resorption of biphasic cements started with the dissolution of its high soluble component (i.e. CSD) through a passive dissolution process, obvious at 3 months (see Fig 8.9), and at later stage it was followed by the CDHA (i.e. the end product of the setting reaction) dissolution, according to their chemical and crystallographic nature. Moreover, the presence of higher solubility cement's phases is an essential requirement for the faster resorption of the *in vivo* hardened set cements; the passive dissolution of CSD in the experimental cements, at the early stage, acts in this sense. In addition, CSD dissolution produces an interfacial supersaturated environment, rich in calcium, that could be favoring cell proliferation, mineralization and new bone bonding, as was mentioned before (see the *in vitro* results) and also demonstrated by others *in vitro* and *in vivo* studies [63,83-85]. Furthermore, CSD dissolution left behind an open-interconnected porosity (see Chapter 3), which offered structural sites favorable for new bone apposition (i.e. osteoconduction).

Various studies have linked the *in vivo* cement dissolution process with the local pH drop as a consequence of cement setting (is not the case in the present study) [23,92] or cell-mediated factors [89]. From this study, it was clear that cement resorption was considerably faster for the CSD-modified cements than for the *CemC*. In fact, the resorption of the experimental cements varied in the following order: *CemC* < *CemC-CSD* < *8IM-CSD*. This was also true for new bone formation that was obviously dependent on the speed of cement resorption. However, cement resorption and new bone formation did not always occur parallel, and in some instances, fibrovascular stroma was apparent at the cement-bone interface (Fig. 8.10.d) towards cement periphery both at 3 and 6

months, as found also in other studies [21,92]. Newly formed osteoid (i.e. partially mineralized bone) was found at the walls of the osseous defects penetrating inside the cement-volume through the porosity developed during the first 3 months. Considering the mechanism of new bone formation, this was slightly similar but with different intensity for *8IM-CSD* and *CemC-CSD*, but different from that observed for *CemC*. Moreover, differences were also found between the mechanisms of cell-mediate resorption among the two types of CSD-modified cements. Thus, at the early observation period (i.e. 3 months), evidence of osteoclast-like cells, containing intracellular *CemC-CSD* cement particles, in direct contact with the residual cement suggested cement degradation by phagocytosis as well as by extracellular resorbtion. In contrast, macrophages containing cement particles were observed at all time points for *8IM-CSD*; they were even more frequently found in the resorption zone close to the cement border. Accordingly, a combination of dissolution with cement disintegration and particle formation followed by phagocytosis through macrophages must be assumed as responsible for the resorption of the new biphasic iron-modified cements (i.e. *8IM-CSD*).

It is generally accepted that fast-degrading cements (i.e. brushite cements) resorb through dissolution combinated with cellular decomposition by macrophages and giant cells, while hydroxyapatite-cements degrade slowly and mainly through a resorption mechanism mediated by osteoclast-like cells (i.e. by creeping substitution) [20,90,93]. Consequently, at this stage, our results seem to be in contradiction with the literature data. Briefly, the presence of macrophages on the implantation site has been associated to the surgical trauma itself or the local pH decrease due to cement setting (i.e. imflamation) [93], the cement particles release (matrix particles or resulted by desintegration) [89,94,95] or the cement surface reactivity [92], but never associated with the mechanism of apatitic cements resorption (known as slow resorption). However, in this study, macrophages seemed to be widely responsible for the resorption of *8IM-CSD*; this was not the case for

CemC and *CemC-CSD*. The fact that differences in resorption found between *8IM-CSD* and *CemC-CSD* suggest that the iron-modification could be responsible for these changes. The appearance of macrophages at the first 3 months has been assigned to a possible chemotaxis phenomenon as response to the exposed iron onto cement surface or as a free iron-ion resulted from cement dissolution or extracellular resorption. Despite cellular iron metabolism is apparently *sine qua non* for cells survival and proliferation, the release of iron-ion from the cement could be toxic, in extreme case, when an excess of ''free'' reactive iron might exceed the cell homeostatic capacity [96-98]. However, it should be highlighted that, under simulated physiological conditions *in vitro*, no iron-ion liberation phenomenon from the cement was found (data not shown). This non-cytotoxic behavior has been related to some stable fixation of iron into the structure of the α-TCP phase (as indicated by XRD; data not shown) as well as to the favored entrapment of iron into the apatitic phase formed during setting [99]. In addition, non-cytotoxic data have resulted after direct-contact cellular cultures with HEp-2 [54] (see also Chapter 6) and MG-63 cells (see *in vitro* results). Moreover, despite macrophages' phagocytic capacity for calcium-phosphate particles and their ability of releasing cytokines (that at higher rate are involved in inflammatory reactions and/or the decrease of bone formation), their role on the homoeostasis of bone formation and resorption has been also widely proved [100-102]. Furthermore, histology sections of *8IM-CSD* at 3 months illustrated significant resorption of the cement with highly vascular penetration (see Fig. 8.10.a,b), ruling out the possibility of inflammatory or osteolytic damage. Assuming that there are no signs of inflammatory or immunologic response of the host tissue to the implanted cement, the appearance of macrophages (generally involved in rapidly resorption of calcium phosphate biomaterials) which, in conjunction with osteoclasts, mediate the resorption of the new apatitic iron-modified cement has to be considered as a normal reaction to this cement formulation, otherwise useful for the enhancement of the well known slowly

resorption of apatitic cements, where iron possibly acts as modulator of apatitic cement resorption. On the other hand, it should be mentioning that the obtained results concerning the macrophage-mediated degradation of the apatitic cements are supported by Kurashina et al. [91], suggesting that the cement may resorb through the same mechanism as resorbable calcium phosphate ceramics (i.e. dissolution process and digestion by phagocitic cells) due to hardened cement body resulted after setting.

In addition, it is known that in the case of injectable bone substitutes, consisting of powder mixtures of various grain sizes, the effect of the particle size has great effect on the intensity of the cellular degradation activity and subsequent cement resorption. From previous studies conducted on the role of particle size on bone ingrowth [101], it has resulted that small particles (10-20 μm) promote bone ingrowth and large particles (80-100 μm) provide suitable granulometry for bone bonding. In addition, small particles can stimulate mitogenesis, support endocytosis and also favor metalloproteinase production [103]. Considering the formulation of the studied experimental cements, their early *in vivo* behavior could also fit into these hypotheses.

In this study, very little resorption of *CemC* took place during the implantation periods, but change of material architecture was observed histologically at 3 and 6 months. Thus, since osteoclasts around residual cement have been rarely found, they have been evidenced inside of remodeling lacunae at the interface between cement surface and contacting bone, suggesting further cement's integration by the creeping substitution process of bone remodeling. Since the apatitic calcium phosphate cement may be resorbed in a process similar to bone remodeling, the time period after which the material finally degrades varies between weeks to years [28-31,104]. Moreover, our present results concerning the osteoclast-mediated slow resorption rate of *CemC* were in agreement with previous studies dedicated to cell-mediated resorption [20,90,93].

The osteoconductive properties of the experimental apatitic bone cements were also proved in this study. Thus, the biphasic cements (i.e. *CemC-CSD* and *8IM-CSD*) showed deep crevices and pores, even at some distance of the original defect walls, covered with osteoid, also demonstrating the bone-bonding property, i.e. bioactivity, because only bioactive materials show apposition of osteogenic cells onto the surface of the pore wall followed by bonding between the *de novo* bone and the biomaterial [105]. In addition, the creeping substitution of *CemC* by bone could be associated to the osteoconduction exhibited by calcium phosphate cements implanted in bone tissue.

The biocompatibility of the cements used in this study has been ensured by the biocompatibility, widely documented, of the start products (i.e. α-TCP and CSD) and the end product of the setting reaction (i.e. CDHA; that has similar chemical composition as the mineral phase in bone) [2-23,44-48]. However, the actual challenge was the iron-modification of the α-TCP main reactant, despite its cytocompatibility has been previously demonstrated *in vitro* [53,54] (see also Chapter 6). Finally, in this study, no inflammation, no necrosis and no any other reaction of the host bone tissue to the implanted cements were observed.

The experimental animal model used in the present study join other ones reported in the literature; previous studies [22,23,93,106] have demonstrated that sheep is a well accepted model for the *in vivo* study of bone substitutes, due to its similar bone structure and remodeling rate as well as to the bone tissue response to the implanted biomaterials, which allow later extrapolation to human conditions [107]. The empty bone defects were used as indicative sites of the metabolic profile of the sheep, concerning the intensity of bone remodeling through spontaneous healing of the bone defect mediated by complex interactions between factors such as hormones, cytokines and mechanical stimuli, which affect the amount and quality of the bone tissue produced [108,109]. These empty-

controls provide only qualitative data without any further relevance for the clinical management of bone substitution/reconstruction.

The results obtained in this study related to the porous apatitic iron-modified bone cement (i.e. *8IM-CSD*) were consistent with previous results [42,52,54] (see also Chapters 3, 5 and 6). This confirms that iron modification of α-TCP in conjunction with CSD addition, as porosity control agent, is a useful approach not only to stabilize the mechanical properties [52] (see Chapter 5) of porous α-TCP based bone cements [42] (see Chapter 3) after setting, without affecting its cytocompatility (see *in vitro* results) [54] (see also Chapter 6) and subsequent biocompatibility, but also to improve *in vivo* cellular colonization (i.e. new bone apposition) and enhance cement resorption.

8.5. Summary conclusion

The present study showed that iron-modified α-TCP based bone cement has cytocompatible and biocompatible features. Both quantitative, morphologic and cytoskeleton evaluations of MG-63 osteoblast-like cells after direct-contact cellular culture showed that adhesion, proliferation and cellular viability were not negatively influenced by the iron-modification of α-TCP main cement reactant. The textural (i.e. biphasic material), microgeometric (i.e. net of entangled crystals of bone-like hydroxyapatite) and topographic (i.e. cement macroporosity) characteristics of its cement surface (attained by progressive hydration reaction of α-TCP followed by passive dissolution of CSD additive) provide favorable substratum for cell proliferation and differentiation, which leads to stable new bone binding (i.e. osteoconduction) as confirmed by the *in vivo* sheep model study. The biocompatibility and resorption of the new porous apatitic iron-modified cement was demonstrated for a period of 3 and 6 months, when no signs of inflammation, necrosis and any reaction of the host tissue against to the implanted

cement were found. The cement resorption occurred by a prevalent macrophage-mediated mechanism and was somewhat higher compared to the controls. The results proved the osteogenic features of this new porous apatitic iron-modified bone cement and might provide new insights into the development of new therapeutic bone cements for cancellous bone replacement of interest to kyphophasty application for the treatment of osteoporotic vertebral compression fractures.

References

1. Brown WE, Chow LC. Dental restorative cement pastes. US Patent No.: 4,518,430. Priority Data: May 21, 1985.

2. Bohner M. Physical and chemical aspects of calcium phosphates used in spinal surgery. Eur Spine J 2001;10:S114-S121.

3. Heini PF, Berlemann U. Bone substitutes in vertebroplasty. Eur Spine J 2001;10:S203-215.

4. Dorozhkin SV, Calcium orthophosphate cements for biomedical application. J. Mater. Sci. 2008;43:3028-57.

5. Lemaitre J, Mirtchi A, Mortier A. Calcium phosphate cements for medical use: state of the art and perspectives of development. Sil Ind Ceram Sci Tech 1987;52:141-6.

6. Bohner M. Calcium orthophosphates in medicine: from ceramics to calcium phosphate cements. Injury 2000;31(S4):D37-D47.

7. Brown WE, Chow LC. Dental restorative cement pastes. US Patent No. 4518430, 1985.

8. Tyllianakis M, Giannikas D, Panagopoulos A, et al. Use of injectable calcium phosphate in the treatment of intra-articular distal radius fractures. Orthopedics 2002;25(3):311-15.

9. Takegami K, Sano T, Wakabayashi H, et al. New ferromagnetic bone cement for local hyperthermia. J Biomed Mater Res: Appl Biomat 1998;43:210-14.

10. Brown WE, Chow LC. A new calcium phosphate water-setting cement. In: Brown PW, editor. Cements Research Progress. Westerville, Ohio. American Ceramic Society; 1986, p. 351-79.

11. Chow LC, Takagi S, Constantino PD, Friedman CD. Self-setting calcium phosphate cements. Mat Res Soc Symp Proc 1991;179:3-24.

12. Chow LC. Development of self-setting calcium phosphate cements. J Ceram Soc Japan (International Edition) 1992;99:927-36.

13. Sugama T, Allan M. Calcium phosphate cements prepared by acid-base reaction. J Am Ceram Soc 1992;75(8):2076-87.

14. Lemaitre J. Injectable calcium phosphate hydraulic cements: new developments and potential applications. Innov Tech Biol Med 1995;16(1):109-20.

15. Fernández E. Bioactive Bone Cements. In: Wiley Encyclopedia of Biomedical Engineering, 6-Volume Set, ISBN: 0-471-24967-X, John Wiley & Sons, Inc. (USA), Metin Akay (Ed.), June 2006, pp. 1-9.

16. Driessens FCM, Boltong MG, Bermu´dez O, Planell JA. Formulation and setting times of some calcium orthophosphate cements: A pilot study. J Mater Sci Mater Med 1993;4:503-08.

17. Bermudez O, Boltong MG, Driessens FCM, Planell JA. Compressive strength and diametral tensile strength of some calcium-orthophosphate cements: A pilot study. J Mater Sci Mater Med 1993;4:389-93.

18. Fernandez E, Gil FJ, Best S, Ginebra MP, Driessens FCM, Planell JA. The cement setting reaction in the $CaHPO_4$-alpha-$Ca_3(PO_4)_2$ system: An X-ray diffraction study. J Biomed Mater Res 1998;42:403-06.

19. Fernandez E, Gil FJ, Best SM, Ginebra MP, Driessens FCM, Planell JA. Improvement of the mechanical properties of new calcium phosphate bone cements in the $CaHPO_4$-alpha-Ca-3(PO_4)(2) system: Compressive strength and microstructural development. J Biomed Mater Res 1998;41:560-67.

20. Ooms EM, Wolke JGC, van der Waerden JPCM, Jansen JA. Trabecular bone response to injectable calcium phosphate (Ca-P) cement. J Biomed Mater Res 2002;61:9-18.

21. Constantz BR, Barr BM, Ison IC, Fulmer MT, Baker J, McKinney L, Goodman SB, Gunasekaren S, Delaney DC, Ross J, Poser RD. Histological, chemical, and crystallographic analysis of four calcium phosphate cements in different rabbit osseous sites. J Biomed Mater Res 1998;43:451-61.

22. Gisep A, Wieling R, Bohner M, et al. Resorption patterns of calcium-phosphate cements in bone. J Biomed Mater Res 2003;66(3):532-40.

23. Apelt D, Theiss F, El-Warrak AO, et al. In vitro behavior of three different injectable hydraulic calcium phosphate cements. Biomaterials 2004;25:1439-51.

24. Bohner M, Gbureck U, Barralet JE. "Technological issues for the development of more efficient calcium phosphate bone cements: a critical assessment". Biomaterials 2005;26:6423-29.

25. Fernández E, Gil FJ, Best SM, Ginebra MP, Driessens FCM, Planell JA. Calcium phosphate bone cements for clinical applications: I. Solution chemistry. J Mater Sci Mater Med 1999;10:169-76.

26. Fernández E, Gil FJ, Best SM, Ginebra MP, Driessens FCM, Planell JA. Calcium phosphate bone cements for clinical applications: II. Precipitate formation during setting reactions. J Mater Sci Mater Med 1999;10:177-83.

27. Fernandez E, Ginebra MP, Boltong MG, Driessens FC, Ginebra J, De Maeyer EA, Verbeeck RM, Planell JA. Kinetic study of the setting reaction of a calcium phosphate bone cement. J Biomed Mater Res 1996;32:367-74.

28. Hankermeyer CR, Ohashi KL, Delaney DC, Ross J, Constantz BR. Dissolution rates of carbonated hydroxyapatite in hydrochloric acid. Biomaterials 2002;23:743-50.

29. Fulmer MT, Ison IC, Hankermayer CR, Constantz BR, Ross J. Measurements of the solubilities and dissolution rates of several hydroxyapatites. Biomaterials 2002;23:751-55.

30. Frankenburg EP, Goldstein SA, Bauer TW, Harris SA, Poser RD. Biomechanical and histological evaluation of a calcium phosphate cement. J Bone Joint Surg Am 1998;80:1112-24.

31. Knaack D, Goad ME, Aiolova M, Rey C, Tofighi A, Chakravarthy P, Lee DD. Resorbable calcium phosphate bone substitute. J Biomed Mater Res 1998;43:399-09.

32. Bohner M. Calcium phosphate emulsions: possible applications. Key Eng Mater 2001;192-195:765-8.

33. Almirall A, Larrecq G, Delgado JA, Martínez S, Planell JA, Ginebra MP. Fabrication of low temperature macroporous hydroxyapatite scaffolds by foaming and hydrolysis of an α-TCP paste. Biomaterials 2004;25:3671-80.

34. Sarda S, Fernández E, Nilsson M, Planell JA. Influence of surfactant molecules as air-entraining agent on bone cement macroporosity. J Biomed Mater Res 2003;65A:215-21.

35. Del Real RP, Wolke JGC, Vallet-Regí M, Jansen JA. A new method to produce macropores in calcium phosphate cements. Biomaterials 2002;23:3673-80.

36. Barralet JE, Grover L, Gaunt T, Wright AJ, Gibson IR. Preparation of macroporous calcium phosphate cement tissue engineering scaffold. Biomaterials 2002;23:3063-72.

37. Takagi S, Chow LC. Formation of macropores in calcium phosphate cement implants. J Mater Sci: Mater Med 2001;12(2):135-9.

38. Markovic M, Takagi S, Chow LC. Formation of macropores in calcium phosphate cements through the use of mannitol crystals. Key Eng Mat 2000;192-1:773-6.

39. Driessens FCM, Planell JA, Boltong MG, Khairoun I, Ginebra MP. Osteotransductive bone cements. Proc Instn Mech Engrs 1998;212H:427-35.

40. Charrière E, Lemaitre J, Zysset Ph. Hydroxyapatite cement scaffolds with controlled macroporosity: fabrication protocol and mechanical properties. Biomaterials 2003;24:809-17.

41. Lu JX, Gallur A, Flautre B, Anselme K, Descamps M, Thierry B, Hardouin P. Comparative study of tissue reactions to calcium phosphate ceramics among cancellous, cortical, and medullar bone sites in rabbits. J Biomed Mater Res 1998;42:357-67.

42. Fernández E, Vlad MD, Gel MM, López J, Torres R, Cauich JV, Bohner M. Modulation of porosity in apatitic cements by the use of α-tricalcium phosphate–calcium sulphate dehydrate mixtures. Biomaterials 2005;26:3395-04.

43. Gisep A. Research on ceramic bone substitutes: current status. Injury, Int J. Care Injured 2002;33:S-B-88-92.

44. Parikh SN. "Bone graft substitutes in modern orthopedics". Orthopedics 2002;25(11):1301-11.

45. Gitelis S, Piasecki P, Turner T, Haggard W, et al. Use of a calcium sulfate-based bone graft substitute for benign bone lesions. Orthopedics 2001;24(2):162-67.

46. Les Substituts Osseoux en 2005. Monographie éditée par L`Association pour l`etude des Greffes Et Substituts Tissulaires en Orthopédie (GESTO); Éditions Romillat 2005; Paris, France.

47. Nelson CL, McLaren SG, Skinner RA, Smeltzer MS, Thomas JR, Olsen KM."The treatment of experimental osteomyelitis by surgical debridement and the implantation of calcium sulfate tobramycin pellets. Journal of Orthopaedic Research 2002;20(4):643-647.

48. Kelly CM, Wilkins RM, Gitelis S, Hartjen C, Watson JT, Kim PT. The use of a surgical grade calcium sulfate as a bone graft substitute. Clin Orthop Rel Res 2001;382:42–50.

49. Bohner M. New hydraulic cements based on α-tricalcium phosphate-calcium sulfate dihydrate mixtures. Biomaterials 2004;25:741-9.

50. Lewis G, Percutaneous vertebroplaty and kyphoplasty for the stand-alone augmentation of osteoporosis-induced vertebral compression fractures: present status and future directions. J Biomed Mater Res Part B: Appl Biomater 2007;81B:371-86.

51. Lewis G, Injectable bone cements for use in vertebroplasty and kyphoplasty: state of the art review. J Biomed Mater Res Part B: Appl Biomater 2006;76B:456-68.

52. Fernández E, Vlad MD, Hamcerencu M, Darie A, Torres R, López J, Effect of iron on the setting properties of a-TCP bone cements. J Mater Sci 2005;40:3677-82.

53. Vlad MD, del Valle LJ, Barracó M, Torres R, López J, Fernández E. Iron oxide nanoparticles significantly enhances the injectability of apatitic bone cement for vertebroplasty. Spine 2008;33(21): 2290-2298.

54. Vlad MD, del Valle LJ, Poeata I, Barracó M, López J, Torres R, Fernández E. Injectable iron-modified apatitic bone cement intended for kyphoplasty: cytocompatibility study. J Mater Sci: Mater Med 2008;19(12):3575-83.

55. Lajeunesse D, Frondoza CG, Schoffield B, Sactor B. Osteocalcin secretion by the human osteosarcoma cell line MG-63. J Bone Miner Res 1990;5:915-22.

56. Lajeunesse D, Kiebzak GM, Frondoza CG, Sacktor B. Regulation of osteocalcin secretion by human primary bone cells and by the human osteosarcoma cell line MG-63. J Bone Miner Res 1991;14:237-50.

57. Boyan BD, Schwartz Z, Bonewald LF, Swain LD. Localization of 1,25-$(OH)_2$ D3-responsive alkaline phosphatase in osteoblast-like cells (ROS 17/2.8, MG63, and cartilage cells in culture. J Biol Chem 1989;264:11879-86.

58. Francheschi RT, James WM, Zerlough G. 1a, 25-Dihydroxyvitamin D3 specific regulation of growth, morphology, and fibronectin in a human osteosarcoma cell line. J Cell Physiol 1985;123:401-09.

59. Mosmann T. Rapid colorimetric assay for cellular growth and survival: application to proliferation and cytotoxicity assays. Journal of Immunological Methods 1983;65:55-63.

60. Standard Test Method: ASTM C266-89. Time of setting of hydraulic cement paste by Gillmore needles. In: Annual book of ASTM standards, vol. 04.01. Cement, lime, Gypsum. Philadelphia, PA: ASTM. 1993;444-72.

61. Emmanual J, Hornbeck C, Bloebaum RD. A Polymethyl Methacrylate Method for Large Specimens of Mineralized Bone with Implants. Biotechnic and Histochemistry 1987;62(6):401-10.

62. Chang YL, Stanford CM, Wefel JS, Keller JC. Osteoblastic cell attachment to hidroxyapatite-coating implant surface in vitro. Int J Oral Maxillofac Implant 1999;14:239-47.

63. Yuasa T, Miyamoto Y, Ishikawa K, Takechi M, Momota Y, Tatehara S, Nagayama M. Effects of apatite cements on proliferation and differentiation of human osteoblasts in vitro. Biomaterials 2004;25:1159-66.

64. Rouahi M, Champion E,Hardouin P, Anselme P. Quantitative kinetic analysis of gene expression during human osteoblastic adhesion on orthopaedic materials. Biomaterials 2006;27:2829-44.

65. Annaz B, Hing KA, Kayser M, Buckland T, Di Silvio L. Porosity variation in hydroxyapatite and osteoblast morphology: a scanning electron microscopy study. J Microsc 2004;215:100-10.

66. Anselme K. Osteoblast adhesion on biomaterials. Biomaterials 2000;21:667-81.

67. Berry CC, Campbell G, Spadiccino A, Robertson M, Curtis ASG. The influence of microscale topography on fibroblast attachment and mobility. Biomaterials 2004;25:5781-88.

68. Anselme K, Bigerelle M, Noel B, Dufresne E, Judas D, Iost A, Hardouin P. Qualitative and quantitative of human osteoblast adhesion on materials with various surface roughness. J Biomed Mater Res 2000;49:155-66

69. Ignjatovic N, Ninkov P, Kojic V, Bokurov M, Srdic V, Krnojelac D, Selakovic S, Uskokovic D. Cytotoxicity and fibroblast properties during in vitro test of biphasic calcium phosphate/poly-di-lactide-co-glycolide biocomposites and different phosphate materials. Microscopy Research and Technique 2006;69:976-82.

70. Suzuki T, Ohashi R, Yokogawa Y, Nishizawa K, Nagata F, Kawamoto Y, Kameyama T, Toriyama M. Initial anchoring and proliferation of fibroblast L-929 cells on unstable surface of calcium phosphate ceramics. Journal of Bioscience and Bioengineering 1999;87(3):320-27.

71. Simon CG, Guthrie WF, Wang FW. Cell seeding into calcium phosphate cement. J Biomed Mater Res 2004;68A:628-39.

72. Kohri M, Miki K, Waite DE, Nakajima H, Okabe T. In vitro stability of biphasic calcium phosphate ceramics. Biomaterials 1993;14:299-04.

73. Kohri M, Miki K, Waite DE, Nakajima H, Okabe T. In vitro stability of biphasic calcium phosphate ceramics. Biomaterials 1993;14:299-04.

74. Harnett EM, Alderman J, Wood T. The surface energy of various biomaterials coated with adhesion molecules used in cell culture. Colloids and Surfaces B: Biointerfaces 2007;55:90-97.

75. Haas TA, Plow EF. Integrin-ligand interactions: a year review. Curr Opin Cell Biol 1994;6:656-62.

76. Yang JY, Ting YC, Lai JY, Liu HL, Fang HW, Tsai WB. Quantitative analysis of osteoblast-like cells (MG63) morphology on nanogrooved substrata with various groove and ridge dimensions. J Biomed Mater Res 2008;00:000-000. (http://dx.doi.org/10.1002/jbm.a.32130).

77. Stamenovic D. Cell mechanics. Two regimes, maybe three?. Nature Materials 2006;5:597-98.

78. Yang Y, Bauer C, Strasser G, Wollman R, Julien J-P, Fuchs E. Integrators of the cytoskeleton that stabilize microtubules. Cell 1999;98:229-38.

79. Hirst LS, Safinya CR. Skin Layer at the Actin-Gel Surface: Quenched Protein Membtanes form Flat, Crumpled, and Tubular Morphologies. Pysical Review Letters 2004;93(1):1-4.

80. In: Bruce Alberts, Alexander Johnson, Julian Lewis, Martin Raff, Keith Roberts, Peter Walter. Molecular Biology of the cell. Fourth edition, pp. 907-1110. Garland Science, NY, 2002.

81. Dalby MJ, Riehle MO, Yarwood SJ, Wilkinson CD, Curtis AS. Nucleus alignment and cell signaling in fibroblasts: Response to a micro-grooved topography. Exp Cell Res 2003;284:274-82.

82. Hott M, Noel B, Bernache-Assolant D, Rey C, Marie PJ. Proliferation and diferantiation of human trabecular osteoblastic cells on hydroxyapatite. J Biomed Mater Res 1997;37:508-16.

83. Matsuoka H, Akiyama H, Okada Y, Ito H, Shigeno C, Konishi J, Kokubo T, Nakamura T. In vitro analysis of the stimulation of bone formation by highly bioactive apatite- and wollastonite-coating glass-ceramics: release calcium ions promote osteogenic differentiation in osteoblastic ROS 17/2.8 cells. J Biomed Mater res 1999;47:176-88.

84. Chang YL, Stanford CM, Keller JC. Calcium and phosphate supplementation indications for hydroxyapatite (HA)-enhanced bone formation. J Biomed Mater Res 2000;52:270-8.

85. Ehara A, Ogata K, Imazato S, Ebisu S, Nakano T, Umakoski Y. Effect of TCP and TetCP on MC3T3-E1 proliferation, differentiation and mineralization. Biomaterials 2003;24:831-6.

86. Yamaguchi T, Chattopadhyay N, Kifor O, Ye C, Vassilev PM, Sanders JL, Brown EM. Expression of extracellular calcium-sensing receptor in human osteoblastic MG-63 cell line. Am J Physiol Cell Physiol 2001;280:C382–C393.

87. Gough JE, Jones JR, Hench LL. Nodule formation and mineralisation of human primary osteoblasts cultured on a porous bioactive glass scaffold. Biomaterials 2004;25:2039-46.

88. Lefaix H, Asselin A, Vermaut P, Sautier JM, Berdal A, Portier R, Prima F. On the biocompatibility of a novel Ti-based amorphouos composite: structural characterisation and in vitro osteoblasts response. J Mater Sci: Mater Med 2008;19:1861-69.

89. Lu J, Descamps M, Dejou J, Koubi G, Hardouin P, Lemaitre J, Proust JP. The Biodegradation Mechanism of Calcium Phosphate Biomaterials in Bone. J Biomed Mater Res (Appl Biomater) 2002;63:408-12.

90. Yuan H, Li Y, de Bruijn JD, de Groot K, Zhang X. Tissue responses of calcium phosphate cement: a study in dogs. Biomaterials 2000;21:1283-90.

91. Kurashina K, Kurita H, Hirano M, Kotani A, Klein CPAT, de Groot K. In vivo study of calcium phosphate cements: implantation of an α-tricalcium phosphate/dicalcium phosphate dibasic/tetracalcium phosphate monoxide cement paste. Biomaterials 1997;18:539-43.

92. Frayssinet P, Roudier, Lerch A, Ceolin JL, Depres E, Rouquet N. Tissue reaction against a self-setting calcium phosphate cement set in bone or outside the organism. J Mater Sci: Mater Med 2000;11:811-15.

93. Theiss F, Apelt D, Brand B, Kutter A, Zlinszky K, Bohner M, Matter S, Frei C, Auer JA, von Rechenberg B. Biocompatibility and resorption of a brushite calcium phosphate cement. Biomaterials 2005;26:4383-94.

94. Harada Y, Wang JT, Doppalapudi VA, Willis AA, Jasty M, Harris WH, Nagase M, Goldring SR. Differential effects of different forms of hydroxyapatite and

hydroxyapatite/tricalcium phosphate particulates on human monocyte/macrophages in vitro. J Biomed Mater Res 1996;31:19-26.

95. Silva SN, Pereira MM, Goes AM, Leite MF. Effect of biphasic calcium phosphate on human macrophage functions in vitro. J Biomed Mater Res 2003;65:475-81.

96. Kakhlon O, Cabantchik ZI. The labile iron pool: characterisation, measurement, and participation in cellular processes. Free Radic Biol Med 2002;33(8):1037-46.

97. Henze MW, Muckenthaler MU, Andrews NC. Balancing acts: molecular control of mamalian iron metabolism. Cell 1004;117:285-97.

98. Cotran R, Kumar V, Abbas AK, Fausto N, in Pathologic Basis of Disease, ed. by Robbins & Cotran, Chapt 1, 7th edn. (WB Saunders Co., 2004), pp. 14–17.

99. M. Jiang, J. Terra, A.M. Rossi, M.A. Morales, E.M.B. Saitovitch, D.E. Ellis, Fe2+/Fe3+ substitution in hydroxyapatite: Theory and experiment. Phys Rev B 2002;66(22):224107-1/15.

100. Pioletti DP, Takei H, Lin T, van Landuyt P, Ma QJ, Kwon SY, Sung KLP. The effects of calcium phosphate cement particles on osteoblast functions. Biomaterials 2000;21:110314.

101. Malard O, Bouler JM, Guicheux J, Heymann D, Pilet P, Coquard C, Daculsi G. Influence of biphasic calcium phosphate granulometry on bone ingrowth, ceramic resorption, and inflammatory reactions: Preliminary in vitro and in vivo study. J Biomed Mater Res 1999;46:103-11.

102. Lassus J, Salo J, Jiranek W, Santavirta S, Nevalainen J, Matucci-Cerinic M, Horak P, Konttinen Y. Macrophages activation results in bone resorption. Clin Orthop Rel Res 1998;352:7–15.

103. Cheung HS, Devine TR, Hubbard W. Calcium phosphate particle induction of metalloproteinase and mitogenesis: Effect of particle sizes. Osteoarthritis Cartilage 1997;5:145-51.

104. Nomoto T, Haraguchi K, Yamaguchi S, Sugano N, Nakayama H, Sekino T, Niihara K. Hydrolyses of calcium phosphates-allografts composite in physiological solutions. J Mater Sci: Mater Med 2006;17:379-85.

105. Okumura M, Ohgushi H, Dohi Y, Katuda T, Tamai S, Koerten HK, Tabata S. Osteoblastic phenotype expression on the surface of hydroxyapatite ceramics. J Biomed Mater Res 1997;37:122-29.

106. Bohner M, Theiss F, Apelt D, Hirsiger W, Houriet R, Rizzoli G, Gnos E, Frei C, Auer JA, von Rechenberg B. Compositional changes of a dicalcium phosphate dihydrate cement after implantation in sheep. Biomaterials 2003;24:3463-74.

107. Sarkar MR, Wachter N, Patka P, Kinzl L. First Histological Observations on the Incorporation of a Novel Calcium Phosphate Bone Substitute Material in Human Cancellous Bone. J Biomed Mater Res (Appl Biomater) 2001;58:329-34.

108. Robling AG, Castillo AB, Turner CH. Biomechanical and Molecular Regulation of Bone Remodeling Annu Rev Biomed Eng. 2006;8:455-98.

109. Kanczler JM, Oreffo ROC. Osteogenesis and angiogenesis: The potential for engineering bone. European Cells and Materials 2008;15:100-114.

Chapter 9

Ultrasonic monitoring of the setting of calcium-based bone cements

9.0. Structured abstract

Mini Abstract. In this study, the setting of calcium sulphate (CS) and calcium phosphate (CP) based bone cements was monitored by ultrasounds in terms of the acoustic impedance $z_c(t)$, the speed of sound $c_c(t)$, the density $\rho_c(t)$ and the reflection coefficient $R_{p,c}(t)$. It has been showed that pulse-echo ultrasound is a reliable method to monitor transient material properties during the early setting of CS and CP bone cements.

Study Design. Experimental study to characterise by ultrasounds the early setting of several CS and CP based bone cements.

Objective. To monitor the acoustic properties linked to material-features of ceramic-based bone cements from the early stages of the cement curing process.

Summary of Background Data. Monitoring of the setting of bone cements is a subject that is relevant to all (polymer and ceramic) bone cements. Traditionally, the start and the end of bone cements' setting has been characterized by the *Gillmore* needles standard. However, this method has been criticized because it is useless for an optimum characterization of the early-setting stages of the new injectable calcium phosphate cements developed for vertebroplasty and kyphoplasty. The *Gillmore* method gives no information on the continuous chemical and physical processes taking place during the cement's setting. For these reasons, ultrasounds, a non destructive technique applied with success to study bone, biomaterials and cement/concrete, has been investigated in this chapter. Thus, the general objective of this research was to monitor by ultrasounds the early setting of several calcium based bone cements (CBCs) in order to both learn more about their setting and microstructural-features and compare the information acquired by the acoustic technique to other more classical characterisation techniques.

Methods. The powder phase of the CS-cement consisted of CS-hemihydrate; the CP-cement was a mixture of α-tricalcium phosphate, CS-dihydrate and hydroxyapatite. For

the CS-cement, the acoustic impedance $z_c(t)$, the speed of sound $c_c(t)$ and the density $\rho_c(t)$ were measured at the interval of liquid-to-powder (L/P) ratios from 0.20 to 3.00 mL/g. For the CP-cement, the acoustic characteristics obtained were the $z_c(t)$ and the reflection coefficient $R_{p,c}(t)$, and the L/P ratio ranged from 0.30 to 0.40 mL/g. Cement setting times were measured both by the *Gillmore* needles method and ultrasonic method by using an ultrasound emitter-receiver transducer (UT) excited with a Pulse Generator.

Results. For CS-cements, the evolution of the acoustic impedance $z_c(t)$ indicated the existence of an optimum L/P ratio around 0.8 mL/g from which the CS-cement started to be less workable (L/P<0.8 mL/g) and more inhomogeneous (increasing amounts of mixing porosity). Acoustic impedance also showed that for L/P>0.8 mL/g, the CS-cements started to be more liquid producing cements with very long setting times (i.e. useless for clinical applications). On the other hand, the speed of sound $c_c(t)$ showed an exponential growth trend that saturated around the characteristic *Gillmore*-FST. Moreover, the evolution of density $\rho_c(t)$ (which is not measured but calculated from $z_c(t)$ and $c_c(t)$ data) was in agreement with data published for dental CS-cements.

Conclusions. It is expected that, after further optimization, the ultrasound technique should help, in combination with recent approaches to measure the injectability features of CBCs, to set up good practice protocols for CBC's injection during minimally invasive surgery. It is also expected that this technology will be implemented in the future during the *in situ* application of injectable CBCs.

Key Points.

- Ultrasounds offered a reliable continuous evaluation of the early curing process by linking acoustic and material properties of ceramic-based bone cements.
- The ultrasounds technique should be further optimized to extent its use and to assure its reliability during bone cement's characterisation.

9.1. Introduction

Monitoring of the setting of bone cements is a subject that is relevant to all bone cements; those used in cemented arthroplasty and those used in vertebroplasty and kyphoplasty. Ultrasound monitoring is a non destructive technique that has been applied with success to study bone [1], biomaterials [2] and cement/concrete [3-6]; literature concerning cement/concrete is really abundant.

Concerning the biomaterials field, recent studies have been performed to monitor by ultrasound the entire setting process of some commercial polymer-based bone cements (PBCs) [7], as well as to monitor the degradation processes of biodegradable polymers [8]. In this field, the curing process of PBCs has been regularly monitored by differential scanning calorimetry (DSC), by recording the rate of heat evolution during polymerization (high exothermic reaction). This method identifies the start and the end of the entire curing process (i.e. characteristic setting times) and allows studying the influence of different experimental factors on the setting [9]. Similar studies have also been performed for calcium-based bone cements (CBCs) to monitor their hydration reactions and to discriminate between different setting mechanisms (i.e. nucleation, precipitation, surface-controlled processes, diffusion-controlled processes, etc.) [10].

However, some CBCs (i.e. calcium phosphate based) have low exothermic reactions [11,12] during setting. For this reason, the common method to easily define the start and the end of these CBCs' setting has been the *Gillmore* needles standard [13]. According to this standard, CBCs start to set at the initial setting time (IST) if one needle exerting a static pressure of 0.3 MPa does not leave a mark that can be visually observed on the cement surface. Similarly, the end of CBCs setting is obtained at the final setting time (FST) for a static pressure of 5 MPa. It should be pointed out that in a clinical situation surgeons have been using IST and FST as a criteria to both place the cement into the bone

damaged cavity (i.e. t<IST) and close the wound (i.e. t>FST) without affecting the mechanical integrity of the cement itself as well as to assure the mechanical stability of the implantation site. Optimum clinical time intervals are considered to be IST<8 min and FST<15 min [14] (see further details in Chapter 1). Unfortunately, this method does not give much information on the continuous chemical and physical processes taking place during the cement's setting. Moreover, this method has been criticized several times because it is useless for the new injectable CBCs that are being developed to treat vertebral compression fractures (VCF) through minimally invasive surgery techniques such as vertebroplasty and kyphoplasty [15-18]. In these applications, the clinical time which is important is the injection time (IT; maximum time available to the clinician for injecting the cement into the bone cavity), which is by far lower than the IST. For these reasons, ultrasound-monitoring has recently entered this field and is being considered as a more appropriate characterisation technique to follow not only the hardening processes of these special injectable bone cements [19], but also the very early stages of their setting [20,21], i.e. when the cement is still injectable.

Thus, the general objective of this research was to monitor by ultrasounds the early setting of several CBCs in order to both learn more about their setting and microstructural-features and compare information acquired by the acoustic technique to other more classical characterisation techniques. This has been approached by investigating the influence of the type of CBCs (i.e. calcium sulphate *versus* calcium phosphate) on key acoustic signatures of the setting process and also by studying these properties as a function of the liquid-to-powder (L/P) ratio in order to account for different cement fluid behaviour.

9.2. Materials and methods

9.2.1. Calcium based bone cements

Calcium sulphate based cement (CS-cement) consisted of a powder phase of calcium sulphate hemihydrate (CSH) and a liquid phase of water (of pharmaceutical quality for injection). L/P ratio ranged from 0.20 to 3.00 mL/g. On the other hand, calcium phosphate based cement (CP-cement) consisted of a powder phase of alpha-tricalcium phosphate (α-TCP; 93, 88 and 73 *wt%*), calcium sulphate dihydrate (CSD; 5, 10 and 25 *wt%*, respectively) and hydroxyapatite seeds (HA; 2 *wt%*); the liquid phase was water (of pharmaceutical quality) solution of disodium hydrogen phosphate (Na_2HPO_4; DHP; 1 and 2 *wt%*), used as a setting accelerator. In this case, the L/P ratio ranged from 0.30 to 0.40 mL/g. CP-cements have been coded as $S_n \equiv$«i/j/k/l», where i=*wt%*α-TCP, j=*wt%*CSD, k=*wt%*DHP and l=L/P. For example, sample $S_1 \equiv$«88/10/1/0.40» is made of a powder phase containing 88 *wt%* α-TCP and 10 *wt%* CSD and a liquid phase containing 1 *wt%* DHP, and the L/P ratio is 0.40 mL/g. Samples selected for further analysis at the results section are $S_2 \equiv$«73/25/1/0.35», $S_3 \equiv$«88/10/1/0.30» and $S_4 \equiv$«93/5/2/0.30». Note that as all samples had 2 *wt%* HA, the codes do not contain this data.

9.2.2. Setting times

Setting times were measured with the *Gillmore* needles standard [13] in order to compare IST and FST with the ultrasound results.

9.2.3. Ultrasound measurements

Ultrasound measurements were made following the general pulse-echo ultrasound set-up described in Fig. 9.1. The ultrasound transducer (UT) was used both as emitter and

receiver. The UT was excited with a Pulse Generator (*Panametric-5025PR*). The pulses P_1 and P_5 and the time of flight of these pulses (i.e. $\Delta t_{P1 \rightarrow P5}$) were recorded in an oscilloscope (*Tektronix TDS-520*). Finally, *MatLab*© was used to develop the interface and the analysis software. The acoustic cement properties monitored with time were the reflection coefficient at the ultrasonic device's interface "Poly-Methyl-Methacrylate/Cement" («PMMA/Cement») $R_{p,c}(t)$, the acoustic impedance of the cement $z_c(t)$, the speed of sound through the cement $c_c(t)$ and the density of the cement $\rho_c(t)$ (see Fig. 9.1 and Eqs. 9.1 to 9.4). These acoustic properties were monitored from 2 min after the start of the powder and the liquid mixture of the cement's phases and during 1 h of the setting reaction.

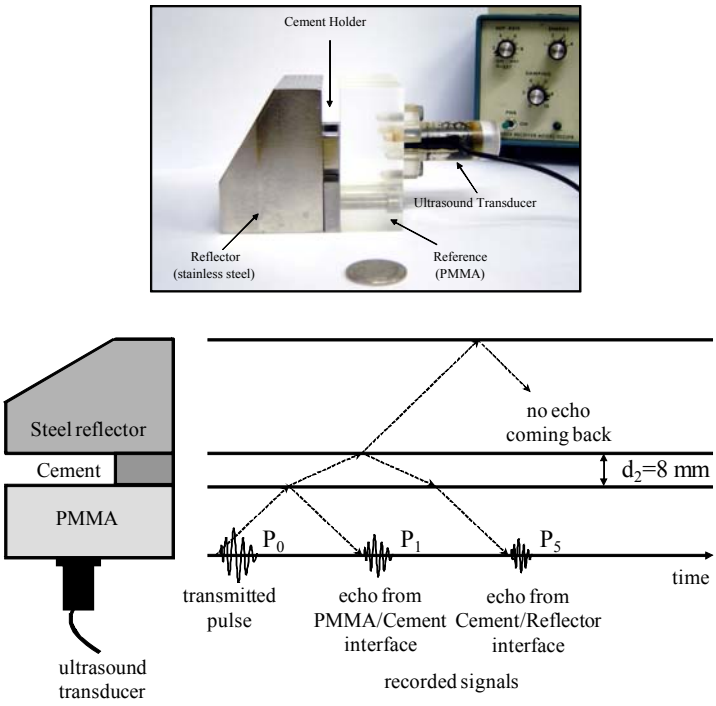

Figure 9.1. Pulse-echo experimental set-up (top) and principle of the probe measurements (bottom): P_1 and P_5 echoes reflected at «PMMA/Cement» and «Cement/Reflector» interfaces, respectively, are recorded to determine the specific acoustic properties of the cement.

$$R_{p,c}(t) = \frac{P_1(t)}{P_0(t)} \quad [9.1]$$

$$z_{cement}(t) = z_{pmma} \times \frac{1 + R_{p,c}(t)}{1 - R_{p,c}(t)} \quad [9.2]$$

$$c_{cement}(t) = \frac{2 \cdot d_2}{\Delta t_{P_1 \to P_5}} \quad [9.3]$$

$$\rho_{cement}(t) = \frac{z_{cement}(t)}{c_{cement}(t)} \quad [9.4]$$

9.3. Results and discussion

9.3.1. Calcium sulphate bone cements

Fig. 9.2 shows the evolution of the acoustic impedance $z_c(t)$ of CS-cement at different L/P ratios. It was observed that for 1.5≤L/P(mL/g)≤3.0, CS-cement behaved as dilute homogeneous ion-containing water solutions with similar constant-like acoustic properties (see Fig. 9.2, cement for L/P=3 mL/g) as that of pure water (z_{water}=1.5 MPa.s/m). In fact, in this L/P ratio range, cements set very slowly; according to the *Gillmore* needles, FST was higher than 2 h. It was also observed from Fig. 9.2 that the average acoustic impedance at saturation, defined as $z_s \equiv \langle z_c \rangle (t>10\ min)$, had a maximum versus the L/P ratio (see Fig. 9.3); this related to the experimental observation that CS-cements made at L/P>0.8 mL/g were more liquid when the L/P ratio increased from 0.8 mL/g. On the other hand, CS-cements made at L/P<0.8 mL/g were more difficult to paste when the L/P ratio decreased from 0.8 mL/g; this indicates that L/P=0.8 mL/g represents a compromise between non-workable and workable cements. In fact, cements made at L/P≤0.4 mL/g were very difficult to mix (very viscous), they were not homogeneous (i.e. presence of porosity) and according to the *Gillmore* needles the IST of these samples equal the FST, i.e.

setting was "instantaneous". Obviously, this was not the case; and, merely, the slurries were so viscous and dried that, under the above conditions, they were able to instantaneously withstand higher *Gillmore*-pressures than 5 MPa.

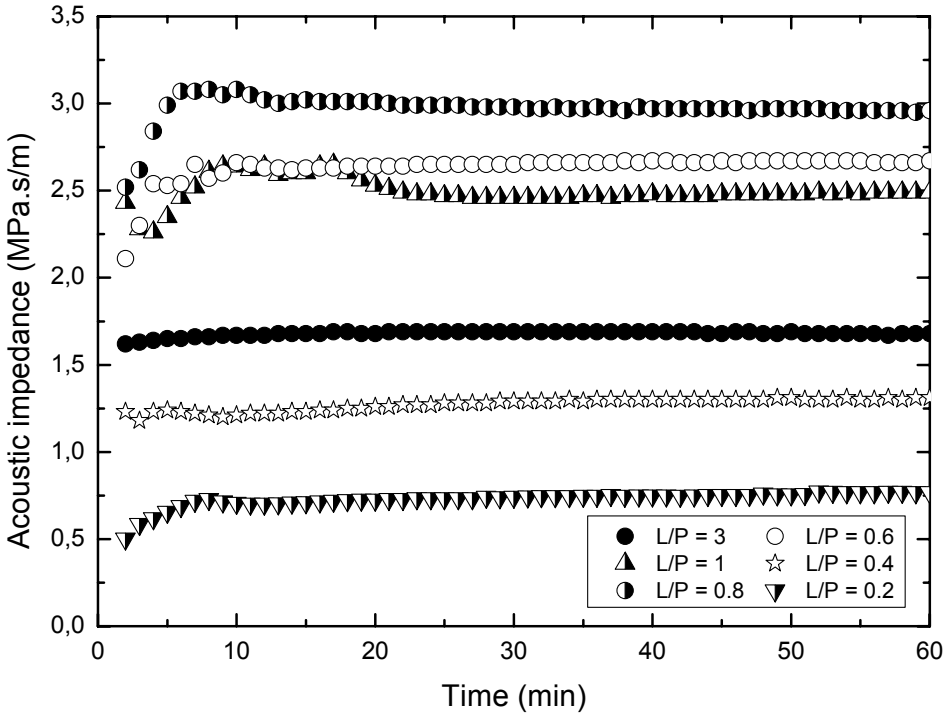

Figure 9.2. Evolution of the acoustic impedance $z_c(t)$ for several CSH-cements made in the interval 0.2≤L/P(mL/g)≤3.

On the other hand, CS-cements prepared at 0.4<L/P(mL/g)≤1 showed FSTs in the range of 4<FST(min)≤12, which was an indication that normal hydration of CSH into CSD [22] was favoured in this interval for increasing L/P ratios. In fact, in this L/P ratio range, the hydration reaction led to a continuous evolution of the speed of sound $c_c(t)$. According to Fig. 9.4, the speed of sound behaved similarly for all L/P ratios; it increased quickly, after the cement mixing (2 min), and then saturated with time, following an

exponential growth trend. This meant (see Fig. 9.1) that the time of flight for the first transmitted pulse to return to the ultrasound receptor (i.e. $\Delta t_{P1 \rightarrow P5}$) diminished gradually with time (up to a constant value) as the setting proceeded, i.e. pulse transmission through CS-cement improved with time (i.e. echo-pulses moved faster up to saturation). It should be remembered that samples made at L/P=3 mL/g were similar to water (see Fig. 9.3; z_s(L/P=3 mL/g)≈1.7 MPa.s/m *vs.* z_{water}=1.5 MPa.s/m). In fact, this sample showed values for the speed of sound around 1500 m/s (data not shown) which is similar to that of water (i.e. c_{water}=1486 m/s) [23].

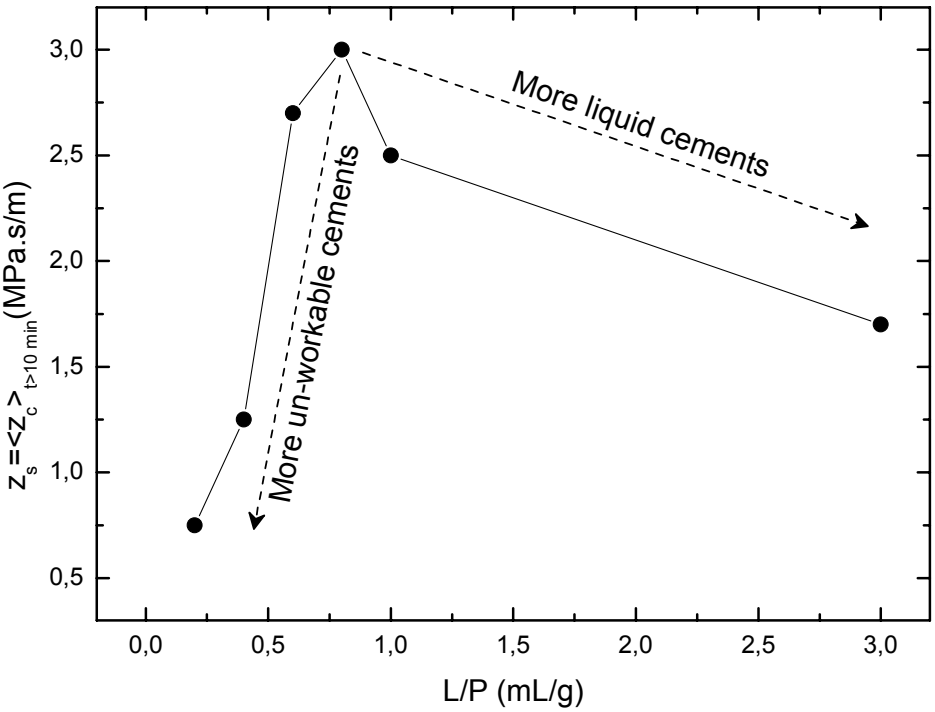

Figure 9.3. Acoustic impedance at saturation as a function of the liquid-to-powder ratio. The value L/P=0.8 mL/g marked the differences between non-workable and workable slurries.

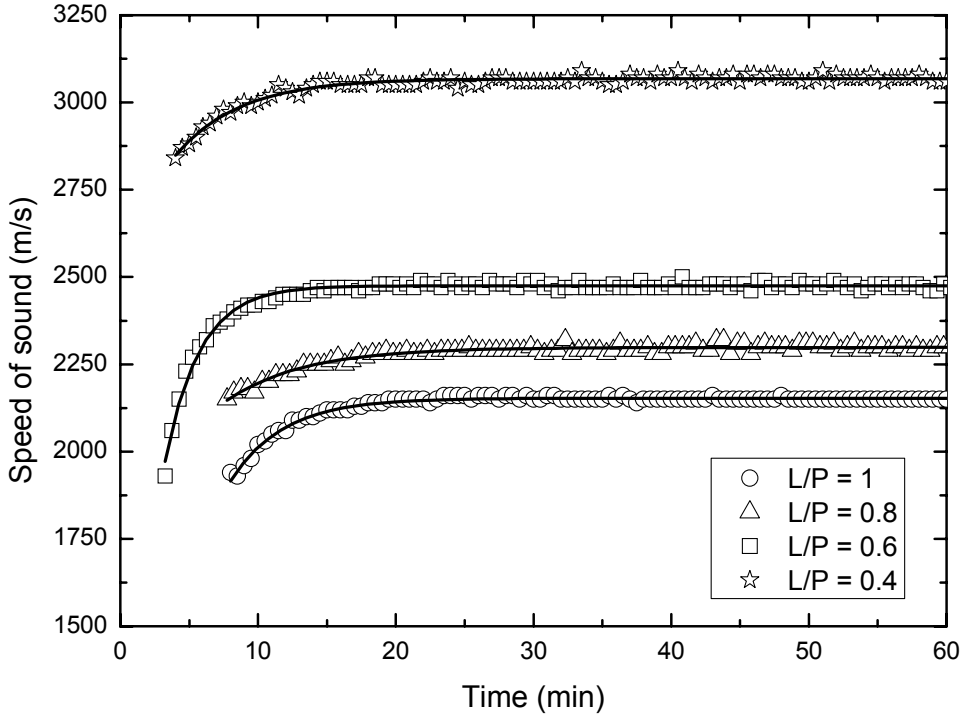

Figure 9.4. Evolution of the speed of sound $c_c(t)$ for several CSH-cements made in the interval 0.4≤L/P(mL/g)≤1.

Another observation should be noted from Fig. 9.4; this concerns the speed of sound observed for L/P=0.4 mL/g, which was very high as compared to the other L/P ratios. As has been commented before, for this L/P ratio, the slurry was difficult to work and paste so that some volume porosity (i.e. air bubbles) was included into the cement. It is thought that this volume-porosity reflected back and attenuated the ultrasound pulses transmitted from the interface «PMMA/Cement» (see Fig. 9.1) before they attained the interface «Cement/Reflector». In fact, for L/P(mL/g)<0.4, the echo-signal $P_5(t)$ was not detected and consequently the speed of sound $c_c(t)$ was not measured for this L/P ratio range. Moreover, according to Fig. 9.2, the acoustic impedance obtained for the L/P=0.2 mL/g had a finite value (i.e. z_s≈0.75 MPa.s/m), which means that the absence of echo-

pulses in this L/P ratio range should be related to pulse attenuation due to the presence of porosity and not to complete pulse reflection (without attenuation) at the cement-pores interfaces, for which situation $z_c(t)$ should tend to infinite (see Eq. 9.1 for $R_{p,c}(t)\approx 1$).

On the other hand, Fig. 9.5 shows the evolution of the cement density $\rho_c(t)$ (i.e. $\rho_c(t)=z_c(t)/c_c(t)$; see Eq. 9.4) as a function of the L/P ratio. These results were useful to clarify why the acoustic impedance $z_c(t)$ decreased so fast from L/P=0.8 mL/g ($z_s\approx 3$ MPa.s/m) to L/P=0.2 mL/g ($z_s\approx 0.75$ MPa.s/m).

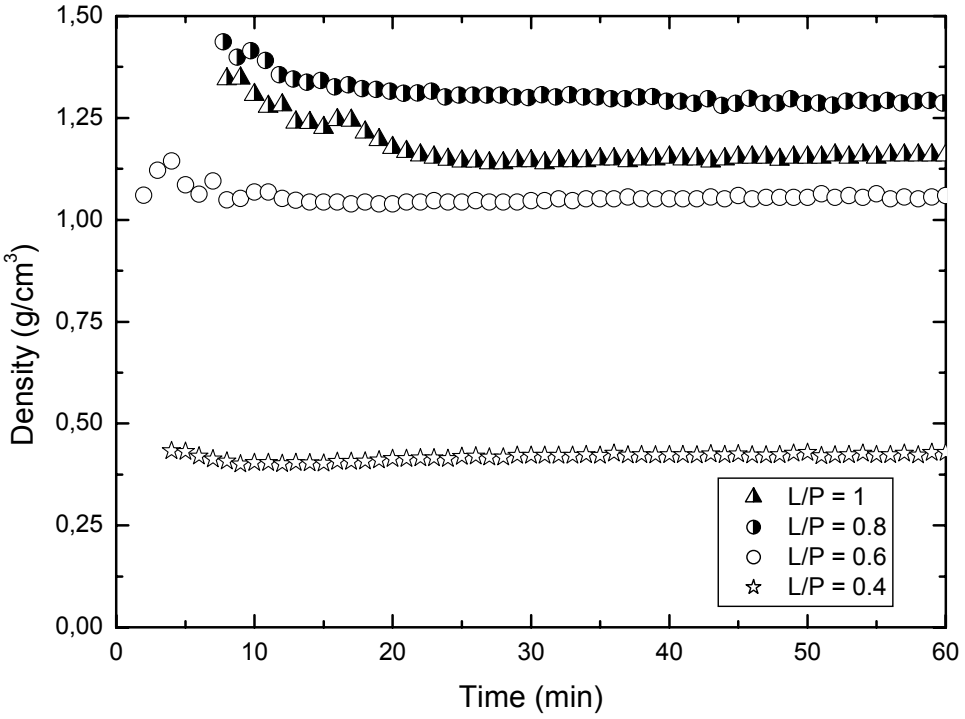

Figure 9.5. Evolution of the density $\rho_c(t)$ for several CSH-cements made in the interval 0.4≤L/P(mL/g)≤1.

As it is observed from Fig. 9.5, for the interval 0.4≤L/P(mL/g)≤1, the density of CS-cements was $0.5\leq\rho(g/cm^3)\leq 1.5$. This was exactly the same interval reported for the

apparent density of rehydrated CSD with different porosities [24]. In fact, the apparent density of calcium sulphate dental plaster (i.e. low porosity cement) has been reported to be 1.58 g/cm^3 [24].

In general, the results showed in Figs. 9.4 and 9.5 agreed with literature and confirmed that porosity is one of the key-factors influencing the acoustic properties of CS-cements [25,26].

9.3.2. Calcium phosphate bone cements

CP-cements behaved differently from CS-cements. In fact, in this case, only the acoustic impedance $z_c(t)$ (see Fig. 9.6) and the reflection coefficient $R_{p,c}(t)$ (see Fig. 9.7) were measured (note that both are related through Eq. 9.2). Fig. 9.6 shows that $z_c(t)$ increased to a maximum value from which, at some time, it decreased to zero; this was the general trend for all the tested cement samples. The general conclusion was that CP-cements shrank with time mostly during the period comprised between the IST and the FST (i.e. samples S1, S2, S3 and S4 shrank between 35-65, 8-19, 21-35 and 9-21 (±1) min, respectively). Only sample S1 showed some departure from the normal observation. In general, shrinkage affected the continuity at the interface «PMMA/Cement» (see Fig. 9.1) and the reflection coefficient (see Fig. 9.7) approached unity, i.e. $|R_{p,c}(t)|\rightarrow 1$. This meant that the actual reflection process took place at a new interface «PMMA/Air» (z_{air}=41.31x10^{-5} MPa.s/m << z_{PMMA}=3.3x10^5 MPa.s/m) formed during CP-cement's shrinkage (i.e. $|R_{p,c}(t)|\rightarrow|R_{p,air}(t)|=|(z_{air}-z_p)*(z_{air}+z_p)^{-1}|\rightarrow 1$; see Eq. 9.2). Unfortunately, cement detachment at the interface «PMMA/Cement» has in itself a statistic nature (note the departure observed for sample S1) and, for this reason, it was not possible to correlate the results with the studied experimental factors, i.e. powder phase chemistry, liquid phase accelerator content and L/P ratio. In order to account for these effects it should be

necessary to assure continuity at the interface «PMMA/Cement» by immersing for example the whole experimental set-up (see Fig. 9.1) under water; this is under study.

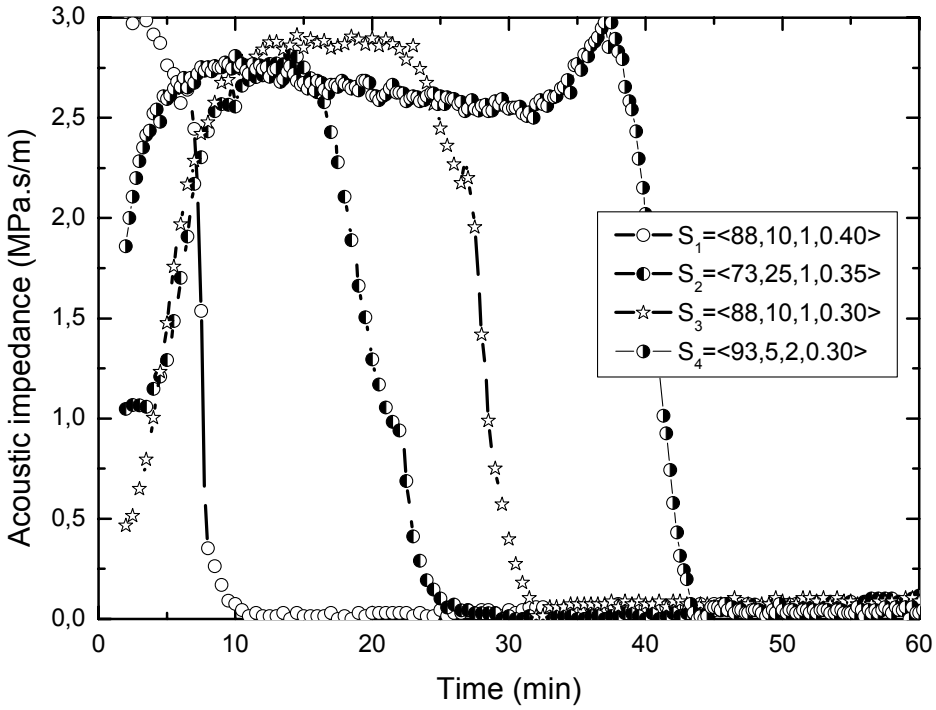

Figure 9.6. Evolution of the acoustic impedance $z_c(t)$ for several CPC-cements. Cement detachment was observed to start between the IST and the FST (see the discussion section). Note: Samples follow the coding S_n=<i,j,k,l> as detailed at Materials and Methods' section.

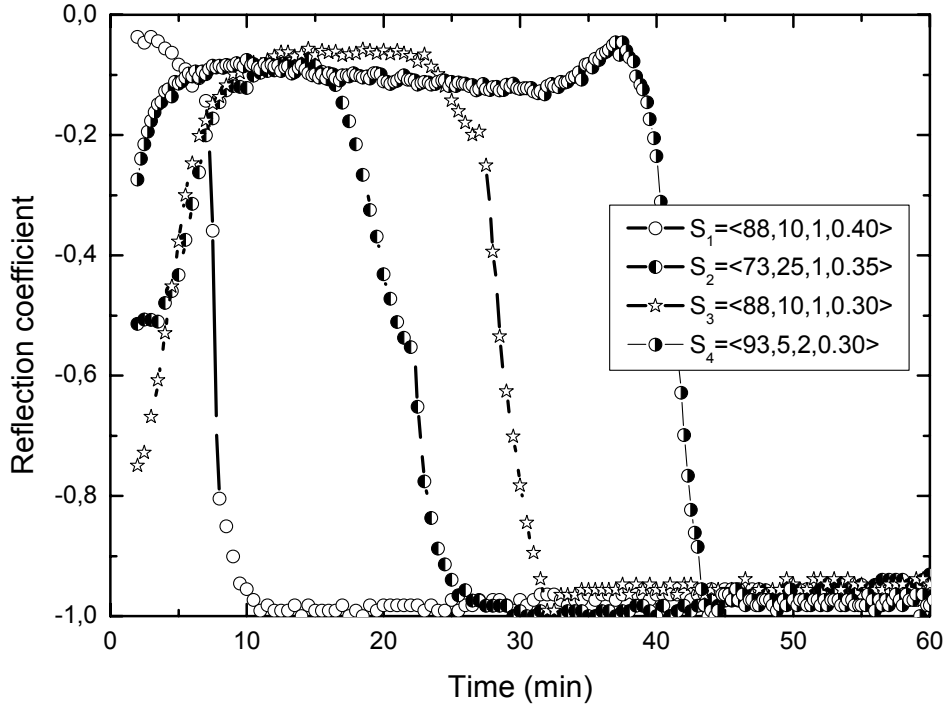

Figure 9.7. Evolution of the reflection coefficient $R_{p,c}(t)$ for several CPC-cements. This figure while showing similar information as that in Fig. 9.6 helps to understand the progressive cement detachment at the interface «PMMA/Cement» (see also the discussion section).

9.4. Summary conclusion

It has been showed that pulse-echo ultrasound is a reliable method to monitor transient material properties during the early setting of CS and CP bone cements.

For CS-cements, the evolution of the acoustic impedance $z_c(t)$ indicated the existence of an optimum L/P ratio around 0.8 mL/g from which the CS-cement started to be less workable (L/P<0.8 mL/g) and more inhomogeneous (increasing amounts of mixing porosity). Acoustic impedance also showed that for L/P>0.8 mL/g, the CS-cements started to be more liquid producing cements with very long setting times (i.e. useless for clinical

applications). On the other hand, the speed of sound $c_c(t)$ showed an exponential growth trend that saturated around the characteristic *Gillmore*-FST (i.e. once cement was set the speed of sound did not further evolved). Moreover, the evolution of density $\rho_c(t)$ (which is not measured but calculated from $z_c(t)$ and $c_c(t)$ data) was in agreement with data published for dental CS-cements.

For CP-cements, the experimental set-up was not appropriate because these cements shrank during setting. Consequently, the contact between the cement and the reference gets lost at some time, from which no further information concerning cement's setting can be obtained.

Finally, it is expected that, after further experimental optimization, ultrasound monitoring should help, in combination with recent approaches that measure certain injectability characteristic for CBCs [16,27], to set up good practice protocols for CBC's injection during minimally invasive surgery. It is also expected that this technology will be implemented in the future during the *in situ* application of injectable bone cements.

References

1. Lee KI, Humphrey VF, Leighton TG, Yoon SW. Predictions of the modified Biot-Attenborough model for the dependence of phase velocity on porosity in cancellous bone. Ultrasonics 2007;46:323-30.

2. Kaczmarek M, Pakula M, Kubik J. Multiphase nature and structure of biomaterials studied by ultrasounds. Ultrasonics 2000;38:703-07.

3. Berriman J, Purnell P, Hutchins DA, Neild A. Humidity and aggregate content correction factors for air-coupled ultrasonic evaluation of concrete. Ultrasonics 2005;43:211-17.

4. Philippidis TP, Aggelis DG. Experimental study of wave dispersion and attenuation in concrete. Ultrasonics 2005;43:584-95.

5. Lee HK, Lee KM, Kim YH, Yim H, Bae DB. Ultrasonic in-situ monitoring of setting process of high-performance concrete. Cement and Concrete Research 2004;34:631-40.

6. Del Río LM, Jiménez A, López F, Rosa FJ, Rufo MM, Paniagua JM. Characterisation and hardening of concrete with ultrasonic testing. Ultrasonics 2004;42:527-30.

7. Viano AM, Auwarter JA, Rho JY, Hoffmeister BK. Ultrasonic characterization of the curing process of hydroxyapatite-modified bone cement. J Biomed Mater Res 2001;56:593-99.

8. Wu HC, Shen FW, Hong X, Chang WV, Winet H. Monitoring the degradation process of biopolymers by ultrasonic longitudinal wave pulse-echo technique. Biomaterials 2003;24:3871-76.

9. Abdulghani S, Nazhat SN, Behiri JC, Deb S. Effect of triphenyl bismuth on glass transition temperature and residual monomer content of acrylic bone cements. Journal of Biomaterials Science, Polymer Edition 2003;14:1229-42.

10. Brunner TJ, Bohner M, Dora C, Gerber C, Stark WJ. Comparison of amorphous TCP nanoparticles to micron-sized α-TCP as starting materials for calcium phosphate cements. J Biomed Mater Res Part B: Appl Biomater 2007;83B:400-07.

11. Liu C, Gai W, Pan S, Liu Z. The exothermal behaviour in the hydration process of calcium phosphate cement. Biomaterials 2003;24:2995-03.

12. Lemaitre J. Injectable calcium phosphate hydraulic cements: new developments and potential applications. Innov Tech Biol Med 1995;16(1):109-20.

13. Standard Test Method for Time of Setting of Hydraulic Cement Paste by the Gillmore Needles, ASTM C266-89, Annual Book of ASTM Standards, vol. 04.01: Cement, Lime, Gypsum. Philadelphia: ASTM 1993;189-91.

14. Khairoun I, Boltong MG, Driessens FCM, Planell JA. Limited compliance of some apatitic calcium phosphate bone cements with clinical requirements. J Mater Sci: Mater Med 1998;9:667-71.

15. Lewis G. Injectable bone cements for use in vertebroplasty and kyphoplasty: state of the art review. J Biomed Mater Res: Appl Biomat 2005;76B(2):456-68.

16. Bohner M, Gbureck U, Barralet JE. Technological issues for the development of more efficient calcium phosphate bone cements: a critical assessment. Biomaterials 2005;26:6423-29.

17. Fernández E. Bioactive Bone Cements. In: Metin Akay, ed. Wiley Encyclopedia of Biomedical Engineering, 6-Volume Set. John Wiley & Sons, Inc. (USA), 2006:1-9. ISBN: 0-471-24967-X.

18. Vlad MD, del Valle LJ, Barracó M, Torres R, López J, Fernández E. Iron oxide nanoparticles significantly enhances the injectability of apatitic bone cement for vertebroplasty. Spine 2008;33(21): 2290-2298.

19. Song Y, Feng Z, Wang T. In situ study on the curing process of calcium phosphate bone cement. J Mater Sci: Mater Med 2007;18:1185-93.

20. Carlson J, Nilsson M, Fernández E, Planell JA. An ultrasonic pulse-echo technique for monitoring the setting of CaSO4-based bone cement. Biomaterials 2003;24:71-7.

21. Nilsson M, Carlson J, Fernández E, Planell JA. Monitoring the setting of calcium-based bone cements using pulse-echo ultrasound. J Mater Sci Mater Med 2002;13(12):1135-41.

22. Lewry AJ, Williamson J. The setting of gypsum plaster. J Mater Sci 1994;29(23):6085-90.

23. Kaye GWC, Laby TH. Tables of Physical and Chemical Constants. Longman, London, 1995.

24. Wirsching F. Calcium sulphate. In: Ullmann's Encyclopedia of Industrial Chemistry 1985;555-584. Fifth, completely revised edition. Vol A4: Benzyl Alcohol to Calcium Sulfate. VCH Publishers, Deerfield Beach FL, USA.

25. Dalui SK, Roychowdhury M, Phani KK. Ultrasonic evaluation of gypsum plaster. Journal of Materials Science 1996;31:1261-63.

26. Sayers CM, Grenfell RL. Ultrasonic propagation through hydrating cements. Ultrasonics 1993;31(3):147-53.

27. Bohner M, Baroud G. Injectability of calcium phosphate pastes. Biomaterials 2005;26(13):1553-63.

Chapter 10

Effect of mixing on the setting of injectable bone cement: an ultrasound study

10.0. Structured abstract

Mini Abstract. In this chapter, experimental calcium sulphate bone cement has been further tested by ultrasounds to characterize and learn more about its progressive setting through the evolution of several acoustic properties. Ultrasound monitorisation and injection experiments were also investigated at different mixing conditions. It has been observed that further mixing after cement's constituency, and before the initial setting time of the cement, drastically affects both the characteristic setting times and the injectability of the cement.

Study Design. Experimental study to characterise the progressive setting of calcium sulphate bone cement through ultrasound monitoring.

Objective. To investigate the early progressive setting and the injectability at different mixing conditions of calcium sulphate bone cement.

Summary of Background Data. Ceramic bone cements (CBCs), i.e. calcium phosphate and calcium sulphate based bone cements are extending its present clinical applications to the management of vertebral compression fractures. However, spinal surgeons have reported problems when performing vertebro- and/or kyphoplasty, such as great difficulties in filling the vertebral bodies (bad injectability of present CBCs), bone press-filtering and/or cement decohesion causing bone instability due to the low mechanical strength and the long setting times of the cement. Thus, this chapter was planned to further investigate the early setting of some experimental cements by ultrasounds in order to continuous monitor the setting and link the influence of some experimental factors on it and on the injectability of the cement.

Methods. The acoustic impedance $z(t)$, the density $\rho(t)$ and the speed of sound $c(t)$ have been monitored versus the curing time during the viscous-to-solid transition of the cement as a function of different mixing conditions. Injectability tests were also

performed and the results have been related to the acoustic properties measured previously. Scanning Electron Microscopy accounted for the influence of the mixing protocols on the developed cement microstructure.

Results. The results indicated that further mixing before the IST can both accelerate the setting (i.e. fast setting cements) and improve the densification of the material (i.e. better mechanical properties). However, after completion of fixed resting times, RTs, additional mixing significantly decreased the injectability as compared to cement samples with no additional mixing. SEM results seemed to corroborate these observations.

Conclusions. It has been shown that mixing actually affects the setting and the injectability of calcium sulphate bone cements. Ultrasound monitoring contributed with relevant information to the understanding of the curing cement's process.

Key Points.

- Further mixing, after cement's constituency and before the initial setting time IST, improved the setting (i.e. lower IST & FST) but reduced the injectability of calcium sulphate based cements.
- Ultrasound monitoring continuously followed the evolution of the curing cement's process by recording the evolution of the acoustic impedance, the density and the speed of sound during the cement's setting.
- The characteristics IST & FST were obtained from the evolution of the speed of sound.
- Ultrasound monitoring should be further investigated to characterize the setting and the injectability properties of more complex bone cements.

10.1. Introduction

Ceramic bone cements (CBCs), i.e. calcium phosphate (CP) and calcium sulphate (CS) based bone cements, have been used in dental and orthopaedic applications to improve the quality of life of patients affected by bone fractures, bone tumours, osteoporosis and dental and/or craniofacial affections. This success has led to the development of several commercial formulations, i.e. Norian SRS©, Cementek©, Biocement-D©, α-BSM©, chronOS Inject©, BoneSource© and/or Biopex©, which have been indicated for certain particular applications [1].

Recently, with the advent of minimally invasive surgery techniques, CBCs have been also applied to spinal surgery (vertebro- and/or kyphoplasty) [2-5]. However, surgeons have reported great difficulties in filling the vertebral bodies (bad injectability of present CBCs) and other problems, such as bone press-filtering and cement decohesion, observed during vertebral body injection, that have resulted in bone instability due to low mechanical strength and long setting times of the cement [6]. For these reasons, the clinicians have indicated that new research on injectable biomaterials is needed because the future of orthopaedic surgery also heads in the direction of minimal invasion, where clinical techniques have lower cost and patients return to their normal activities much sooner. Thus, as interest in vertebro- and kypho-plasty continues, the application of injectable cements through minimally invasive techniques in the management of skeletal defects has become popular and scientists have approached the rheological properties of these materials in several ways [6-10].

The present research aims at furthering the understanding of injectable CBCs, as those used in spinal surgery, to elucidate which rheological properties are needed to inject these biomaterials into bone cavity before their setting. This general objective has been approached by monitoring the acoustic properties of experimental CS bone cement

during its setting by ultrasounds [11]. However, as these materials have progressive setting, it is not known how the injectability can be maintained in a clinical procedure. For this reason, ultrasound monitoring and injection experiments were also investigated at different mixing conditions. Broadly speaking, the present chapter extends the knowledge acquired in previous Chapter 9.

10.2. Materials and methods

Cements were made by mixing, by hand with a pestle in a mortar during 30 s, calcium sulphate hemihydrate (CSH) with water of pharmaceutical quality at different liquid-to-powder L/P ratios ($0.5 \leq L/P(mL/g) \leq 3.5$). The setting was monitored, 30 s later, at room temperature by ultrasounds during 1 h following the method outlined by Carlson et al. [12]. Cement made at L/P=2 mL/g was selected for further studies. It set under static conditions to obtain, from the evolution of the speed of sound *versus* time's curve (see the results section), the ultrasound's initial and final setting times (IST, FST). Then, replicas were prepared in a glass tube and set up to resting times RT lower than the IST, where *resting time* means that time for which the cement sets without further continuous or discontinuous mixing (i.e. under static conditions). After completion of those fixed RTs, cements were mixed by agitation (*YelloLab Test Tube Shaker, Ika Works, Inc.*) at 1600 rpm during 30 s and monitored again (as above, [12]), 30 s later, by ultrasounds during 1 h. The acoustic impedance $z(t)$, the density $\rho(t)$ and the speed of sound $c(t)$ were measured with this method [12] (see also Chapter 9).

The injectability was approached, following the method outlined by Driessens et al. [13] (see also Chapter 7), by extruding syringes of 5 mL, filled with cement up to ≈4.6 mL (i.e. ≈3.7 cm), at a crosshead speed of 50 mm/min (i.e. maximum extruding time to empty the syringe ≈45 s) and up to a maximum load of 300 N, using an *MTS Insight 5* universal testing machine. Following this method, the evolution of the extrusion force was

recorded against the extruding time for different mixing conditions; i.e. samples setting at rest up to different RTs and then injected, and samples mixed again at 1600 rpm for 30 s after completion of fixed RTs and then injected.

Scanning Electron Microscopy SEM was performed for some cement samples setting up to fixed resting times, before (i.e. RT=0 min) and after (i.e. RT=0, 1.5, 3 & 9 min) the application of further mixing during 30 s at 1600 rpm, in order to see any effect on cement's crystals distribution that could be related to cement's densification (see *10.3. Results and discussion*). Samples were quenched in acetone immediately after both, the completion of RTs or the additional mixing protocol to stop further hydration of cement.

10.3. Results and discussion

10.3.1. Acoustic properties

Fig. 10.1 shows the evolution of the speed of sound of ultrasound pulses traversing a cement sample *versus* the curing time, and as a function of the L/P ratio. These curves are used to calculate the characteristic initial and final setting times of the curing cement reaction [11]. The speed of sound is constant for times both lower than the IST and higher than the FST; between the IST and the FST (i.e. the setting period) the speed of sound increases at constant rate. Fig. 10.1 shows that the IST and the FST increased as the L/P ratio, indicating that high L/P ratio retards the setting. Moreover, the initial constant speed of sound before the IST decreased as the L/P ratio increased, approaching the value of 1500 m/s, characteristic of sound traversing water, i.e. the condition L/P>2 mL/g produced very liquid cements (non useful for the present study). Similar behaviour is observed for the speed of sound at saturation after the FST, i.e. it decreased as the L/P ratio increased. In general, these results indicated that cements set faster and were more compact for lower L/P ratios.

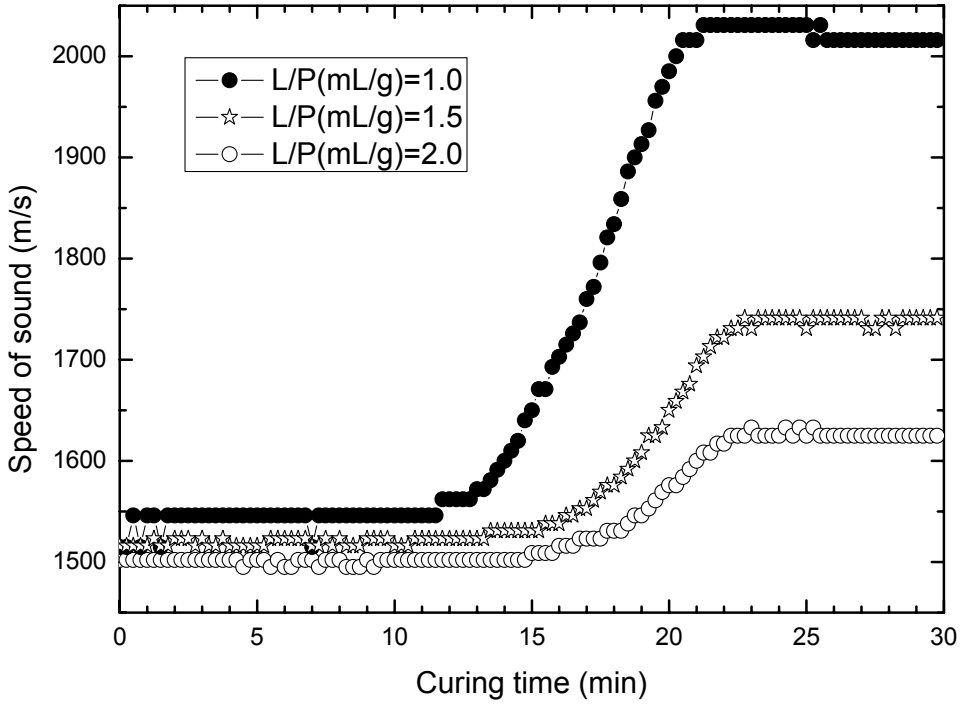

Figure 10.1. Speed of sound *vs.* Curing time: Effect of the liquid-to-powder ratio L/P for CS-cement.

Figs. 10.2 and 10.3 show the evolution of the acoustic impedance $z(t)$ and the density $\rho(t)$, respectively, *versus* the curing time for cement made at L/P=2 mL/g, and as a function of resting times RT. This L/P ratio showed good workability, it had the highest useful IST of the series (IST≈14(±1) min) and allowed for more experiments at RT<IST. Figs. 10.2 and 10.3 show that, if cement mixing (30 s at 1600 rpm) is again performed at some time (RT=3 or 9 min) after the initial powder and liquid cement mixture, the acoustic impedance and the density increased with RT, as compared to the control cement for which no additional mixing is performed at any time.

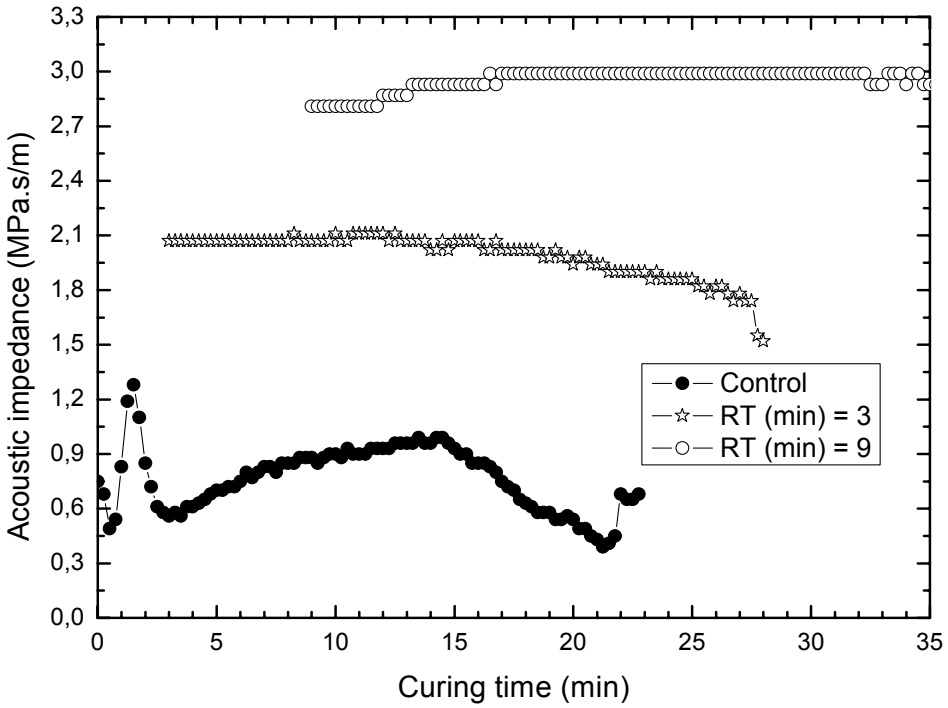

Figure 10.2. Acoustic impedance *vs.* Curing time: Effect of further mixing (30 s at 1600 rpm) after completion of resting times RT=3 & 9 min of CS-cement at L/P=2 mL/g.

These results indicated that further mixing before the IST compacts and makes the cement more homogeneous (i.e. more constant $z(t)$ and $\rho(t)$ values along the whole curing period) probably by eliminating air bubbles introduced during hand mixing and also by favouring a better distribution of reactant and product crystals, i.e. CSH and CS-dihydrate (CSD) crystals. SEM results seemed to corroborate this conclusion (see later). An interesting observation is that more compact and homogenous cements are produced as RT approaches the IST, i.e. higher nearly-constant values of both $z(t)$ and $\rho(t)$. In fact, values around 0.5(±0.1) g/cm^3 (i.e. sample at RT=0 min) are typical of porous CS cements while values around 1.2(±0.1) g/cm^3 (i.e. sample at RT=3 min) and 1.8(±0.1) g/cm^3 (i.e.

sample at RT=9 min) are also known for compact CS cements [14]. It should be noted in Fig. 10.3 that data acquisition for curves RT=3 & 9 min start at 3 & 9 min, meaning that before these times (i.e. before the application of 30 s mixing at 1600 rpm) the setting condition was exactly the same as that of the control and so the density of cements before the application of further mixing is the same as that reported by the control curve. This means that further mixing actually densifies the cement material. It should be mentioned that no thermal effect, that could accelerate the setting of the cement, was noticed with a thermometer after mixing at 1600 rpm for 30 s (data not shown).

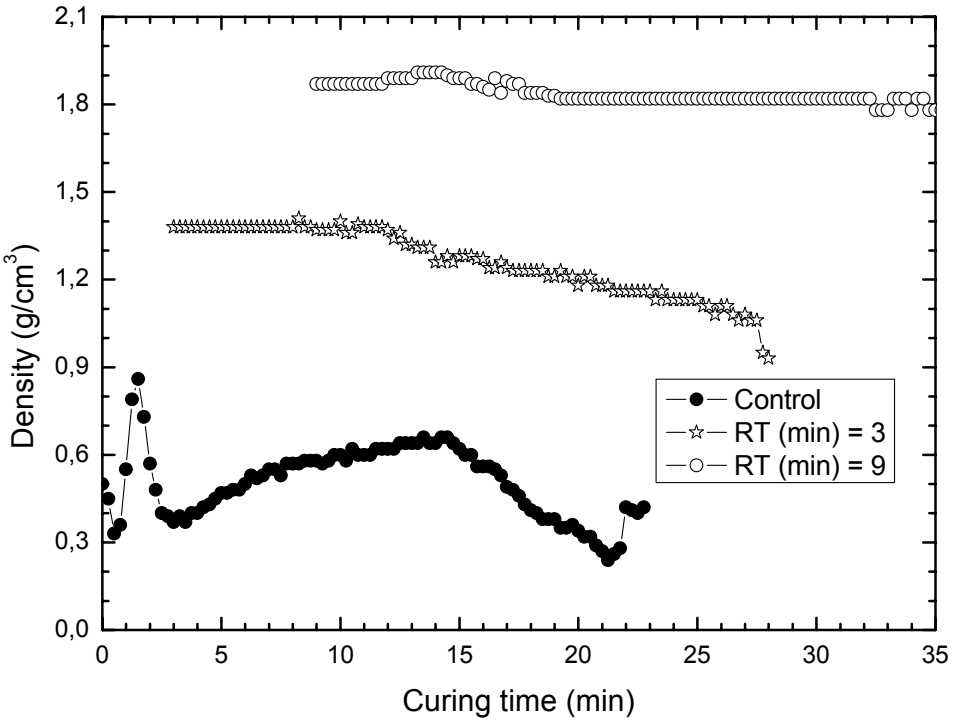

Figure 10.3. Density *vs.* Curing time: Effect of further mixing (30 s at 1600 rpm) after completion of resting times RT=3 & 9 min of CS-cement at L/P=2 mL/g.

Fig. 10.4 shows the evolution of the speed of sound *versus* the curing time for cement made at L/P=2 mL/g, and as a function of RT. It shows how setting times (IST and FST) can be drastically reduced if appropriate mixing protocols are conducted just after the initial mixture of the powder and liquid cement phases. Interestingly, when cement set at rest during 1.3 min and then was mixed during 30 s at 1600 rpm, the IST reduced from 14(±1) min (i.e. the control) to 4(±1) min, and the FST reduced from 23(±1) min to 10(±1) min. In that particular case, the setting reaction was heavily accelerated. On the other hand, when RT approached the IST the effect on the setting times reduced.

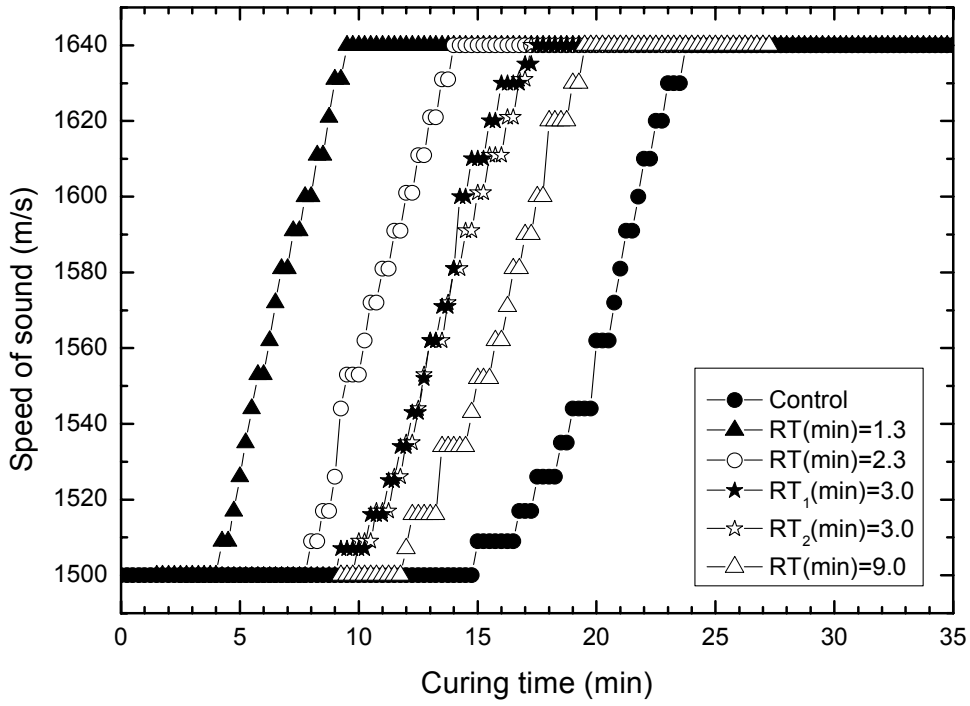

Figure 10.4. Speed of sound *vs.* Curing time: Effect of further mixing (30 s at 1600 rpm) after completion of resting times RT=1.3, 2.3, 3 & 9 min of CS-cement at L/P=2 mL/g. (Note: two curves are shown for sample RT=3 min to show that standard deviation (not drawn for clarity) of ultrasound measurements was less than 2%).

Fig. 10.4 also shows that the observed results had good reproducibility (see curves for series RT_1 and RT_2, both made at RT=3 min), which is a characteristic of ultrasonic measurements (inherent error less than 2%; standard deviation not drawn for clarity). In fact, the differences observed between curves in Fig. 10.4 showed to be statistically significant at a probability level of 95% (α=0.05).

It is thought, based of SEM observations (see *10.3.3. Scanning electron microscopy*), that the results in Fig. 10.4 should be related with the number and size of CSD crystals which are formed at the beginning of the hydration reaction of CSH crystals and on how these crystals are distributed in volume when further mixing is applied. However, more research is needed to clarify these observations. On the other hand, Figs. 10.3 and 10.4 shows that further mixing before the IST can both accelerate the setting (i.e. fast setting cements) and improve the densification of the material (i.e. better mechanical properties). It is also important to note that the speed of sound of all samples for times lower than their IST was 1500 m/s, which is the same as that of ultrasound pulses traversing water. This means that before the IST cement behaves as a liquid phase similar to water; thus, when injection was performed before the IST, injectability was similar for all the cements tested in that condition (i.e. measured speed of sound around 1500 m/s) to that observed for sample RT(min)=0 in Fig. 10.5 (see *10.3.2. Injectability properties*). Moreover, the speed of sound at saturation was also the same for all the samples, i.e. 1640 m/s. This means that the differences observed for the cement's density (see Fig. 10.3) are not enough to change the speed of sound traversing the cement, i.e. from the point of view of ultrasound pulses the physical properties of the cement's crystal microstructure is the same after their FST.

10.3.2. Injectability properties

Fig. 10.5 shows the evolution of the extrusion force *versus* the extruding time during the injectability experiments of cement made at L/P=2 mL/g. Cement samples were prepared

following the same protocol. Syringes of 5 mL filled with cement were allowed to set at different resting times without further agitation (RT=0N, 14N, 17N, 22N, 27N, 32N min; where "N" stands for "No-further agitation") and then extruded (see *10.2. Materials and methods*). Sample at RT=0N min was the control for the injectability experiments, i.e. sample extruded immediately after cement's constituency; RT=14N min is a sample at the IST; RT=17N is a sample between the IST and the FST; RT=22N min is a sample at ≈FST; and RT=27N & 32N min are samples at RT>FST.

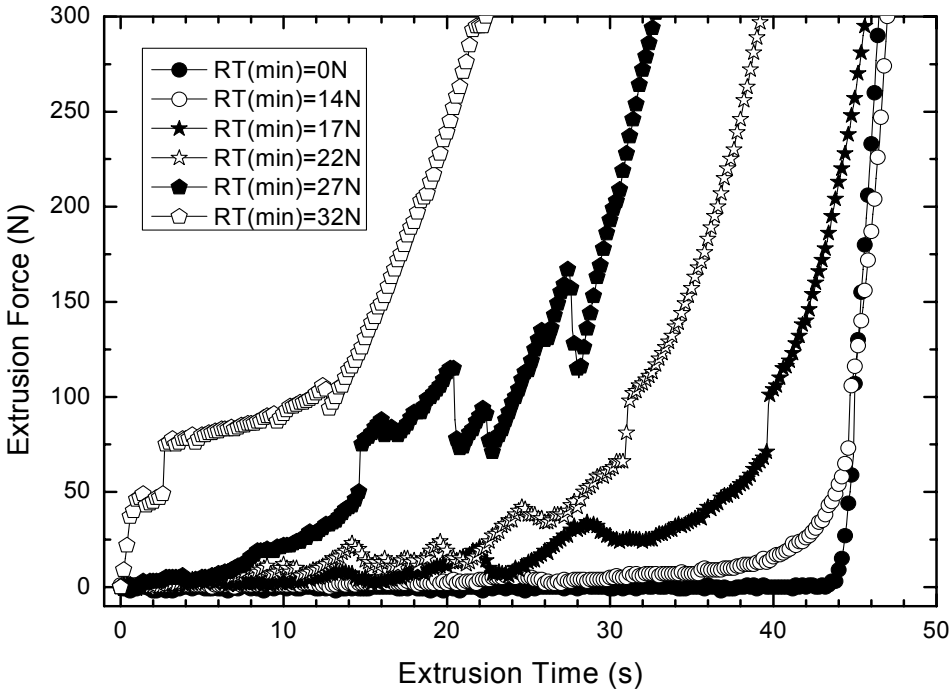

Figure 10.5. Extrusion force *vs.* Extrusion time: Effect of RT on CS-cement's injectability at L/P=2 mL/g.

The general observation is that cement's injectability decreased (as expected) with the increase of RT; i.e. with the progress of the hydration setting reactions. If a force value is taken constant (200 N, for example) it is observed that this level of force was attained in

shorter time for higher RTs, i.e. more set and less injectable cements. Other specific observations such as cement-water filtration and cement blockage (force step-drop variations) inside the syringe can be also observed in Fig. 10.5. It is worth-mentioning that the control cement (i.e. RT=0N min) was fully injectable during the maximum allowed extruding time period, i.e. ≈45 s. In fact, if cements mixed at different RTs are injected before their characteristic IST (see Fig. 10.4) the extrusion behaviour (i.e. minimum constant extrusion force or maximum injectability) was the same as that of the control sample (i.e. RT=0N min; in Fig. 10.5). This was also in agreement to the results observed in Fig. 10.4, where the speed of sound for times t<IST was 1500 m/s, i.e. the speed of sound through water (very liquid cements). Statistic analysis performed on three series of experiments confirmed the above observations.

Fig. 10.6 shows the effect on the extrusion force *versus* the extruding time of applying further mixing of 30 s at 1600 rpm to samples setting at rest up to RT=14N & 17N min. According to Fig. 10.4, it is not expected to observe any acceleration effect on the setting times IST & FST. However, Fig. 10.6 shows that, after completion of fixed RTs, additional mixing (i.e. samples RT=14A & 17A in Fig. 10.6) significantly decreased the injectability as compared with cement samples with no additional mixing (i.e. RT=14N & 17N). This means that, after the IST, further mixing is still able to compact the cement. In fact, from the point of view of the injectability, the additional mixing applied to samples RT=14 & 17 was equivalent to those samples setting at rest (i.e. with no additional mixing at any time) for curing times t>27 min (see Fig. 10.5). Moreover, the effect of compactation due to the additional mixing is so notable that liquid phase press-filtering and cement blockage inside the syringe were also noted in Fig. 10.6 (see force step-drop variations).

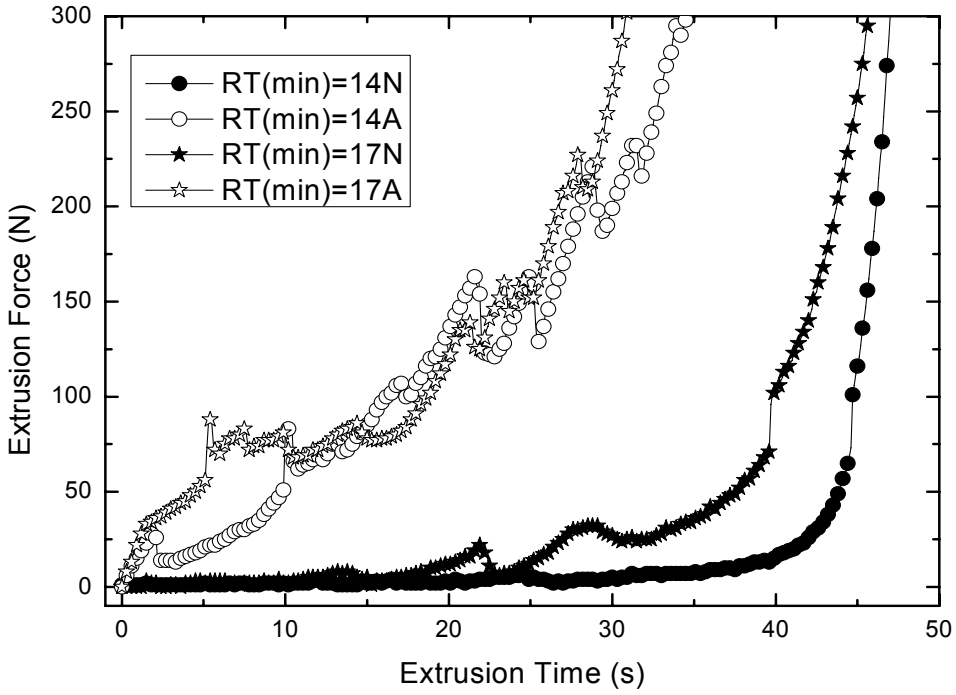

Figure 10.6. Extrusion force *vs.* Extrusion time: Effect of further mixing (30 s at 1600 rpm) on CS-cement's injectability at L/P= 2 mL/g, i.e. non-further agitation (N) versus further agitation (A) after completion of fixed resting times RT=14 & 17 min.

10.3.3. Scanning electron microscopy

Fig. 10.7 is a survey of SEM pictures taken at different mixing conditions. Left-top picture shows the reactant powder phase of the cement, i.e. CSH crystals. These crystals are as large as 20 μm with an aspect ratio of ≈0.25. Right-top picture shows the cement after hand mixing of the powder and the liquid phases during 30 s and then quenched in acetone to stop further CSH-crystals hydration (see *10.2. Materials and methods*). The microstructure showed a network of needle shape (aspect ratio of ≈0.08) mild entangled CSH & CSD crystals (equally oriented in all directions). Middle-left picture is the same

cement as that in right-top picture but with an added mixing of 30 s at 1600 rpm. In that case, it was observed that needle-shape CSH & CSD crystals oriented preferably following centrifugal forces. Similar behaviour was observed for those samples setting at rest for 1.5 (middle-right picture) & 3 (bottom-left picture) min and mixed again for 30 s at 1600 rpm. This general effect seemed to stop as the IST of the sample was approached; see bottom-right picture for resting time of 9 min and further mixing of 30 s at 1600 rpm. Although these observations are quite subjective, these should be at the base of a possible explanation for the acceleration (see Fig. 10.4) and the densification (see Figs. 10.3 & 10.6) effects observed in this study.

10.4. Summary conclusion

It has been put forward that further mixing, after cement's constituency and before the initial setting time IST, improves the setting (i.e. lower IST & FST) but reduces the injectability of calcium sulphate based cements. Ultrasound monitoring contributed with relevant information to the understanding of the curing cement's process by recording the evolution of the acoustic impedance, the density and the speed of sound during the cement's setting. The characteristics IST & FST were obtained from the evolution of the speed of sound. SEM observations helped to clarify that cement's densification was related to preferential orientation, due to agitation, of the needle-shape CSH & CSD crystals formed during the initial stages of the hydration reaction. The final conclusion is that mixing actually affects the setting of injectable calcium sulphate bone cements.

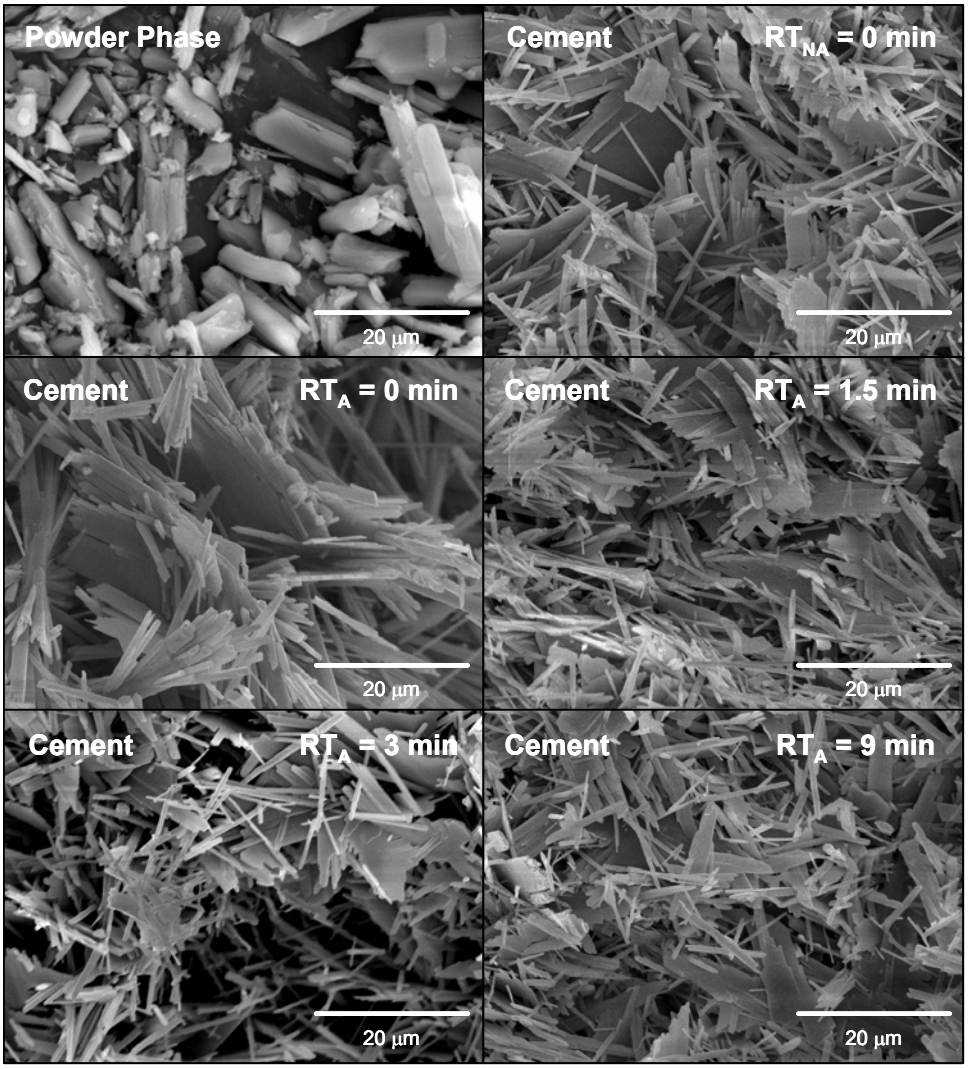

Figure 10.7. SEM pictures at different mixing conditions. See the text for comprehensive description of the microstructures. (Top-left: reactant powder phase of CSH crystals; Top-right: cement control quenched without further mixing; Middle-left: cement control with further mixing of 30 s at 1600 rpm and quenched; Middle-right & bottom pictures: cement set at different times (i.e. 1.5, 3 & 9 min), mixed again for 30 s at 1600 rpm and quenched).

References

1. Bohner M. Physical and chemical aspects of calcium phosphates used in spinal surgery. Eur Spine J 2001;10:S114-S121.

2. Moore DC, Maitra RS, Farjo LA, Graziano GP, Goldstein SA. Restoration of pedicle screw fixation with an in situ setting calcium phosphate cement. Spine 1997;22(15):1696-05.

3. Mermelstein LE, McLain RF, Yerby SA. Reinforcement of thoracolumbar burst fractures with calcium phosphate cement: a biomechanical study. Spine 1998;23(6):664-70.

4. Bai B, Jazrawi LM, Kummer FJ, Spivak JM. The use of an injectable, biodegradable calcium phosphate bone substitute for the prophylactic augmentation of osteoporotic vertebrae and the management of vertebral compression fractures. Spine 1999;24(15):1521-26.

5. Heini PF, Berlemann U, Kaufmann M, Lippuner K, Fankhauser C, Landuyt P. Augmentation of mechanical properties in osteoporotic vertebral bones: a biomechanical investigation of vertebroplasty efficacy with different bone cements. Spine 2001;10:164-71.

6. Bohner M, Baroud G. Injectability of calcium phosphate pastes. Biomaterials 2005;26(13):1553-63.

7. Gbureck U, Barralet JE, Spatz K, Grover LM, Thull R. Ionic modification of calcium phosphate cement viscosity. Biomaterials 2004;25:2187-95.

8. Barralet JE, Hoffman M, Grover LM, Gbureck U. High-strength apatitic cement by modification with α-hydroxy acid salts. Adv Mater 2003;15(24):2091-4.

9. Fernández E, Sarda S, Hamcerencu M, Vlad MD, Gel M, Valls S, Torres R, López J. High-strength apatitic cement by modification with superplasticizers. Biomaterials 2005;26:2289-96.

10. Baroud G, Bohner M, Heini P, Steffen T. Injection biomechanics of bone cements used in vertebroplasty. Bio-Medical Materials and Engineering 2004;14,4:487-504.

11. Viano AM, Auwarter JA, Rho JY, Hoffmeister BK. Ultrasonic characterization of the curing process of hydroxyapatite-modified bone cement. J Biomed Mater Res 2001;56:593-99.

12. Carlson J, Nilsson M, Fernández E, Planell JA. An ultrasonic pulse-echo technique for monitoring the setting of CaSO4-based bone cement. Biomaterials 2003;24:71-7.

13. Khairoun I, Boltong MG, Driessens FCM, Planell JA. Some factors controlling the injectability of calcium phosphate bone cements. J Mater Sci Mat Med 1998;9:425-8.

14. Ullmann's Encyclopedia of Industrial Chemistry. Volume A4: Benzyl Alcohol to Calcium Sulfate, 1985, pp.555-584.

Chapter 11

Summary

In this Doctoral thesis several calcium phosphate bone cements (CPBCs) have been proposed and characterised in order to develop new injectable, high strength and/or porous cementitic-like materials with biocompatible/osteogenic behaviour, for application in the spinal management of vertebral compression fractures through minimally invasive surgery techniques (MIST), such as vertebroplasty and/or kyphoplasty. This work provides new insights into: (A) the development of new apatitic CPBCs through methods that have resulted in new cement formulations with improved: (a.1) mechanical (Chapter 2, 5 & 7), (a.2) porosity (Chapter 3 & 6), and (a.3) injectability properties (Chapter 7); and with optimum (a.4) *in vitro* (Chapter 6, 7 & 8) and (a.5) *in vivo* (Chapter 8) osteogenic behaviour. It also provides new insights into: (B) the application of: (b.1) new sintering routes for the control of the setting properties of the main cement reactant (Chapter 4 & 5); (b.2) ultrasounds to monitor the early stages of the setting reaction of ceramic based bone cements (Chapter 9 &10).

The following are the central and major findings of this work.

- Civil engineering superplasticizers affect apatitic CPBCs' properties as expected, i.e. by enhancing (at constant liquid-to-powder ratio): (a) cement particle dispersion and hydration; (b) cement workability and flowing properties; and (c) mechanical properties at saturation. These effects were plasticizer-type dependent and opened the

search for new biocompatible superplasticizers to develop new injectable high-strength CPBCs of use for MIST applications (Chapter 2).

- Apatitic CPBCs can be made progressively porous during its normal setting. The macroporosity of alpha-tricalcium phosphate (α-TCP) based bone cement can be tailored in advance by adding into the powder phase passive dissolution phases such as calcium sulphate dihidrate (CSD). The setting and hardening properties are the result of α-TCP hydration into an entangled net of calcium deficient hydroxyapatite (CDHA) crystals surrounding passive dissolving CSD crystals (active creating porosity). The resulting mechanical properties during setting are suitable for cancellous bone applications. The resulting porous material has potential ability to assure new bone apposition after implantation *in vivo* (Chapter 3).

- There is strong correlation between the calcium-to-phosphorus (Ca/P) ratio of high-temperature sintered cement reactants and their chemical reactivity in solution at low temperature. It has been shown that the Ca/P ratio of the main cement reactant controls the setting and hardening properties of the resulting cement. It has been shown that there is an optimum value for this Ca/P ratio around the α-TCP's reactant and that small deviations from Ca/P=1.50 can have drastic effects on the cement setting. In this sense, it has been concluded that uncontrolled ionic contamination of the main cement reactant, affecting its Ca/P ratio, can explain the non-setting reactivity of some cements after scale production (Chapter 4).

- Iron modified calcium phosphates obtained from the ternary system «CaO-P_2O_5-FeO» by sintering at high-temperature have cement-like properties in solution at low temperature. These new cement reactants can be tailored with different acidities and

magnetic strength depending on the addition of iron. The resulting cements can be optimized to show maximum magnetic and mechanical strength after setting by increasing the amount of iron of the main cement reactant. The nature of the physico-chemical setting reactions controlling the setting of the new apatitic-iron-modified based cements is not affected by the iron addition, i.e. a net of entangled calcium deficient apatite crystals evolved during the setting is still responsible for the mechanical strengthening of the cement-material. Finally, the new sintering route has proved suitable to improve the chemical reactivity of unreactive (unbalanced Ca/P ratio or ionic-contaminated; see Chapter 4) α-TCP cement reactant, thus assuring cement setting properties' reproducibility (Chapter 5).

- The addition of iron oxide nanoparticles (IO) into the cement powder phase of an α-TCP based bone cement significantly enhanced: (a) the initial workability (longer setting times); (b) the injectability; and (c) the maximum compressive strength of the resulting cement pastes, without affecting their: (d) physico-chemical setting reactions; and (e) cytocompatibility. The conclusion is that IO-cement modification could be suitable to improve the initial cement's flowing properties without affecting further cement hardening of this or other similar CPBCs' systems (Chapter 7).

- Iron-modified α-TCP based bone cements have cytocompatible features *in vitro*; i.e. these new cements have the ability to support cellular colonization, proved by the fact that the adhesion, proliferation and viability of HEp-2 cells were not negatively influenced by iron concentration in a dose-dependent manner (Chapter 6). In addition, biphasic cement materials based on iron-modified α-TCP (as main reactant) and CSD crystals (as passive dissolving/active creating porous phase) showed favorable cement substratum properties for osteoblast-like cells proliferation and

differentiation *in vitro*, which leads to stable new bone binding (i.e. osteoconduction) as confirmed by the *in vivo* sheep model study. The biocompatibility and resorption of the new porous apatitic iron-modified cement was demonstrated for a period of 3 and 6 months, when no signs of inflammation, necrosis and any reaction of the host tissue against to the implanted cement were found. The cement resorption occurred by a prevalent macrophage-mediated mechanism and was somewhat higher compared to the controls, proving the osteogenic features of this new porous apatitic iron-modified bone cement and providing new insights into the development of new therapeutic bone cements for cancellous bone replacement of interest to kyphophasty for the treatment of osteoporotic vertebral compression fractures (Chapter 8).

- Ultrasound monitoring offered a reliable evaluation of the early curing process of ceramic based bone cements by linking acoustic and material properties during the early setting of calcium sulphate (CS) and calcium phosphate (CP) based bone cements. Ultrasound monitoring continuously followed the curing cement's process by recording the evolution of the acoustic impedance, the density and the speed of sound during the cement's setting. The characteristics initial and final setting times (IST & FST) were obtained from the evolution of the speed of sound. Finally, it has been put forward that further mixing, after cement's constituency and before the IST, improves the setting (i.e. lower IST & FST) but reduces the injectability of CS based cements. It is expected that, after further experimental optimization, ultrasound monitoring should help, in combination with recent approaches to measure the injectability property of CPBCs, to set up good practice protocols for CPBCs' injection during minimally invasive surgery (Chapter 9 & 10).

Published articles

E. Fernández, S. Sarda, M. Hamcerencu, M.D. Vlad, M. Gel, S. Valls, R. Torres, J. López. *High-strength apatitic cement by modification with superplasticizers*. Biomaterials 2005;26:2289-2296.

E. Fernández, M.D. Vlad, M. Gel, J. López, R. Torres, J.V. Cauich, M. Bohner. *Modulation of porosity in apatitic cements by the use of α-tricalcium phosphate-calcium sulphate dihydrate mixtures*. Biomaterials 2005;26:3395-3404.

E. Fernández, M.D. Vlad, M. Hamcerencu, A. Darie, R. Torres, J. López. *Effect of iron on the setting properties of α-TCP bone cements*. Journal of Materials Science 2005;40:1-6.

M.D. Vlad, R. Torres, J. López, M. Barracó, J.A. Moreno, E. Fernández. *Does mixing affect the setting of injectable bone cement? An ultrasound study*. Journal of Materials Science: Materials in Medicine 2007;18:347–352.

M.D. Vlad, L.J. del Valle, M. Barracó, R. Torres, J. López, E. Fernández. *Iron oxide nanoparticles significantly enhances the injectability of apatitic bone cement for vertebroplasty*. Spine 2008;33(21): 2290-2298.

M.D. Vlad, L.J. Valle, I. Poeata, M. Barracó, J. López, R. Torres, E. Fernández. *Injectable iron-modified apatitic bone cement intended for kyphoplasty: cytocompatibility study*. Journal of Materials Science: Materials in Medicine 2008;19(12):3575-83.

Articles submitted

M.D. Vlad, L. González, R. Torres, J. López, J.E. Carlson, M. Barracó, E. Fernández. *Ultrasonic monitoring of the setting of calcium-based bone cements*. Ultrasonics 2008;00:000-000.

M.D. Vlad, M. Barracó, R. Torres, J. López, E. Fernández. *Effect of the calcium to phosphorus ratio of α-tricalcium phosphate on the setting properties of calcium phosphate bone cement*. Journal of Biomedical Materials Research 2009;00:0000-0000.

M.D. Vlad, L.J. del Valle, I. Poeată, M. Barracó, J. López, R. Torres, E. Fernández. *Osteogenic features of biphasic calcium sulfate dihydrate/iron-modified alpha-tricalcium phosphate bone cements intended for kyphoplasty: in vitro study*. Biomaterials 2009;00:0000-0000.

M.D. Vlad, E.V. Şindilar, M.L. Mariñoso, I. Poeată, M. Barracó, J. López, R. Torres, E. Fernández. *Osteogenic features of biphasic calcium sulfate dihydrate/iron-modified alpha-tricalcium phosphate bone cements intended for kyphoplasty: in vivo study*. Biomaterials 2009;00:0000-0000.